Pechora Sea Environments: Past, Present, and Future

Edited by
H. A. Bauch, Yu. A. Pavlidis, Ye. I. Polyakova,
G. G. Matishov, N. Koç

Ber. Polarforsch. Meeresforsch. 501 (2005)
ISSN 1618 - 3193

Pechora Sea Environments: Past, Present, and Future

H.A. Bauch[1], Yu.A. Pavlidis[2], Ye.I. Polyakova[3], G.G. Matishov[4], N. Koç[5] (eds.)

[1]Akademie der Wissenschaften und der Literatur, Mainz, Geschwister-Scholl-Str. 2, D-55131 Mainz.

[2]Shirshov Institute of Oceanology, 36 Nakhimovskii prospekt, 117856 Moscow, Russia.

[3]Department of Geography, Moscow State University, Vorob'evy Gory, 119899 Moscow, Russia.

[4]Murmansk Marine Biological Institute, 17 Vladimirskaya ul., 183010 Murmansk, Russia

[5]Norwegian Polar Institute, Polar Environmental Centre, N-9296 Tromsø, Norway.

TABLE OF CONTENTS

INTRODUCTION

Page

Bauch, H.A., Pavlidis, Yu.A., Polyakova, Ye.I., Matishov, G.G., Koç, N.
Past, modern, and future state of the Pechora Sea.....1

MODERN ENVIRONMENTAL CONDITIONS

Nikiforov, S.L., Dunaev, N.N., Politova, N.V.
Modern environmental conditions of the Pechora Sea (climate, currents, waves, ice regime, tides, river runoff, and geological structure).....7

Kaplin, P.A., Selivanov, A.O.
Holocene sea-level changes in the European sector of the Russian Arctic.....39

Pogodina, I.A.
Modern benthic foraminiferal assemblages in the Pechora Sea.....49

Denisenko, S.G., Denisenko, N.V., Dahle, S., Cochrane, S.J.
The zoobenthos of the Pechora Sea revisited: a comparative study.....55

BOTTOM TOPOGRAPHY

Pavlidis, Yu.A., Dunaev, N.N., Nikiforov, S.L., Artem'ev, A.V., Politova, N.V.
Submarine terraces in the Pechora Sea.....75

Biryukov, V.Yu., Ogorodov, S.A.
Seafloor morphology of the Pechora Sea (based on bathymetry).....85

Pavlidis, Yu.A., Nikiforov, S.L., Artem'ev, A.V., Dunaev, N.N., Politova, N.V.
New data on the Pechora Sea bottom topography evidenced by geoacoustic profiling.....91

COASTAL DYNAMICS AND MORPHOLOGY

Ogorodov, S.A.
Coastal morphology and dynamics of the Pechora Sea.....103

Ogorodov, S.A.
The role of sea ice in coastal and sea bottom dynamics of the Pechora Sea.....113

QUATERNARY STRATIGRAPHY AND PALEOGEOGRAPHY

Pavlidis, Yu.A., Dunaev, N.N., Nikiforov, S.L.
Sediment sequence of the Southern Novaya Zemlya trough (Pechora Sea): Facial and stratigraphic interpretations.....125

Bondarev, V.N., Rokos, S.I., Tarasov, G.A., Kostin, D.A., Dlugach, A.G., Polyakova, N.A.
Cryogenic processes and phenomena in the upper sediment layer of the Pechora Sea 141

Rudenko, O.V., Polyakova, Ye.I.
Quaternary palynostratigraphy of the Pechora Sea.....155

Tarasov, G.A., Pogodina, I.A., Matishov, G.G., Bauch, H.A., Kukina, N.A.
The Late Pleistocene history of the Pechora Sea.....167

Ogorodov, S.A., Polyakova, Ye.I., Kaplin, P.A., Parunin, O.B., Taldenkova, E.E.
Evolution of the barrier beaches in the Pechora Sea.....177

GEOECOLOGY

Ogorodov, S.A.
Technogenic impact on the coastal dynamics in the Varandei Region, Pechora Sea.....185

Dunaev, N.N., Nikiforov, S.L., Pavlidis, Yu.A., Politova, N.V.
Geoecological situation in the "Prirazlomnoe" oilfield area, Pechora Sea.....195

FUTURE DEVELOPMENTS

Pavlidis, Yu.A.
Possible sea-level changes at the beginning of the third millennium.....201

Kaplin, P.A., Selivanov, A.O., Sobolev, V.M.
Evolution of the southern Pechora Sea coasts during the present century as expected from future changes in climate and sea-level 211

Leont'ev, I.O.
Modeling the sedimentary evolution of the Pechora Sea coast.....231

PAST, MODERN, AND FUTURE STATE OF THE PECHORA SEA

H.A. Bauch[1]*, Yu. A. Pavlidis[2], Ye.I. Polyakova[3], G.G. Matishov[4], N. Koç[5]

[1]Alfred Wegener Institute for Polar and Marine Research, Bremerhaven, Germany;
*now at Academy of Sciences, Humanities and Literature, Mainz, Germany
[2]Shirshov Institute of Oceanology, Moscow, Russia
[3]Department of Geography, Lomonosov Moscow State University, Moscow, Russia
[4]Murmansk Marine Biological Institute, Murmansk, Russia
[5]Norwegian Polar Institute, Polar Environmental Centre, Tromsø, Norway.

Abstract

The Pechora Sea is quite unique among Arctic seas as it is a region directly influenced by both Atlantic and Polar waters as well as river waters (Fig. 1). This area has important economic value due to the existence of extensive oil and gas fields, but it is also home to traditional fishing and reindeer breeding. Because exploitation of the natural resources will start in the nearest future, an establishment of regional sustainable development strategies seems necessary. Since the Pechora Sea will soon be increasingly influenced by these anthropogenic factors, such strategies should be based on a detailed analysis of the ongoing situation, but even more so, should consider those environmental changes which occurred in this area during the past. Hence, there is a need to investigate the pre-anthropogenic phase in order to better understand any possible future environmental changes. Such investigations were carried out by various groups from Russia, Germany and Norway between the years 2000 and 2002, in a project which was financially supported by INTAS (No. 1489-99).

Introduction

Large oilfields recently explored in the Pechora Sea are now ready for exploitation. Therefore, this region will undergo considerable changes due to man-induced technogenic impact. Unlike the Barents Sea, the semi-enclosed and rather small Pechora Sea is much shallower and ice-covered for a considerable time of the year. Moreover, its coasts are being actively eroded. Altogether, this allows the assumption that the Pechora Sea basin could undergo major environmental change due to climate warming and sea-level rise. Because of the increasing economic interest in the Pechora region there is a demand to develope a strategy for widespread territorial exploration, for instance, for suitable construction sites.

An example, which points to the necessity of ecologically substantiated approach for industrial exploitation of the new coastal areas, is the Varandei area. Active industrial exploitation of the Varandei area started in the seventies. Varandei Island experienced maximum technogenic impact, because here the main industrial objects together with Novyi Varandei settlement are located. There is ample evidence from this region that, for instance, enhanced coastal abrasion observed more recently resulted from improper exploitation of the area without understanding the characteristics of the coastal relief and its dynamics.

Because the Arctic environment is known for its sensitivity, it is especially important to minimize negative anthropogenic impacts. However, to do this properly requires profound knowledge of the present and past geoecological state of this territory as basis for a better forecast of possible future environmental changes.

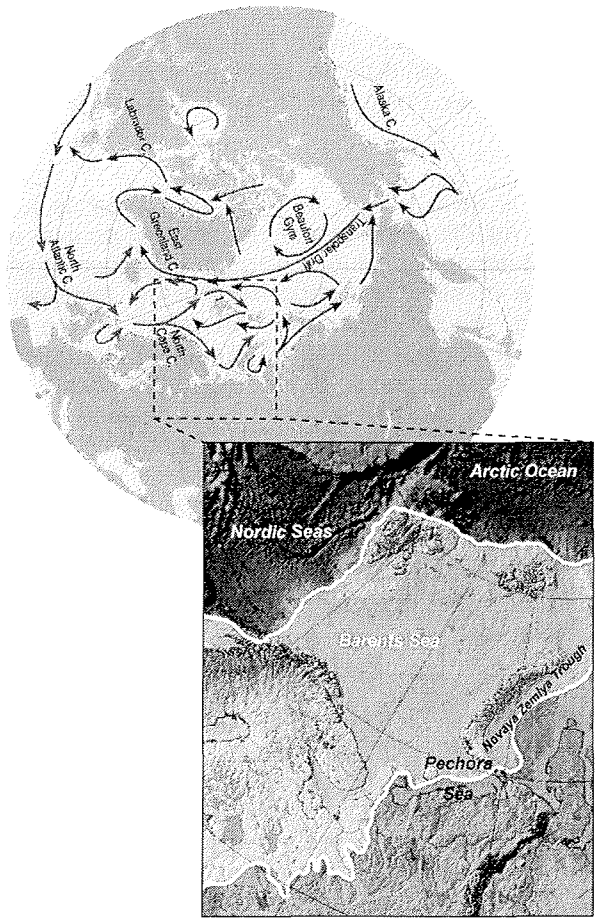

Fig. 1 Main surface ocean circulation in the Arctic Ocean, its shelf seas and neighbouring ocean basins (top). Inset below shows Barents Sea region with the Pechora Sea. The white line marks the outer limit of glacial ice extent during the last glacial maximum according to the most recent reconstruction (adopted from Svendsen et al., 2004). The reconstruction for the Pechora Sea and Novaya Zemlya Trough region is thereby based on Polyak et al. (2000) and Gataullin et al. (2001)

So far, a number of questions concerning the Quaternary history of the Pechora Sea region still remain unanswered (Fig. 1). These relate to the stratigraphic subdivision and facial characteristics of the seafloor sediment sequences, the shelf geomorphology, the lack of information of the sediment sequence in the southern Novaya Zemlya trough, and the uncertainty of the impact of glaciological activity on this particular shelf during the last glaciation.

Because of the various abovementioned issues, scientific interest in the Pechora Sea region became more eminent and, eventually, led to the initiation of an INTAS-funded project (No 1489-99) entitled *The Pechora Sea – Late Pleistocene paleogeography, present state of the shelf and coastal zone and forecast for the 21st century.*

The various articles compiled in this report deal with the main goals of the Pechora Sea project. These may be summarized as follows:

- to reconstruct the paleoenvironmental evolution of the Pechora Sea during the Late Pleistocene and Holocene on the basis of geological evidence (e.g., seismic, lithological, geochemical, and micropaleontological data) in order to link the past and recent environmental changes with possible future development of this region;
- to study the morphology and sedimentary dynamics of the Pechora Sea coastal and shelf zones and to outline patterns of change as expected due to future climate warming and associated sea-level rise;
- to analyze natural sedimentological processes in the shelf and coastal zones as well as the anthropogenic impact upon natural environment caused by the existing sources of pollution and those that will appear due to intensified oil/gas exploitation;
- to forecast possible evolution of the Pechora Sea shelf and coastal zones according to the following scenarios: stable climate and sea-level conditions; climate warming and sea-level rise in the 21st century.

To tackle these problems, several scientific teams and respective team leaders from various countries and research institutes were formed. These included

1) Alfred Wegener Institute for Polar and Marine Research, Germany (H.A.Bauch - now at Mainz Academy of Sciences, Humanities and Literature, Germany)

2) Norwegian Polar Institute, Polar Environment Center, Norway, (N. Koç)

3) Shirshov Institute of Oceanology, Laboratory of shelf and coastal studies, Russia (Yu. Pavlidis)

4) Kola Scientific Center, Murmansk Marine Biological Institute, Department of geology and chemistry of sea, Russia (G. Matishov)

5) Lomonosov Moscow State University, Geography Department, Laboratory of Recent Sediments and Pleistocene Paleogeography, Russia (Ye. Polyakova)

To successfully meet the stated objectives, several research tasks were conducted by either one or both partners. These activities included the following:

Task 1: Establishment of a Late Pleistocene - Holocene stratigraphical scheme for the Pechora Sea on the basis of geochronological, seismostratigraphical, lithostratigraphical, biostratigraphical, and ecostratigraphical data.

Task 2: Reconstruction of the paleoenvironmental conditions of the Pechora region during specific time intervals of the Late Pleistocene and Holocene.

Task 3: Analysis of the modern and past sedimentological processes and its application to the present and possible future pollution, its sources and sinks.

Task 4: Determination of the coastal evolution and development of coastal processes over various time scales.

Task 5: Forecast of the Pechora Sea shelf and coast evolution in the 21st century.

Summary of Results

The scientific teams of the project developed new concepts of shelf and coastal evolution of the Pechora Sea during Late Pleistocene and Holocene times by linking together past and recent environmental change in order to deduce possible future developments of this region as they are related to both natural and anthropogenic factors.

A subdivison of Upper Quaternary sediments was carried out using facial analysis and high-resolution acoustic profiles. A further stratigraphical refinement of the late Pleistocene to Holocene deposits was constructed on the basis of geochronological, seismostratigraphical, lithostratigraphical, and biostratigraphical approaches. By studying micrfossils in surface and downcore sediments the main biostratigraphical events were determined and correlated with the seismostratigraphical units. The distribution of modern benthic organisms and sediments was also used to reconstruct different aspects of paleoenviornmental conditions (e.g., paleocurrents, paleosalinity, paleoproductivity). Paleogeographical models of the Pechora Sea for three different time slices were then developed.

Various maps were compiled that demonstrate the schematic geomorphological nature of the Pechora Sea bottom and the principal character of dominant coastal features. The main factors of coastal development and directions of alongshore sediment movement were identified and their intensity evaluated. Ten morphodynamic regions with specific dynamic and morphological characteristics were distinguished and mapped. The main stages of barrier beach formation were established for the southern Pechora Sea.

By evaluating the various morphological and sedimentological features, past and modern dynamics of coasts and shelf regions were interpreted. Assuming a further increase in climate warming, sea-level rise and anthropogenic activity, different scenarios were developed. It is found that in the economically most developed and developing areas, namely those of oil and gas prospection, extraction, storage and transportation, intensity of the anthropogenic impact during the present century will reach a crucial level. Using semi-quantitative models of coastal evolution, which were elaborated in form of maps for various types of coasts, it is further concluded that barrier coasts and icy-rich coastal escarpments will suffer much from the future

changes. Applying these models to several coastal segments, the shoreline retreat by the end of the present century was estimated.

Acknowledgements
All project participants are very thankful for the financial support granted by INTAS. The individual manuscripts included in this report benefited from careful editorial work by E. Taldenkova (Moscow State University, Moscow) and K. Volkmann-Lark (IFM-GEOMAR, Kiel). Financial administrative work on behalf of the project co-ordinator (H.A. Bauch) was kindly assisted by C. Audebert (AWI, Bremerhaven).

References

Gataullin,V.,Mangerud,J.,Svendsen,J.I. (2001). The extent of the Late Weichselian ice sheet in the southeastern Barents Sea. Global and Planetary Change 31, 453–474.

Polyak,L.,Gataullin,V.,Okuneva,O.,Stelle,V. (2000). New constraints on the limits of the Barents-Kara ice sheet during the Last Glacial Maximum based on borehole stratigraphy from the Pechora Sea.Geology, 28, 611–614.

Svendsen et al. (2004). Late Quaternary ice sheet history of northern Eurasia Quaternary Science Reviews, 23, 1229–1271.

MODERN ENVIRONMENTAL CONDITIONS OF THE PECHORA SEA (CLIMATE, CURRENTS, WAVES, ICE REGIME, TIDES, RIVER RUNOFF, AND GEOLOGICAL STRUCTURE)

S.L. Nikiforov, N.N. Dunaev, N.V. Politova
Shirshov Institute of Oceanology RAS, Moscow, Russia

Abstract

The article deals with detailed information on environmental conditions, geological structure, bottom topography, and tectonics of the Pechora Sea shelf. It is outlined that specificity of climate as the basic exogenic factor of relief formation and sedimentation is determined here by high-latitudinal position of the region and, partly, by warming influence of the North Atlantic. The data on river runoff, permafrost evolution, ice regime and wave activity are analyzed. The geological section, besides a brief stratigraphic and tectonic review, contains detailed description of the recent stage in the evolution of this area.

Climate

Environmental peculiarity of the Pechora Sea, as well as the other Arctic seas, is determined by their high-latitudinal position. Not only do climatic conditions in the Arctic determine the intensity of the processes shaping the seabed, but they also control the character of sediment input to the coastal zone. This primarily concerns river runoff, ice and wave processes, tidal currents and other hydrodynamic factors. In polar areas, where average annual temperatures below zero are dominant, ice regime, frost weathering, solifluction and thermal abrasion are extremely important and in some areas play the leading role in modern relief formation.

Distribution of atmospheric precipitation and other climatic parameters is a result of complex interaction of circulation processes. Basic synoptic situations depend on location and intensity of dominant baric centers. The western Arctic seas are distinguished by intrusion of Atlantic cyclones carrying the greatest amount of atmospheric precipitation. It should be noted that climatic characteristics of polar coasts and adjacent hinterland largely depend on terrestrial relief. For example, at the eastern coast of the Novaya Zemlya archipelago very strong gusty winds – "novozemel'skaya bora" – with wind blows of up to 50–60 m/s are quite frequent. Local atmospheric features influence manifestation of exogenic processes including changes of hydrodynamic regime on adjacent parts of the sea basin.

Climatic conditions also determined manifestation of exogenic processes in the past. Global changes of atmospheric and oceanic circulation resulted in periodic climate coolings, accumulation and degradation of ice caps, exposure of vast shelves and subsequent flooding and alteration of its topography. The last late Pleistocene (Würm) glaciation had the greatest impact on evolution of modern shelf relief due to deep regression and, consequently, exposure of vast shelf areas in periglacial regions.

The main feature of the Arctic radiation regime is practically complete absence of solar heating during polar night, thus during 50–150 days the surface is subjected to continuous cooling. In summer, a significant amount of solar energy is lost due to cloudiness and reflection from water surface. As a result, radiation balance in the central Arctic regions is negative during the greatest part of the year, but on coasts and islands its annual value is positive and equals 2–15 kcal/sm^2 (Kaplin et al., 1991).

Climatic conditions determine domination of physical weathering and specificity of material input from the coastland. Cracking of rocks due to frost weathering produces a stable coarse debris cover over watersheds and slopes. Therefore, loose deposits inherit practically all minerals of mother rocks including unstable ones.

Frost weathering is the main coast-forming process on denudation coasts. Sharp temperature fluctuations and periodic moistening of rocks with different lithology result in destruction of coasts. Therefore, frost weathering is the major factor of sediment material mobilization, transportation and input to the coastal zone and further downslope to lower hypsometric levels.

Permafrost is also responsible for transformation of initial sediment material. Only superficial waters are able to evacuate clay particles and dissolved matter from the active soil layer. Sediments underlying the active layer are stuck with ice, and no weathering takes place. Under conditions of seasonal thawing water-bearing material creeps downslope due to solifluction (Aksenov et al., 1987). Presence of permafrost, excess moistening of the active layer, its low temperature, and long freezing period slow down the rates of chemical and biochemical processes of soil formation in the polar zone. Therefore chemical weathering produces only 1-3% of eluvium (Lisitsin, 1978). Under such conditions the liquefacted gleyish soil horizon is formed, that is easily eroded and, hence, is the source of fine clay particles input into water basins.

Thus, diverse material, i.e. coarse-grained polymictic and clay (mainly chlorite-hydromica), is supplied to the coastal zone.

In many respects, environmental and climatic conditions of the Pechora Sea, as well as the whole Barents Sea, are determined by their high-latitudinal position and warming influence of the North Atlantic and temperate air masses. Their interactions initiate variability of meteorological parameters during a year (Table 1).

As a result of interaction between Icelandic low, high-pressure polar air and Siberian high, the Arctic air moves southwestward, and warm air of the middle latitudes moves to the northeast. At the border of these two basic fluxes the atmospheric Arctic front is formed that is directed from the northern point of the Novaya Zemlya through the Medvezhii and Jan Mayen islands to Iceland. In winter, the Icelandic low deepens, the Siberian anticyclone is formed, and the Arctic front becomes aggravated. As a result, intensive cyclonic activity above the central Barents Sea develops, which considerably affects the situation in the Pechora Sea. Seasonal southwesterly winds with a strength of 3–5 to 7–8 prevail. However, northerly (~85 %) and subordinated southerly winds predominate over the coast (Dobrovol'skii and Zalogin, 1982). In winter, air temperature above the sea surface is negative. Average temperature of the coldest month (March) is -4°C on Kolguev Island and -7°C in the southeastern part of the sea.

Table 1. Meteorological parameters and phenomena in the Pechora Sea and adjacent regions of the Barents-Kara region (Danilov and Efremkin, 1998)

Parameter and phenomenon	Shtokmanovskoe	Pechora Sea	Bayadarat-skaya Bay	Northwestern coast of the Yamal Peninsula
1. Air temperature, °C				
Average annual	-1.2	-5.6	-9.0	-9.7
summer				
Minimum	–	-9	-4	-6
Average (monthly)	–	7–10	5–7	5–6
Maximum	23	30–32	28–32	29
winter				
Minimum	-28	-48	-50	-49
Average (monthly)	–	-13-19	-20-22	-20-25
Maximum	–	2–5	0–2	0–2
2. Duration of the cold period, days	160	240	240	250
3. Wind speed, m/s				
Mean for 10 minutes	43	35	26	28
Mean for 2 minutes	53	40	40	34
Mean for 3 seconds	–	49	–	–
4. Average duration of wind with speed exceeding 15 m/s (in hours)	8–10	7 (max 60)	–	–

In spring, the branch of the Icelandic low stretching northeastward reduces in size. The Polar high moves to the pole, and the Siberian anticyclone is destroyed. In most areas the weather is cloudy, with strong winds of different directions (wind strength 6–7), snow and rain.

In summer, the stable anticyclone is formed above the Barents Sea, and cloudy weather with northeasterly winds is established. In the warmest months (July and August) air temperature in the southeastern area is about +7°C. Intrusion of Atlantic air masses often disturbs weather conditions especially in the western and central areas. During such periods southwesterly up to 6-7 strong winds predominate.

At the beginning of fall, wind direction frequently changes, but by the end of this period southwesterly winds become dominant. Wind speed increases up to storm values, and the general cooling starts. From the second half of fall onwards, the fast transition to winter conditions occurs.

A characteristic feature of the region is the polar night lasting from 40 to 70 days.

The observed climate warming and ice cover reduction do not exclude extreme hydrometeorologic conditions especially in winter.

The data collected by International scientific centers on climate and global changes and the Russian Hydrometeocenter clearly demonstrate global climate warming for the last 150 years of observations as shown in the diagram of temperature anomalies variations (Fig. 1).

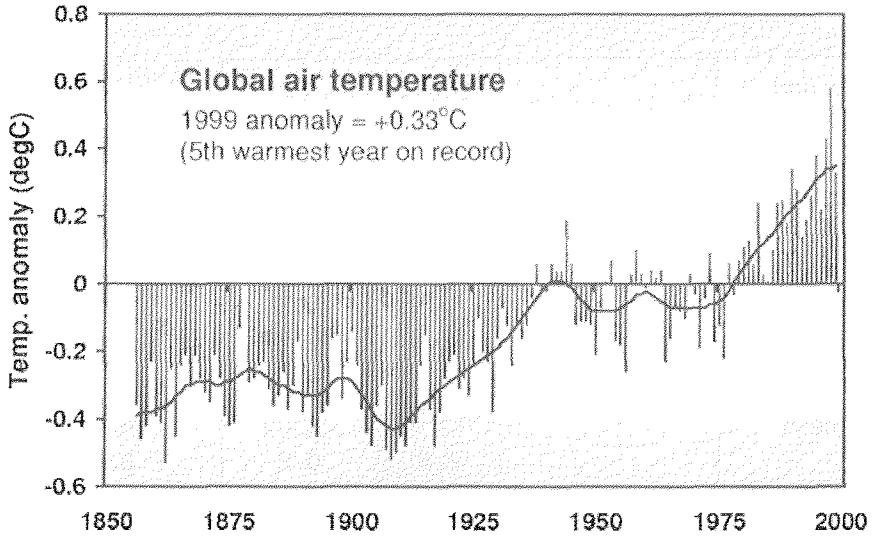

Fig.1. Variations in the average global air temperature since 1850 util 2000 (Climate trends and scenarios. (Http://www. Besis.uaf.edu/ak climate.html)

Paleoclimatological evidence demonstrates that the most pronounced climate changes occurred in high latitudes. For instance, during the Pliocene epoch air temperature in high latitudes exceeded the modern one by up to 14°C, while in the low latitudes it was even less than the modern temperature. During the last interglacial climate optimum (*ca.* 125 ka), when the average annual global air temperature was up to 2°C higher than the modern one, the temperature rise in the Barents Sea reached 5°C. During the Holocene climate optimum (5.5-6.0 ka) the average global temperature was 1°C higher than at present, while in the Arctic regions it exceeded the modern one by 3-4°C.

The expected average global climate warming by 1°C by 2025 allows modeling environmental conditions at the Russian Arctic coasts by analogy with the Holocene climate optimum. At the average annual global climate warming of 1-2°C, temperature increase in the Arctic regions will reach 4-8°C. Steady positive temperature anomalies are already evident in the high latitudes, temperatures exceed the period of 1966-1995 by 2°C. This warming will inevitably result in reduction of ice cover extent in the inner shelf zone and activization of hydrodynamic processes including increasing influence of storm waves over the seabed. Increasing coastal abrasion and, primarily, thermoabrasion lead to enhanced removal of sedimentary matter from land (Pavlidis and Leont'ev, 2000).

Hydrology

Hydrodynamic regime of ***the Barents Sea*** is determined by the system of quasi-stationary and non-stationary currents, tidal and inertial movements, wave processes on the surface and in the water column, vortical formations of various size. Water movement is accompanied by wind-induced sea-level oscillations, horizontal and vertical turbulent mixing (Table 2).

Table 2. Hydrological parameters of the Pechora Sea and adjacent marine regions (Danilov and Efremkin, 1998).

Parameter and phenomenon	Shtokmanovskoe	Pechora Sea	Bayadaratskaya Bay	Northwestern coast of the Yamal Peninsula	Ob-Taz region
1. Sea surface temperature, °C					
Minimum	-1.7	-1.8	-1.9	-1.9	-1.9
Average	2.4	2.8	0.9	–	–
Maximum	8.2	10.9	12.9	8	16.5
2. Sea surface salinity, ‰					
Minimum	34.68	12.67	20.65	0.19	–
Average	34.86	31.55	31.8	–	0–31
Maximum	35.03	33.46	35.44	30.56	–
3. Bottom water temperature, °C					
Minimum	-1.7	-1.7	-1.9	–	0.5
Average	–	0	0.05	–	–
Maximum	0.8	4.0	12.2	–	2.0
4. Tides, relative to the average sea level, cm					
Minimum	-46	-61	-51	–	–
Average	0	0	0	–	–
Maximum	51	83	55	–	–
Amplitude	97	144	106	60–100	50–200
5. Extreme sea level, cm (once in a century)					
Minimum	-86	-170	-106	–	–
Average	0	0	0	–	30–40
Maximum	107	222	167	–	–
6. Current velocity, cm/s					
Tidal	38	38	40	20–30	12–30
Summary	146	123	84	100	80–148
7. Wave height, m (0.1% probabilty)	23.7	9.0–10.0	–	5–7	3–4

The warmest transparent dark blue waters of the Atlantic Ocean with temperature ranging from +4 to +12°C and salinity about 35 come with the North Cape branch of the North Atlantic current. Close to 25°E the current is divided into the coastal branch with a surface velocity of about 40 cm/s and the northern branch with a surface velocity of about 13 cm/s. The coastal current partly deviates to the southeast and flows into the White Sea, while the remaining part flows northeastward and forms the Murmansk current. Near the Northern Kanin shoal, the Kolguev-Pechora branch of the current is formed, which enters the Pechora Sea. The greatest part of the Northern branch of the North Cape current turns to the west and southwest, though a small part keeps the northeastern direction and in the region near 73°N and 30°E is included into cyclonic circulation. Due to considerable inflow of warm Atlantic waters the Barents Sea is one of the warmest in the Arctic Ocean. The greatest part of the North Cape current heat storage (about 90%) is spent for heating the atmosphere. That is why positive temperature anomalies appear over the Norwegian and Barents seas. As a result of thermal and mass-exchange between the ocean and atmosphere cyclones gain additional energy. The environmental conditions hamper freeze-up, and an open-ocean circulation pattern is established. The volume of Atlantic water inflow is estimated at 50–75,000 km^3 per year.

Cold currents flow westward along the Persei rise. Near Nadezhdy Island they form the Medvezhinskoe current with a current velocity of about 50 cm/s. Cold waters of the Litke Current come via the Karskie Vorota Strait (Dobrovol'skii and Zalogin, 1982; Pfirman et al., 1995).

At the convergence of warm and cold currents the North Atlantic polar hydrological front is formed. Its waters are enriched in oxygen and favor bioproductivity growth in this zone. Oceanic polar fronts are global climatic formations, so they have many common features. In the North Atlantic and the Norwegian, Greenland and Barents seas, rather salty (35–36) and warm (10–20°C) water of the North Atlantic current (Gulf Stream) interacts with colder (less than 5–10°C) and freshened Arctic and Subarctic waters of different origin.

In general water circulation is determined by interaction of the two basic opposite currents, the Atlantic and Arctic ones. Warm water enters the Barents Sea with the North Atlantic current, which is the extension of the Gulf Stream, and with its branches, the North Cape and West Spitsbergen currents. The Gulf Stream water is found near Spitsbergen, Novaya Zemlya, North Pole and other areas, thus determining the hydrological regime of the North-European basin (Khimicheskie..., 1997).

Surface water temperature decreases in northeastern and northern directions. In winter, surface water temperature equals +4 to 5°C in the south, +3°C in the central part and falls below zero in the north. In summer, surface water temperature is close to air temperature. In the southern part of the sea, it averages +8 to 9°C, in its central part - +3 to 5°C, and to the north of 79°N temperature is close to the freezing point. The highest surface water temperature all over the Barents Sea is recorded in August. Down the water column a natural delay in achieving the temperature maximum occurs, that is closely related to spatial-temporal variability of the turbulent heat exchange coefficient.

Vertical temperature distribution in the water column almost entirely depends on penetration of warm Atlantic waters, winter cooling and bottom topography. In the southwestern part of the sea, that is strongly affected by the Atlantic waters, temperature smoothly decreases with depth remaining positive down to the bottom. In the north, east, and southeast, the Atlantic water influence is considerably less pronounced. When penetrating these areas Atlantic waters cool down, and their temperature remains negative all the year round. Thus, the Atlantic water masses undergo considerable alteration by colder local waters of the Barents Sea.

In the bottom water layer, the dates of minimal temperature approach differ with space. In the shallow southeastern areas and in the coastal zone minimum heat storage is simultaneous within the whole water column. In deep areas (200–300 m), bottom temperature reaches minimum values in May–June and, sometimes, in July. In the southwestern region and in the areas with water depths exceeding 300 m advection component of thermal balance plays the basic role in seasonal bottom water temperature variations. Therefore, here the annual temperature record may have some extremes with time of approach dependent on interannual advection fluctuations (Khimicheskie..., 1997).

In the polar front zone (60–70° N), hydrological summer begins in June–July and lasts for 2–3 months. Transition seasons, spring and fall, are short and last for less than one month. Structure of the Arctic polar front is determined by sharp (1–2°C/km) temperature gradients, meanders, various vortexes, intrusions of cold freshened waters, and other natural phenomena.

Seasonal thermocline is a typical feature of polar waters. As a rule, it is formed in spring and summer at the depths of 50–100 m. In fall and winter it is destroyed due to surface water cooling in the presence of strong winds. An important condition for the spring thermocline is the presence of a fresh surface-water layer providing initial density gradient near the ice edge and in the nearshore zone of meltwater discharge (Khimicheskie..., 1997).

In summer, different planktic organisms inhabit various water layers: diatoms predominate in mixed waters, small flagellates, Decapoda and Euphausiacea in stratified waters above the thermocline, and dinoflagellates inside the thermocline. The role of temperature in formation of density gradient in the frontal zone increases from summer to winter, while that of salinity decreases. Short-term frontal variability is governed by winds, while seasonal variability depends on a complex of factors including variations in the heat storage of Atlantic waters, ice edge position, and atmospheric circulation pattern (Zabruskova, 1988; Khimicheskie..., 1997).

In ***the Pechora Sea,*** the system of general quasi-stationary circulation is formed by two flows of warm and salty Atlantic waters (Kanin and Kolguev-Pechora), by the White Sea and Pechora discharge currents, and by the Litke current carrying cold waters from the Kara Sea (Gidrometeorologicheskie..., 1985; Gidrometeorologiya..., 1990; Potanin et al., 1985). Transit of the Barents Sea waters to the Kara Sea occurs in the surface water layer. In the Pechora Sea they are essentially transformed and change their thermohaline properties. The Barents Sea and the Atlantic waters are distributed in the intermediate, deep, and bottom water layers.

Velocities and directions of wind currents depend on baric situation and atmospheric conditions. For instance, in summer when cyclonic activity in the Pechora Sea is rather low, wind currents are relatively weak especially in the shallow areas where they are slowed down by friction between water and seabed.

It should be noted that polar front waters in the Norwegian-Greenland basin and Barents Sea are enriched in biogenic elements. Primary production has a well expressed seasonal character. Zooplankton biomass exceeds 500 mg/m^3 in summer, and in some regions reaches even 1000 mg/m^3 and more (Pavshtiks, 1979). The Barents Sea is the most productive northern water basin of Russia due to active light regime of polar summer, favorable geographical position, and penetration of the warm North Atlantic current. Biological and oceanological processes in the sea have a well manifested seasonality because of climatic zonality. The influence of the Atlantic waters as well as taxonomic diversity of flora and fauna decrease eastward.

Waves

Wave activity is one of the basic factors responsible for evolution of the coastal zone and its present-day shaping. Prevailing types of wave activity in the Barents Sea are wind-induced waves and mixed waves produced by winds of changing directions during fast moving cyclones. Therefore, the average wave periods mainly depend on the degree of wind wave activity (Nauchno-metodicheskie..., 1997).

Unlike other Arctic seas, vast areas in the Barents Sea remain ice-free all the year round. In combination with cyclonic activity this results in high frequency of storm waves. In winter, at steady westerly winds the maximum height of waves in the central part of the sea may reach 10–11 m. Close to the coast, the strongest storm waves are related to northerly and northwesterly winds producing up to 8-m-high waves. In summer, frequency of strong waves reduces and equals 1–4% for 5–6-m-high waves and up to 10% for 3–5-m-high waves (Veter..., 1974).

In the Pechora Sea, the most probable twenty-years maxima of average wave heights in the central part equal 4.5 m and decrease down to 4 m in the Karskie Vorota Strait. During ice-free season the length and period of storm waves decrease from the west to the east. In certain coastal areas interaction of waves with strong tidal or discharge currents may give rise to random waves called "crowds". Ice floes smoothen waves by removing secondary elements from their basic surface. Nevertheless, storms in the open sea with drift ice are very dangerous because of ice-floe impacts against boards of ships and mountings of stationary constructions (Table 3).

Table 3. Height (h, m) and period (τ, s) of waves in deep water (>25 m); and wind speed (v, m/s) with different probabilities in some parts of the Pechora Sea during active storm season (October–December).

Ele-ment	Probability, %				Recurrence, time in n years					Recurrence of calms, %
	50	20	5	1	1	5	10	20	50	
69° 10' N, 46° 00' E										
H	1.1	1.8	2.4	3.0	3.5	4.0	4.2	4.5	4.6	31
τ	5.0	6.2	7.2	8.1	8.8	9.1	9.5	9.8	10.1	
V	8.2	12.8	17.5	22.0	25.0	25.0	30.0	32.0	34.0	
70° 30' N, 52° 00' E										
H	0.7	1.5	2.3	2.9	3.5	4.0	4.3	4.4	4.8	39
τ	4.0	6.0	7.2	8.2	8.9	9.7	10.1	10.5	10.7	
V	7.2	12.0	16.6	20.4	22.0	25.0	25.4	25.6	27.7	
69° 50' N, 55° 00' E										
H	0.9	1.5	2.2	3.0	3.5	4.0	4.3	4.5	4.7	39
τ	4.5	6.0	7.1	8.2	8.9	9.7	10.00	10.2	10.7	
V	8.3	12.0	16.6	20.0	22.0	25.0	26.5	27.5	29.0	
69° 40' N, 57° 00' E										
H	0.8	1.4	2.2	2.8	3.3	3.7	4.0	4.3	4.5	39
τ	4.4	5.6	6.6	7.2	7.5	8.0	8.2	8.3	8.3	
V	7.5	12.0	17.2	20.0	25.0	28.5	31.0	32.0	33.0	

Storm activity increase in westward direction is explained by higher frequency of gales in the western areas and presence of ice cover limiting momentum of storm waves in the east. So, the seasonal storm wave heights usually average 7–9 m in winter and 5–6 m in the summer (shipboard records). At the same time, extremely strong gales occur in the eastern areas, too. In October and December 1987, the maximum height of a single wave exceeded 13.6 m in the region north of the Kanin Peninsula (Nauchno-metodicheskie..., 1997). In 1984, under strong steady westerly wind and displacement of ice edge towards "Prirazlomnoe" oilfield in the Pechora Sea the height of a wave exceeded 8 m (Danilov and Efremkin, 1998). Relatively strong wave activity, when water turbidity rises up to 150–200 g/m^3 (at usual values of 50–80 g/m^3), is characteristic for the Pechora Bay (Mikhailov, 1997). Despite predominance of wind-induced short-period waves in the Arctic seas, ripple waves are important relief-forming

agents. This is especially typical for the western Barents Sea where in some years the abundance of ripple waves mixed with wind-induced waves reaches 70–80% (Ionin, 1992).

Ice regime

The first ice observations in the Barents Sea and, accordingly, Pechora Sea date back to the beginning of the 20th century. In 1913–1916 polar stations (Kanin Nos, Bolvanski Nos, Yugorskii Shar, Marre-Sale) were founded in this region, and regular standard meteorological, ice, and hydrological investigations began. In the thirties regular aerial ice observations allowed for obtaining the data on ice-cover distribution for certain winter months and for all summer months. In the same period the basic network of coastal and island hydrometeorological stations was organized. In the seventies and eighties instrumental methods of ice investigation (air survey, radar survey, etc.) were introduced, and regular remote sounding of sea ice with the help of meteorological satellites started. Since 1986, the Arctic and Antarctic Research Institute (AARI) has published weekly complex maps of ice conditions in the Russian Arctic and has created the database on ice-cover distribution with the use of GIS-technologies (Mironov et al., 1998).

Ice regime considerably influences sedimentation and bottom topography in the Arctic seas. Extensive ice fields, drift ice, and grounded ice hummocks ("stamukhi") preserved during the greatest part of the year hamper wave activity. Due to this, in a number of coastal areas an abnormally gentle profile of submarine coastal slope is formed and fine-grained deposits occur in the nearshore zone, which is not typical for inner shelf areas. At the same time, ice cover promotes better preservation of relic landforms and transit of sediments along the shelf edge with further evacuation beyond the shelf limits.

According to estimations (Kaplin, 1971), ice factor limits duration and intensity of wave abrasion. It slows down abrasion-accumulative processes by approximately 3–4 times in the Subarctic, and 7–10 times in the Arctic region, and reduces the total lithodynamic effect.

Sea ice exerts dynamic, thermal, and chemical influence on the coastal-shelf zone. By hummocking and "stamukhi" formation ice removes sediment material from seabed and beaches and forms barriers, furrows, and depressions. According to the data of American researchers (Reimnitz et al., 1972, 1978), ice exaration is evident down to the depth of 75 m. However, only on the inner shelf ice furrows have modern age. They are 1-2 m deep and have typical marginal ramparts.

The chemical impact of ice on the seabed is observed in shallow nearshore areas and lagoons that are almost completely isolated from the sea till the end of winter, when fast ice gains maximum thickness, and the specific local temperature and salinity regime is formed. For example, investigations in neighboring patches within the Sharapovy Koshki Islands (Kara Sea, western coast of the Yamal Peninsula) have shown that in winter under the fast-ice cover strongly mineralized waters occurred in depressions between barriers. Water temperature was about –4.4°C within the depth interval of 0.2–0.5 m (Grigor'ev, 1987).

Low water temperature favors preservation of relict permafrost. Where fast ice adfreezes to bottom grounds new generations of frozen grounds are formed.

Unlike other Arctic seas, the Pechora Sea, as the whole Barents Sea, never becomes completely ice-covered, and about 1/4 part of their area remains ice-free all the year round (Fig. 2). Every year the warm Atlantic waters bring $177{,}369 \times 10^{12}$ kcal of heat to

the Barents Sea (Timofeev, 1960). These waters serve as a natural barrier to ice drifting from the north. Ice inflow from the Kara Sea is insignificant (Table 4).

Ice extent differs from year to year. Its fluctuations are dependent on the intensity of the North Cape current and general climate fluctuations (information databases on the series of observations on ice regime in the Pechora Sea for 50–70 years are available at the AARI).

One prominent feature of ice regime in the Pechora Sea is the presence of only one-year ice during an annual cycle (Mironov et al., 1998). The Pechora drift-ice massif is dynamically active. Ice formation starts at the end of November and ends in March. The average multiannual location of its western margin corresponds to 47°E. During the years of intensive ice discharge, the ice massif is small and occupies the area close to the Novaya Zemlya straits. If discharge is absent under prevalence of easterly and northeasterly winds, the ice massif grows to a size of several times bigger, and its margin shifts westward close to the Kola Peninsula. In the southwest the ice massif feeds ice to the drift ice flow from the White Sea. The total amount of the White Sea ice is about 6.7 km^3 (Zubakin, 1998).

Input of ice (average multiannual data) from the Kara Sea equals 4.6 km^3 being far less than ice discharge from the Pechora Sea through the Karskie Vorota Strait (21,4 km^3) (Mironov et al., 1998).

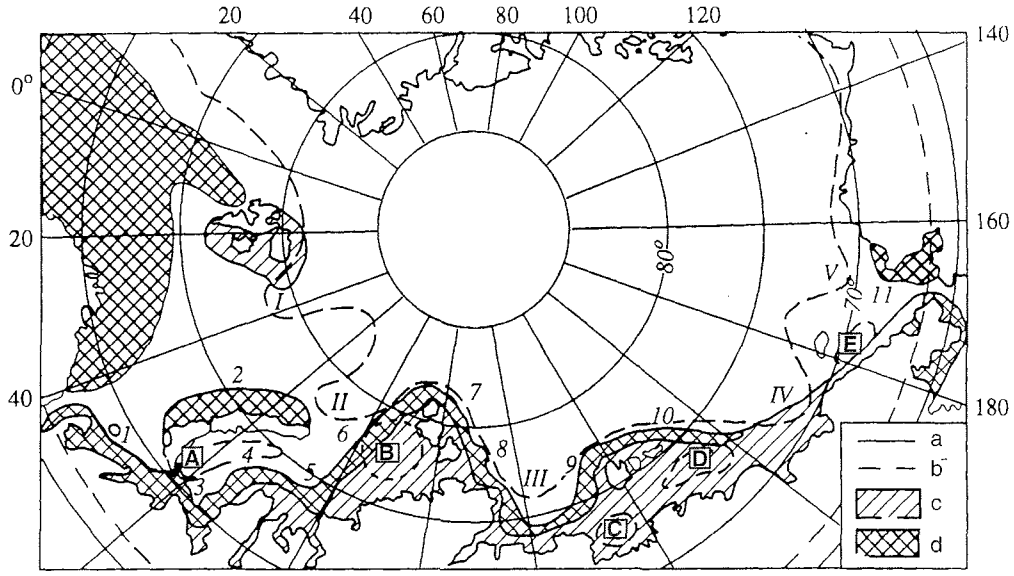

Fig. 2. Arctic Ocean ice cover (Severnyi Ledovityi ..., 1985):
a - ice margin in winter; b - ice margin in summer; c - fast ice; d - polynyas
(1-Pechora, 2-Western Novaya Zemlya, 3-Amderma, 4-Yamal, 5-Ob'-Yenisei, 6-Western Severnaya Zemlya, 7-Eastern Severnaya Zemlya, 8-Taimyr, 9-Lena, 10-New Siberian, 11-Alaska.
Branches of oceanic ice fields: I - Spitsbergen, II - Kara, III - Taimyr, IV - Aion, V - Chukotka. Local ice fields: A - Novaya Zemlya, B - Severnaya Zemlya, C - Yana, D - New Siberian, E - Wrangel.

River runoff has a warming influence on coastal ice conditions. In the Pechora Bay fast-ice freeze-up occurs later than the Pechora River freeze-up (second half of November).

Fast-ice break-up follows the river-ice break-up. Thermal river runoff plays an essential role in fast ice break-up. The estuarine polynya appearing at the river mouth rapidly grows in direction of the river runoff spreading. The rate of ice-edge displacement is about 3–5 km/day. The average ice thickness is up to 90 cm. Ice melts away at the end of June - beginning of July (Mikhailov, 1997).

Table 4. Ice parameters and phenomena in the Pechora Sea and adjacent areas of the Barents-Kara region (Danilov and Efremkin, 1998).

Parameter and phenomenon	Shtokmanov-skoe	Pechora Sea	Bayadarat-skaya Bay	Northwestern coast of Yamal Peninsula
1. Beginning of ice freeze-up, date				
early	XII	25.X	5.X	28.IX
average	IV	18.XI	17.X	7.X
late	V	23.XII	2.XI	30.X
2. Fast ice freeze-up, date				
early		23.XII	7.X	6.X
average		22.II	1.XI	5.XI
late		11.IV	4.XI	30.XI
3. Beginning of fast ice break-up				
early		5.IV	12.VI	21.VI
average		23.V	7.VII	
late		7.VII	21.VII	24.VII
4. Total disappearance of ice cover, date				
early	25.III	10.IV	12.VI	29.VI
average	29.V	19.V	4.VIII	5.VIII
late	7.VII	30.VIII	26.IX	5.IX
5. Duration of ice-covered season, days				
minimum	0	131	239	
average	45	213	300	300
maximum	186	272	365	
6. Fast ice				
extent, km		3–15	5–20	15
average thickness, cm		110	140	150
7. Drift ice				
thickness, cm				
average	150	80	100	90
maximum		145		
size of ice fields, km				
average	1.4	1.4	0.5–2.0	1.2
maximum		17.5		
continuity, units	7–8	10	9–10	9–10
hummocks, %	60	60–90	60	60
mass of hummocks, 10^3 tons		47–130	168	
8. Seabed exaration (observations), m			1–2	< 0.5

The calculated maximum ice thickness in the Pechora Sea that could be achieved once in N years is given below (Gudoshnikov et al., 2003).

Number of years	Maximum ice thickness, cm
5	110
10	120
25	130
50	138
100	145

Zones of intensive hummocking are located in the southeastern Pechora Sea and in the Karskie Vorota Strait.

Icebergs are one of the most dangerous natural phenomena. Glaciers of the archipelagoes of Spitsbergen, Franz Josef Land, Novaya Zemlya, and Severnaya Zemlya are potential sources of icebergs in the Barents Sea. Spitsbergen has the greatest ice stocks where approximately 30% of the whole volume of glacial ice of all Eurasian Arctic islands is concentrated. Ice storages of the Northern Novaya Zemlya Island and Severnaya Zemlya Archipelago rank second. Ice stocks of the Franz Josef Land are by three times smaller than those of Spitsbergen. It should be noted that in winter icebergs usually concentrate near the centers of their formation. In spring, during the fast-ice break-up icebergs begin to drift offshore. Sometimes in June they drift as far as the Norwegian and Kola Peninsula coast. Abnormal distribution of icebergs in the southern Barents Sea was recorded in 1989 when they were observed to the north of the Kanin Nos Cape (Nauchno-metodicheskie..., 1997). During one hundred years of observations (1888–1991) icebergs in the southeastern Barents Sea were marked 11 times. Calculation of extreme values has shown that at sea routes westward from Kolguev Island icebergs could be met 5 times in 100 years (Mironov et al., 1998) (Table 5).

Table 5. Statistic characteristics of the linear size (m) of above-water parts of icebergs in the Barents Sea, cruise observations (Nauchno-metodicheskie..., 1997).

Statistic characteristic	Length	Width	Height
Arithmetical mean	64	46	11
Mode	54	35	6,5
Root-mean deviation	38	33	6
Factor of variation, %	62	71	58
Maximum	180	160	30
Minimum	5	5	5
Range	175	155	25
Series, length	97	38	87

The environmental conditions established by the beginning of the Subatlantic period, ca. 2.7 ka, could be referred to as relative cooling (in comparison with the Holocene climate optimum). Ice cover extent increased in both the Arctic seas and North Atlantic. Considerable cooling in the Arctic regions between 860 and 1800 was followed by gradual warming, and during the last 200 years ice cover in the Arctic basin has been essentially reduced. The electronic version of ACSYS Forecast journal (1998) published by the International Center on Arctic Climate Systems Study (ACSYS) contains archival data on location of the drift ice fields in the Western Arctic regions at the end of the 19th century (1881) in April, July and September. Comparison of archival data and modern satellite images provides evidence for significant reduction of ice fields in the spring-

summer period. The greatest reduction of ice fields in the Norwegian and Barents seas (1997 against 1881) is especially evident for April. In the 19th century at this time of the year the southern ice limit stretched from the Kola Peninsula coast and the North Cape to the southeastern coast of Iceland, while in 1997 the whole southwestern Barents Sea, from Novaya Zemlya to the southern Spitsbergen, remained ice-free (Pavlidis and Leont'ev, 2000) (Fig. 3).

Hence, at present climate and ice conditions of the Arctic regions are gradually becoming as warm as their warmest analogues observed during the "Atlantic optimum" of the Holocene 5-7,000 years ago.

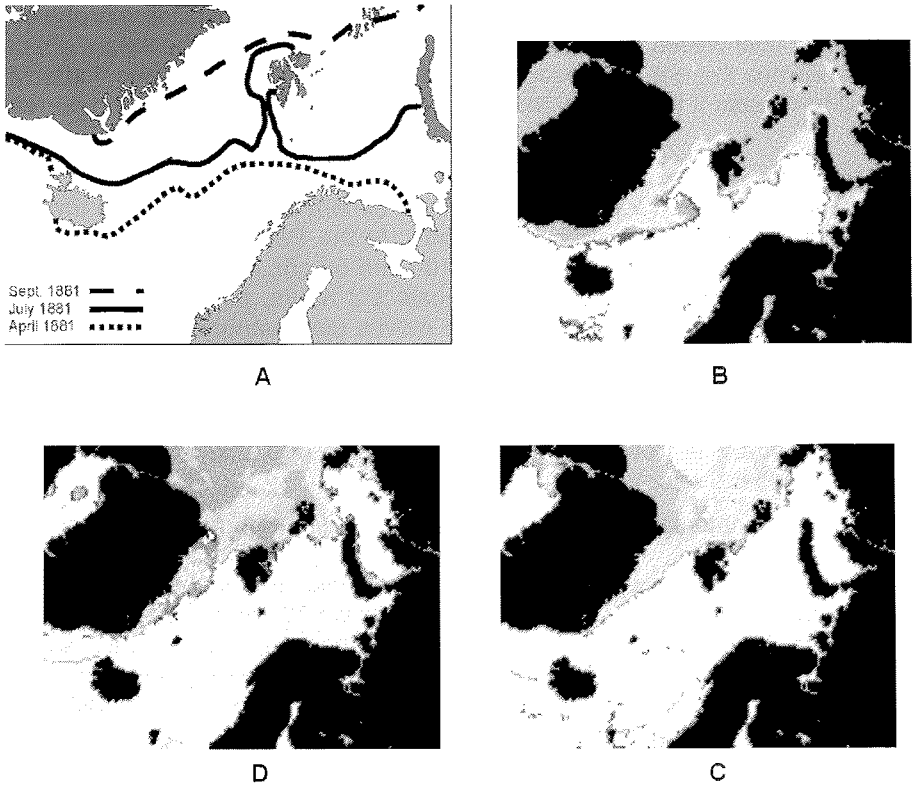

Fig. 3. Drift ice margin in Western Arctic in April, July, and September 1881 (A) (R.Colony and T.Vinje, 1998, (www.npolar.no/acsys/jan98), and ice conditions in Western Arctic in April, July, and September 1997 (B, C, D) (space images). (Sea Ice Analysis History Page. http://polar.wwb.noaa.gov/seaice/Historical.html).

Tides

Tidal currents belong to non-stationary quasi-periodical movements. They are especially active within the coastal zone, in straits and gulfs. Sometimes their velocity reaches

160-250 cm/s. Velocity of tidal currents strongly depends on the moon phases. It grows during syzygy and reduces during neap.

In ***the Barents Sea*** tides are mainly caused by the eastward moving Atlantic tidal wave, that reaches Novaya Zemlya. To the west from the Matochkin Shar it turns to the northeast and, partly, to the southeast. Northern areas are affected by the tidal wave coming from the Arctic Ocean. This produces interference of the Atlantic and northern tidal waves at the northeastern Spitsbergen coast and at Franz Josef Land.

Tidal fluctuations in the Barents Sea have regular semidiurnal character. The strongest tidal currents are marked along the Murmansk coast, at the entrance into the White Sea, on the Kanin and Southern Spitsbergen shallows. Near the Murmansk coast, the tidal sea-level rise reaches 6 m, near Spitsbergen 1–2 m, and near Franz Josef Land – 0.4–0.5 m. Such differentiation results from bottom topography, coastline morphology, and interference of tidal waves. East and north of the Kola Peninsula the height of tides decreases. Sometimes there is not enough time to fill some narrow bays and fiords with tidal water and to release it from them, therefore, the level gradient and strong currents are formed.

In ***the Pechora Sea,*** syzygy tidal currents velocity is 1.5 to 2.5 times greater than that of neap tidal currents. The tidal wave approaches the Pechora River mouth from the west and moves along the Gulyaevskie Koshki Islands. At the Pechora Bay entrance the average, syzygy, and neap tides are about 80, 100 and 58 cm, respectively (Mikhailov, 1997). The tide is asymmetrical: rising tide equals 5.3 hours, falling tide equals 6.7 hours. During summer low water, the tide wave moves upstream the river for 160 km. The limit for the upstream movement of tidal wave is about 190 km, while the minimum one – during high water – is only 10–15 km. Tidal currents determine water exchange between the Pechora Bay and the sea. The total tidal water discharge through the Gulyevskie Koshki straits is tremendous and reaches 162,000–258,000 m^3/s. Current velocities in the straits are about 2 m/s.

The calculated tidal deviations from the average sea-level are non-uniform and increase from the open sea (50 cm) towards coastline (up to 150 cm). Wind-induced sea-level rises have the following values and frequencies: once a year the rise reaches 20 to 30 cm; once in 5 years 45 to 147 cm; once in 10 years 50 to 172 cm; once in 25 years 60 to 205 cm; once in 50 years 60 to 230 cm. Seasonal sea-level falls are the following: once a year - 10 to 40 cm; once in 5 years – 40 to 95 cm; once in 10 years – 40 to 100 cm; once in 25 years – 45 to 120 cm; once in 50 years – 45 to 130 cm (Mikhailov, 1997).

In order to obtain the data on sea-level fluctuations in the open Pechora Sea tide gauges were deployed in August 1998 at two sites located at a distance of about 8 miles (13th cruise of RV "Akademik Sergei Vavilov", stations 1092 and 1093). The tide gauges measured time-dependent changes of bottom hydrostatic pressure. Water depths at the sites were 13.4 and 13.0 m, respectively. Two tide gauges per site were fixed on a vertical bar at a distance of 1 m above the seafloor. Both tide gauges recorded distinct sea-level oscillations (Table 6). Semidiurnal periodicity (about 12 hours) with variable ranges was dominant. Unequal ranges of the two successive semidiurnal fluctuations point to the presence of tides with daily periodicity. The estimated range of daily fluctuations was 5 to 15 cm; that of semidiurnal fluctuations 70 to 115 cm.

Table 6. Maximum range of sea-level oscillations.

Datum mark	H, cm	Datum mark	H, cm
Mikulkin Cape	577	Konstantinovskii Cape	469
Indiga	399	Varandei	399
Sengeiskii Shar	287	Belyi Nos	406
Tobseba	338	Bugrino	348
Bolvanskii Cape	469	Belush'ya	181

River runoff

The river runoff to the Barents Sea equals about 163,000 km^3/year (Romankevich and Vetrov, 2001). The Pechora River brings approximately 90% of the total river runoff to the Pechora Sea. Its average multiannual discharge at Oksino (141 km from delta margin) is 4120 m^3/s. On average, the Pechora River delivers about 130 km^3 of water every year. In terms of river runoff, it is one of the largest rivers in Russian Arctic after the Yenisei (597 km^3/year that makes 31.9% of the total river runoff into the Russian Arctic seas), Lena (530, 19.4%), and Ob' (402, 14.7%). The length of the Pechora River is about 1810 km, its catchment area is 322,000 km^2 (Mikhailov, 1997; Romankevich and Vetrov, 2001). Interannual distribution of runoff is extremely non-uniform (Table 7).

Table 7. Interannual distribution of river runoff in the Pechora River delta head (Mikhailov, 1997).

month	I	II	III	IV	V	VI	VII	VIII	IX	X	XI	XII	year
km^3	778	609	522	1080	11200	16700	5390	2660	3480	3850	1970	1150	4120
%	1,6	1,2	1,1	2,2	22,7	33,8	10,9	5,4	7,0	7,8	4,0	2,3	100

More than 67% of the annual runoff is discharged during spring flood (May–July) and more than one third of this (34%) in June. The spring flood often has two stages – the main ("spring") and later ("usinskaya" when the meltwater runoff from the Usa River comes).

Distribution of the runoff among the main branches of the Pechora delta is given in Table 8.

At transition from high to low water the share of runoff through most lateral branches decreases. When runoff is low, practically no water flows through small branches. This regularity results from the presence of one deep-water passage to the Pechora Bay through the Big Pechora and extreme shallowness of the small branches.

Maximum water levels in the mouth are related to the flood wave passing. The level rise is redoubled by ice blocking and reaches 8–9 m in the delta head and about 5 m near Nary'an-Mar.

Table 8. Distribution of the runoff among the main branches of the Pechora River delta (100% corresponds to the total runoff at the delta head, data for 1977–1980) (Polonskii, 1984).

Branch, transit point	%
Delta head	
Pechora, Oksino	95,5
Golubovskii Shar, source	4,2
Gorodetskii Shar, Nar'yan-Mar	4,5
Pechora, Bol'shaya Sopka	91,3
Small Pechora, Bol'shaya Sopka	48,6
Big Pechora, Bol'shaya Sopka	42,7
Andega unit	
Small Pechora, Bol'shaya Sopka	48,6
Utcher (Tndrovyi Shar), source	5,5
Krestovyi Shar, source	1,2
Srednii Shar, source	17,5
Mesin, Mesino	24,4
Lower reaches of the Big Pechora	
Big Pechora, Koryagovka	75,2
Glubokii Shar, source	4,2
Kamennyi Shar, source	1,2
Nevolin Shar, source	4,9
Big Pechora, mouth	64,9

The average multiannual solid discharge in the mouth is 8.5 million t/year. Ninety percent of this flux passes during flood. The average water turbidity is 65 g/m^3. Ionic discharge equals 67.5 mg/l (Romankevich and Vetrov, 2001). Suspended matter content in the surface water layer is about 1.5-5.0 g/m^3 (Mikhailov, 1997).

It should be noted that though the total water river runoff to the Arctic Ocean is tremendous, turbidity of riverine waters is low. So, the total solid discharge of the 11 biggest northern rivers equals about 110 million t/year, which is approximately 5 times less than solid discharge of the Mississippi River solely. Due to differences in water runoff and turbidity, the total particulate matter flux into the Russian Arctic seas differs from the liquid river runoff values: the Laptev Sea receives 31.4; the Kara Sea 27.3; the East Siberian Sea 27.4; the Barents Sea 10.5, and the White Sea 6.0 million tons per year (Table 9).

Table 9. River discharge against the area and water storage of the sea (Romankevich and Vetrov, 2001).

Sea	Sea area, 10^3km^2 (_)	Water storage, 10^3km^3 (B)	Suspended matter discharge, 10^6 tons/year (C)	Specific suspended matter discharge	
				Total discharge against the sea area, g/m^2 per year (C/_)	Total discharge against water storagre, g/m^3 per year (C/B)
White	90	6,0	6,0	66,7	1,0
Barents	1424	316	10,5	7,4	0,03
Kara	885	98	27,3	30,8	0,28
Laptev	663	353	31,4	47,4	0,09
East Siberian	913	49	27,4	30,0	0,56
Chukchi	582	45,4	-	-	-

The area of freshening in the Pechora Bay depends on the runoff. During summer low water, the zone of riverine and sea water mixing is located within the bay. The average width of the mixing zone is about 50–60 km. Seawater salinity is about 33. During flood, the mixing zone spreads beyond the limits of the Pechora Bay and stretches offshore into the Pechora Sea. In this case, seawater salinity at marine side of the Gulyaevskie Koshki Islands drops down to 0. The average water salinity at Varandei and Khodovarikha during summer low water is 24, while in winter it reaches 35 (Mikhailov, 1997).

The bay penetrates far inland for more than 150 km. It is shallow even in its deepest part in the east. Only in a number of deltaic channels there are erosive trenches with depths of up to 15 m. At present they are probably deepened by reversal tidal currents. It should also be noted that the Pechora Bay is a relict estuary. It was shaped by erosive processes aging back to Tertiary times. Wide distribution of accumulative terraces at the heights of 46-66, 16-29, 8-12, and 3-5 m usually composed of alluvial-marine deposits evidences that coastal land was not subjected to exaration and accumulative impact of the Late Pleistocene ice covers. During the Pleistocene epoch, erosional and accumulative fluvial processes and sea-level oscillations repeatedly affected this territory.

The basic tendencies in the modern development of the Pechora River mouth is silting and gradual disappearance of small western channels, silting of the delta and Korovinskaya Inlet, protruding of the Big Pechora fan, and further consolidation of the coastal barrier – the Gulyaevskie Koshki Islands.

Some time ago it was proposed to transfer part of the Pechora runoff (about 13–30 km^3/year) to the Volga basin with artificial reduction of the natural runoff by 10–13%. For the Pechora River mouth, negative consequences of water transfer would obviously outbalance the positive ones. The only positive consequence is reduction of delta silting in spring. The main negative consequence is salinization of the Pechora Bay and increasing inflow of salt water into the river channels.

Recently the region has become exposed to intensive anthropogenic impact. In this connection it should be noted that changeable ecosystems of the river mouth are extremely vulnerable. Negative ecological consequences are marked not only in the areas of hydraulic engineering constructing, but also on adjacent territories including deltas and estuaries. Water transfer and regulation of river runoff result in reduction of deltaic flood-plain area, silting of the deltaic branches and channels, enhanced inland penetration of tidal wave, strengthening of storm wind-induced surges, coastal abrasion, degradation of soil cover, impoverishment of fish populations, etc.

Geology

The Pechora Sea shelf occupies the submarine continuation of the Timan-Pechora Epibaikalian plate and is completely located within the limits of the continental crust. It is not a typical shelf basin because one of the three zones characteristic for shelves with platform geotectonic regime is absent here, namely the outer one. At the same time, the inner (down to the depth of 20 m) and middle shelf zones are well expressed. From the east and north, the shelf is bounded by the Hercynian mountains of the Novaya Zemlya and Pai-Khoi. In the west it is linked to the Central (sometimes called Southern) Barents Sea depression by the system of faults of the Kurentsovskaya structural terrace. The depression includes an area with suboceanic crust distinguished by increased thickness of sediment cover (up to 24 km). Submarine structures of the Baikalian folding structures, the Timan ridge, bound the shelf from the southwest. According to geothermal data (thermal flux measurements), the thickness of the lithosphere within

the Pechora shelf is 190 km. The mantle, basalt, and granite layers have thicknesses of 160, 15, and 15 km, respectively (Verzhbitskii, 2001).

Geological shelf sequence (Fig. 4) consists of three groups. The lower one is represented by heterogeneous rocks of different ages forming the fold-blocky basement that became stable about 650-550 million years ago. Its surface is covered by metamorphic complexes and folded sedimentary strata formed by the Baikalian and Hercynian tectonic activity and also by epiplatform stirring up of the Earth's crust. The depth of the basement submergence under the sedimentary cover load reaches 8 km (Korobkin and Boiko, 1999). The middle group is represented by platform deposits, mainly the Early Paleozoic-Early Permian carbonate sediments with a thickness of up to 4 km. This unit is subdivided into the Epibaikalian and Epihercynian subunits according to tectonic cycles. The inner structure of the group has not yet been investigated in detail. The upper group consists of terrigenous Late Permian – Cenozoic deposits represented by shelf formations that reflect structural isolation of the Arctic geodepression whose syn-oceanic development began at the Early-Late Cretaceous boundary.

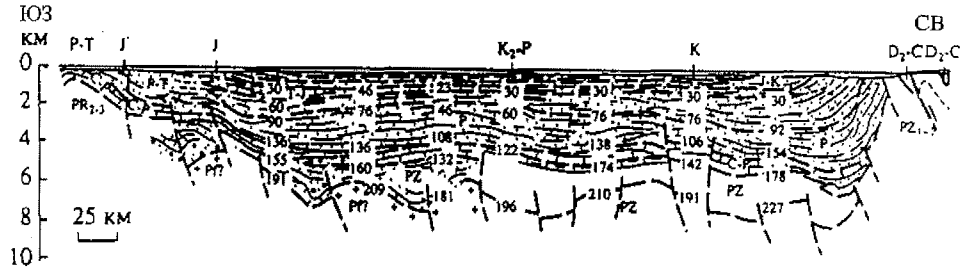

Fig. 4. Geological-geophysical profile of the northwestern Pechora Sea and temperatures of sediment cover, in °C (Verzhbitskii, 2001).

The group is subdivided into four structural subgroups: Late Permian–Triassic (pre-oceanic), Jurassic–Early Cretaceous, Late Cretaceous (both transitional to sin-oceanic), and Oligocene-Quaternary (syn-oceanic). By analogy with the adjacent areas of the Barents Sea shelf it is possible to subdivide the last subgroup into several sedimentary complexes: Oligocene–Miocene lacustrine-alluvial complex corresponding to regressive conditions, Pliocene-Quaternary complex with sediments of marine, glacial, and glacial-marine origin reflecting transgressive-regressive conditions, and Late Pleistocene–Holocene deposits evidencing transgressive conditions. The Quaternary deposits consist of continental and terrigenous-marine high-latitudinal sediment facies. Some researchers think that the natural cyclic spatial-temporal succession of rift complexes by plate deposits is characteristic for the general process of regional sedimentary cover formation. The main phase of the Earth's crust destruction in the region is dated by the Middle (?)–Late Devonian (Shipilov, 1993).

The thickness of the Quaternary deposits on the shelf ranges from zero up to tens of meters (Figs. 5-7). The thickness of the Holocene deposits sometimes is close to 10 m, but averages 0.1-5 m. Depending on local conditions, deposits are represented by clays, sands, silts or polygranular sediments.

The Quaternary deposits of the southeastern Barents Sea are well enough investigated seismoacoustically (AMIGE and MAGE, Murmansk) and geologically (drilling carried out by AMIGE). Most researchers suggest subdividing the Quaternary deposits into three seismoacoustic complexes separated by unconformities (Chistyakova, 1997).

III-d seismoacoustic complex, Upper Valdai moraine, is characterized by massive mainly chaotic type of seismoacoustic record. It occurs throughout the whole area and dominates in the sequence. It has an even subhorizontal base and uneven ridge-like top. Glacial deposits compose this complex. Their age is determined as the Late Valdai since they represent the basement of last glacial cycle. However, it probably incorporates relics of more ancient moraines as evidenced by occurrence of internal boundaries.

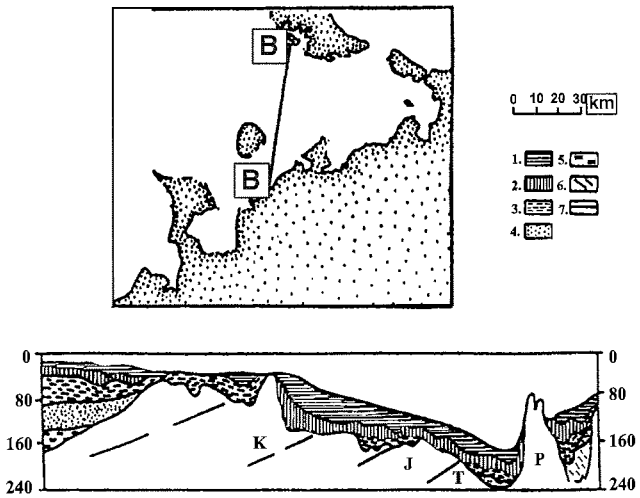

Fig. 5. Seismo-stratigraphic section of loose sediment unit. Key: Sediment seismostratigraphic (sedimentation) complexes: 1 Upper Pleistocene Holocene; 2 Upper Pleistocene; 3 Upper-Middle Pleistocene; 4 Lower-Middle Pleistocene; 5 Lower Pleistocene; 6 pre-Cenozoic deposits; 7 boundaries of sediment complexes.

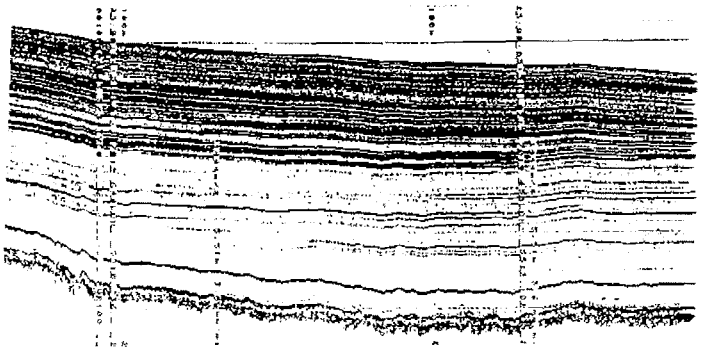

Fig. 6. Fine bedding of Quaternary sediments in the Southern Novaya Zemlya trench.

II-nd seismoacoustic complex, Lateglacial deposits, occurs in the form of lenses filling depressions of the III-d seismoacoustic complex. Deposits of this complex have a basin-like character of accumulation covering all roughnesses of the underlying morainic deposits. Their thickness reaches 30-40 m. The complex is dated to 12.7-9.4 ka. Sediment composition studied in many cores is represented by flat-bedded, sometimes rhythmic-bedded, clays, clayey silts, and, rarely, clayey-silty sands. Sediments have characteristic brown and brownish grey coloring, that sharply distinguishes them from greenish grey deposits of the Holocene sea basin.

I-st seismoacoustic complex is represented by stratified **Holocene deposits** (not older than 9.4 ka). In the coastal zone they consist of sands and silts with a thickness of up to 5-10 m. Farther offshore they are represented by silty-clayey deposits (up to 2-3 m thick). Diagenetic mineral transformations in the form of various hydrotroillite accumulations are marked in the Holocene beds. An up to 65-70 m thick body of the Holocene deltaic and prodeltaic deposits of the Pechora River is traced to the east from its mouth. Distribution of surface sediments is shown in Fig. 8.

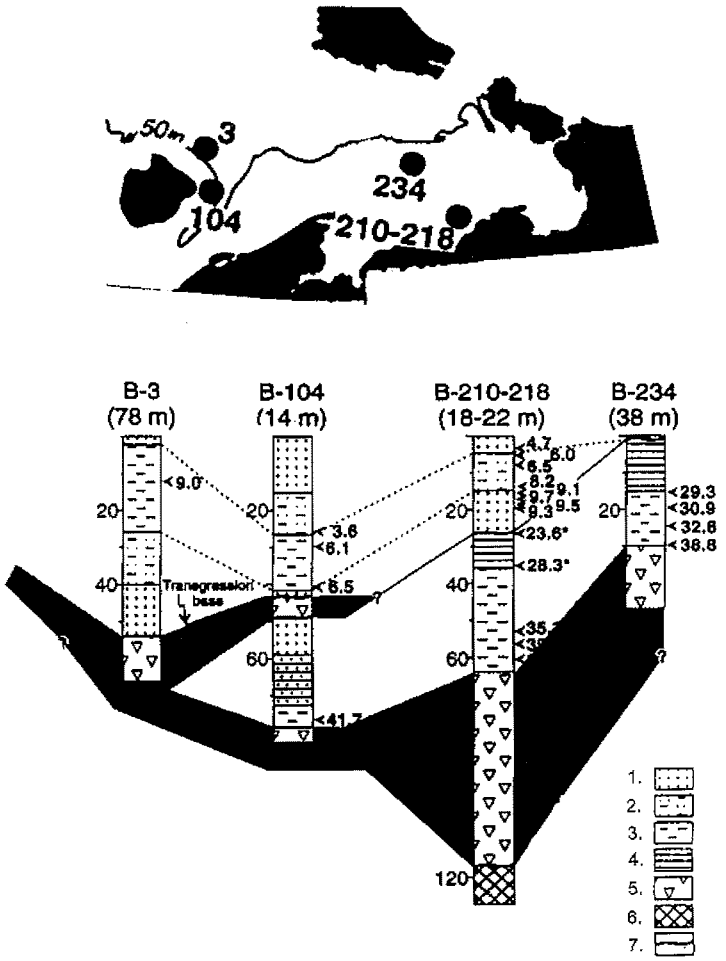

Fig. 7. Location of boreholes and core sections (Polyak et al., 2000).

However, some researchers do not agree with this opinion about the structure and origin of the Quaternary deposits. The basic disagreement concerns the role of the Valdai glacial factor. Field investigations carried out by the Institute of Oceanology RAS have shown that glacial activity in this area was insignificant, and the Pechora Sea shelf was mainly covered by arctic tundra (Pavlidis et al., 1998; Avenarius and Dunaev, 1999).

There is not much evidence about permafrost deposits on the Barents Sea shelf (Figs. 9, 10).

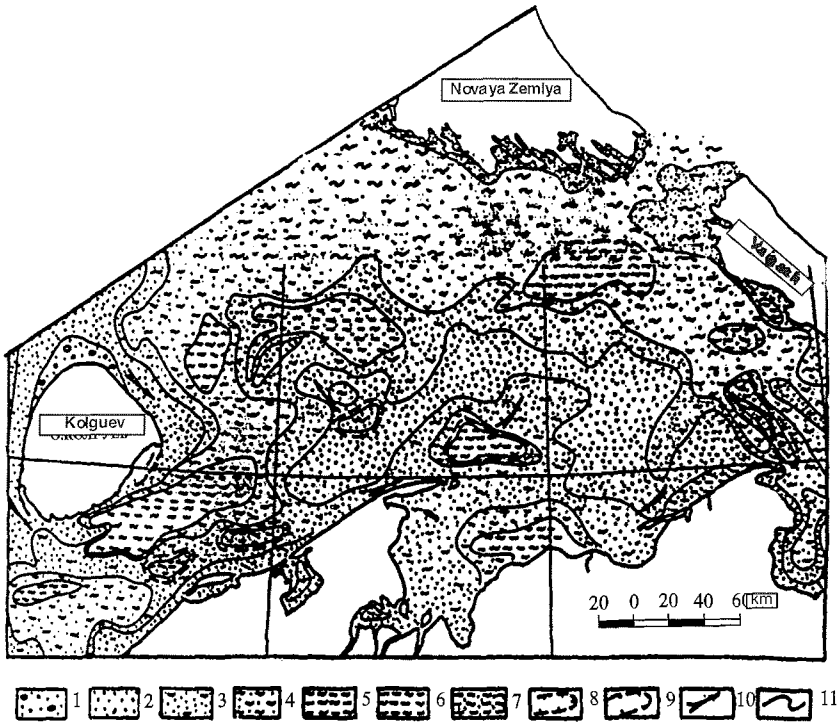

Fig. 8. Bottom grounds (Ekosistemy..., 1996 with additions).
Key: 1 - sand-gravel-pebble sediments; 2 - sands; 3 - silty sands; 4 - sandy silts; 5 - pelitic silts; 6 - silty pelites; 7 - sand-silt-pelite sediments; 8 - bottom abrasion of Pleistocene beds; 9 - bottom abrasion of Paleozoic beds; 10 - directions of sand and silt transportation; 11- lithologic boundaries.

Within the limits of the Pechora shallow their thickness may reach 30 m, and their top is located 25 m below the seafloor. In the Kolguev Island laida, permafrost base runs along the depth of 10-20 m. However, taking into account low heat flux on the Arctic shelf ($\approx$1-1,5x1%$^{-3}$ cal/cmxsxdegree) and short-term postglacial period in the Barents Sea, there could probably be other places with relict permafrost. According to Mel'nikov and Spesivtsev (1995), perennially frozen grounds and, also, relict permafrost lying in the depth range between 25-40 and 50-100 m below the seafloor are typical for the Pechora Sea. It is supposed that the modern submarine cryolithozone could be formed on the Arctic shelf within water depths of 0-2.5 and 40-150 m (Rozenbaum and Shpolyanskaya, 1998).

Different opinions exist about tectonic structure and the character of tectogenesis of the Pechora shelf (Aksenov et al., 1987). Recent evidence (Senin, 1993) suggests that since the end of the Baikalian stage the regime referred to as metoplatformian has been established in the Barents Sea-Pechora Sea region. This area has been separated from the continent since the Late Mesozoic and in the modern structural plan represents a pericontinental mobile platform bounded by flexures and faults of continental slopes from the west and north, by the Caledonian and Baikalian folded structures from the south, and by the Hercynian-early Cimmerian structures from the east. It is noted that

the structure of the upper stage is rather independent from the tectonic plan of the basement. Riftogenesis plays an important role in development of the region. There are no reliable data on the relation of its tectonic structure to horizontal movements of lithospheric plates (Mitrofanov et al., 1998).

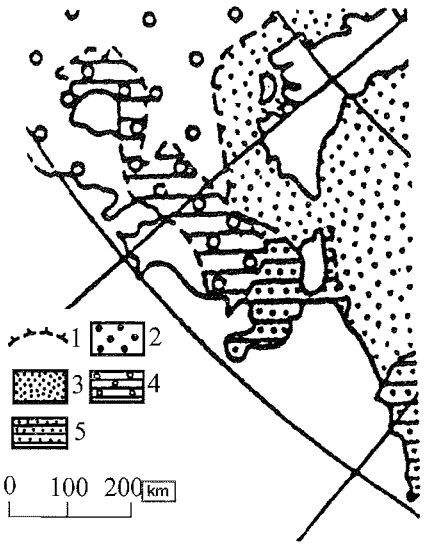

Fig. 9. Schematic map of the cryolithozone (Osnovy..., 1996).
Key: 1 shelf boundary; 2 area of positive water temperatures; 3 mainly unfrozen cryolithozone with cryopegs; 4-5 relict insular permafrost within the area of (4) positive bottom temperatures and (5) cryopegs.

In recent times the shelf has gained its modern borders. It replaced an epicontinental sea that adjoined the Central-Arctic rise. Re-arrangement of the former structural plan occurred. The latter was predetermined by platform geological structure formed in the post-Baikalian time and further evolution in the Late Mesozoic-Cenozoic. Structural forms include depressions, troughs, rises, terraces, archs, etc., often complicated with folds and faults. At that time, new block associations and relationship between faulting zones were created by selective activation of more ancient structural fragments. The biggest structural forms reflected in bottom topography correspond to the structural plan of the sedimentary cover sole and basement. Peculiarities of the modern structural plan are discussed in several publications (Geologicheskoe ..., 1984; Makhotina, 1982; Musatov, 1990).

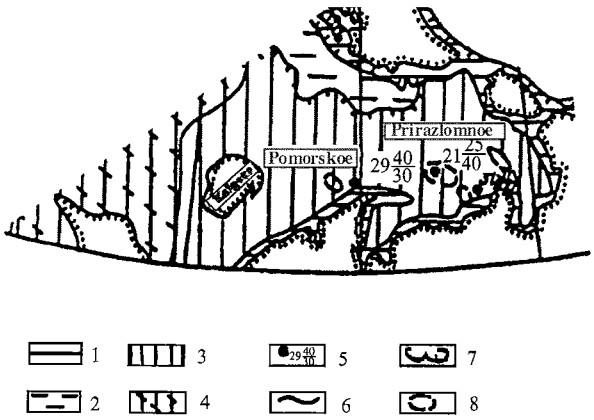

Fig. 10. Map of geocryological zonation (Mel'nikov and Spesivtsev, 1995). **Key**: 1-4 - geocryological regions: 1 - continuous freezing during the Pleistocene: permafrost sediments of submerged continental and abrasion types developed along abrasion coasts and, partly, along stable ones, 2 - freezing during the Late Pleistocene: insular permafrost with permafrost top located at the depths of 15 to 40 m, 3 - continuous distribution of 0 to 50-m-thick perennially cooled sediments, 4 - post-cryogenic sediments with positive temperature; 5 - boreholes penetrating permafrost sediments (figures: at the left water depth, m; numerator depth of permafrost top, m; denominator depth of permafrost base, m); 6-8 - boundaries of: 6 - neocryologic regions, 7 - paleoland; 8 - perspective oil and gas fields.

There is no agreement among geologists regarding the timing of neotectonic stage in this sector of the Arctic, that is dated to the end of Oligocene, Miocene, Late Miocene, Middle Neogene, Late-Middle Pliocene boundary, the end of Pliocene (Matishov, 1984; Makhotina, 1982; Zarkhidze, 1985). Study of paleomagnetic anomalies suggests Early Oligocene age for the cardinal reorganization of geological conditions in this region (Savostin, 1981). It correlates with deformations of the youngest regional peneplanation plane, that was formed, by analogy with adjacent hinterland, during the Paleocene-Eocene. As applied to subaquatic conditions, the beginning of neotectonic stage could be correlated with formation of the Thule basaltic province in the Barents Sea. Comparison of the elevations of the peneplanation plane fragments with the modern sea level enabled estimating amplitudes of neotectonic movements. One variant of neotectonic scheme (Musatov, 1990) is based on elevations of the lower boundary of the Neogene-Quaternary deposits. Musatov (1990) considers the modern shelf structure to have sub-latitudinal zonality, while in the pre-Quaternary period the latter was sub-longitudinal. The main neotectonic process implies destruction of the Earth's crust and subsidence of inner shelf. The general tendency of tectonic movements is the replacement of differential movements with small amplitudes by less differential ones but with greater amplitude. Most mappable rises are the result of their slower subsidence in comparison with adjacent seafloor areas and could be, therefore, referred to as relative ones. Some researchers consider neotectonic movements to be oscillatory, since the investigated sediment sequences are rhythmic. Others trace a wavy character of these movements because of the eastward reduction of tectonic activity in the Paleogene, and the southward reduction in the Neogene-Quaternary time. Recent tectonic activity is emphasized by relatively high differentiation of structural

forms, considerable total amplitude of vertical movements, etc. Nevertheless, the region as a whole is considered to be isostatically balanced. The general trend of the Holocene epoch is subsidence.

From the seismic point of view the area is stable. The estimated potential seismotectonic danger is less than magnitude 3.9 – the lowermost value recorded by the most closely located seismic stations (Assinovskaya, 1994).

Morphostructural analysis of the shelf area allows distinguishing between positive (vaults, rises, archs), negative (depressions, troughs, trenches), and transitional (terraces) diamorphs (structural forms) along with different lineaments identified as dislocations, that are an important criterion of the tectonic structure organization. An example of structurally dependent relief is given in Fig. 11, and an example of morphostructural zonation in Fig. 12. Recent morphostructural elements of the shelf are usually shown as a group with northwestern strike following tectonic zonality typical for this area (Takki and Buivolenko, 1976). Our investigations have shown that from the Timan-Kanin Ridge and further northward to the western edge of the Southern Novaya Zemlya Trough the recent morphostructural elements have northwestern strike. However, to the east of this zone, the morphostructural plan expressed in neotectonic ridges, furrows, depressions, and rises gains northeastern strike. Farther eastward from the Kolvinskaya Ridge expressing itself by Pesyakov Island, the northwestern orientation of morphostructural elements (Fig. 13) is re-established. These zones differ not only in the degree of destruction, deposit thickness, etc., but also in neotectonic activity. The eastern zone is the most active. Some researchers rather attribute small dislocations on the seafloor to glacial pressure than to tectonic causes. However, Krapivner (1992) has clearly demontrated the inconsistency of this supposition. In particular, subsurface plicative dispositions (up to several hundreds of meters deep), often referred to as glacial ones, are created due to subsurface flattening of reversed and reversed-shift faults. At the same time, small dislocations occur here that belong to lithobaric (structure of loading) and cryogenic (produced by deposit freezing and further ice crystallization) types. Danilov (1985) considers cryogenic deformations to be dozens of kilometers wide and dozens of meters deep.

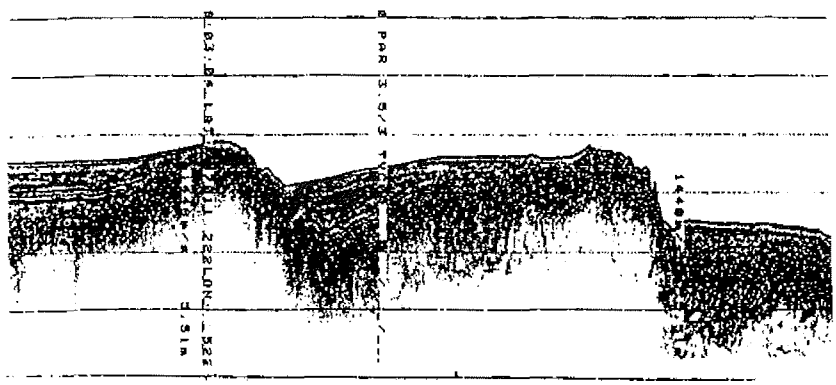

Fig. 11. Pattern of structural-tectonic relief record at the southern flank of the Southern Novaya Zemlya trench.

The data on modern tectonic movements are available only for coastal areas and separate upper shelf regions. In general, direction of these movements is in a good accordance with the results of structural-geomorphological analysis. The highest rates

of upward movements are characteristic of the Novaya Zemlya coasts (1-3 mm/year). Submergence prevails at the southern Pechora Sea coasts (up to 3 mm/year) and Kolguev Island (1-2 mm/year) (Nikonov, 1978; Borisov, 1976; Veinbergs, Stelle, 1995).

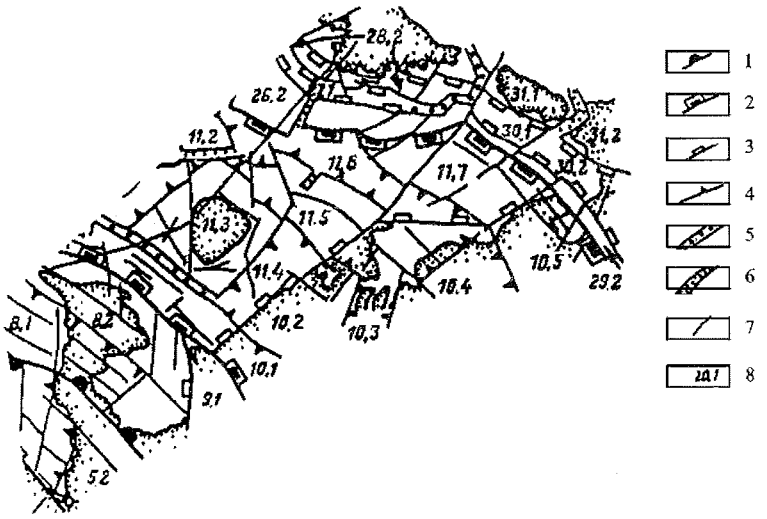

Fig. 12. Morphostructural zonation of the eastern Barents Sea (Avenarius et al., 1999). Key: Boundaries of morphostructural elements: 1 super-provinces, 2-- provinces, 3 - areas, 4 - regions. Graben-forming boundary zones: 5 - between morphostructural elements, 6 - complexifying morpho-structural elements, 7 - lineaments corresponding to active tectonic dislocations, 8 - numbers of morphostructural areas (first figure) and regions (second figure).

The local postglacial Earth's crust movements have not yet been enough studied even in such a thoroughly investigated area as Fennoscandia. The most important questions are the role of tectonics and glacioisostasy, size and timing of glacioisostasy, its morphological manifestation, etc. Some researchers believe that in this area compensating rebound of the Earth's crust in response to removal of the glacial loading has already finished (Freiwald et al., 1991), while the others consider that it is still present (Nikolaev, 1988). As to the shelf, some researchers share the opinion that there should be practically no glacioisostatic rebound, since melting ice was immediately replaced by water. Moreover, the problem of the Earth's crust isostasy is still poorly developed. One of the models of the last glaciation in the studied region is substantiated in Avenarius and Dunaev (1999) (Fig. 14).

Conclusions

In order to analyze the mechanisms and characteristics of the anthropogenic impact on the shelf and coast, it is necessary to understand the nature of environmental processes in the region. Environmental conditions of the Pechora Sea shelf are determined by its high-latitudinal position and warming influence of the North Atlantic.

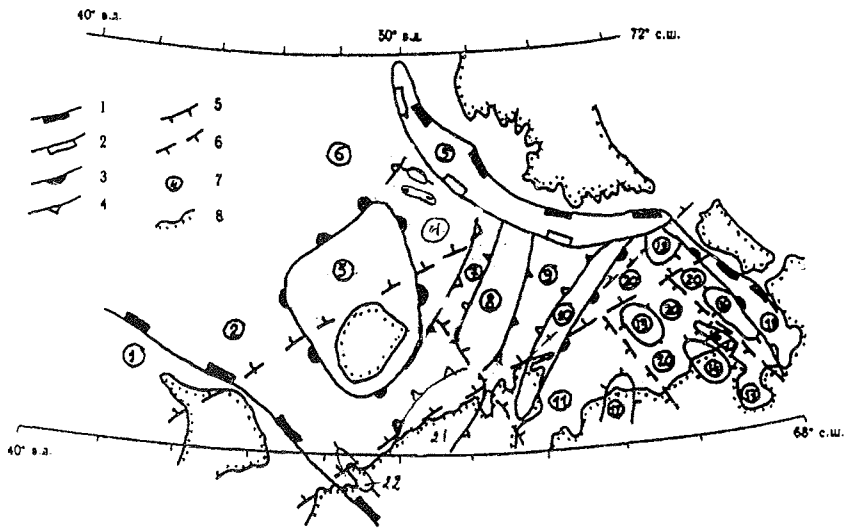

Fig. 13. Morphostructural scheme of the Pechora Sea (Arkticheskii..., 1998). Key: 1-5 - boundaries of major morphostructures; 6 - fractures; 7 - structural elements (1 - Timan-Kanin uplift, 2 - Kanin-Kolguev depression, 3 - Kolguev uplift, 4 - Kolguev step, 5 - Southern Novaya Zemlya trench, 6 - Kurentsovo structural terrace, 7 - Pomorskii trench, 8 - Sengei uplift, 9 - Sengei trench, 10 - Malozemel'skoe uplift, 11 - Ust'-Pechora depression, 12 - Dresven uplift, 13 - Kolva uplift, 14 - Varandei uplift, 15 - Medyn uplift, 16 - Dolgii Ostrov uplift, 17 - Khaipudyr depression, 18 - Vaigach trench, 19 - Eastern Pechora uplift, 20 - Eastern Pechora step); 8 - land boundaries.

As a result, the sea remains at least partially ice-free even in the most severe winters. Regional climatic peculiarities are clearly manifested in the specific exogenic relief and composition of bottom sediments, mainly represented by sedimentary material produced by physical weathering.

At present, as a result of global processes climate and ice conditions of the Arctic regions gradually become comparable with the Holocene "Atlantic climate optimum" (5-7 ka). Already now steady positive temperature anomalies are observed in high latitudes, which achieve 2°C (in relation to the period of 1966-1995). Warming will inevitably result in reduction of ice fields on the inner shelf, activization of hydrodynamic processes including increasing influence of storm waves upon the seabed. Strengthening of coastal abrasion and, primarily, thermoabrasion will cause increasing sediment discharge from land.

Specificity of ice regime lies in development of one-year ice that decreases wave impact on the coast. Sea ice has a dynamic, thermal, and chemical influence on the coast-shelf zone. Ice extent varies from year to year depending on the intensity of the North Cape Current and general climate fluctuations. River runoff has additional warming influence upon nearshore ice conditions. The Karskie Vorota Strait and the southeastern Pechora Sea are the most strongly hummocked zones. Comparison of the archival data and satellite images revealed considerable reduction of ice fields.

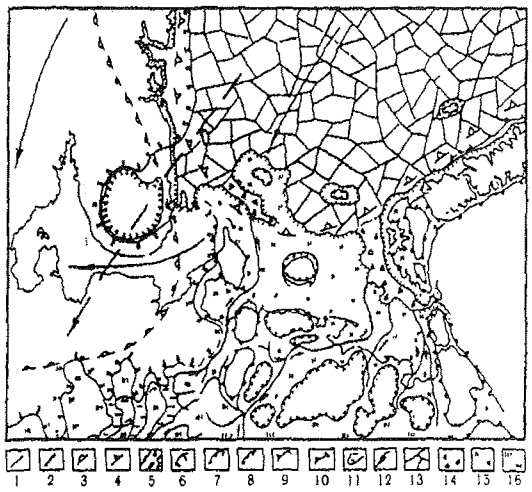

Fig. 14. Paleogeographical scheme of the Barents Sea and adjacent land (Avenarius and Dunaev, 1999).
Coastline: 1- modern, 2 - Late Valdai. Regions with anomalous precipitation: 3 - negative during cold season; 4 - positive during warm season. 5 - main routes of anticyclonic air masses: a - winter, b - summer. Boundaries of ice caps: 6 - thick and active, 7 - small moving, 8 - local, thin and stable. Boundaries of mountain glaciers: 9 - big, 10 - small and slightly active. 11 - glacial lakes; 12 - expected river beds; 13 - perennial pack ice; 14- seasonal ice cover. Alluvial, alluvial-lacustrine, and alluvial-marine plains with predominance of cryogenic and nival processes within: 15 - arctic tundra, 16 - tundra-forest-steppes.

The total river runoff to the Pechora Sea equals 147,000 km^3/year; 90% of this amount are supplied by the Pechora River. Its average multi-annual water discharge is about 4120 m^3/s, i.e. the Pechora on average delivers about 130 km^3 of water to the sea. In terms of water runoff it is one of the biggest rivers of the Russian Arctic ranking fourth after the Yenisei (597 km^3/year that makes 31.9% of the total river runoff to the Russian Arctic seas), Lena (530, 19.4%) and Ob (402, 14.7%). The average multi-annual solid runoff reaches about 8.5 million t/year. Ninety percent of this discharge falls on the flood period, when water turbidity is as high as 65 g/m^3. Discharge of ions is 67.5 mg/l. Suspended matter content in the surface layer is about 1.5-5.0 g/m^3. The area of freshening in the Pechora Bay depends on runoff. In summer low-water, the zone of river and sea water mixing is located within the limits of the bay. The average width of the mixing zone is about 50-60 km at background seawater salinity of 33. During flood the zone extends offshore into the sea. In this case water salinity at the seaside of the Gulyaevskie Koshki Islands falls down to zero.

Changeable ecosystems of river mouths are extremely vulnerable. Negative ecological consequences of anthropogenic regulation of water regime are evident not only in the areas of hydraulic engineering construction, but also on adjacent territories including deltas and estuaries. Water transfer and regulation of river runoff result in reduction of deltaic flood-plain area, silting of deltaic branches and channels, enhanced inland penetration of tidal wave, strengthening of storm surges, coastal abrasion, degradation of soil cover, impoverishment of fish populations, etc.

Geological shelf sequence consists of the three groups: Baikalian folded block

basement, Epibaikalian and Epihercynian metaplatform cover, and Late Permian – Cenozoic plate complex reflecting isolation of the Arctic geodepression. The latter includes a series of structural subgroups and sedimentary complexes. Isolation of the shelf in its modern borders occurred at the neotectonic stage (Late Oligocene - Holocene). It replaced an epicontinental sea that adjoined the Central-Arctic rise. Dominant neotectonic process is destruction of the Earth's crust and submergence of inner shelf regions.

References

Aksenov, A.A., Dunaev, N.N., Ionin, A.S. et al., 1987. Arkticheskii shel'f Evrazii v pozdnechetvertichnoe vremya (Eurasian Arctic shelf in the Late Quaternary time). Moscow, Nauka, 277 pp. (in Russian).

Assinovskaya, B.A., 1994. Seismichnost' Barentseva morya (Seismicity of the Barents Sea). Moscow, Nation. Geophys. Com. RAS, 128 pp. (in Russian).

Avenarius, I.G., Dunaev, N.N., 1999. Some aspects of relief evolution during the Late Valdai in the eastern Barents Sea and adjacent land. Geomorphologiya, 3, 57-62 (in Russian).

Avenarius, I.G., Belozerov, S.N., L'vov, L.A., Repnina, T.Yu., 1999. Morphostructural division and some features of the newest geodynamic of a shelf of the East Barents Sea. Byulleten' komissii po izucheniyu chetverichnogo perioda, 63, 57-62 (in Russian).

Borisov, L.A., 1976. Modern oscillations of average sea-level in the Kara and the Barents seas. Okeanologiya, 2, 302–309 (in Russian).

Chistyakova, I.A., 1997. Sedimentation and history of Quaternary shallow glacial shelf (Pechora Sea as an example). Candidate Thesis, GIN RAS, 24 pp. (in Russian).

Danilov, I.D., 1985. Development of the Northern Eurasia continental margin in the Late Cenozoic. In: Geologiya i geomorfologiya shel'fov i kontinental'nykh sklonov (Geology and geomorphology of shelves and continental slopes). Moscow, Nauka, P. 48–57 (in Russian).

Danilov, A.I., Efremkin, I.M., 1998. Natural-climatic conditions in the regions of oil-gas fields on the Arctic shelf. In: Osvoenie shel'fa arkticheskikh morei Rossii (Exploration of the Russian Arctic shelf). St.Petersburg, Krylov TsNII, 479-487 (in Russian).

Dobrovol'skii, A.D., Zalogin, B.S., 1982. Morya SSSR (Seas of the USSR). Moscow, Mysl', 196 pp. (in Russian).

Ekosistemy, bioresursy i antropogennoe zagryaznenie Pechorskogo morya (Ecosystems, bioresources and anthropogenic pollution of the Pechora Sea), 1996. Apatity, Kola Sci. Center RAS, 162 pp. (in Russian).

Freiwald, A., Henrich, R., Shafer, P., Willnomm, H., 1991. The significance of high-boreal to subarctic marine deposits in Northern Norway to reconstruct Holocene climatic changes and sea level oscillations. Facies, 25, 315–340.

Geologicheskoe stroenie SSSR i zakonomernosti razmeshcheniya poleznykh iskopaemykh (Geological structure of the USSR and regularities in distribution of mineral resources). V. 9: Soviet Arctic seas, 1984. Leningrad, Nedra, 280 pp. (in Russian).

Gidrometeorologicheskie usloviya shel'fovoi zony morei SSSR (Hydrometeorological conditions of the shelf zone of the USSR). V. 6, Is. 1/2: Barents Sea, 1985. Leningrad, Gidrometeoizdat, 262 pp. (in Russian).

Gidrometeorologiya i gidrokhimiya morei SSSR (Hydrometeorology and hydrochemistry of the seas of the USSR). V. 1, Is. 1: Barents Sea., 1990. Leningrad, Gidrometeoizdat, 280 pp. (in Russian).

Grigor'ev, N.F., 1987. Cryolithozone of a coastal zone of the Western Yamal. Reports of Permafrost Institute, Siberian Branch Acad. Sci. USSR, Yakutsk. (in Russian).

Gudoshnikov, Yu.P., Zubakin, G.K., Naumov, A.K., 2003. Morphometric characteristics of ice formations in the Pechora Sea according to multiannual field data. Proceedings of RAO-03, St.Petersburg, 295-299 (in Russian).

Ionin, A.S., 1992. Rel'ef shel'fa Mirovogo okeana (Relief of the World Ocean shelf). Moscow, Nauka, 255 pp. (in Russian).

Kaplin, P.A., 1971. Peculiarities of coastal dynamics in the polar seas (Chukchi Sea coast as an example). In: Novye issledovaniya beregovykh protsessov (Recent investigations of coastal processes). Moscow, Nauka, 22–34 (in Russian).

Kaplin, P.A., Leont'ev, O.K., Luk'yanova, S.A., Nikiforov, L.G., 1991. Berega (Coasts). Moscow, Mysl', 479 pp. (in Russian).

Khimicheskie protsessy v ekosistemakh severnykh morei: gidrokhimiya, neftyanoe zagryaznenie (Chemical processes in ecosystems of the northern seas: hydrochemistry, geochemistry, petroleum pollution), 1997. Apatity, Kola Sci. Center RAS, 404 pp. (in Russian).

Korobkin, A.V., Boiko, N.I., 1999. Structure of the Quaternary deposits in the southeastern Barents Sea (the Pechora Sea). Izvestiya VUZov. Geologiya i razvedka, 4, 160-164 (in Russian).

Krapivner, R.B., 1992. Are there any subsurface dislocations connected to glacial pressing? Bull. MOIP. Geologiya, 67, 6, 29–42 (in Russian).

Lisitsin, A.P., 1978. Protsessy okeanskoi sedimentatsii: litologiya i geomorfologiya (Processes of ocean sedimentation: Lithology and geomorphology). Moscow, Nauka, 392 pp. (in Russian).

Makhotina, G.P., 1982. Peculiarities of evolution and recent structure of the Barents-Kara shelf. In: Stratigrafiya I paleogeografiya pozdnego kainozoya Arktiki (Stratigraphy and paleogeography of the Late Cenozoic in Arctic). Leningrad, Sevmorgeologiya, 9–15 (in Russian).

Matishov, G.G., 1984. Dno okeanov v lednikovyi period (Seafloor in glacial epoch). Leningrad, Nauka, 176 pp. (in Russian).

Mel'nikov, V.P., Spesivtsev, V.I., 1995. Inzhenerno-geologicheskie i geokriologicheskie usloviya shel'fa Barentseva i Karskogo morei (Engineering-geological and geocryologic conditions of the Barents and Kara shelf). Novosibirsk, Nauka, 197 pp. (in Russian).

Mikhailov, V.N., 1997. Ust'ya rek Rossii i sopredel'nykh stran: proshloe, nastoyashchee I budushchee (Mouths of the rivers of Russia and adjacent countries: past, present and future). Moscow, GEOS, 413 pp. (in Russian).

Mironov, E.U., Zubakin, G.K., Lebedev, A.A., Tyuryakov, A.B., 1998. Ice cover extent in the Pechora Sea and estimation of ice export from the Kara Sea. Osvoenie shel'fa arkticheskikh morei Rossii (Exploration of the Russian Arctic shelf). St.-Petersburg, Krylov TsNII, 53-56 (in Russian).

Mitrofanov, F.P., Predovskii, A.A., Lyubtsov, V.V. et al., 1998. Pre-Cambrian stage in development of oil-gas fields, the Barents province as an example: importance for the new criteria of the forecast. In: Osvoenie shel'fa arkticheskikh morei Rossii (Exploration of the Russian Arctic shelf). St.Petersburg, Krylov TsNII, 356-359 (in Russian).

Musatov, E.E., 1990. Neotectonics of the Barents-Kara shelf. Geologiya i razvedka, 5, 20-27 (in Russian).

Nauchno-metodicheskie podkhody k otsenke vozdeistviya gazo-neftedobychi na ekosistemy morei Arktiki (na primere Shtokmanovskogo proekta) (Scientific-methodical approaches in estimating the influence of oil-gas exploitation on ecosystems of the Arctic seas (Shtokman project as an example), 1997. Apatity, Kola Sci. Center RAS, 393 pp. (in Russian).

Nikolaev, N.I., 1988. Noveishaya tektonika i geodinamika litosfery (Recent tectonics and geodynamics of lithosphere). Moscow, Nedra, 491 pp. (in Russian).

Nikonov, A.A., 1978. Vertical movements of polar seas coasts. Priroda, 6, 16–22 (in Russian).

Osnovy geokriologii, chast' 2: Litogeneticheskaya geokriologiya (Basics of geocryology. Part 2: Lithogenetic geocryology), 1996. Moscow, Izd. MGU, 397 pp. (in Russian).

Pavlidis, Yu.A., Ionin, A.S., Shcherbakov, F.A., Dunaev, N.N., 1998. Arkticheskii shel'f. Pozdnechetvertichnaya istoriya kak osnova prognoza razvitiya (The Arctic shelf. Late Quaternary history as the base for forecast of future development. Moscow, GEOS, 187 pp. (in Russian).

Pavlidis, Yu.A., Leont'ev, I.O. 2000. The forecast of coastal zone development in the East Siberian Sea at sea-level rise and climate warming. Vestnik RFBR, 1, P. 58–69 (in Russian).

Pavshtiks, E.A., 1979. Seasonal changes in age structure of populations of copepods *Calanoida* in the Arctic basin. In: Ekologiya morskogo planktona (Ecology of marine plankton). Leningrad, Nauka, 56–73 (in Russian).

Pfirman, S.L., Kogeler, J., Anselme, B., 1995. Coastal environments of the western Kara and eastern Barents Seas. Deep-Sea Research, II, 42, 1391–1412.

Polonskii, V.F., 1984. Distribution of water discharge in the Pechora River estuarine area and tendency of its change. Reports of State Oceanographic Institute, 172, 96–110 (in Russian).

Polyak, L., Gataullin, V., Okuneva, O., Stelle, V. 2000. New constraints on the limits of the Barents-Kara ice sheet during the Late Glacial Wurm based on borehole stratigraphy from the Pechora Sea. Geology, 28 (7), 611-614.

Potanin, V.A., Denisov, V.V., Ershtadt, M.A., 1985. Water dynamics. Zhizn' I usloviya ee sushchestvovaniya v pelagiali Barentseva moray (Life and environments in pelagic areas of the Barents Sea). Apatity, Kola Sci. Center RAS, P. 18–30. (in Russian).

Reimnitz, E., Barnes, P., Forgatsch, T., Rodeick, C., 1972. Influence of grounding ice on the Arctic shelf of Alaska. Marine Geology, 13 (5), 323–334.

Reimnitz, E., Toimil, L., Barnes, P., 1978. Arctic continental shelf morphology related to sea-ice zonation, Beaufort Sea, Alaska. Marine Geology, 28, 3-4, 179–210.

Romankevich, E.A., Vetrov, A.A., 2001. Tsikl ugleroda v moryakh Rossiiskoi Arktiki (Carbon cycle in the Russian Arctic seas). Moscow, Nauka, 302 pp. (in Russian).

Rozenbaum, G.E., Shpolyanskaya, N.A., 1998. Cryolithozone of the Russian Arctic regions in the Middle Pleistocene–Holocene. Izvestiya Russian Academy of Science. Geography, 3, 32–48 (in Russian).

Savostin, L.A., 1981. Cenozoic tectonics of plates in the Arctic regions, Northeastern and Inner Asia, and global paleodynamic reconstructions. Doctor Dissertation Thesis, IO AN USSR, 47 pp. (in Russian).

Senin, B.V., 1993. Geological structure of Western Arctic shelf of Eurasia (Barents and Kara seas). Doctor Dissertation Thesis, MSU, 82 pp. (in Russian).

Severnyi Ledovityi i Yuzhnyi okeany (The Arctic and Southern oceans), 1985. Leningrad, Nauka, 501 pp. (in Russian).

Shipilov, E.V., 1993. Rifting of the Eurasian-Arctic continental margin. Doctor Dissertation Thesis, MSU, 85 pp. (in Russian).

Takki, D.F., Buivolenko, E.V., 1976. Morphostructural map of the southeastern Barents Sea. Okeanologiya, 3 (4), 639–644 (in Russian).

Timofeev, V.T., 1960. Vodnye massy Arkticheskogo basseina (Water masses of the Arctic basin). Leningrad, Gidrometeoizdat, 191 pp. (in Russian).

Veinbergs, I.G., Stelle, V.Ya., 1995. Late Quaternary history of coastal development in the Pechora Sea. In: Korrelyatsiya paleogeograficheskikh sobytii: materik-shel'f-okean (Correlation of paleogeographic events: continent-shelf-ocean). Moscow, Izd. MGU, 106–112 (in Russian).

Verzhbitski, E.V. 2001. Geothermal conditions in the Pechora Sea. Oceanology (English Translation), 41 (3), 453-461.

Veter i volny v okeanakh i moryakh (Wind and waves at oceans and the seas), 1974. Leningrad, Gidrometeoizdat, 360 pp. (in Russian).

Zabruskova, M.M., 1998. Sezonnye osobennosti polyarnoi frontal'noi zony Barentseva morya (Seasonal features of polar frontal zone in the Barents Sea). Apatity: Kola Sci. Center RAS, 28 pp. (preprint) (in Russian).

Zarkhidze, V.S., 1985. The recent stage in evolution of the Arctic shelf. In: Geologiya i geomorphologiya shel'fov i materikovykh sklonov (Geology and geomorphology of shelves and continental slopes). Moscow, Nauka, 58–65 (in Russian).

Zubakin, G.K., 1998. Ice regime of the Pechora Sea and local specifications for "Prirazlomnoe" oilfield. In: Osvoenie shel'fa arkticheskikh morei Rossii (Exploration of the Russian Arctic shelf). St.Petersburg, Krylov TsNII, 510-517 (in Russian).

HOLOCENE SEA-LEVEL CHANGES IN THE RUSSIAN SECTOR OF THE EUROPEAN ARCTIC

P.A. Kaplin, A.O. Selivanov
Faculty of Geography, Lomonosov Moscow State University, Moscow, Russia

Abstract

The paper summarizes results obtained by the authors and numerous other investigators. A broad variety in interpretations of glacial history and, therefore, intensity and pattern of isostatic rebound results in significant differences between the various estimates of sea-level changes in the Russian sector of the European Arctic. However, in general, two primary regions of the coast may be distinguished. The decreasing trend in the relative sea level in the Kola Peninsula and Karelia, where the highest Late Glacial terraces are situated at 90-125 m above the present sea level, was superimposed by fluctuations in the order of 8-12 m or even more, whereas in the eastern White Sea and in the Pechora Sea a fluctuating pattern of sea-level changes became established after the drainage of periglacial lakes.

Over the whole region major periods of sea-level rise are dated to the Atlantic period (probably Middle and Late Atlantic) and the Middle Subboreal. Fluctuations in relative sea level during the Middle and Late Holocene were possibly in the order of 5-7 m.

Introduction

The European Arctic coast of Russia is characterized by a broad variability of morphology and recent history. This variability results primarily from the differences in glacial history during the Late Pleistocene. The Kola Peninsula and the western coast of the White Sea in Karelia were covered by the thick Fennoscandian continental ice sheet and represent an area of intensive glacial erosion and isostatic uplift whereas the southeastern coast of the Barents Sea experienced steady submergence during the Pleistocene and was an area of marine transgressions. The origin of fine-grained Pleistocene sediments has various interpretations but the combination of lithologic, faunal, pollen and other evidence generally proves their marine and glaciomarine origin (Danilov, 1989; Kostyaev et al., 1992).

According to some authors, an extensive ice sheet or a number of small ice caps of the specific "glacial shelf type" existed in the present basin of the Barents Sea during the Late Pleistocene. The ice possibly advanced from the sea basin onto the shelf area and the present Mezen' and Pechora lowlands thus creating a backwater effect (Grosswald, 1989). In contrast, according to Matishov (1984) and Biryukov et al. (1988), the Late Pleistocene continental ice sheet advanced onto the Barents Sea basin from the Kola Peninsula and Novaya Zemlya Islands to a depth of 200 m. The latest extensive study by Pavlidis et al. (1998) generally supports this hypothesis.

Most of the European Arctic coasts of Russia are meso and microtidal. Tidal range in narrow inlets of the White Sea called "guba" ("lip") is as high as 10.5 m (Mezen' Inlet). Wave intensity varies from low in inlets to high at the open coast.

Climate-driven fluctuations in the warming influence of the northeastern Atlantic current on the western sector of the European Arctic coast of Russia govern the migration of Boreal malacofauna species, which serve as palaeogeographical and stratigraphical markers in the area and provide reliable material for radiometric dating. The general stratigraphic scheme of the Late Glacial and Postglacial periods in the area was developed by Lavrova (1960, 1969) on the basis of changes in mollusc assemblages. The successive basins were correlated with the seven principal shorelines (a-h) by Tanner (1930) on Fennoscandian coasts, presumably in the Finnmark region, distinguished by morphological data (Table 1).

Table 1. Correlation of shorelines in the Kola Peninsula

Assemblages of malacofauna (Lavrova,1960)	Regional shore-line in Fenno-scandia (Tanner, 1930)	Elevation of shoreline in Kola Pen., m (Koshechkin, 1979)	Possible correlation with climatic periods	Radiocarbon age (uncal. yr B.P.)
Late Glacial	h	88-97, up to 120	Alleröd	
Late Glacial	g ("main")	80-120	Younger Dryas	
Portlandia 1	f	50-80	Preboreal	
Portlandia 2	e	25-40	Preboreal	10,030±130
Littorina	d5-d1	16-40	Preboreal	9,490±100 8,980±180
Folas 1	d	45-75, up to 90	Early Boreal	8,890±180 8,980±180
Folas 2	c4-c1	0-10?	Late Boreal	7,890±150
Tapes 1	c	24-29	Middle Atlantic	6,870±60
Tapes 2	b	22-26, up to 45	Late Atlantic	5,650±80 6,480±60
Trivia 1 Late	a9-a7	20-25	Late Atlantic-Early Subboreal	5,000±120
Trivia 2	a4	15-18, up to 27	Middle Subboreal	4,170±70 4,100±70
Trivia 3	a3	10-15, up to 20	Late Subboreal	3,590±200 3,490±200 3,090±140
Ostrea 1	a2	15-8, up to 14	Early Subatlantic	1,950±150 1,800±100 1,720± 80
Ostrea 2	a1	2.8-6.0	Late Subatlantic	730± 60

This paper summarizes results obtained by the authors and numerous other investigators. Radiocarbon measurements in the area have remained scanty and controversial so far. Only a few of the most recent measurements were analyzed by accelerated mass-spectrometry. All datings in this paper are cited in the non-calibrated form. A broader analysis of this problem was earlier presented in Russian (Kaplin and Selivanov, 1999).

Late Glacial sea levels in the European Arctic of Russia

A series of submerged shorelines is found in the southwestern part of the Barents Sea at the depths of 400-500, 200-300, 125-140, 100-115 and 60-75 m (Strelkov, 1971; Lastochkin and Fedorov, 1978). Their coastal origin has not yet been reliably established but the sea-level fall to at least minus 200-250 m is beyond any doubt and has been proven by the existence of the submerged ancient river deltas (Grosswald, 1989).

During the Late Glacial almost the whole basin of the present White Sea was filled by the lobes of the Fennoscandian continental ice sheet. In the lower reaches of the Severnaya Dvina, Mezen' and some other rivers, extensive lakes existed during the Late Glacial due to the backwater effect of the glacial lobes. These lakes at elevations of 50-140 m above the present sea level drained southwards, presumably through the existing river valleys (Gerasimov and Velichko, 1982).

Anomalously elevated shorelines of fluvioglacial lakes (127-138 m and up to 260 m at some locations), dated to the Alleröd and Younger Dryas (12-10,500 yr B.P.), are typical for the White Sea coast of the Kola Peninsula (Koshechkin, 1979). On the basis of the reconstruction of isostatic deformation, initial elevation of these shorelines is estimated at 15-60 m above the present mean sea level (Badyukov and Kaplin, 1979), which is, in any case, at least one hundred metres higher than the mean sea level during the Late Glacial.

On the coast of the Onega Peninsula in the east of the White Sea ancient coastal terraces of fluvioglacial or glaciomarine origin have been distinguished at elevations of up to 60-80 m (Lavrova, 1969). However, field observations of one of the authors do not prove the existence of terraces at the elevations exceeding 20 m above the present sea-level (Selivanov, 1984). Moreover, the highest depositional terrace (13-20 m) obviously is of lacustrine origin.

In coastal bluffs in the eastern and southeastern corner of the White Sea, boulder tills of the last glaciation at 10-18 m above the present sea-level are usually covered by laminated grey clays and silts with Arctic freshwater and mixed diatom and mollusc assemblages and periglacial spore-pollen complexes (Selivanov, 1984). In coastal sections with less intensive sediment supply, the erosion of glacial tills during that time is marked by erosional escarpments up to 16-20, rarely 25-30 m above the present sea-level. To the southwest of the Onega Peninsula, in the Solovki Archipelago a series of erosional terraces in pre-Quaternary rocks lies at elevations of up to 21-23 m (Nikishin, 1981). Therefore, the maximum water level of the periglacial lake was possibly nearly 15-20 m above the present sea level.

Direct radiocarbon measurements from lacustrine sediments do not yet exist. However, on the eastern coast of Onega Bay the covering peats are dated to

7,980±270 and 7,570±250 yr B.P., thus confirming the possible Early Holocene age for the lacustrine clays and silts.

According to the data from bottom cores, the central basin of the White Sea and the Onega Bay were still covered by extensive glacial masses during the Boreal period (9,000-8,000 yr B.P.) (Nevesskii et al., 1977). Intrusion of typical marine fauna into the central basin of the sea is dated to 8,200 yr B.P. (Koshechkin and Strelkov, 1976), and the steady bidirectional water exchange of the White Sea and the Barents Sea as part of the Arctic Ocean became established 7,700-7,000 yr B.P. (Nevesskii et al., 1977). The latest estimate of the "opening" of the strait between the White Sea and the Barents Sea is approx. 8,000 yr B.P. (Pavlidis et al., 1998). However, marine mollusc fauna was found on the Kola Peninsula in the sediments of terraces dated back as far as 12,000 yr B.P. This discrepancy may preliminarily be explained by the "dead ice" character of glacial masses in the central part of the sea basin that could survive in the periglacial marine basin for several millennia (Nevesskii et al., 1977).

Farther east, the largest Pechora Lake possibly formed approximately 11,500 yr B.P. in the lower reaches of the Pechora River. The highest lacustrine shoreline lies at 80-100 m and the lowest at 30-45 m above the present sea-level (Arslanov et al., 1985; Lavrov and Potapenko, 1989). However, the hypothesis of the existence of this lake as well as the Late Würmian glaciation of the area has been strongly criticized by several authors (see Danilov, 1989 for discussion).

Holocene marine shorelines

Raised shorelines of the Barents Sea coast of the Kola Peninsula and Novaya Zemlya Island

The Kola Peninsula experiences an intensive glacio-isostatic uplift. There is a well-pronounced series of Late Glacial and Postglacial marine terraces on the northern coast of the peninsula. The terraces usually have erosional character, but beach sediments with shells may be found in embayments. The terraces lie up to 120 m above sea level and are tentatively correlated along the coastline by geomorphological evidence, mollusc fauna and few radiocarbon datings (Table 1).

The highest elevations are typical for the upper Kola and Kandalaksha inlets, which are situated closer to the former glacial centre and experience more intensive glacio-isostatic uplift (Fig. 1). The earliest terrace is correlated with the Alleröd interstadial and the best developed shorelines date from the Littorina (8,500 yr B.P. by uncalibrated ^{14}C dates), Tapes 2 (6,500-5,600 yr BP.) and Trivia 1 (nearly 5000 yr B.P.) transgressive periods and are situated at the elevations of 44-90, 22-45 and 14-27 m, respectively. Shorelines of the two stages of the Tapes transgression are marked by the most abundant and best studied mollusc assemblage and by a pumice layer. The shoreline of the last transgressive period Ostrea (3-6 m) is possibly dated to early A.D.

Intermittent periods of sea-level fall shown in the terrace sections near the centre of the former ice sheet are marked by regional unconformities whereas in the distant areas thick series of continental sediments formed during these periods. The most intensive fall in relative sea level occurred between the Younger Dryas and Late Preboreal and was as fast as 95-100 m in 2,000-2,500 years (Fig. 1).

During the next millennium (9,100-8,300 yr B.P.) the relative sea-level possibly rose by 35-40 m. Subsequent fluctuations in the sea level in the order of 8-12 m superimposed the general negative trend (Koshechkin, 1979). However, these fluctuations are possibly overestimated by the correlation of the areas with differing tectonic regime.

Shorelines of the earlier periods of the Pleistocene are not known in the Kola Peninsula whereas the series of terraces on Novaya Zemlya Islands up to 410-420 m above sea level represents different periods of Quaternary history. Only terraces up to 60 m can be reliably correlated with the Late Glacial and Postglacial periods. Dominant altitudes are 42-60, 22-40, 12-20, 6-10 and 3 m (Veinbergs, 1986). They are tentatively correlated with the transgressive stages of the Kola Peninsula.

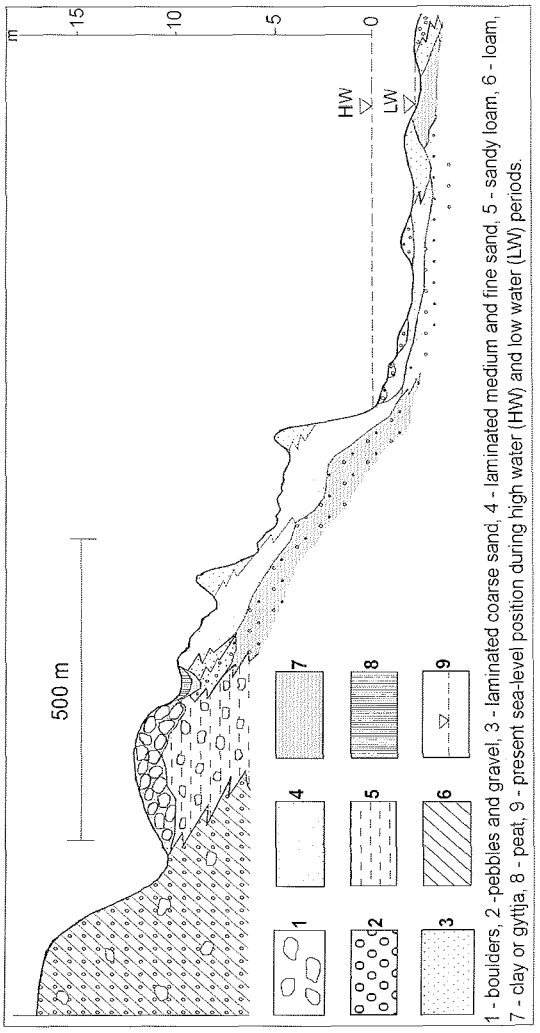

Fig.1. Schematic profile of the coastal zone in the eastern part of Onega Bay, White Sea

However, the precise synchronism of terraces along the Arctic coast and their representation of large-scale sea-level fluctuations are doubtful. It is worth noting that the stratigraphy based on mollusc complexes remains the principal basis for their division.

Shorelines of the White Sea

Kola coast of the White Sea is characterized by the existence of 5 to 12 depositional and erosional-depositional terraces with marine mollusc fauna at elevations of up to 100 m (Lavrova, 1960). The best developed terraces are traced along the altitudes of 50, 20-35 and 7-10 m (Koshechkin, 1979). In embayments, glacial tills form a significant part of outcrops in the higher terraces, whereas the lower terraces are usually characterized by an exclusively depositional character. Terraces on capes usually lack a sedimentary cover and are characterized by higher elevations. Near the Vyg River mouth, in the south of the sea, a detailed stratigraphy of Holocene sea-level and climate changes was established by archeological investigations and pollen analysis of coastal terraces up to 45-50 m above the present sea level (Devyatova, 1976). It was supposed that sea-level fluctuations during the Middle and Late Holocene were as high as 15-20 m in amplitude. However, these conclusions were not supported by detailed lithological analysis and by tracing terraces along the coast.

On the Onega Peninsula, in the east of the sea, marine depositional terraces at 8-15 and 3-8 m above the present sea level are traced along several segments of the coast but have not been dated yet. Bluffs in the 8-15-meter terrace outcrop are composed of glacial tills overlain by residual boulder causeways and a relatively thin layer of coarse sand with beach lamination. This terrace may be tentatively correlated with the "main postglacial shoreline" of the Kola Peninsula.

Sections of the 3-8-meter terrace, which is developed presumably in embayments, consist usually of two transgressive-regressive sequences of sand and mud facies of the upper shelf, intertidal flat, beach and lagoon (Selivanov, 1984). Peats indicating falls in relative sea level were dated to 8,705-7,825 and 4,030±70 yr B.P. (Koshechkin et al., 1977).

On the open eastern coast of the Onega Bay stretching along the belt of end moraines dated to 13-12,000 yr B.P., erosional features are obvious in the seaward slope of the moraine ridge, which is situated several hundred meters inland from the present beach (Selivanov, 1984; Fig. 1). Sediments of the ancient lagoon at the altitudes of 6-9 m are reliably dated to the Middle Atlantic period: 6,455±80, 5,940+7-250, 5,600+7-250; 5,240+7-200 yr B.P. (Boyarskaya et al.,1986).

During the following sea-level fall a series of coastal ridges and a coastal dune formed at the present altitude of 7-10 m. The subsequent transgressive-regressive cycle in the relative sea level is marked in this coastal segment by a layer of beach gravel and sand at 3-4 m above the present sea level and a series of coastal sand ridges and a coastal dune at 5-6-meter altitudes. This depositional coastal terrace may be tentatively attributed to the Subboreal period by the information on the Late Neolite archaeological site (approx. 4,000-4,500 yr B.P. in the regional chronology) found in its upper sediments. This age is confirmed by two radiocarbon dates of the upper transgressive layer from the

Holocene terrace in the adjacent embayment: 4,800+7-180; 4,100±150 yr B.P. (Boyarskaya et al., 1986). Pollen analysis reveals a general coincidence of the periods of rising sea levels and climate amelioration (Boyarskaya et al., 1986).

Summarizing the above data, the relative sea level during the Atlantic transgressive period may be estimated as exceeding the present sea level by 5-7 m and during the Subboreal transgressive period by 3-5 m (Fig. 2). According to the existing data, it is doubtful that sea level was higher than the present one during the Subatlantic period. The possible influence of relatively slow coastal emergence on the altitudinal position of these shorelines can not be excluded. Similar to Boyarskaya et al. (1986), Selivanov (1984) did not find any traces of a relative sea level below the present one during the Preboreal-Early Boreal and Late Subboreal-Early Subatlantic regressive periods. Therefore, drastic Holocene sea-level fluctuations by over 8-10

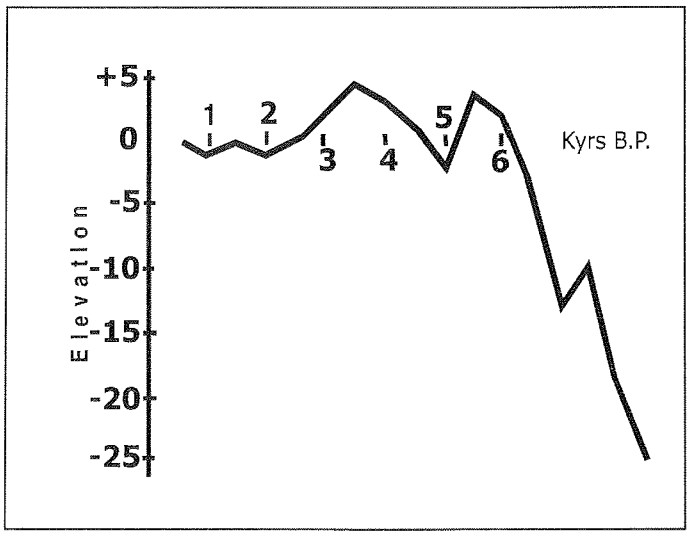

Fig. 2. Possible changes in the relative sea level in the eastern White Sea during the Holocene

m, assumed for Kola Peninsula (see above) and the Vyg River mouth, are not supported by these data. The latter conclusions possibly reflect the local block deformation of coastal areas (Selivanov, 1984).

Shorelines of the Pechora Lowland

According to the "non-glacial" interpretation of the Late Glacial history of the Pechora Lowland (Danilov, 1989), a series of typical marine depositional terraces at 40-60, 16-20, 8-12 and 3-5 m above the present sea level dominates the morphology of the area. In view of the lack of radiometric age determinations, the highest terrace is tentatively correlated with the Kargian (Middle Würmian) transgression in the adjacent West Siberian Lowland, whereas the three lower terraces are attributed to the Holocene.

In contrast, according to Lavrov and Arslanov (1977), depositional surfaces at 40-150 m above the present sea level in the south of the Pechora Lowland represent terraces of the extensive Pechora Lake and local periglacial lakes in front of marginal glacial features. The terrace at 100-110 m is dated to 9,000-8,000 yr B.P., that at 70-80 m to 8,000-7,700 yr B.P. and that at 40-50 m to 5,950 yr B.P. According to this hypothesis, marine history of the Pechora Lowland began only in the Late Atlantic period. A more recent paper of Lavrov and Potapenko (1989) dates the 15-17 m terrace, which is traced for 500 km along the coast, to 10,500-8900 yr B.P. and regards it as a terrace of an extensive perigracial lake with limited water exchange with the sea.

Conclusions

The Late Glacial and Postglacial history of the sea level in the Russian sector of the European Arctic depended, to a large extent, on the glacial history of the region. Various interpretations of the latter phenomenon, from continental glaciers spreading onto the shelf to "glacier shelves" and extensive masses of "dead ice" in sea basins, as well as the lack or low reliability of radiocarbon dates determine the broad variety of possible sea-level histories for the region. The situation is complicated by difficulties in tracing terraces along shorelines due to intensive glacioisostatic rebound in the western sector of the region and block character of tectonic movements.

In general, the decreasing trend in the relative sea level in the Kola Peninsula and Karelia was superimposed by fluctuations in the order of 8-12 m or even more, whereas in the eastern White Sea and the Pechora Lowland a fluctuating pattern of sea-level changes became established after the drainage of periglacial lakes.

Over the whole region major periods of sea-level rise are dated to the Atlantic period (probably Middle and Late Atlantic) and the Middle Subboreal. Intensive sea-level rise in the Boreal period is only typical for the formerly glaciated areas of the Kola Peninsula and possibly resulted from the deceleration of postglacial rebound superimposed on continuing fast eustatic rise in sea level. Fluctuations of the relative sea level during the Middle and Late Holocene were possibly in the order of 5-7 m, and the higher estimates for the Kola Peninsula reflect the inadequacy of methodology, namely the comparison of areas with differing tectonic regime.

Acknowledgements: This study was supported by INTAS project 99-1489 and by the Russian Foundation for Basic Research (projects 01-05-64181 and 02-05-65105). The paper is a contribution to the International Geological Correlation Programme (IGCP) Project 437 "Coastal Environmental Change During Sea-Level Highstands".

References

Arslanov, Kh.A., Lavrov, A.S, Potapenko, L.M., Tertychnaya, T.V., Chernov, S. B., 1985. New data on geochronology and palaeogeography of the Late and Early Holocene of the north Pechora Lowland. In: Punning, Ya.-M. K. (ed.), Geochronologiya Chetvertichnogo perioda (Geochronology of the Quaternary Period), Tallinn, 40-47 (in Russian).

Badyukov, D.D., Kaplin, P.A., 1979. Sea-level changes on the coasts of the USSR during the last 15,000 years. In: Suguio, K., Fairchild, T. R., Martin, L., Flexor, J. M. (eds.), Proc. Int. Symp. Coastal Evolution in the Quaternary, San Paulo, 1978, 135-169.

Biryukov, V.Y., Faustova, M.A., Kaplin, P.A., Pavlidis, Y.A., Romanova, E.A., Velichko, A.A., 1988. The paleogeography of Arctic shelf and coastal zone of the Eurasia at the time of the last glaciation (18,000 yr B.P.). Palaeogeogr. Palaeoclimatol., Palaeoecol., 68, 117-125.

Boyarskaya, T.D., Polyakova, Ye.I., Svitoch, A.A., 1986. New data on the Holocene transgression of the White Sea. Reports Acad. Sci. USSR, 290, 964-968 (in Russian).

Danilov, I.D., 1989. Rhythmostratigraphic method for marine Pleistocene sediments. In: Alekseev, M.N. (ed.), Chetvertichnyi period: Stratigrafiya. Sovetskiye doklady na 28 sessii Mezhd. Geol. Congr. (Quaternary Period: Stratigraphy. Soviet Reports on the 28th Session of the Int. Geol. Congr.). Nauka, Moscow, 188-195 (in Russian).

Devyatova, E.I., 1976. Geologiya i palinologiya golotsena i khronologiya arkheologicheskikh pamyatnikov yugo-zapadnoi chasti Belogo morya (Geology and Palynology of the Holocene and Chronology of Archaeological Sites in the Southwestern White Sea Area). Leningrad, Nauka, 122 pp. (in Russian).

Gerasimov, I.P., Velichko, A.A. (eds.), 1982. Paleogeografiya Evropy v poslednie 100,000 let (Palaeogeography of Europe during the last 100,000 years). Moscow, Nauka, 156 pp. (in Russian, English summary).

Grosswald, M.G., 1989. "Submerged shorelines" on glaciated continental shelves: Solving the puzzle? J. Coast. Res., 5, 113-121.

Kaplin, P.A., Selivanov, A.O., 1999. Izmeneniya urovnya morei Rossii i razvitie beregov: proshloe, nastoyashchee, budushchee (Sea-level changes and coasts of Russia: Past, present, future). Moscow, GEOS, 299 pp. (in Russian).

Koshechkin, B.I., 1979. Golotsenovaya tektonika vostochnoi chasti Baltiiskogo shchita (Holocene tectonics of the eastern part of the Baltic shield). Leningrad, Nauka, 160 pp. (in Russian).

Koshechkin, B.I., Strelkov, S.A., 1976. Shoreline movement and shelf glaciation in the North, Barents and White seas in the Late Pleistocene and Holocene. Abstr. 23rd Int. Geogr. Congr. 1, Moscow, P. 212-213.

Koshechkin, B.I., Devyatova, E.I., Kogan, L.Ya., Punning, Ya.M.K., 1977. Postglacial marine transgressions in the Onega region of the White Sea. In: Koshechkin, B. I. (ed.), Stratigrafiya i paleogeografiya chetvertichnogo perioda na severe Evropeiskoi chasti SSSR (Stratigraphy and Palaeogeography of the Quaternary Period in the North of European USSR). Petrozavodsk, Karelia, 5-16 (in Russian).

Kostyaev, A.G., Kulikov, O.A., Malaeva, Ye.M., Surkov, A.V., 1992. On the extension, age and causes of the polar marine transgression on the plains of north-west Eurasia. Water Resources, 19 (4), 51-57.

Lastochkin, A.N., Fedorov, B.G., 1978. Morphology and recent history of the northern shelf of Eurasia. Geomorphologiya, 3, 19-27 (in Russian).

Lavrov, A.S., Arslanov, Kh.A., 1977. Age and genesis of terraces in the Pechora Lowland: New geological and radiocarbon data. In: Chalov, R.S. (ed.), Rechnye sistemy i melioratsiya (River Systems and Amelioration), vol. 1. Novosibirsk, Nauka, 78-85 (in Russian).

Lavrov, A.S., Potapenko, L.M., 1989. Comparative characteristics of the Late Glacial ice features and terraces in the north of the Pechora Lowland and West Siberia. In: Velichko, A.A. (ed.): Paleoklimaty i oledenenie v pleistotsene (Palaeoclimates and Glaciation in the Pleistocene). Moscow, Nauka, 204-211 (in Russian).

Lavrova, M.A., 1960. Chetvertichnaya geologiya Kol'skogo poluostrova (Quaternary Geology of the Kola Peninsula). Moscow, Leningrad, Acad. Sci. USSR Publ., 233 pp. (in Russian).

Lavrova, M.A., 1969. Postglacial history of the White Sea. In: Alekseev, M.N. (ed.), Poslednii lednikovyi pokrov severo-zapada evropeiskoi chasti SSSR (The Last Ice Sheet in the North-West of the European USSR). Moscow, Nauka, 124-145 (in Russian).

Matishov, G.G., 1984. Dno Mirovogo okeana v lednikovyi period (The Seabed during the Glacial Period). Leningrad, Nauka, 176 pp. (in Russian).

Matoshko, A.V., Lomakin, I.E., Palansky, M.G., Sorokin, A.L., Vanyushin, B.I., 1989. Geomorphological correlation of the Late Pleistocene and Holocene terraces in the central part of the Onega Bay. Reports Inst. Geol. and Geophys., 657, 145-150 (in Russian).

Nevesskii, E.N., Medvedev, V. S., Kalinenko, V.V., 1977. Beloe more: sedimentogenez i golotsenovaya istoriya (The White Sea: Sedimentogenesis and Holocene History). Moscow, Nauka, 236 pp. (in Russian).

Nikishin, N.A., 1981. On the role of the sea in morphological evolution of the Solovki Islands. Abstr. Sci. Conf. on Problems of the White Sea. Arkhangelsk, 87-88 (in Russian).

Pavlidis, Yu.A., Ionin, A.S., Shcherbakov, F.A., Dunaev, N.N., Nikiforov, S.L., 1998. Arkticheskii shel'f: Pozdnechetvertichnaya istoriya kak osnova prognoza razvitiya (Arctic Shelf: Late Quaternary History as a Predicting Base of Future Changing). Moscow, GEOS, 187 pp. (in Russian).

Selivanov, A.O., 1984. Coastal evolution of tidal inlets and the possibility of construction of freshwater reservoirs, exemplified by the Onega Bay, White Sea. Ph.D. Thesis. Lomonosov Moscow State University, 245 pp. (in Russian).

Strelkov, S. A., 1971. Shoreline movement in the eastern Soviet Arctic during the last 12,000 years. In: Matishov, G. G. (ed.), Problemy razvitiya rel'efa i noveishie otlozheniya kol'skogo poluostrova (Problems of formation of morphology and recent sediments of the Kola Peninsula). Leningrad, Nauka, 141-150 (in Russian).

Tanner, V., 1930. Studier over kvartarsystemet i Fennoscandias nordliga delar, IY. Bull. Comm, Geol. Fin. 88. 96 pp.

Veinbergs, I.G., 1986. Drevnie berega sovetskoi Baltiki i drugikh morei SSSR (Ancient Coasts of the Soviet Baltic and Other Seas of the USSR). Riga, Zinatne, 168 pp. (in Russian).

MODERN BENTHIC FORAMINIFERAL ASSEMBLAGES IN THE PECHORA SEA

I.A. Pogodina
Murmansk Marine Biological Institute, Murmansk, Russia

Abstract

Benthic foraminifers from coretop sediments collected at 29 localities from different parts of the Pechora Sea were taken for modern assemblage studies. Four main assemblages were established. The most widespread *Eggerella advena – Hyperammina subnodosa* assemblage is restricted to coarse sandy grounds within the water depth range of 20 to 100 m and slightly freshened bottom waters (34.5-32) subjected to considerable summer warming (up to 9°C). *Elphidium clavatum - Buccella frigida* assemblage occurs on silty grounds around the Novaya Zemlya Archipelago and in the Karskie Vorota Strait at the depths of 10 to 200 m in more stable bottom water environments with temperatures ranging from –1 to 0°C and salinity exceeding 34. The impoverished *Haynesina orbiculare – Cibicides lobatulus* assemblage inhabits the shallow hydrodynamically active region around the Kanin Peninsula coast (20-40 m) with bottom waters experiencing freshening down to 33 and summer warming up to 7°C. The taxonomically poor assemblage without any well-defined dominant species occupies the most freshened (down to 5) southern part of the sea with the highest summer warming (up to 11°C). Samples from this area are dominated by "live" specimens.

Introduction

The southeastern part of the Barents Sea called the Pechora Sea is bordered by Kolguev Island in the west, southern Novaya Zemlya Island in the north, Vaigach Island in the east and Bol'shezemel'skaya tundra coast in the south. Seafloor is represented by a flat plain gently sloping to the north. The average depth is less than 20-60 m reaching 200 m only in the Novaya Zemlya trough (Matishov, 1997).

The environmental and biotic conditions of the Pechora Sea are primarily dependent upon water dynamics and sea ice cover extent. The greatest part of the year the sea is ice covered. Seasonal ice cover exists from October-November till July. Ice freeze-up starts in several distinct places in the southeastern (October-December) and central (January-March) parts of the sea. Ice break-up is also restricted to several centers. The zone of the most intensive ice melting is located in the eastern Pechora Sea in April-May (Potanin et al., 1986). The Pechora Sea is the only part of the Barents Sea basin, where freshwater runoff plays the main role in the hydrometeorological regime. The average annual runoff of the Pechora River equals 131.4 km^3 (Gidrometeorologicheskie usloviya..., 1984). Except the shallow area affected by the Pechora River, where the whole water column is freshened down to the depths of 20 m, the runoff influence is evident down to the depths of 10 m, and below 25 m sea waters are located.

Obviously, the fauna inhabiting the Pechora Sea (especially its southern part) must be able to survive under strong salinity variations (daily, seasonal, annual) and considerable freshening during flood period. Thus, our data provide evidence for foraminiferal fauna of a polar sea strongly affected by freshwater runoff and

summer warming. Similar investigations were carried out in the Pechora Bay by Maier (1974), and in the neashore zone of Kolguev Island by Digas (1969) and Gus'kov (1998).

Material and methods

Sediment samples for foraminiferal studies were obtained by the van Veen grab sampler during the cruise of R/V "Dal'nie Zelentsy" in September 2000 (stations 26-74) and July 2001 (stations 6-13). A total of 29 samples were analyzed. Each sample represented 20 cm^3 of sediment taken from the upper 1 cm of bottom sediments and fixed with 70° ethanol. Later it was stained with Bengal Rose and washed over 63 μm sieve. Both colored ("live") and non-colored ("dead") foraminifers were counted.

Results and discussion

Sixty-one species of Foraminifera have been recorded in the Pechora Sea sediment samples (Table 1). Of these twenty-five are agglutinated forms, and thirty-six calcareous ones. Four assemblages of benthic foraminifers named after dominant species were established in the Pechora Sea (Fig. 1).
Eggerella advena – Hyperammina subnodosa assemblage predominates over the greatest part of the Pechora Sea occurring within the water depth range of 20-100 m on sands and sandy silts. Detailed description of surface sediments is given in the article of G.A. Tarasov and co-authors (this volume). In summer, bottom water temperature reaches 9°C. Bottom salinity varies from 34.5 to 32. The assemblage consists of 25 agglutinated and 28 calcareous species. The number of species in a sample ranges from 17 to 31. Agglutinated foraminifers usually constitute half of this number, but their abundance is higher. The total abundance of foraminifers is 29-195 specimens per 1 cm^3 of sediment and that of agglutinated forms 24-131 specimens/cm^3. Relative abundances of *Eggerella advena* and *Hyperammina subnodosa* are 48-65% and 16-19%, respectively. Relative abundance of *Ammotium cassis* is the highest (up to 23%) at 20-40 m water depth. The group of calcareous foraminifers is taxonomically diverse, but inconsiderable in number. Typical representatives of high-arctic zone *Elphidium clavatum, Cassidulina reniforme, Buccella frigida* predominate among calcareous forms. The ratio between "live" and "dead" calcareous foraminifers is 2 to 1. This ratio was found to be species-dependent. For instance, for *Elphidium clavatum* and *Cassidulina reniforme* it equals 4:1. Only "live" specimens of *Pyrgo williamsoni* were recorded, while for *Buccella frigida* the ratio is opposite with 1:6. Probably, the tests of *Buccella frigida* are the most resistant to dissolution in course of sedimentation.

Elphidium clavatum - Buccella frigida assemblage is restricted to the northeastern part of the sea and occupies the nearshore area around the Novaya Zemlya Archipelago and the Karskie Vorota Strait within the water depth range between 10 and 200 m. Summer bottom water temperatures do not exceed 0°C. Bottom salinity is higher than 34. Bottom sediments are represented by dark grey silts.

Table 1. Taxonomic composition of the benthic foraminiferal assemblages

Textulariata Mikhalevich, 1980	**Lagenata Maslakova, 1990**
Astrorhiza sp.	*Dentalina baggi* Galloway & Wissler, 1927
Rhabdammina abyssorum M. Sars, 1868	*Dentalina frobischerensis* Loeblich & Tappan, 1953
Rhabdammina discreta Brady, 1881	*Dentalina* sp.
Proteonella atlantica (Cushman, 1944)	*Lenticulina* sp.
Hyperammina elongata Brady, 1878	*Lagena semilineata* Wright, 1886
Hyperammina subnodosa Brady, 1884	*Polymorphina* sp.
Ammodiscus sp.	*Oolina melo* d'Orbigny, 1839
Reophax curtus Cushman, 1920	
Reophax dentaliniformis Brady, 1884	**Rotaliata Mikhalevich, 1980**
Reophax scorpiurus Montfort, 1808	*Robertina arctica* d'Orbigny, 1846
Reophax scotti Chaster, 1892	*Rosalina* sp.
Reophax sp.	*Cibicides lobatulus* (Walker & Jacob, 1798)
Ammotium cassis (Parker, 1970)	*Nonion umbilicatulum* (Walker & Jacob, 1798)
Adercotryma glomerata (Brady, 1878)	*Nonionella auricula* Heron-Allen & Earland, 1930
Recurvoides turbinatus Brady, 1881	*Nonionellina labradonca* (Dawson, 1960)
Alveolophragmium crassimargo (Norman, 1892)	*Astrononion gallowayi* Loeblich & Tappan, 1953
Cribrostomoides jeffreysi (Williamson, 1858) *Cribrostomoides subglobosum* (G.O. Sars, 1872)	*Melonis barleeanus* (Williamson, 1858)
Trochammina inflata Montagu, 1808	*Haynesina orbiculare* (Brady, 1881)
Trochammina sp.	*Buccella frigida* (Cushman, 1922)
Tritaxis nana (Brady, 1881)	*Elphidium asklundi* Brotzen, 1943
Spiroplectammina biformis (Parker & Jones, 1865)	*Elphidium subarcticum* Cushman, 1944
Textularia torquata F. Parker 1952	*Elphidium bartletti* Cushman, 1933
Eggerella advena (Cushman, 1922)	*Elphidium clavatum* Cushman, 1930
Miliammina agglutinata (Cushman, 1917)	*Elphidiella arctica* (Parker & Jones, 1864)
	Elphidiella groenlandica (Cushman, 1933)
Miliolata Saidova, 1981	*Cassidulina reniforme* Norvang, 1945
Quinqueloculina arctica Cushman, 1933	*Islandiella norcrossi* (Cushman, 1933)
Quinqueloculina seminula (Linne, 1758)	*Islandiella helenae* Feyling-Hanssen & Buzas, 1976
Quinqueloculina stalkeri Loeblich & Tappan, 1953	*Bolivina pseudopunctata* Hoeglund, 1947
Miliolinella subrotunda (Montagu, 1803)	*Trifarina fluens* (Todd, 1947)
Triloculina trichedra Loeblich & Tappan, 1953	*Stainforthia loeblichi* (Feyling - Hanssen, 1954)
Pyrgo williamsoni (Silvestri, 1923)	*Globobulimina auriculata* (Bailey, 1894)

Calcareous foraminifers dominate this assemblage (36 species) constituting one third of it. Thirteen species of agglutinated foraminifers were identified. The number of species per sample is 35-52. The total abundance of foraminifers per 1 cm^3 of sediment is 89-114 specimens. In the zone affected by the Novaya Zemlya glaciers (station 32) subdominant species are represented by *Cassidulina reniforme* (16-21%) and *Nonionellina labradorica* (15-18%), and in the Karskie Vorota Strait – by *Cibicides lobatulus* (25-34%). The ratio between "dead" and "live" species in this assemblage is 3:1, which is in marked contrast with other foraminiferal assemblages of the Pechora Sea.

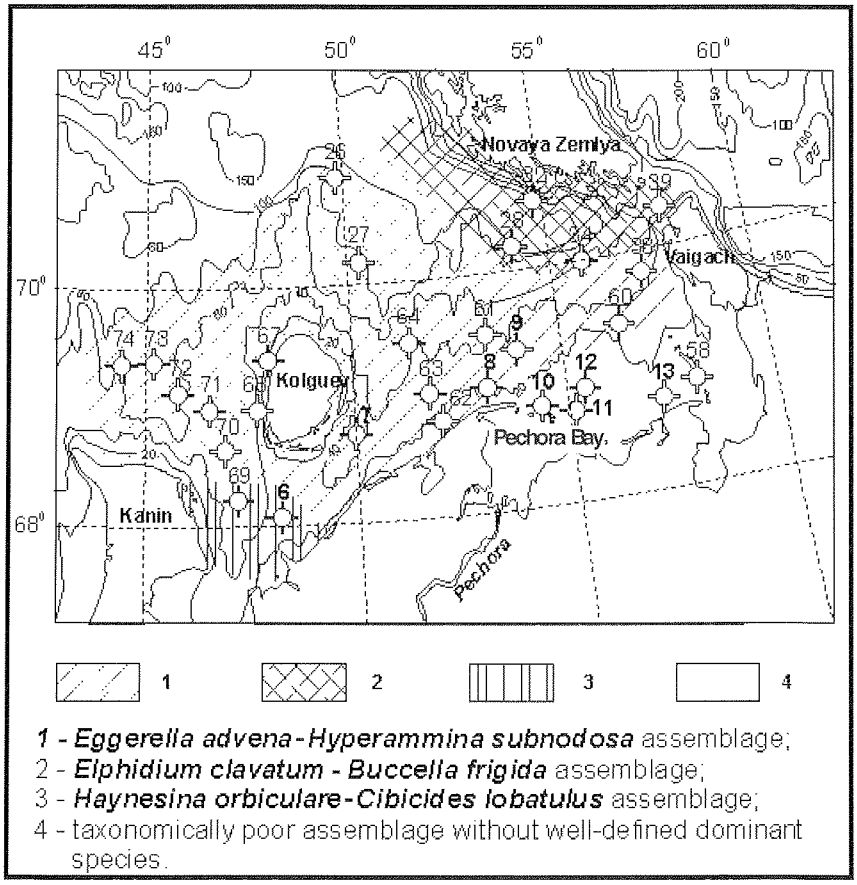

Fig. 1. Modern benthic foraminiferal assemblages in the Pechora Sea

Haynesina orbiculare – Cibicides lobatulus assemblage inhabits the Kanin Peninsula nearshore area within the water depth range of 20-40 m. Surface sediments are represented by coarse- and medium-grained sands. The summer bottom water temperatures here reach 5-7°C. Bottom water salinity is about 33. The total abundance of foraminifers is less than 50 specimens per 1 cm^3 of sediments. Among fourteen species identified in this assemblage only four are agglutinated ones. The ratio between "live" and "dead" specimens is about 1:1. The samples contain abundant *Balanus* shells, worm tubes, ostracods, bivalves, hydroids and bryozoans. Together with abundance of *Cibicides lobatulus* this provides evidence for the active hydrodynamics of coastal waters.

In the southern part of the sea no well-defined dominant species was found. Samples in this zone contain only nine foraminiferal species. Impoverishment of species composition is probably related to the short summer combined with strong freshening of waters (down to 20-14, in the Pechora Bay down to 5), sharp seasonal salinity variations, shallowness and considerable summer warming of bottom waters (up to 11°C). "Live" specimens predominated among calcareous foraminifers. Among agglutinated foraminifers, "live" and "dead" specimens showed

equal abundance. Single "live" specimens had semi-dissolved calcareous tests. That was the case with all tests of *Quinqueloqulina stalkeri* and *Elphidium clavatum*.

Conclusions

Based on the distribution of modern foraminifers and the ratio between "live" and "dead" specimens, four assemblages were established in the Pechora Sea. The greatest part of seafloor with coarse- and medium-grained sands at the depths of 20-100 m is occupied by *Eggerella advena – Hyperammina subnodosa* assemblage dominated by agglutinated foraminifers. In summer, bottom waters in this area are warmed up to 9°C and slightly freshened down to 34.5-32. *Elphidium clavatum - Buccella frigida* assemblage is restricted to silty grounds at the depths of 10-200 m and more stable bottom water environmental conditions with temperatures ranging from –1 to 0°C and salinity exceeding 34. This assemblage is dominated by calcareous forms typical of polar shelf areas. It is also distinguished by a high relative abundance of "dead" specimens (about 75%). Hydrodynamically active shallow regions (20-40 m) experiencing summer freshening (down to 33 ppt) and warming (up to 7°C) are occupied by the taxonomically poor *Haynesina orbiculare – Cibicides lobatulus* assemblage. The southern zone with the strongest summer freshening (down to 5) and heating (up to 11°C) is inhabited by the poorest assemblage without any well-defined dominant species. "Live" specimens dominate in the samples from this zone, which is a result of active post-mortal dissolution and destruction of foraminiferal tests.

Acknowledgments: The author is grateful to Dr. V.B. Khasankaev for sampling and providing the data on bottom water temperature and salinity and N.V. Frygina for sample processing. The research was supported by INTAS (project 1489).

References

Digas, L.A., 1969. Distribution of foraminifers in surface sediments of the Barents Sea and adjacent parts of the Norwegian-Greenland basin. PhD Thesis, Saratov, 27 pp. (in Russian).

Gidrometeorologicheskie usloviya shel'fovoi zony morei SSSR (Hydrometeorological conditions of the shelf seas of the USSR), 1984. Vol. 6. The Barents Sea, part 3. The southeastern part of the sea, 273 pp. (in Russian).

Gus'kov, S.A., 1998. Holocene Foraminifera of the Barents Sea. PhD Thesis, Novosibirsk, 24 pp. (in Russian).

Maier, E.M., 1974. Foraminifera fauna of the Pechora Bay. In: Biologiya Belogo morya (Biology of the White Sea), 4, 123-139 (in Russian).

Matishov G.G., 1997. Bathymetric Map of the Barents and West Kara seas. Russian Academy of Sciences, Murmansk Marine Biological Institute. Mercator projection. Scale 1:2.313.000 at latitude 72°N.

Potanin, V.A., Korotkov, S.V., Savel'eva, S.P. et al., 1986. Environmental conditions of the southeastern Barents Sea shelf. In: Priroda i khozyaistvo Severa (Environment and economics of the North), 14, 37-42 (in Russian).

THE ZOOBENTHOS OF THE PECHORA SEA REVISITED: A COMPARATIVE STUDY

S. G. Denisenko[1], N.V. Denisenko[1], S. Dahle[2] and S. J. Cochrane[2]

[1]Zoological Institute RAS,199034, St. Petersburg, Russia
[2]Akvaplan-niva, Polar Environmental Centre, 9296 Tromsø, Norway

Abstract

Samples of benthic macrofauna from the Pechora Sea (southeastern part of the Barents Sea) were collected during r/v "Dal'nie Zelentsy" cruise in 1992. Parallel sampling and analyses by Russian and Norwegian scientists allow comparing the two datasets, and thus integrating Russian and other international knowledge on benthic fauna of this region. Contrary to the previous opinion about low biodiversity in this region, the fauna richness (446 taxa) appeared to be two times larger. Independent of differences in the sampling equipment and washing procedure, the number of taxa in both Russian and Norwegian datasets was comparable. Some discrepancies in the records of certain faunal groups are attributed to differences in species distribution and identification literature on some systematic groups. In the Russian data, the abundance varied from 666 to 2378 ind./m^2, and the biomass - from 8 to 920 g/m^2. Community-based approach to the numerical analyses of benthic production compared with faunal assemblages (Dahle et al., 1998) shows a general similarity in species composition and abundance distribution only in environmentally stressed areas, where the benthic organisms generally have lower biomass. In the largest part of the Pechora Sea, there is greater heterogeneity among dominant species within the Dahle et al. (1998) data, because the present work incorporates production derived from abundance and biomass.

Introduction

Analyses of benthic communities could be used to assess the effects of different human impacts (Pearson and Rosenberg, 1978), as well as to perform retrospective studies of climatic changes (Deryugin, 1924). Russian scientists have carried out investigations of benthic fauna in the arctic seas (Deryugin, 1928; Pergament, 1945; Zenkevich, 1963). Denisenko et al. (1995) reviewed the studies of macrobenthic fauna of the Pechora Sea (southeastern part of the Barents Sea). However, the focus of these investigations has varied to such an extent that it is difficult to compare the results of the studies over time. In addition to the problem of compensating for and standardizing the different approaches used throughout the years, another important issue is the differences in methodology and analytical approaches used between Russian and other, international laboratories. In Soviet times, a large amount of Russian data did not reach the international scientific community. Therefore, there is an urgent need for mutual exchange of methods and results, as well as for building bridges to earlier findings.

The Murmansk Marine Biological Institute of the Russian Academy of Sciences and Akvaplan-niva, Norway, have been co-operating in the studies of the arctic benthic macrofauna since 1990. In 1992, a cruise aboard r/v "Dal'nie Zelentsy" was organized to study the benthic fauna of the Pechora Sea. During this cruise, parallel sets of samples were collected, using the standard methodology of the respective Russian and Norwegian participating institutes. The Norwegian team used a 50 kg 0.1m^2 Van Veen grab (Van Veen, 1933), and the samples were washed through a 1-mm-meshsize sieve with round holes. The description of the faunal associations was based on a numerical quantification of the species present, as well as on the ecology of the dominant taxa. Using canonical correspondence analyses (CCA), the connection between the faunal data and environmental variables was analyzed (Dahle et al., 1998).

The present work documents the findings of the Russian team, who used a modified Petersen grab (Petersen and Boysen Jensen, 1911) with a sampling area of 0.25 m^2. An integrated, community-based approach to the numerical analyses was applied, combining the species biomass and abundance into a purpose-devised formula to achieve an index of benthic production. The latter is a suitable parameter for estimating the role of each species in a community because it is based on a combination of both abundance and biomass. Although the two datasets are not extensive enough to be used to reveal statistically significant relations between the two approaches, the fact that both sets of samples were collected at the same locations and at the same time allows for a first comparison of the results from the two different sampling and analytical approaches.

Study area

The Pechora Sea occupies the southeastern part of the Barents Sea and is bordered by Kolguev, Novaya Zemlya, and Vaigach islands in the west, north, and east, respectively, and by the mainland in the south (Fig. 1)

The Pechora Sea is a heterogeneous area in terms of water depth (Fig. 1) and sediment type (Adrov and Denisenko, 1996; Dahle et al., 1998). Temperature and salinity of bottom and surface water layers show strong seasonal and spatial variations. Bottom water temperatures reach their maximum in August-September, and generally range from –1°C in the north to 6°C in the southwest, close to the coast (Adrov and Denisenko, 1996). The average bottom salinity in the open part of the Pechora Sea ranges from 34 in winter to 30-31 in early spring due to large amounts of freshwater runoff from the Pechora River and ice melting.

In short, the Pechora Sea forms a mixing zone of four main water masses (Il'in and Matishov, 1992): coastal water masses in the south, waters of Atlantic origin in the central parts, Barents Sea bottom water in the deep trench south of Novaya Zemlya, and Arctic water extending from the Kara Strait and flowing northwards along the Novaya Zemlya coast.

Material and methods

Sampling

Sampling was carried out in July 1992 from the MMBI research vessel "Dal'nie Zelentsy". The station locations (Fig. 1) correspond to those of Dahle et al. (1998). Two additional stations, 6a and 7a, were sampled in the western open sea.

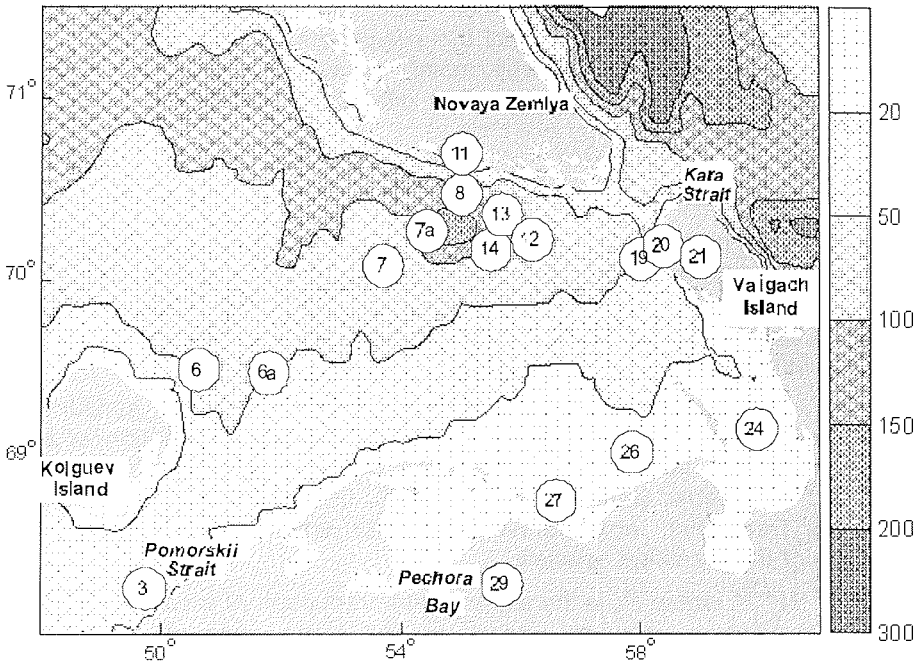

Fig. 1. Location of stations sampled for analysis of benthic fauna in the Pechora Sea. Bathymetry in meters.

Quantitative samples were collected using an Ocean grab (Lisitzin and Udintsev, 1955) with a sampling area of 0.25 m^2. The weight of this grab is *c.* 70-90 kg depending on the additional weight, and its penetration into the ground is 20-25 cm depending on sediment softness. Two or three replicate samples were collected at each sampling station. The samples were gently flushed through a nylon net bag with a square meshsize of 0.75 mm (i.e. diagonal opening close to 1 mm). After washing to remove fine sediment particles, the remaining sediment and animals were fixed in 4% formaldehyde buffered by sodiumtetraborate (hexamine).

Laboratory analyses

In the laboratory, the samples were sieved through a soft nylon mesh with a square meshsize of 0.5 mm in running water to remove formaldehyde and any remaining fine sediment particles. The animals were sorted to different taxonomic groups using a microscope. They were preserved in 70% ethanol, and, subsequently, identified either to species or the lowest taxonomic level possible. Specimens that could not be accurately identified to species level due

to taxonomic difficulties (*Spongia, Cnidaria, Nematoda, Sipuncula, Tunicata*) were identified to generic or family levels, and recorded in the total number of 'taxa'.

The identified species in each sample were counted and weighed (wet mass in alcohol) to 3 decimal points using a calibrated scale. Molluscs, bryozoans, and barnacles were weighed including shell skeleton. The annelids were removed from their tubes for weighing, except the polychaete *Spiochaetopterus typicus*, which was weighed inclusive of tube, mainly because it is entirely self-secreted by the animal, and, also, because it is difficult to remove the tube without destroying the fragile animal.

Numerical analyses

The species numbers and abundance data from the two or three 0.25 m^2 replicates were combined for each station, giving a total sampling area for each station of 0.5 m^2 or 0.75 m^2, respectively. For all stations a mean value for the number of taxa per 0.25 m^2 was calculated, while the abundance and biomass were calculated per one square meter.

Clustering of the benthic communities was carried out using similarities of samples based upon calculations of species production. Estimation of a given species production from its abundance and biomass was suggested by Brey (1990) and Denisenko and Denisenko (1990). In our calculations, the formula derived by Denisenko and Denisenko (1990) was used to figure out the production of the identified species:

$P_s = k\, B_s^{0.75} * N_s^{0.25}$, where P_S is the approximate production of a species in a given sample per year or seasonal growth (in the same units as biomass), B_S biomass, and N_S abundance of 's'-species.

To calculate the inter-station similarity, we applied the Czekanowski-Soerensen index (Czekanowski, 1909; Soerensen, 1948). The production value of each species was used in the calculations as follows:

$$Cz = 2 * \_ [\min (P_{sa}, P_{sb})] / \_ [(P_{sa} + P_{sb})],$$

where P_{sa} is the estimated production of 's-th species at station 'a', P_{sb} the estimated production of 's-th' species at station 'b'.

To determine faunal communities, a standard hierarchical clustering procedure (Pesenko, 1982) with the average linkage method was used. To define the level at which the samples should be assigned to separate communities, the average level of similarity for the whole matrix was calculated (Sirotinskaya, 1975).

The dominant species, after which the communities are named, are the species having the highest "validity". The validity of a given species is calculated as the product of the species production and its frequency of occurrence within samples incorporated into the community.

Station grouping by their similarity on the basis of standardized environmental characteristics (such as depth, bottom temperature, salinity, dissolved oxygen content, type of bottom sediments) was carried out by hierarchic clustering using Euclidean distances as similarity coefficients.

Results

Species composition

A total of 446 different taxa were recorded, of which 343 were identified to species level. The number of taxa at different stations varied between 15 and 129 (per 0.25 m^2).

A total of 16 phyla, 19 classes, and 134 families were recorded. The species number of different systematic groups is presented in Table 1 and Fig. 2A. The highest species richness (129 taxa per 0.25 m^2) was recorded on the mixed bottom sediments near the Kata Gate Strait (St.19, 21, see Fig. 2A).

Table 1. Fauna structure in the Pechora Sea, comparison of the two studies carried out during the same cruise in 1992.

Phylum	Russian data set		Norwegian data set (after Dahle et al., 1998)	
	Total taxa	Species	Total taxa	Species
Protozoa	1	-	1	1
Porifera	1	-	1	-
Cnidaria	31	23	10	3
Nemertini	1	-	1	-
Nematoda	1	-	1	-
Sipuncula	6	4	4	2
Priapulida	3	2	3	2
Echiurida	1	-	2	1
Polychaeta	118	90	117	77
Pantopoda	1	-	2	-
Crustacea	102	76	73	46
Mollusca	93	72	91	68
Bryozoa+ Brachiopoda	61	56	87	76
Echinodermata	22	17	17	14
Tunicata	4	1	6	4
Total	446		416	

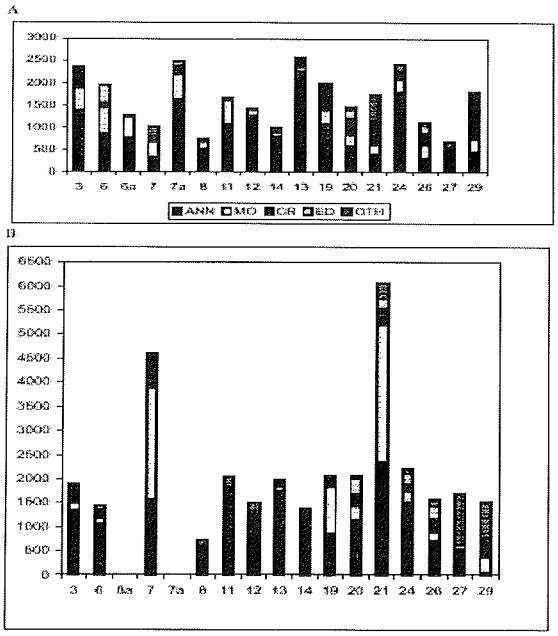

Fig. 2. Faunal structure of zoobenthos at different stations in the Pechora Sea.
A – According to the data set collected by the Russian team in 1992; B – according to the data set collected by the Norwegian team in 1992.
Key: ANN - Annelids; CR - Crustaceans; ED - Echinoderms; MO - Molluscs; OTH - others. Diameter of a circle reflects the number of species found at each station.

The remaining stations located on sandy-mud or muddy-clay sediments contained from 71 to 85 taxa. An impoverished benthic fauna was found in and close to the Pechora Bay (15 and 41 taxa at St. 29 and St. 27, respectively). At all stations *Polychaeta* showed the highest taxonomic diversity.

Abundance

The highest number of individuals at stations 3, 7a, 13 and 24 (Fig. 3A) exceeded 2000 ind./m^2. The lowest abundance was recorded at St. 27 (666 ind./m^2). In general, polychaetes represented the most abundant faunal group, and their abundance varied from 152 (St. 21) to 2248 ind./m^2 (St.13). Polychaetes predominated throughout the whole area except the Pechora Bay (St. 29) and Kara Strait area (St. 19, 21), where crustaceans were dominant with the abundance equal to 1066, 489 and 465 ind./m^2, respectively. The highest abundance of molluscs (573 ind./m^2) was registered at St. 6, and the lowest at stations 12 and 27 (38 and 44 ind./m^2, respectively). Echinoderms were not numerous, and their frequency varied from 6 (St. 6a, 7) to 188 ind./m^2 (St. 6).

Biomass

Fig. 4 presents variations in biomass within the study area. The biomass ranges between 108 and 446 g/m^2 in the northern part of the Pechora Sea with mixed bottom grounds. At St. 6, to the northeast of Kolguev Island, the recorded biomass equals 710 g/m^2. However, this high value is attributed to the presence of a single large specimen of the echinoderm *Henricia scoricovi*. Exclusion of this species reduces the biomass value down to approximately 400 g/m^2. Stations 8, 21, and 24 (the latter two on coarse sediments) are characterized by intermediate biomass values (108, 103, and 122 g/m^2, respectively). In the Pechora Bay, the biomass is 44 g/m^2. The lowest biomass, 8 g/m^2, is found at St. 27, on sandy sediments in the southern part of the study area.

Community structure

Based on the similarity analyses, the benthic fauna of the 16 stations may be grouped into six communities, subsequently referred to as Groups A to F (Fig. 5). Fig. 6 shows the spatial distribution of these communities, and their main characteristics are given in Table 2. The community referred to as Group A includes only one station (7a) located southwest of Novaya Zemlya at the depth of 120 m on soft silty clay sediments with a small sand portion. This community is dominated by two species, *Ctenodiscus crispatus* and *Macoma calcarea*.

Group B (Table 2) is made up of 5 stations (3, 8, 11, 12, 13, 14), four of which (8, 12, 13, 14) are located close to each other in the depression south of Novaya Zemlya, at the depths between 180 and 250 m, which is the deepest part of the Pechora Sea. Stations 3 and 11 are located in shallow areas - in the strait between Kolguev Island and the mainland, and in the Chernaya Fjord. At all five stations characterized by high concentration of organic matter in the sediment surface and subsurface, deposit feeders predominate. The dominant species is *Spiochaetopterus typicus*.

Group C (Table 2) is made up of stations 6, 6a, 7, 19, and 20, all at depths between 88 and 126 m on sandy mud sediments. Stations 6, 6a, and 7 are influenced by currents from the western Barents Sea, while stations 19 and 20 are influenced by the Kara Sea water. This community is dominated by the mobile filter-feeder *Tridonta borealis*. This species has neither the highest abundance nor the biomass, but it occurs in more than half of the samples, which in combination gives the highest species validity within the community. Despite the large biomass of *Henricia scorikovi*, its very low frequency and abundance prevent it from being a dominant or subdominant species for this community.

Group D (Table 2) comprises station 21 located in the Kara Strait. This station is influenced by strong bottom currents and is, therefore, characterized by mixed sediments with a large portion of coarse components such as gravel and pebbles. Due to its high biomass, the dominant species *Strongylocentrotus pallidus* has a twice greater validity than the subdominant species, the erect filter-feeding bryozoan *Myriapora gracilis*, even though the latter is very abundant and present in all samples.

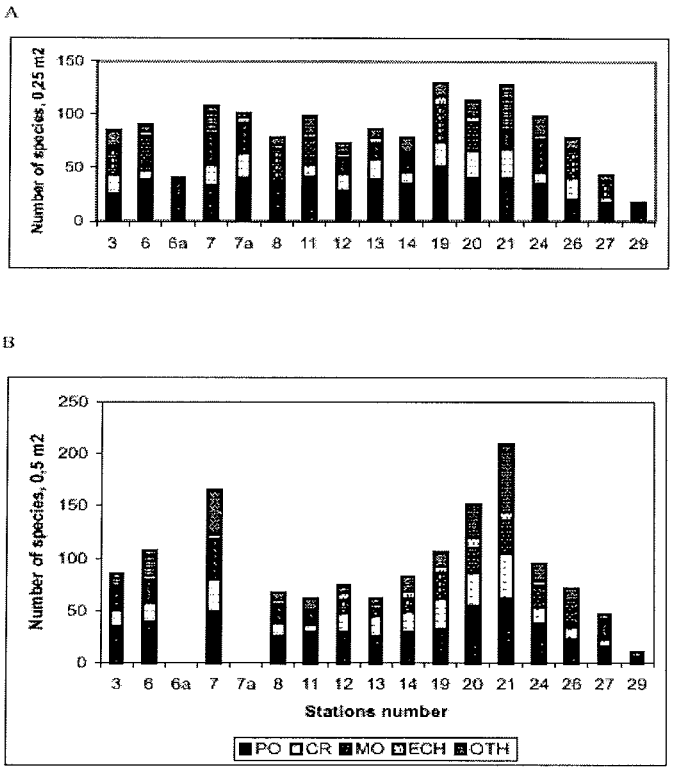

Fig. 3. Abundance (ind./m^2) of the bottom fauna and the share of different systematic groups. A – According to the data set collected by the Russian team in 1992; B – according to the data set collected by the Norwegian team in 1992. Key for group description is the same as in Fig. 2.

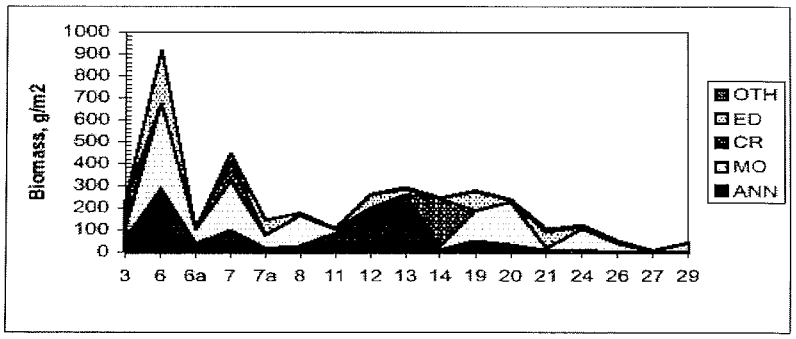

Fig. 4. Biomass (g/m^2) of the bottom fauna and the share of different groups in the study area. Key for group description is the same as in Fig. 2.

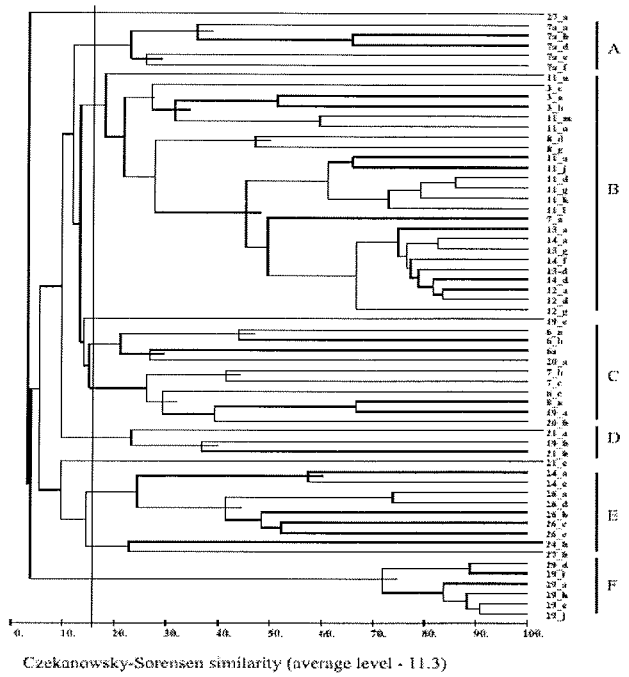

Fig. 5. Cluster diagram showing station grouping based on the similarity of the fauna production data.
A – *Ctenodiscus crispatus-Macoma calcarea* community; B – *Spiochaetopterus typicus* community; C – *Tridonta borealis* community; D – *Strongylocentrotus pallidus* community; E – *Serripes groenlandicus* community; F – *Macoma balthica* community.

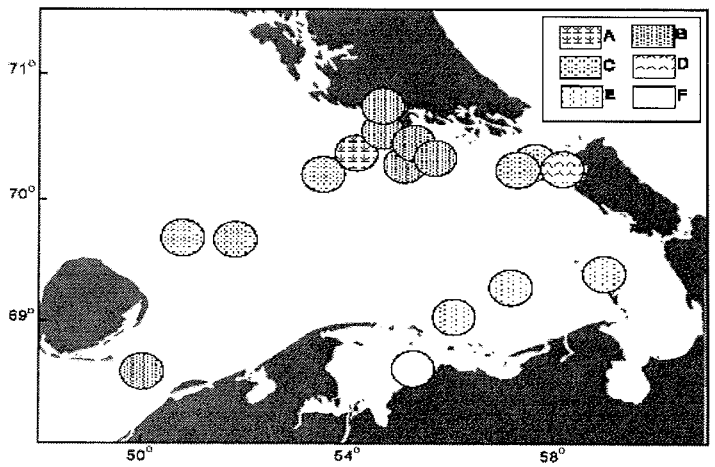

Fig. 6. Distribution of bottom communities in the study area. Key is the same as in Fig. 5.

Table 2. The ten most significant taxa according to their validity *) for every of the six established benthic communities (A-F) in the study area of the Pechora Sea. Average abundance, biomass, frequency, and relative production are indicated for each taxon. Additionally, average biomass, number of species, and samples for every community are given.

Community group with ten most common taxa	Abundance, ind./m^2	Biomass, g/m^2	Frequency of occurrence	Relative production	Species validity*
Group A					
Ctenodiscus crispatus	34	68.11	0.80	57.06	45.64
Macoma calcarea	529	35.87	0.40	70.10	28.04
Yoldia amygdalea	46	18.12	0.60	22.67	13.60
Ophioctén sericeum	44	8.52	1.00	12.84	12.84
Macoma moesta	660	28.88	0.20	63.14	12.62
Portlandia arctica	33	16.73	0.60	19.15	11.49
Nuculana pernula	40	9.67	0.60	13.71	8.22
Lumbriconereis sp.	340	1.68	1.00	5.75	5.75
Scalibregma inflatum	269	1.19	1.00	4.53	4 53
Golfingia margaritacea	4	35.76	0.20	20.68	4.13
Number of samples: 5, Number of taxa: 112, Average biomass: 145.38					
Group B					
Spiochaetopterus typicus	220	110.86	0.82	129.91	107.32
Maldane sarsi	264	22.27	1.00	38.85	38.85
Chaetozone setosa	516	2.42	0.95	9.12	8.72
Ctenodiscus crispatus	11	21.65	0.47	16.50	7.89
Yoldia amygdalea	74	21.49	0.21	23.47	5.10
Priapulus caudatus	17	6.95	0.56	6.15	3.48
Lumbriconereis sp.	288	1.22	0.69	4.74	3.30
Ophiocten sericeum	36	3.87	0.47	6.70	3.20
Nicania montagui	37	7.78	0.26	11.26	2.93
Thyasira gouldi	135	1.58	0.52	4.63	2.41
Number of samples: 23, Number of taxa: 257, Average biomass: 166.80					
Group C					
Tridonta borealis	39	126.34	0.55	87.54	48.63
Travisia forbesii	27	155.36	0.33	99.65	33.21

Henricia skorikovi	10	698.00	0.11	241.48	26.83
Cillatocardium ciliatum	9	80.01	0.55	45.33	25.18
Golfingia margaritacea	17	99.08	0.33	63.75	21.25
Nicania montagui	62	16.55	0.88	21.48	19.09
Balanus crenatus	94	82.54	0.22	81.78	18.17
Spiochaetopterus typicus	64	9.18	0.88	14.31	12.72
Maldane sarsi	97	5.39	0.88	10.66	9.48
Macoma calcarea	28	51.58	0.22	41.2	59.16

Number of samples: 9, Number of taxa: 229, Average biomass: 427.25

Group D

Strongylocentrotus pallidus	12	98.36	1.00		
	57.72	57.72			
Myriapora subgracilis	212	11.72	1.00	23.91	23.91
Celleporina incrassata	36	11.10	1.00	14.86	14.86
Macoma calcarea	60	17.36	0.50	23.67	11.83
Ophiura robusta	88	6.24	0.50	12.09	6.04
Alvania viridula	8	6.80	0.50	7.08	3.54
Nephtys ciliata	4	7.28	0.50	6.27	3.13
Rhodine gracilior	86	0.40	1.00	1.52	1.52
Polychaeta varia	4	1.27	1.00	1.48	1.40

Number of samples: 2, Number of taxa: 112, Average biomass: 150.91.

Group E

Serripes groenlandicus	10	55.89	0.66	35.01	23.34
Stegophiura nodosa	135	4.88	0.77	11.04	8.58
Bivalvia g.sp.	61	5.28	0.77	9.17	7.13
Ascidiacea g.sp.	34	5.37	0.44	8.49	3.77
Pelonaia corrugata	56	11.16	0.22	16.50	3.66
Owenia fusiformis	74	1.23	1.00	2.78	2.78
Modiolus modiolus	12	23.72	0.11	20.00	2.22
Myriochele oculata	338	0.35	1.00	1.93	1.93
Scoloplos armiger	68	0.55	1.00	1.78	1.78
Edwardsiidae g.sp.	23	1.14	0.77	2.25	1.75

Number of samples: 9, Number of taxa: 146, Average biomass: 70.64

Group F

Macoma balthica	245	38.51	1.00	60.39	60.39

Pontoporeia femorata	790	2.36	1.00	10.07	10.07
Halicriptus spinulosus	121	1.24	1.00	3.75	3.75
Spionidae g.sp.	71	0.78	1.00	2.23	2.23
Diastylis sulcata	201	0.22	1.00	1.22	1.22
Nemertini g.sp.	16	0.66	0.83	1.40	1.17
Nephtys minuta	208	0.07	1.00	0.56	0.56
Polychaeta varia	12	0.12	1.00	0.36	0.36
Amphipoda g. sp.	72	0.04	1.00	0.29	0.29
Yoldielia intermedia	10	0.50	0.16	1. 05	0.17

Number of samples: 6, Number of taxa: 16, Average biomass: 44.08

*) Species validity is the species production multiplied by their frequency of occurrence.

Group E (Table 2) encompasses stations 24, 26, and 27 located in the shallow southern part of the study area on sandy sediments with low organic content. The area is influenced by coastal water masses with highly variable temperature and salinity. The benthic community is dominated by filter-feeding bivalve *Serripes groenlandicus*. Due to its large biomass, *S. groenlandicus* has a validity three times higher than that of the subdominant species, the carnivorous brittle-star *Stegophiura nodosa*, although the abundance of the latter species is ten times higher than that of the former.

Group F (Table 2) contains samples from St. 29 in the estuarine part of the Pechora Bay. The muddy sediments in this area are under strong influence of brackish water. Species richness, abundance, and biomass are relatively low; the dominant species is the deposit feeding mollusc *Macoma balthica*. Although the abundance of the subdominant species, the amphipod *Pontoporeia femorata*, is approximately three times higher than that of *M. balthica*, the latter taxon has a far higher biomass (38.5 g/m^2).

Discussion

Zenkevich (1927) recorded only 220 species of macrozoobenthos from the Pechora Sea, and considered the region to be relatively poor in species. The number of species recorded during the present study is 446, while the Norwegian team reported 416 species (Dahle et al., 1998). Some discrepancies were found between the two datasets in certain faunal groups, for instance, the phyla *Polychaeta* and *Crustacea,* resulting from differences in species identifications and synonyms of the taxa in the taxonomic literature used by the two teams. In addition, the phylum *Hydroidea,* was identified to species level in the Russian but not the Norwegian samples.

Nevertheless, the two datasets demonstrate similar results in terms of species composition and spatial distribution of species numbers (Fig. 2 A, B). The highest species richness in both sets of samples was observed near the Kara Strait, where the seafloor consists of mixed grounds offering a wide range of habitat types. A sparser benthic fauna found in the Pechora Bay and in the area around the Pechora river mouth reflects a benthic fauna which has to cope with low salinity (Remane and Schpileper, 1971) and a strong seasonal variation in temperature and salinity (Adrov and Denisenko, 1996). The low species

richness, abundance and biomass, found immediately outside the bay as well as in the other seas influenced by strong freshwater discharge (Denisenko et al., 1999), most probably reflect a quite uniform shallow water habitat of unstable sand, as is the case around the mouth of the Ob' Bay (Milliman and Syvitski, 1992; Lisitzin, 1995).

In general, the proportion of species from different systematic groups is similar in the Russian and Norwegian samples from the same stations. But at the stations 7 and 21, the number of species in the Russian samples was approximately 2/3 as compared to the findings of the Norwegian team. Small forms of crustaceans, such as *Byblis gaimardi* and *Protomedia fasciata,* and some species of echinoderms and polychaetes were not recorded in the Russian samples. These differences are attributed either to patchy occurrences of the organisms concerned, or to differences in sampling on stony or sandy sediments between the van Veen and "Ocean" grabs.

The environmental conditions, particularly bottom topography, sediment type, and water depth, strongly influence benthic community structure (Figs. 7, 8) as has been demonstrated for the study area (Dahle et al., 1998), which is not subjected to any significant anthropogenic impact (Loring et al., 1995).

The accumulation areas with high concentrations of total organic carbon (TOC) correlative to the fine fraction portion in bottom sediments (Klenova, 1960; Loring et al., 1995) are located in the Chernaya Fjord (St.11), Pomorskii Strait between Kolguev Island and the mainland (St.3), in the depression south of Novaya Zemlya (St. 7a, 8, 12-14), and near Dolgii Island (St. 24) (Loring et al., 1995). Surface and sub-surface deposit-feeding polychaetes are the most abundant faunal group in all these areas (Fig. 3 A, B). At station 29 located in the Pechora Bay, where TOC content is high, but salinity is very low, the deposit-feeding brackish-water bivalve *Macoma balthica* is the most abundant. Co-dominance of filter-feeding molluscs and bryozoans was observed in the nearshore zone (St. 21) and farther offshore at St. 7 located on the coarse grounds close to the Kara Gate Strait. This area is affected by strong bottom currents. Similar groups predominate at shallow St. 26 with water depth less than 15 m and strong water mixing. Like in the case with abundance, the biomass of polychaetes is the highest in organic-rich soft muddy sediments (St. 11, 12, 13) in the deepest northern part of the Pechora Sea. Polychaetes constitute the main part of the total biomass, because big molluscs with heavy shells, such as *Tridonta borealis* or *Nicania montagui*, are rare there.

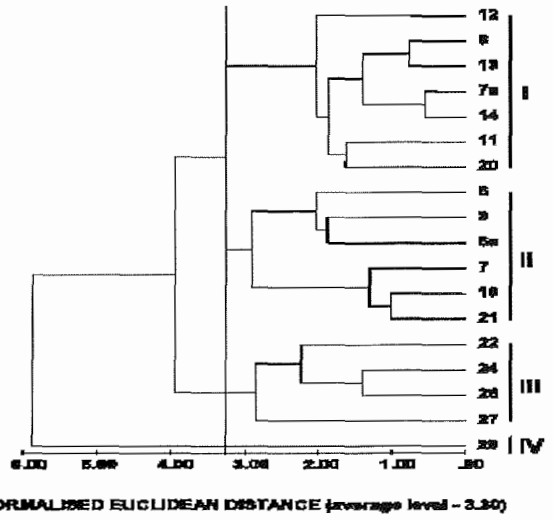

Fig. 7. Cluster diagram showing station grouping based on the similarity of environmental data.

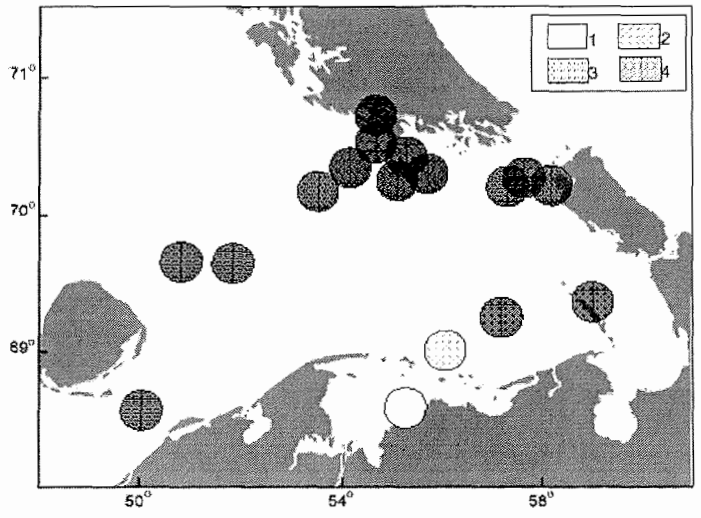

Fig. 8. Distribution of station groups according to their environmental characteristics (bottom sediments, depth, temperature, and salinity). Key: 1 – estuarine shallow station; 2 – marine shallow stations with low TOC; 3 - marine stations with intermediate TOC; 4 – deep marine stations with high TOC.

An increase in coarse fraction portion leads to a change in the dominant group constituting the main part of the total biomass of zoobenthos, and detritovorous polychaetes are substituted by filter-feeding molluscs. At St. 6 and 7 on mixed grounds, the biomass of polychaetes is still quite high, but molluscs become more abundant compared to muddy sediments and, as a result, they dominate over polychaetes. Mobile and very large carnivorous animals, such as starfishes

and crabs, are rarely caught by grab in the offshore area, but their occasional appearance can sometimes considerably increase the total biomass, as is the case with St. 6. It is an accidental fact, because biomass of echinoderms in the Pechora Sea does not usually exceed 50 g/m^2 (Khodkina, 1964).

The predominance in biomass of a detritovorous feeder, sea urchin *Stongylocenthrotus pallidus,* at St. 21 on mixed grounds with low organic content is due to the presence of fine fraction in the surface sediment layer. The presence of diverse bryozoans, immobile filter-feeders with comparatively large biomass, testifies to the considerable portion of coarse fraction in the sediment of the area with good water exchange and high content of suspended organic matter in water column (Zenkevich, 1927).

As shown by Kuznetsov (1970), the trophic structure of fauna in a certain area is, in general, determined by a species, or several species with the same type of feeding, which have the biggest share in the total biomass of zoobenthos. Figures 7 and 8 show the four discrete groups of stations that differ from each other mainly in water depth and salinity. Group One occupies the areas deeper than 100 m, and Group Two occurs at the depths between 50 and 100 m. The stations of both groups are restricted to organic-rich sediments (Loring et al., 1995). Surface (*Spiochaetopterus typicus, Macoma calcarea*) and sub-surface (*Maldane sarsi*, *Pectinaria hyperborea*) deposit feeders predominate in Group One. Group Two is dominated by mobile filter-feeding species (*Tridonta borealis, Nicania montagui, Ciliatocardium ciliatum*). Group Three includes shallow stations located at depths of 10-20 m. Suspension feeders, such as bivalve *Serripes groenlandicus*, bryozoans, and the ascidian *Pelonaia corrugata* predominate in the southern regions of the Pechora Sea and Kara Strait. A single station in the Pechora Bay forms Group Four, where deposit feeders predominate. In general, the bay represents a typical high latitude estuarine zone (Denisenko et al., 1999), where the distribution of abundance and biomass, as well as trophic structure, agree well with the generalized scheme for the whole Pechora Sea plotted on the basis of the data collected in 1992-1994 and the present data set (Denisenko et al., 1997).

As noted by Dahle et al. (1998), there are two main quantitative approaches to determine benthic communities or faunal associations. One approach mainly uses abundance (Petersen, 1913), whereas the other approach, usually adopted by Russian scientists, uses biomass or some other derivative (Moebius, 1877; Brodskaya and Zenkevich, 1939; Vorob'ev, 1949). The role of an organism in the transformation of matter and energy can be estimated knowing its respiration and production. Using the calculated production values reflecting the integrated data on abundance and biomass allows determining the functional role of each species in the community (Alimov, 1989; Brey, 1990; Denisenko and Denisenko, 1990). Owing to the use of production values, the importance of numerous small-bodied organisms and a single individual of a large-size species in the total production of a community can be compared and estimated. Thus, production characteristics allow statistically grouping samples collected throughout the year, including periods of mass juvenile recruitment. Comparison of the present results with previously published data (Zenkevich, 1927 *in* Dahle et al., 1998; Fig.6), which were based on analysis of biomass only, demonstrates a certain similarity in the structure of bottom communities of the Pechora Sea. The main

difference lies in a slightly reduced significance of large-size molluscs in the given outcome.

The present results show similar trends in community boundary determination to those outlined by Dahle et al. (1998), who used only numerical abundance in the faunal analyses. In both studies, a similar distribution pattern and similar dominant species were found in the areas subjected to environmental stress, such as the fjordic Chernaya Bay, the cold-water depression south of Novaya Zemlya, and the estuarine Pechora Bay. Opposite to this, in the open part of the Pechora Sea the dominant species of the communities determined with the use of production values differ markedly from those determined by abundance data only.

The reliability of the results in faunal groups analysis increases with growing number of stations and replications involved in the calculations. Thus, when the data of the present study are incorporated into larger-scale analyses (Denisenko et al., 1997), the minor difference is not unexpected. The distribution area of some communities determined during the present calculations was reduced, because some stations were included in the neighboring communities and integrated with them. It happened because in large-scale calculations significance for some species was decreased, while for other species it was increased. The last group of species is more regularly distributed as it is present in all investigated samples and replications.

Conclusions

Contrary to the existing opinion about sparse benthic fauna in the Pechora Sea resulting from long ice-covered period, insignificant Atlantic influence, and considerable freshwater runoff of the Pechora River (Zenkevich, 1927) the number of species appeared to be comparable with the number of species in the western Barents Sea (Brodskaya and Zenkevich, 1939). The present study supports previous investigations that have described plentiful sublittoral zoobenthos in this area (Denisenko et al., 1995; Antipova, 1975).

Trophic structure of zoobenthos, its biomass and abundance strongly depend on environmental conditions in the study area, as has been demonstrated by zoobenthos abundance in parallel data sets from the same cruise (Dahle et al., 1998).

Compared to the parallel data sets from the same stations analyzed using numerical abundance only (Dahle et al., 1998), the present study reveals differences in the species considered as dominant ones. However, in environmentally stressed areas, such as the Chernaya Bay and the depression south of Novaya Zemlya, where the dominant animals are relatively low in biomass, bottom communities were dominated by the same species.

Acknowledgements: We thank the European Community for financial support within the framework of INTAS Project 1489-99 «The Pechora Sea – Late Pleistocene paleogeography, present state of the shelf and coastal zone and forecast for the 21st century», and the Research Council of Norway for financial support within the framework of the cooperation program between Eastern

Europe and Russia (project 120429/730). The captain and the crew of RV "*Dalnie Zelentsy*", Lars-Henrik Larsen (Akvaplan-niva), and Natalia Anisimova (MMBI) are acknowledged for fieldwork. Elena Frolova (MMBI), Elena Luppova (MMBI), Runo Palerude (Akvaplan-niva), Natalia Anisimova (MMBI) and Ninel Panteleeva (MMBI) identified polychaetes, crustaceans, echinoderms and hydroids, respectively.

References

Adrov, N.M., Denisenko G.S., 1996. Oceanographic characteristics of the Pechora Sea. In: Matishov, G.G., Tarasov, G.A., Denisenko, S.G., Denisov, V.V., Galaktionov, K.V. (eds.), Biogeocoenoses of glacial shelf of the western Arctic Seas. Apatity, Kola Centre RAN, 166-179 (in Russian).

Alimov, A.F., 1989. Introduction in productive hydrobiology. Leningrad, Gidrometeoizdat, 152 pp. (in Russian).

Antipova, T.V., 1975. Distribution of zoobenthos biomass in the Barents Sea. PINRO proceedings, 35, 121-123 (in Russian).

Brey, T. ,1990. Estimating productivity of macrobenthic invertebrates from biomass and mean individual weight. Meeresforsch., 32, 329-343.

Brodskaya, V.A., Zenkevich, L.A., 1939. Quantitative distribution of zoobenthos in the Barents Sea. Trudy VNIRO. Moskow. 4, 3-159 (in Russian).

Czekanowski, J., 1909. Zur Differential diagnose der Neandertalgruppe. Korrespl. Dtsch. Ges. Anthropol., 40, 44-47.

Dahle, S., Denisenko, S.G., Denisenko, N.V., Cochrane, S., 1998. Benthic fauna in the Pechora Sea. Sarsia, 83,183-210.

Denisenko, N.V., Denisenko, S.G., 1990. Biomass, density of populations, and their contribution to productivity of bottom communities. In: Problems of nature preservation in the Northern areas. Proceedings of the conference of young scientists, Murmansk, 53-54 (in Russian).

Denisenko, G.G., Denisenko, N.V., Dahle, S., 1995. Baseline Russian investigations of the bottom fauna in the south-eastern part of the Barents Sea. In: Skjodal, R.H., Hopkins, C., Erikstad, K.E., Leinaas, H.P. (eds.), Ecology of Fjords and Coastal Waters, Elsevier Science B.V., 293-302.

Denisenko, S.G., Denisenko, N.V., Frolova, E.A., Anisimova, N.A., Sandler, H,, Dahle, S., 1997. Current state of bottom fauna and structure of bottom communities in the Pechora Sea. In: Volkov, V., Kosheleva, G.J., Smolyanitskii, V., Vinje, T. (eds.), Natural conditions of the Kara and Barents seas. Proceedings of the Russian-Norwegian workshop-95, Norsk Polarinstitutt rapportserie, Oslo, 97, 390 –394.

Denisenko, S., Sandler, H., Denisenko, N., Rachor, E., 1999. Current state in two estuarine bays of the Barents and Kara seas. ICES Journal of Marine Science, 56,187-193.

Deryugin, K.M.,1924. The Barents Sea along the Kola section. Proceedings of the Northern science-fishery expedition,19, 3-103 (in Russian).

Deryugin, K.M. 1928. The White Sea fauna and environment of its existence. Explorations of the seas of the USSR, 7-8, 512 pp. (in Russian).

Il'in, G.V., Matishov, G.G., 1992. Oceanographic conditions in the Pechora Sea in July. In: An international (American-Norwegian-Russian) ecological expedition in the Pechora Sea, Novaya Zemlya, Vaygach, Kolguyev and

Dolgiy islands, July, 1992 (R.V. "Dalnie Zelentzy"). MMBI report, Russian Academy of Science, Apatity, Kola Science Centre, 7-11 (in Russian).

Khodkina, I.V., 1964. Echinoderms of the southern part of the Barents Sea. New investigations of plankton and benthos in the southern part of the Barents Sea Moskva-Leningrad: Nauka. 41-71 (in Russian).

Klenova, M.V., 1960. Geology of the Barents Sea. Moscow-Leningrad, Ac. of Sci. of the USSR, 367 pp. (in Russian).

Kuznetsov, A.P., 1970. Distribution patterns of bottom invertebrate trophic groups in the Barents Sea. Proceedings of the Oceanographic Institute 88, 5-80. (in Russian).

Lisitzin, A.P., 1995. The marginal filter of the Ocean. Oceanology, 34(5), 671-682 (in Russian).

Lisitzin, A.P., Udintsev, G.B., 1955. A new type of grab. Proceedings of the USSR Hydrobiological Association. 6, 217-222 (in Russian).

Loring, D.H., Naes, K., Dahle, S., Matishov, G.G., Ilyin, G., 1995. Arsenic, trace metals, and organic micro contamination in sediments from the Pechora Sea, Russia. Marine Geology, 2,153-167.

Moebius, K., 1877. Die Auster und die Austerwirtschaft. Berlin, 59 pp.

Milliman, J.D., Syvitski, J.P.M., 1992. Geomorphic/tectonic control of sediment discharge to the oceans: The importance of small mountainous rivers. Journal of Geology, 100, 525-544.

Pearson, T.H., Rosenberg, R., 1978. Macrobenthic succession in relation to organic enrichment and pollution of the marine environment. Oceanography and Marine Biology Annual Review,16,229-311.

Pergament, T.S., 1945. Benthos of the Kara Sea. Problems of the Arctic, 1, 3-54 (in Russian).

Pesenko, J.A., 1982. Principles and methods of quantitative analyses in faunistic studies. Moscow, Nauka, 287 pp. (in Russian).

Petersen, C.G.J., 1913. Valuation of the sea. 2. The animal communities of the sea bottom and their importance for marine zoogeography. Report of the Danish Biological Station, 21, 1-44.

Petersen, C.G.J., Boysen Jensen P., 1911. Valuation of the sea. I. Animal life of the sea bottom, its food and quantity. Report from the Danish Biological Station, 20, 81.

Remane A., Schpileper, C., 1971. Biology of brackish water. Second edition. Die Binnengewässer, 25, 372 pp.

Sirotinskaya, S.V., 1975. Logic-informational decisions of geological tasks. Moscow, Nauka. 262 pp. (in Russian).

Soerensen, T.A., 1948. A new method of establishing groups of equal amplitude in plant sociology based on similarity of species content and its application to analysis of vegetation on Danish commons. Rgl. Dan. Videnskab. selskab. Biol. Skr., 5(4), 1-34.

Van Veen, J., 1933. Onderzoek naar het zandtransport von rivieren. De Ingenieur, 48, 151-159.

Vorob'ev, V.P., 1949. Sea of Azov benthos. AzCherNIRO Proceedings, 13, 193 pp. (in Russian).

Zenkevich, L.A., 1927. Quantitative estimation of the bottom fauna of the Pechora region, the Barents and White Seas. Proceedings of Floating Marine Scientific Institute, 2(4), 3-64 (in Russian).

Zenkevich, L.A., 1963. The biology of the seas of the USSR. Moscow, Academy of Sciences of the USSR, 739 pp. (in Russian).

SUBMARINE TERRACES OF THE PECHORA SEA

Yu.A. Pavlidis, N.N. Dunaev, S.L. Nikiforov, A.V. Artem'ev, N.V. Politova

Shirshov Institute of Oceanology RAS, Moscow, Russia

Abstract

For the first time, well-defined submarine terraces were recorded on the Pechora Sea floor, which was previously referred to as a gently sloping submarine plain. These conclusions are based on "Parasound" acoustic profiling. The terraces were found at the depths of 140, 120, 110, 100-104, 60, 50-54, 40, 32, and 25 m. The terraces located at depths of 50-54 and 120 m show the best preservation. The 120 m deep terrace is tentatively correlated with the Late Glacial sea-level lowstand, and the one at 50-54 m water depth with the pre-Holocene time (12-11 ka). The presence of submarine terraces on the Pechora Sea floor is inconsistent with the existence of the Late Würm ice cap on the Pechora Sea shelf, and contradicts coalescence of the Northern Ural and Novaya Zemlya ice caps.

Introduction

There are many questions in the Late Pleistocene-Holocene history of the Pechora Sea that remain to be answered. The most debatable one is the problem of existence or, on the contrary, absence of the Late Würm ice cap. However, there is no agreement among defenders of the ice cap existence regarding the extent of the ice cover. Whereas some of them support the idea of panarctic glaciation, the others consider the Pechora Sea to be the place of coalescence of the Novaya Zemlya and Northern Ural ice caps. Some scientists including the authors support the hypothesis of the limited extent of ice caps and believe that during the last glacial maximum the studied region represented an arctic tundra, and only in the Southern Novaya Zemlya Trough (SNZT) there was a sea basin covered by pack and seasonal ice. Here we present new data on distribution of a series of submarine terraces on the Pechora Sea floor along with certain paleoenvironmental reconstructions. The lower terrace at 120 m water depth corresponds to the generally assumed depth interval of sea-level lowstand during the last glacial maximum, without corrections on the thickness of the Holocene sediments and tectonic movements.

The conclusions based on the geomorphological analysis of bottom topography, morphology and morphometry of terraces are preliminary. Paleoenvironmental reconstructions for the Late Valdai epoch in the Pechora Sea require additional drilling data, biostratigraphical evidence, absolute age dating, and facial-genetic analysis of the Holocene sediment sequence.

Materials and terminology

The article analyzes materials of echo sounding carried out during the 8th cruise of r/v "Professor Shtokman" (1982), and "Parasound" seismoacoustic records with 0.5 m resolution obtained during the 11th (1997) and 13th (1998) cruises of r/v "Akademik Sergei Vavilov". For our purposes the most informative transects are those crossing the Pechora Sea from the SNZT to the coastline, which allowed

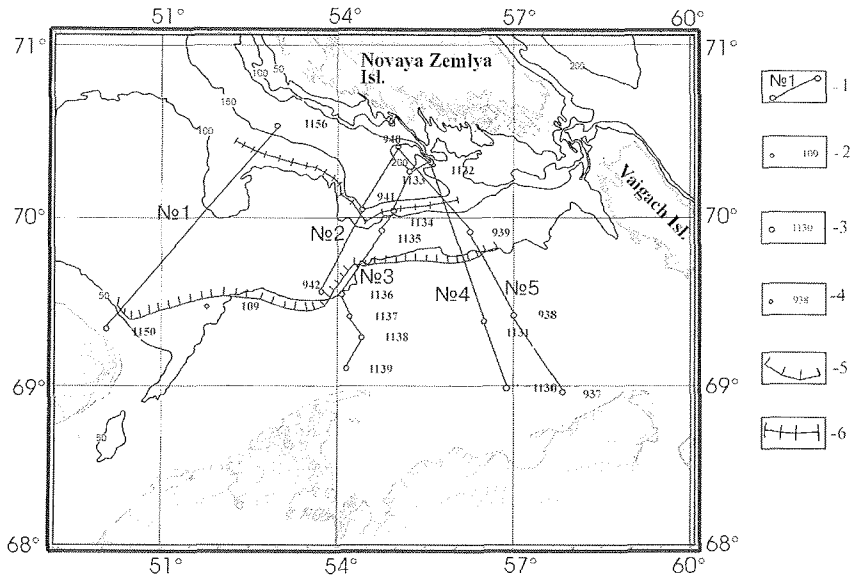

Fig. 1. The Pechora Sea.
Key: 1 - locations and numbers of bottom profiles; 2 - boreholes; 3 - stations of RV "Professor Shtokman"; 4 - stations of RV "Akademik Sergei Vavilov"; Submarine terraces at: 5 - 50-54 m; 6 - 120 m.

tracing the submarine terraces on the gently sloping towards SNZT seabed. For convenience these profiles were numbered from 1 up to 5 (Fig. 1).

A marine terrace is a subhorizontal or gently sloping surface of marine origin limited by a cusp that was formed during previous epochs of sea-level high or lowstands.

Morphometry and morphostructure of terraces

Until recently the Pechora Sea floor was characterized as a gently sloping plain slightly inclined towards the SNZT, as is shown in all bathymetric maps. The profiling revealed the plain to have a number of terrace levels stretching across the whole sea, approximately along the isobaths.

Seismoacoustic profile № 1 (Fig. 2A) stretches southwestward from the Novaya Zemlya Archipelago, through the SNZT, to Kolguev Island. The northern rocky slope of the SNZT is steep and formed by a series of tectonic faults. It has no terraces. The southern slope is gentle and consists of sedimentary rocks overlain by a poorly consolidated sediment cover. A trough bed represents a relatively plane surface with 20-m-deep and 4-km-wide V-shaped trench at the depth of 166-167 m.

At least three distinct terraces could be traced at the southern SNZT slope. ***The first,*** lowermost, terrace is located at the depths from 118 m (inner border) to 120 m (terrace cusp) (Fig. 3A). Its nearly 2-km-wide surface is almost horizontal with a very small inclination (φ=0,001) to the trough thalweg. It has a rough surface with relative height range of about 1-3 m. The gentle 5-m-high bench separates the 120-m-high terrace from ***the second*** one located at the depth of 110 m.

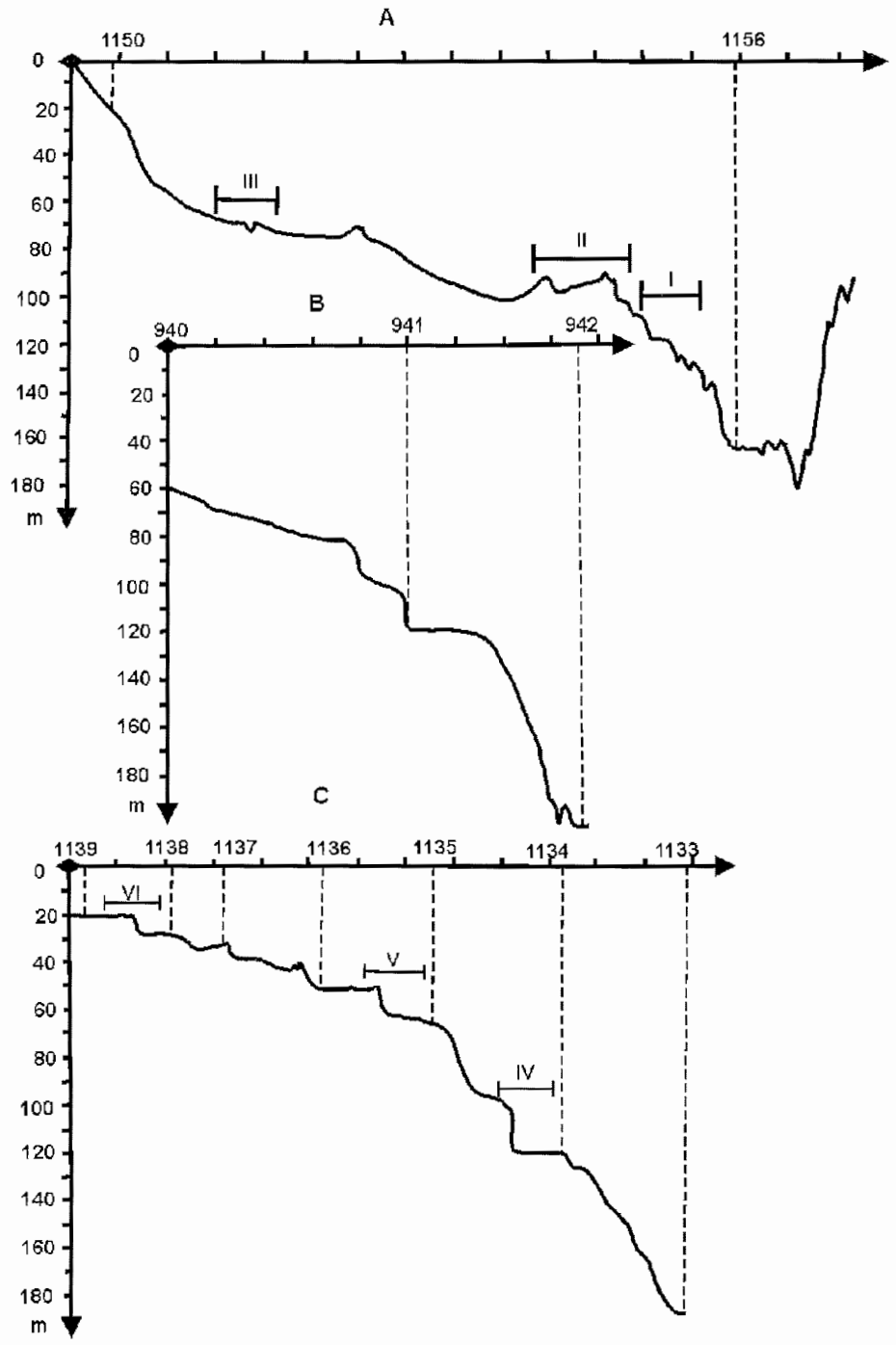
A
1150
1156
0
20
40
60
80
100
120
140
160
180
m
III
II
I
B
940
941
942
C
1139
1138
1137
1136
1135
1134
1133
VI
V
IV

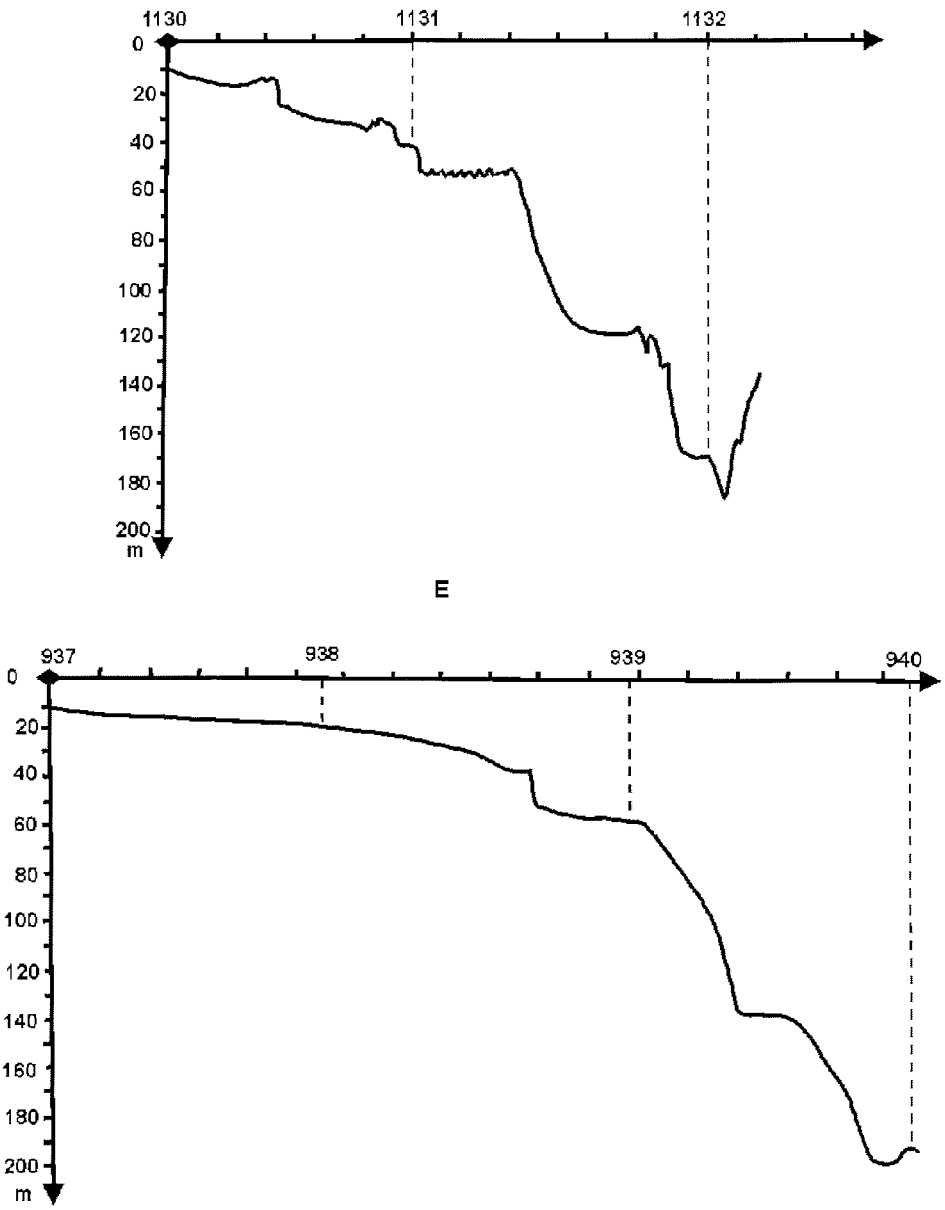

Fig. 2. Bottom profiles: **a)** A - seismoacoustic profile 1; B - echo sounding profile 2; C - seismoacoustic profile 3; **b)** D - seismoacoustic profile 4; E - echo sounding profile 5.
The Roman figures on profiles designate fragments of "Parasound" record.

The latter has a convex wavy cusp and slightly concave (about 2 m) surface with a width of 4 km and a depth of 110 m. A 6-m-high gentle bench separates this terrace from ***the third*** terrace located within the southern SNZT slope at the depth of 105 m (Fig. 3B). Seismoprofiling record allows assuming accumulative origin of

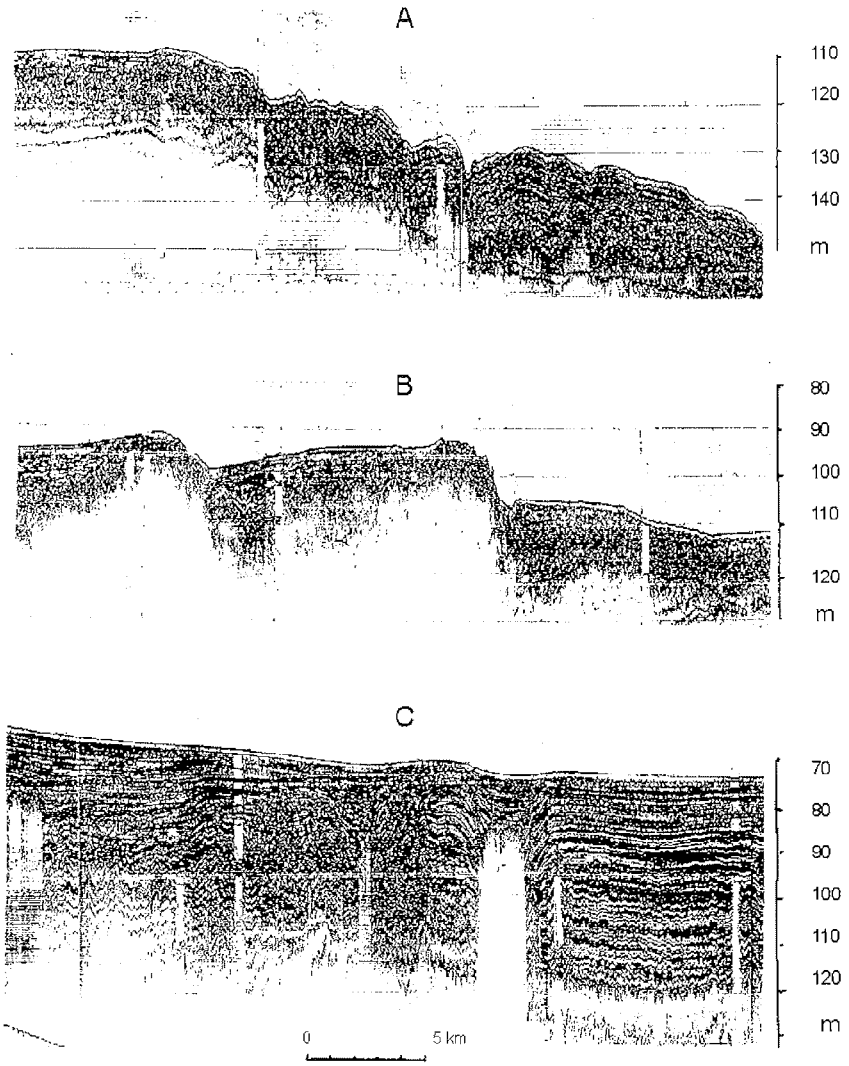

Fig. 3a

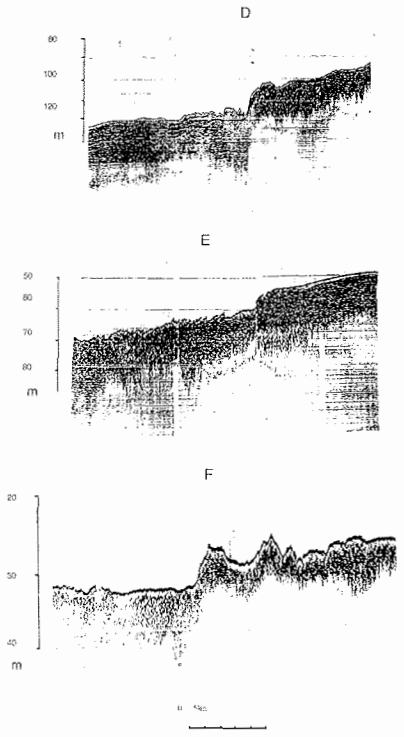

Fig. 3. Fragments of "Parasound" records:
a) A - fragment I: terrace at the depth of 120 m (profile 1); B - fragment II: terrace at the depth of 105 m divided by listric faults (profile 1); C - fragment IIIa: bottom structure at the depth of 70-75 m with cryogenic deformations (profile 1);
b) D - fragment IV: terrace at the depth of 120 m (profile 3); E - fragment V: terrace at the depth of 60 m with surface of sandy waves (profile 3); F - fragment VI:

these terraces. The thickness of stratified deposits ranges from 15 to 20 m. The 105-m-high terrace is separated by a rather steep bench from the flat rise at the top of the SNTZ border. The top of this rise is located at the depth of 91-92 m and is cut by the so-called listric faults. This surface and the rise itself mark a zone of slope discontinuity and transition to the central Pechora Sea shelf. The latter has a structural rise in the middle that represents a northwestern pericline of the Zakhar'inskii arch. The arch separates two depressions filled with stratified loose sediments. Maximuml sediment thickness in the depression located to the north from the arch reaches 35-40 m as determined by sounding, while in the southern depression it exceeds 50 m. Borehole 109 recovered southeastward from this profile has the following sediment sequence, that has been palynologically studied by Rudenko (2001):

0-2,5 m - dark gray silty mud with sand and gravel. Pollen of dwarf birch, pine, fur; spores of arctic lycopodiums.

2,5-5,0 m - fine-grained sand and silt with gravel. Pollen of wormwood and grass.

5,0-9,1 m - dark gray clay with gravel and pebbles. Only ancient redeposited pollen and spores.

9,1-12,0 m - fine-grained laminated sand with gravel. Only ancient redeposited pollen and spores.

12,0-41,0 m – lacustrine clayey laminated deposits (continental). Pollen of Mesozoic conifers.

Rudenko (2001) regards the upper 5-meter layer as the Holocene sediments, and the underlying layer (5-9.1 m) as the Late Würm deposits. The basal lacustrine clays yield pre-Cenozoic (probably Late Cretaceous) age.

Sediments filling the depression between the Zakhar'inskii arch and Kolguev Island exhibit obvious signs of cryogenic alteration as evidenced by cryogenic deformations and possible presence of ice wedges (Fig. 3C).
Towards Kolguev Island sounding reveals a surface of denser consolidated deposits underlying the loose sediment cover. It occurs from the depth of about 75 m that corresponds to the bedrock depth at the Zakhar'inskii arch. Also, towards Kolguev Island, two smooth slope discontinuities forming terrace-like levels occur at the depths of 50-51 and 20-22 m.

Echo sounding profile № 2 (Fig. 2B) shows a distinct terrace on the southern SNZT slope at the depth of 120 m with 8-km-wide horizontal surface bounded by a 16 m high cusp. Besides this, two horizontal surfaces are traced at the depths of 96 and 60 m with a width of 1.3 and 0.6 km, respectively. The lower one marks a watershed of small valley-shaped depressions ending in the SNZT, while the upper surface is restricted to one of the local rises stretching northwestward from the Gulyaevskie Koshki Islands. These rises apparently belong to a single structural-tectonic arch-like form that we name the Gulyaevskii arch.

On the seismoacoustic profile № 3 (Fig. 2C) the terrace at the depth of 120 m on the southern SNZT slope is especially distinct. It has a horizontal surface with a width of 4.5 km and practically vertical 18-m-high upper slope (Fig. 3D). The high abrupt slope and considerable width of the terrace, probably, result from prolonged stabilization of sea level at these depths, but also by fast downslope evacuation of abrasion material. Apparently, the material was not accumulated in the coastal zone and, therefore, did not hamper abrasion and thermoabrasion during the sea-level lowstand at the depth of 120 m.

Another subhorizontal 1.2-km-wide surface occurring upslope at the depth of 100 m gradually turns into a slightly inclined (φ=0,0006) 8-km-wide terrace with distinct juncture at the depth of 60 m. Its surface mesorelief is represented by sandy waves (Fig. 3E). The 7-m-high bench connects this terrace with the subhorizontal surface of the next, 9.6 km wide, terrace located at the depth of 50 m. Its surface is cut by local up to 5 m deep trenches filled with laminated sediments. Another well-defined terrace is traced at the depth of 32 m (Fig. 3F). At the depth of 22 m it is separated from the topmost surface of the Gulyaevskii arch by a 10 m high scarp.

On the seismoacoustic profile № 4 (Fig. 2D) the terrace at the depth of 120 m occurs on the SNZT slope. Its 6-km-wide surface is covered with a 5 m thick layer of stratified deposits. As evidenced by seismoacoustic records, this layer overlies denser deposits. Here, the initial terrace at the depth of 125 m (lower than in other locations) was covered by younger deposits moving down the relatively steep (φ=0,01) slope. At the depth of 54 m, the profile crosses a distinct accumulative terrace apparently composed of sands. Its horizontal 16-km-wide surface is covered with sand ridges (Fig. 3F). The 8 m high bench separates this terrace from

a higher terrace with slightly inclined surface located within the depth range of 40 m (inner border) and 45 m (cusp). Another slightly inclined surface covered with muddy sediments occurs at the depths of 25-33 m. Its width is 16 km. A gently sloping surface located further upward at the depth of 17 m belongs to the Pakhtusova shoal. The slightly sloping surfaces at the depths of 40, 25 (inner border), and 15 m are separated by two beach barriers with their tops reaching the depths of 30 and 17 m. According to acoustic record, they are formed of sand and represent ancient coastal accumulative forms.

Although the echo sounding profile № 5 (Fig. 2E) runs close to profile № 4, it has one essential difference. The lowermost terrace is located at the depth of 140 m, and not 120 m. This is not because of different age, but rather due to their location on local tectonic blocks. The latter experienced subsidence with different amplitudes along the faults on the most deeply concave slope of the SNZT. This profile displays another characteristic terrace level of the Pechora Sea at the depth of 54 m.

Thus, among terraces with different heights at the Pechora Sea floor two levels are the best developed ones, namely those at the depths of 120 m and 50-54 m (Fig. 1).

Paleogeographical concept of the authors

We think that the 120 m terrace is the most interesting from the paleogeographical point of view. Now it is commonly accepted that the glacioeustatic regression of the World Ocean during the last glacial maximum about 18-20,000 years ago reached the depths of 110-130 m below the present sea level. Therefore, the terrace with morphological signs of the coastal landform stretching along the SNZT was probably formed during this epoch. Existence of this terrace confirms our point of view about the Pechora Sea paleoenvironment during the Lastglacial maximum (Chistyakova, 1997; Pavlidis et al., 1998), when the Pechora shelf was occupied by arctic tundra, and the SNZT represented a sea basin extending along the Novaya Zemlya Archipelago as a gulf of the Barents Sea.

Absence of an ice cap on the exposed Pechora Sea shelf is evidenced by seismograms revealing fine-grained laminated deposits on the southern SNZT slope without any signs of glacioturbidites that appear due to melting of big ice masses. No morainic beds are recorded on the north-south transects. Also, no distinct continuous terrace levels could be formed under an ice cover.

We suppose the terrace of the SNZT slope at the depth of 120 m to date to the Late Würm. The terrace formed in loose deposits could not be older because otherwise subsequent exodynamic processes should have reworked it. It can hardly have formed during the Holocene because in this case we must assume subsidence of the trough slope by 50 m between 15 and 10 ka, which is extremely doubtful. There is no reason to believe that the cusp of the 120 m submarine terrace is of tectonic origin, since "quick" fault, for example, due to seismic impacts must have produced gravitational deposits at the inner terrace border, which, in fact, are absent. Also, persistence of the terrace depth, besides the zone of tectonic subsidence, testifies exogenous origin of the terrace as a coastal landform.

In the Late Würm, the sea bay at the southern Novaya Zemlya coast was narrow and extended in sublatitudinal direction. It was ice-covered during the greatest part of the year, and only during 1-2 months a year it probably remained ice-free. Under such conditions, action of wave coast-forming processes was rather limited. The only active process able to form the terrace cusp and subhorizontal terrace surface was thermoabrasion. This is quite reasonable also because the SNZT slope, especially its upper part (as evidenced by seismic records), consists of loose deposits. Thermoabrasion produces sediment material at the slope base, which is practically immediately evacuated, and an extremely flat and shallow seabed surface is formed. Such a process is presently observed in the East Siberian and Laptev seas (Are, 1985).

Reconstruction of the process of terrace formation at the -50 m sea-level lowstand is a much more complicated task. Some scientists think that in the studied region the main deglaciation occurred 15-9.5 ka (Spasskaya et al., 1992; Rybalko, 1998). By analogy with the other areas of the World Ocean it is possible to assume that during postglacial transgression the sea level reached the 50-meter level 11-12 ka, i.e. at the time of the Bering Strait opening.

Younger terraces were obviously formed at the final stage of postglacial transgression. These are the terraces at the depths of 40, 32, and 25 m. Some coastlines, i.e. terraces, have original morphosculptural forms probably generated by significant slowdown or stabilization of sea-level rise. These include, for instance, a big accumulative form located to the northeast from Kolguev Island. We identify it as an ancient river mouth bar. The river incorporated all inflows from the Timan coast of the Malozemel'skaya tundra. The bar is 18 km long, its width is 5 km, and the foot and top are located at -65 and -54 m water depth, respectively. This level (~-60 m) might be correlated with the coastline location at the beginning of the Holocene.

Peculiarities of submarine topography, primarily morphology and morphometry of flooded coastlines represented by submarine terraces can tell much about the history of postglacial transgression. According to Lastochkin (1978), the concave slope discontinuity, reduced cusp height and terrace width are the signs of increase in the rate of sea-level rise, while convex slopes, considerable cusp height and terrace width indicate decrease in the rate of sea-level rise. The relative constancy of slope gradients evidences stabilization of the rate of sea-level rise; smaller gradients being related to slower rates, and bigger ones to faster rates. Growing density of submarine coastlines, especially within the Pakhtusova shoal, shows that slowdowns in the sea-level rise became more frequent. This stage corresponds to sea-level highstand at the depths of 25-30 m and can be tentatively dated to the beginning of the Atlantic period.

The main conclusion made by the authors implies that there was no ice cap on the exposed Pechora Sea shelf during the Late Würm. Therefore, our results do not confirm the opinion of Spasskaya et al. (1992) about coalescence of the Northern Ural and Novaya Zemlya ice caps.

Acknowledgements: This investigation is part of the INTAS project No 99-1489 "The Pechora Sea – Late Pleistocene paleogeography, present state of the shelf and coastal zone and forecast for the 21st century". Geomorphological analysis of

the Pechora Sea bottom topography was executed according to FCP project "World Ocean" No 5.10 and RFBR project No 00-05-64077.

References

Are, F.E., 1985. Osnovy prognoza termoabrazii beregov (Principles of the forecast of coastal thermoabrasion). Novosibirsk, SB RAN, 172 pp. (in Russian).

Chistyakova, I.A., 1997. Osadkonakoplenie i istoriya chetvertichnogo razvitiya melkovodnogo glyatsial'nogo shel'fa (na primere Pechorskogo morya) (Sedimentation and Quaternary evolution of the shallow glacial shelf (Pechora Sea as an example)). Abstract of PhD Thesis, GIN RAS, 24 pp. (in Russian).

Lastochkin, A.N., 1978. Strukturno-geomorfologicheskie issledovaniya shel'fa (Structural-geomorphologic researches of shelf). Leningrad, Nedra, 247 pp. (in Russian).

Pavlidis, Yu.A., Dunaev, N.N., Shcherbakov, F.A., 1997. The late Pleistocene palaeogeography of Arctic Eurasian shelves. Quaternary International, 41/42, 3-9.

Pavlidis, Yu.A., Ionin, A.S., Shcherbakov, F.A., Dunaev, N.N., 1998. Arkticheskii shel'f. Pozdnechetvertichnaya istoriya kak osnova prognoza (The Arctic shelf. Late Quaternary history as a basis for forecast). Moscow, GEOS, 187 pp. (in Russian).

Rudenko, O.V., 2001. Istoriya razvitiya rastitel'nosti barentsevomorskogo regiona v pleistotsene-golotsene (A history of development of vegetation in the Barents Sea region during the Pleistocene-Holocene). Abstract of PhD Thesis, MSU, 26 pp. (in Russian).

Rybalko, A.E., 1998. Pozdnechetvertichnyi sedimentogenez vnutrennikh morei glyatsial'nykh shel'fov Rossii (Late Quaternary sedimentation in the inner seas of the glacial shelves, northwestern Russia). Abstract of PhD Thesis, St.Petersburg, VSEGEI, 48 pp. (in Russian).

Spasskaya, I.I., Astakhov, V.I., Glushkova, O.J. et al., 1992. Development of landscapes and climate of the Northern Eurasia. In: Pozdnii pleistotsen-golotsen, elementy prognoza (Late Pleistocene-Holocene, elements of forecast). Moscow, Nauka, 102 pp. (in Russian).

BATHYMETRY-BASED SEAFLOOR MORPHOLOGY OF THE PECHORA SEA

V.Yu. Biryukov, S.A. Ogorodov
Faculty of Geography, Lomonosov Moscow State University, Moscow, Russia

Abstract

The article gives a detailed description of the seafloor morphology of the Pechora Sea primarily based on bathymetry. A geomorphological chart was plotted showing dominant types of seafloor relief and major bottom landforms. The main geomorphological regularities in the seafloor morphology are revealed, allowing to reconstruct the evolution of the bottom relief during Pleistocene-Holocene times. The boundary between the "young" and "ancient" relief was identified allowing to distinguish between original subaqueous and subaerial landforms.

Introduction

Exploitation of oil and gas in the Pechora sea shelf area implies construction of new ports, navigation channels, artificial islands, drill platforms, terminals, above-ground and submarine pipelines. Therefore, it is necessary to take account of the bottom morphology in order to find the optimal positioning of hydrotechnical constructions in terms of safeness and minimization of the negative impact on shelf geosystems.

The aim of the current investigation is to analyze the previously compiled geomorphological chart of the Pechora seafloor (1:1000000) without reconstructing sea-level oscillations. The chart is based on the bathymetric map plotted with the use of navigation maps 1:500000 and 1:200000. The chart is highly informative and gives a detailed image of the bottom morphology, structure, geomorphology and evolution of the Pechora Sea shelf.

To plot geomorphological data, we worked out key symbols suitable for the applied scale that correspond to all types of relief and landforms. To clarify the genesis of certain landforms, we used archive and published materials on geology and geomorphology of the area (Mel'nikov and Spesivtsev, 1995; Lastochkin, 1982). Detailed analysis of the shelf bathymetry allowed us to distinguish between elements of marine and subaerial relief. The latter include channels, as well as slopes of ancient erosional forms, flooded beach ridges, and lagoonal depressions. Also, elements of structural and gravitational relief (scarps, troughs) were mapped. Four morphogenetic complexes were established, which are amply described in this paper.

Formation of relief

In the Pechora Sea, formation of bottom relief is mainly dependent on regional structures. The Kolguev highland and Pechora-Kolva mega-arch are the biggest positive morphostructures on this shelf (Mel'nikov and Spesivtsev, 1995). They are divided by the Eastern Kolguev trough. In its southern part, the Pechora-Kolva mega-arch has two depressions, the Malozemel'skaya and Ust'-Pechora ones. The

Eastern Pechora depression with local highs (Gulyaevskii arch, Medyn' arch, Sorokin arch) is located to the east from the mega-arch. In the north, the depression and mega-arch are bordered by the Southern Novaya Zemlya (Yuzhno-Novozemel'skii) trough.

The morphostructures of the shallow Pechora Sea are mainly composed of the Quaternary marine and glacial marine deposits (Mel'nikov and Spesivtsev, 1995). Depending on the structural plan of the territory, their thickness varies from 10 to 100 m. Interglacial deposits are preserved only in depressions and are not found in positive structures. Drilling has shown that most part of sediment sequence is represented by middle and late Pleistocene clays, gravel, shell debris and single sand layers (Mel'nikov and Spesivtsev, 1995). In depressions, middle-late Pleistocene clays and loams are underlain by lower Pleistocene fine sands with the average thickness of about 30 m. In the shallow regions, the uppermost 1-5-m-thick sediment layer is represented by Holocene fine sands and loamy sands. Where clays are eroded, coarse debris exposures are formed. Surface sediments in the deep Pechora Sea consist of pelite muds.

The Pechora Sea bottom relief is a result of land-ocean interactions. The Arctic Ocean experienced significant sea-level oscillations during the Pleistocene and Holocene. Geological and geomorphological indicators evidence that the Pechora Sea bottom relief consists of two generations: the relatively young Late Pleistocene-Holocene landforms and older landforms of probably Pre-Late Pleistocene age (Lastochkin, 1982). The conventional boundary between these generations corresponds to the water depths of 50-60 m. The young landforms appeared during the Late Pleistocene regression when the present inner shelf was subject to subaerial erosion. Later, the subaerial relief underwent transformation by wave activity and tides in the course of the postglacial transgression. Notwithstanding the considerable ruggedness of the Pre-Pleistocene relief, it is still rather smooth due to tidal activity and accumulation of muds. At present, currents of different origin are shaping the old landforms, while waves and tides affect landforms of the younger generation.

Thus, taking into account the evolution history and modern lithodynamic conditions, the following types of bottom relief have been distinguished in the Pechora Sea (Fig. 1): 1) nearshore-accumulative; 2) accumulative-abrasion; 3) abrasion-accumulative; 4) deep-sea accumulative. The first two types correspond to the "young" relief, the third and fourth to the "ancient" one.

Types of relief

The elements of the ***nearshore-accumulative relief*** could be found in the bays of the Pechora Sea: Pechora, Pakhancheskaya, Perevoznaya, Khaipudyrskaya and Kolokolkova bays (Fig. 1). The shallow bays serve as sediment traps for terrigenous material supplied by thermoabrasion of coasts, solid river discharge, alongshore sediment flow and tides. Here, vast coastal territories are represented by sandy and, rarely, muddy tidal flats formed by tidal and wind-induced sea-level oscillations. Channels and valleys of different origins make the generally flat accumulative relief of the bays more complicated. Most of them are subaerial forms maintained by discharge and rip currents.

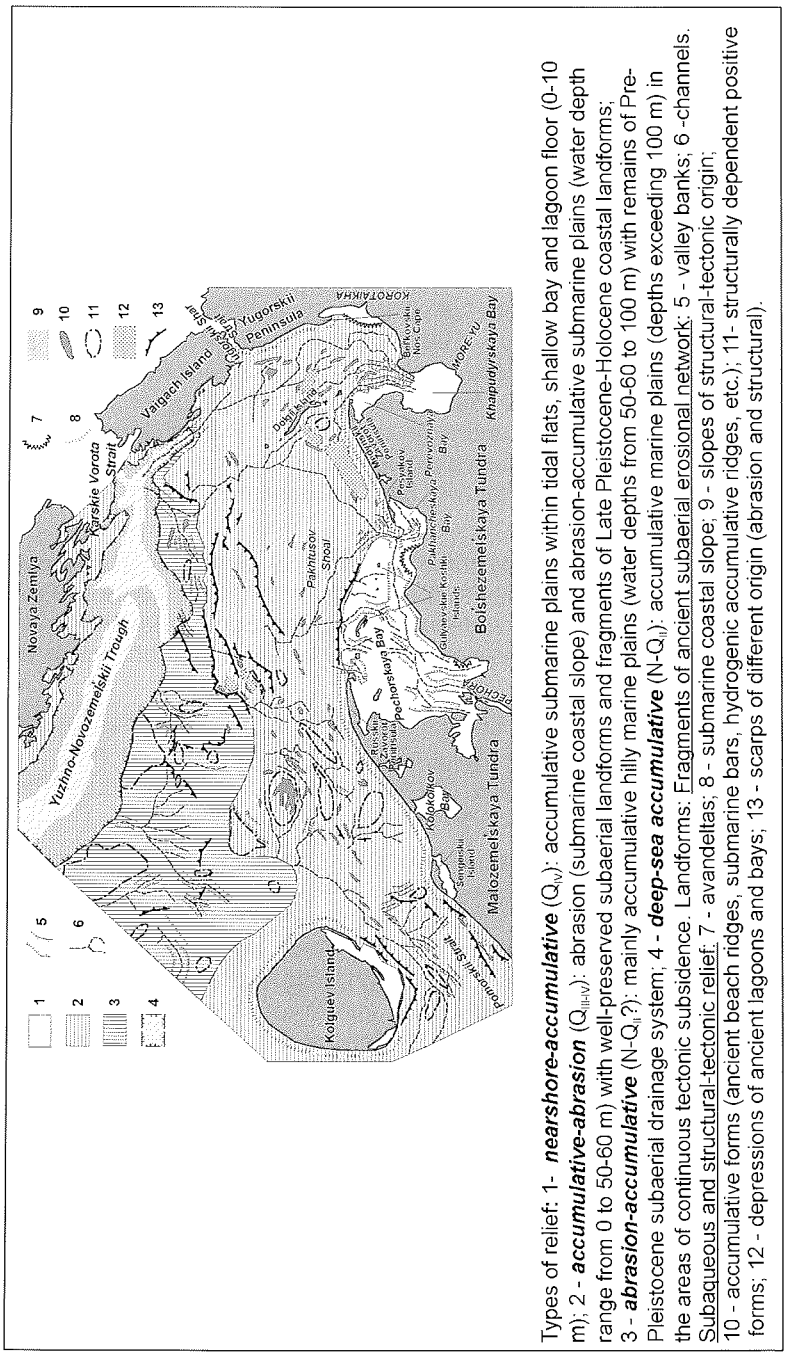

Types of relief: 1- ***nearshore-accumulative*** (Q_{IV}): accumulative submarine plains within tidal flats, shallow bay and lagoon floor (0-10 m); 2 - ***accumulative-abrasion*** (Q_{III-IV}): abrasion (submarine coastal slope) and abrasion-accumulative submarine plains (water depth range from 0 to 50-60 m) with well-preserved subaerial landforms and fragments of Late Pleistocene-Holocene coastal landforms; 3 - ***abrasion-accumulative*** (N-Q_{II}?): mainly accumulative hilly marine plains (water depths from 50-60 to 100 m) with remains of Pre-Pleistocene subaerial drainage system; 4 - ***deep-sea accumulative*** (N-Q_{II}): accumulative marine plains (depths exceeding 100 m) in the areas of continuous tectonic subsidence. Landforms: Fragments of ancient subaerial erosional network: 5 - valley banks; 6 -channels. Subaqueous and structural-tectonic relief: 7 - avandeltas; 8 - submarine coastal slope; 9 - slopes of structural-tectonic origin; 10 - accumulative forms (ancient beach ridges, submarine bars, hydrogenic accumulative ridges, etc.); 11- structurally dependent positive forms; 12 - depressions of ancient lagoons and bays; 13 - scarps of different origin (abrasion and structural).

Fig. 1. Geomorphological chart of the Pechora Sea floor

The biggest of these bays, the Pechora Bay, is protected from the sea by the Russkii Zavorot Peninsula and Gulyaevskie Koshki Islands. Depending on the water depth, the Pechora Bay is subdivided into two big parts, the shallow northwestern and deep eastern ones. The whole northwestern Pechora Bay is occupied by a vast poorly investigated shallow with prevailing depths of 1-3 m. This shallow is probably located within the ancient Pechora River delta formed during postglacial transgression when sea level was 8-10 m below its modern position. The straits between the islands and shallows of the Guilyaevskie Koshki archipelago have big tide-developed troughs with depths of up to 10 m and more. The so called channel fans are formed on the shallows at the outflows of these linear depressions (Morskaya..., 1980).

The fairway of the bay with depths of up to 6-13 m, i.e. the submarine paleovalley of the Pechora River (Lastochkin, 1982), begins at the Pechora River mouth and runs along the Bol'shezemel'skaya tundra coasts and further offshore from Pesyakov Island. Single 0.5-1.0-m-high bar-like forms occur on the smooth valley bottom. Some of these are probably relic forms, which formed at sea-level lowstand. North of the eastern Gulyaevskie Koshki islands, the submarine Pechora valley is replaced by a distinct alluvial fan. The minimum water depth at its top is about 4.5-5 m.

A modern bay-mouth bar cut by three big channel depressions is located in the southern part of the bay opposite to the mouth of the main Pechora River branch (Bol'shaya Pechora). The outer convex slope of the Pechora avandelta is oriented to the northeast, and its southern part gradually turns into the shallow accumulative plain of the Bolvanskaya Bay.

Accumulative-abrasion relief occupies shallows of the open Pechora Sea down to depths of 50 m (around the Kolguev Island down to 60 m) (Fig. 1). Besides hydrogenic subaqueous landforms, big remnants of the subaerial Late Pleistocene-Holocene relief have been preserved here.

Wave-affected shores show well-pronounced convex-concave submarine coastal slopes typical for thermoabrasion coasts. Their height and gradient depend on lithological and hydrological characteristics. For instance, at the Yugorskii Peninsula coast, between the Yugorskii Shar Strait and Bel'kovskii Nos Cape, the submarine coastal slope is up to 8-10 m high, and its gradient is 0.005. Southward from the cape, the slope is overlain by the Korotaikha River avandelta. In the region stretching further eastward to the Medynskii Zavorot Peninsula, the slope gradually disappears due to intensive sediment accumulation. In the area between the Medynskii Zavorot Peninsula and Pesyakov Island, the height of the submarine coastal slope is 7-10 m, and the gradient varies between 0.003 and 0.005; both the height and gradient decrease towards Pesyakov Island. The submarine coastal slope of the Timan coast differs from that of the Bol'shezemel'skaya tundra coast. Its height rises to 10-17 m, and the gradient increases to 0.005-0.007. The submarine coastal slope of Kolguev Island is 15-20 m high, and its gradient is 0.007-0.01.

At the depths of 8-10 m (around Kolguev Island 15-20 m), the submarine coastal slope turns into the gentle accumulative-abrasion submarine plain. Its surface is slightly uplifted in its central part (Pakhtusov shoal) and gently slopes in the western, northern and northeastern directions.

The plain still bears some indications of river erosion during the period of subaerial development in the Late Pleistocene. Orientation of thalwegs provides evidence that the river runoff was directed to the Southern Novaya Zemlya trough and, also, that the drainage system has undergone considerable changes. When the Pechora paleovalley reaches the outer shelf it is divided into two channels. One channel directed to the northwest can be traced down to water depths of 25-27 m. The other channel flows to the northeast and further to the north. At the depth of 53-56 m it again turns to the northeast towards the Karskie Vorota Strait, cuts the slope and disappears in the Southern Novaya Zemlya trough.

Another system of thalwegs has been preserved between the Dolgii Island and western Yugorskii Peninsula coast. They belong to the paleovalleys of the present Korotaikha and More-Yu Rivers. One of them can be traced down to depths of 10 m. It flows northward, enters the canyon running along the western coast of Vaigach Island, and reaches the Southern Novaya Zemlya trough. Another channel begins in Khaipudyrskaya Bay and flows northwestward meandering along the Yugorskii Peninsula coast. In the direct line with the Yugoskii Shar Strait it crosses the first channel and then disappears at the depth of 27 m.

Bottom subaqueous landforms are clearly defined on the plain. In the central part of the plain (Pakhtusov shoal) and eastward from it near the Yugorskii Peninsula coast water depths do not exceed 25 m. The surface gently slopes to the west and north (gradients ranging from 0.0002 to 0.0006). The number of single accumulative landforms occurring there increases in the southeastern part of the plain. Relative height of the accumulative subaqueous forms (ridges, spits) is not greater than 1 m. Abrasion-accumulative planation seems to be the main process of relief formation in the central part of the plain with depths less than 25 m. Inundated lagoonal depressions found at the depths of 40-45, 28-30 and 12-15 m evidence stabilization of the sea level during postglacial transgression.

To the west from the Pakhtusov shoal, water depths increase up to 30-35 m, and close to Kolguev Island up to 45-50 m. In this part of the plain, several arch-like uplifts, i.e. structural forms of the second order, occur at the depth of 30-35 m. Their relative height does not exceed 20 m, and their length reaches 30-40 km. A group of thalwegs reflects the structural morphology of the area. All thalwegs end at the depths of 50-52 m. Accumulative forms are also common. Sedimentation processes in this part of the plain are not related to wave activity.

The seafloor around Kolguev Island is smoothened by abrasion. Gradients (0.002-0.004) are much greater than those observed on the plain east of the island. A trough-like depression is located on the seafloor of the Pomorskii Strait between Kolguev Island and Timan coast. The slope close to the island is steeper than the opposite one. Both slopes bear several structural scarps and were shaped by abrasion. The bottom is relatively flat but shows some traces of erosional activity. Several arch-like uplifts with a relative height of 5-10 m stretch along the trough-like depression. Also, small (not more than 1 m high) accumulative ridges are found.

Abrasion-accumulative relief is represented by a rather dissected accumulative submarine plain with depths ranging from 50(60) to 100 m (Fig. 1). According to morphological differences, the plain can be subdivided into a western and an eastern part. The latter forms a narrow band stretching along the southern slope of the trough at the depths of 50-60 m and ending in the form of a canyon in the

Southern Novaya Zemlya trough. The canyon runs parallel to the western Vaigach coast. Its average depth is 30-40 m. The plain slopes towards the trough in a step-like form and includes fragments of the Pre-Pleistocene drainage system (Lastochkin. 1982).

The western part of the plain with depths varying from 50 to 100 m slopes more gently towards the trough (gradient 0.0015). Typical landforms are represented by big, probably structural, hills and highlands and fragments of ancient valleys. The relative height of the hills does not exceed 30 m. The fragments of ancient valleys are about 5 km wide and up to 20 m deep. It should be noted that these valleys do not have anything in common with the subaerial drainage system found in the shallow zone. Some of them are "cut" by the slope of the Southern Novaya Zemlya trough. In general, marine processes have considerably changed the bottom relief.

Deep-sea accumulative relief occurs in the Southern Novaya Zemlya trough. The latter is a sub-meridional superimposed negative morphostructure (Fig. 1). In the eastern Pechora Sea, its bottom has a two-step structure. The upper step lies at water depths of 100-110 m. The western step is lower and corresponds to water depths of 190-200 m. Relative to the surrounding submarine plain, the depth of the trough is 90-60 m. Its flat bottom is up to 30 km wide. The cross-section is asymmetric, the northern bank being higher and steeper. The trough serves as a sediment trap for fine-grained material.

Conclusions

Four morphogenetic complexes with certain geomorphological features were established in the Pechora Sea. Shelf morphology shows the following peculiarities: 1) the Pleistocene-Holocene subaerial drainage system could be traced only down to depths of 50-55 m; this level can probably be referred to as the natural boundary between the "young" and "ancient", Pre-Late Pleistocene, relief; 2) the Southern Novaya Zemlya trough cuts the fragments of the Pre-Late Pleistocene valleys, thus providing evidence for its superimposed character; 3) the fact that the Southern Novaya Zemlya trough has a two-step structure argues for the hypothesis that there were two stages of neotectonic activity.

References:

Lastochkin, A.N., 1982. Metody morskogo geomorfologicheskogo kartografirovaniya (The methods of marine geomorphological mapping). Leningrad, Nedra, 272 pp. (in Russian).

Mel'nikov, V.P., Spesivtsev, V.I., 1995. Inzhenerno-geologicheskie i geokriologicheskie usloviya shel'fa Barentseva i Karskogo morei (Engineering-geological and geocryological conditions of the Barents and Kara shelf). Novosibirsk, Nauka, 197 pp. (in Russian).

Morskaya geomorfologiya. Terminologicheskii spravochnik. Beregovaya zona: protsessy, ponyatia, opredeleniya (Marine geomorphology. Reference book. Coastal zone: processes, terms and definitions), 1980. Zenkovich, V.P., Popov, B.A. (eds.), Moscow, Mysl', 280 pp. (in Russian).

NEW DATA ON THE PECHORA SEA BOTTOM TOPOGRAPHY EVIDENCED BY GEOACOUSTIC PROFILING

Yu.A. Pavlidis, S.L. Nikiforov, A.V. Artem'ev, N.N. Dunaev, N.V. Politova
Shirshov Institute of Oceanology RAS, Moscow, Russia

Abstract

The article deals with detailed description of the Pechora Sea bottom topography based on morphogenetic analysis. The main landforms of the Pechora Sea are represented by: 1 – inner shelf (underwater coastal slope); 2 – subhorizontal mid-shelf plain; 3 – slopes and sea bottom of the Southern Novaya Zemlya Trough (SNZT) and the Korotaikhinskaya depression composed of a complex with relic and modern landforms.

Pechora Sea bottom topography

The Pechora Sea is not exactly a typical shelf basin since there is no outer shelf, while inner and middle shelf zones are well expressed.

The main bottom landforms of the Pechora Sea are represented by: 1 – inner shelf (underwater coastal slope); 2 – subhorizontal midshelf plain; and 3 – slopes and bottom of the Southern Novaya Zemlya Trough (SNZT) and the Korotaikhinskaya depression. Additionally, a zone of lagoons is formed along the coast.

By inner shelf (underwater coastal slope) is meant the seabed area directly adjoining the coast that is exposed to the constant influence of modern hydrodynamic and ice processes of different intensity. The outer limit of the inner shelf corresponds to the underwater coastal slope discontinuity that is usually restricted to depths lesser than 20 m. The width and inclination of the inner shelf zone differ at various coasts. On accumulative coasts, the inner shelf is, on average, 4-6 km wide, and the inclination angle is about 0.003 (here and below in tangent); on abrasion coasts the values are 1-2 km and about 0.005, respectively; and, finally, on thermoabrasion ones 2-3 km and 0.005-0.003, respectively. The inner shelf on Vaigach Island varies in width from 1.5 to 3 km, and the inclination angle is considerably larger (0.013-0.003), while on Kolguev Island it is 4-8 km and 0.005-0.003, respectively (Figs. 1, 2). The thickness of the Holocene deposits is insignificant ranging from 0.2 to 4.0 meters, and bedrock exposures occur in the eastern part of the sea.

Two to four submarine bars are usually found in the coastal zone. Their occurrence is sporadic. Several generations of submarine bars were found in the coastal zone near the Polyarnyi Cape. The first generation with its top at the depths of about 1.2-2.0 m (relative height of the bars is 2 m) is located 250-500 m off the coast. The second generation is also well expressed in bottom topography, its top occurs at the depths of about 2.5-3.2 m, and the relative height of the bars is about 1 m. The third generation located approximately 1500 m offshore is less evident. Its top reaches 7 m water depth, and the relative height of the bars is about 1 m.

A modern abrasion step is found in some parts of the coast at the depth of 4-5 m. It is formed by annual strong fall storms (Gidrodinamicheskie..., 1985). Numerous

cross-hollows created by joint action of tidal, wind-induced, and wave currents occur on the inner shelf. In most cases, increasing hydrodynamic activity produces small fans on these hollows, which are, however, quickly washed away.

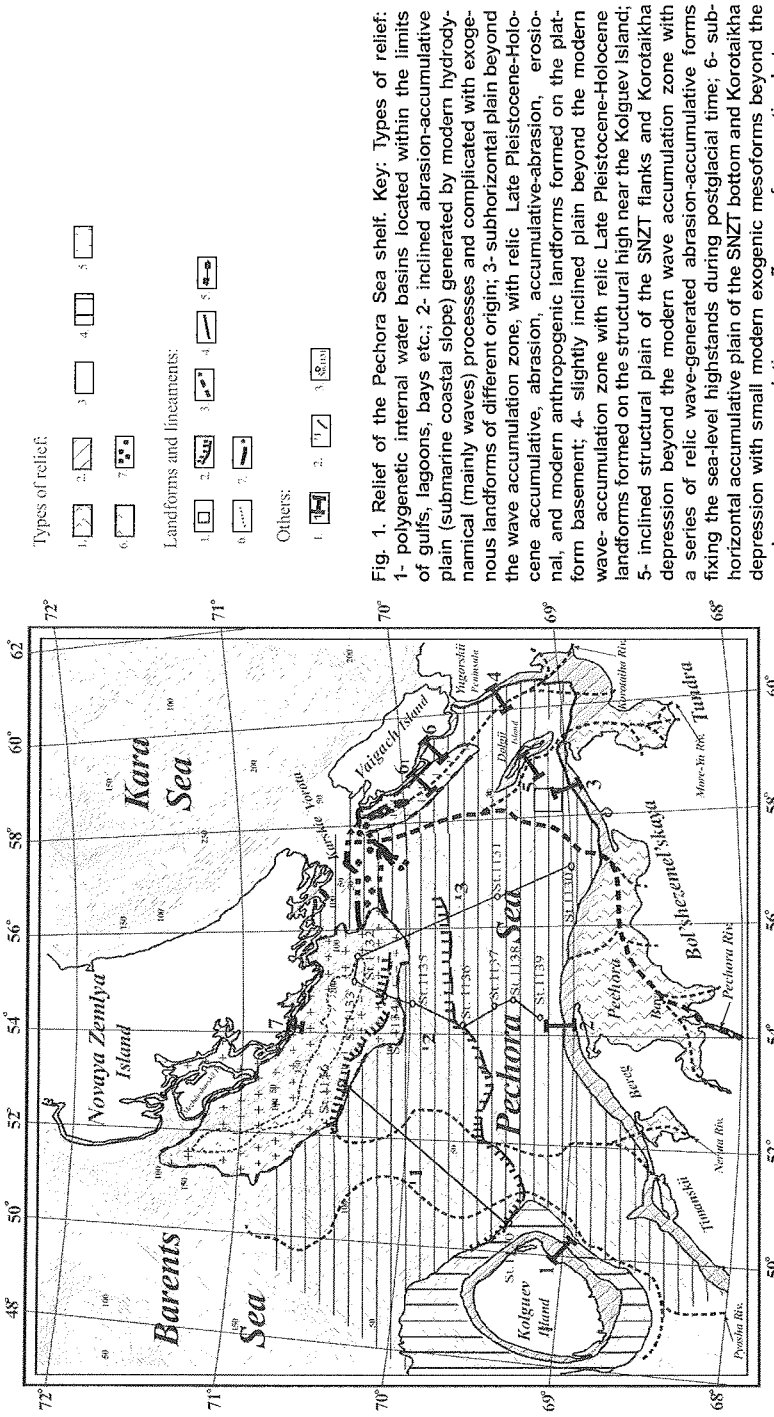

Fig. 1. Relief of the Pechora Sea shelf. Key: Types of relief: 1- polygenetic internal water basins located within the limits of gulfs, lagoons, bays etc.; 2- inclined abrasion-accumulative plain (submarine coastal slope) generated by modern hydrodynamical (mainly waves) processes and complicated with exogenous landforms of different origin; 3- subhorizontal plain beyond the wave accumulation zone, with relic Late Pleistocene-Holocene accumulative, abrasion, accumulative-abrasion, erosional, and modern anthropogenic landforms formed on the platform basement; 4- slightly inclined plain beyond the modern wave- accumulation zone with relic Late Pleistocene-Holocene landforms formed on the structural high near the Kolguev Island; 5- inclined structural plain of the SNZT flanks and Korotaikha depression beyond the modern wave accumulation zone with a series of relic wave-generated abrasion-accumulative forms fixing the sea-level highstands during postglacial time; 6- subhorizontal accumulative plain of the SNZT bottom and Korotaikha depression with small modern exogenic mesoforms beyond the modern wave accumulation zone; 7- zone of connection between the SNZT and Korotaikha depression structures with dissected topography. Landforms and lineaments: 1- area of fixed anthropogenous landforms; 2- submarine terraces; 3 - probable directions of river discharge in the Late Valdai glacial epoch; 4- boundaries of the relief types of the inner shelf and Kolguev rise; 5- slopes of the SNZT and Korotaikha depression; 6 - bottom of the SNZT and Korotaikha depression; 7- probable borders of zone of connection between the SNZT and Korotaikha depression structures. Others: 1- location of coastal transects; 2- position and numbers of bottom transects; 3- stations of RV "Akademik Sergei Vavilov".

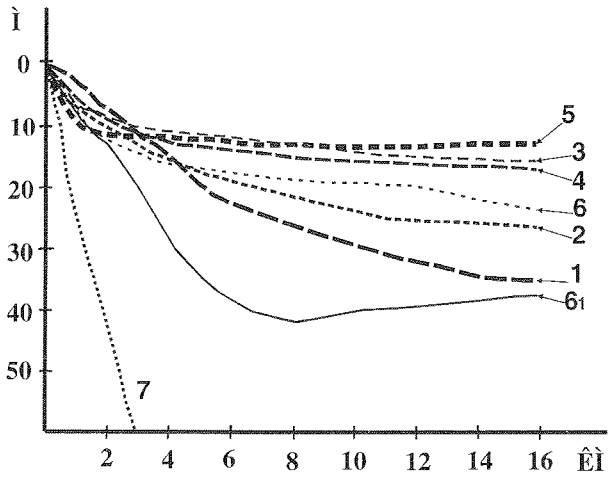

Fig. 2. Characteristic transects for various coasts of the Pechora Sea:
1- Kolguev Island, accumulative coasts; 2- Bol'shezemel'skaya tundra near the

5- Dolgii Island, abrasion-accumulative coasts; 6- Vaigach Island (Lyamchin Bay) abrasion-accumulative coasts; 6- Vaigach Island (Lyamchin Bay), abrasion-bay and accumulative coasts; 7- Novaya Zemlya archipelago (near Cape Rakovi), erosion-tectonic fjord coasts.

Transverse sediment drift is characteristic of the inner shelf zone. Given the underwater coastal slope near Novyi Varandei settlement as an example, one should expect the greatest deformations of the seafloor, and, accordingly, considerable sedimentary matter transfer at the depths of down to 5 m, and during strong storms down to 10 m and more (Ogorodov and Lugovoi, 2000; Ogorodov, 2001). Nevertheless, small thickness of modern loose deposits allows assuming inconsiderable thickness of wave load and its discharge of less than 100-200 m^3/h. Small size of accumulative waveforms indicates relative deficiency of sand at the underwater coastal slope, where submarine bars are about 1 m high, and sand waves even smaller. Offshore the underwater coastal slope suspended matter flux is directed to the east.

This means that the inner Pechora Sea shelf represents a slightly inclined abrasion-accumulative plain shaped by the modern hydrodynamic processes, with small-size exogenous landforms of different origin.

The central (or middle) shelf is located beyond the modern wave-affected zone in the water depth range from the underwater coastal slope base down to approximately 90 meters. It represents a subhorizontal plain stretching northward for about 100-140 km, and in the perpendicular direction for 350-400 km. Its inclination is about 0.0003-0.0006, reaching 0.001-0.002 at big rises. Bottom sediments are represented by the Holocene deposits unconformably overlying more ancient (Late Pleistocene) clays.

These data are confirmed by the results of drilling from aboard b/v "Bavenit". The deepest core yielding the highest number of ^{14}C datings (N 210-218) was recovered in the nearshore southeastern part of the sea at the depth of 20 m. Sediment sequence consists of the Holocene sand layer, which yielded 8 datings ranging from 4.7 to 9.7 ka, underlain by varved clays aging back to 23.6-28.3 ka, in turn underlain by loams dated to 35-36 ka. At the base of the core, dense clays overlie Mesozoic sedimentary rocks. The total core thickness is 118 m (Polyak et al., 2000). Structurally, the subhorizontal plain lies on the submarine continuation of the Timan-Pechora Epibaikalian plate and is completely located within the limits of the continental Earth's crust. Inclination angles in the zones of rises are about 0.002-0.001.

The big structurally dependent positive landforms occur on the mid-shelf around the Kolguev rise and in the eastern part of the sea, where they form a linear bedrock protrusion near the Matveev and Malyi Zelenets islands. Parallel to the barrier chain northwestward and, also, southward from Dolgii Island wide structural blocks (6 to 8 km) are located. Submarine outliers are separated from the islands by a narrow linear trough with a depth of about 15 m. Such geological-geomorphological combination of outliers and linear trough with a width of about 10 km stretching along the barrier chain on the prolongation of the Chernov Ridge allows assuming presence of lineaments that bound the zone of recent lateral movements at the western margin of the Novaya Zemlya-Paikhoi orogen.

During the 13th cruise of r/v "Akademik Sergei Vavilov", detailed geological-geomorphological investigations including seismoacoustic profiling by "Parasound" and sediment sampling were carried out off Varandei at the depths of 12-21 m. Of special interest are the arch-like rises with relative height of 1 m above the generally gentle seabed that occur within the water depths of 15-18 m. It should be noted that similar landforms are quite common on the Pechora Sea floor. They are mainly composed of sands overlying the dense clayey basement. Taking into account the morphometric signs, lithology, location depth of about 18 m, geomorphological structure of adjacent areas, and geophysical data, it is possible to conclude that these landforms are ancient (relic) wave accumulative formations tracing one of the former Holocene coastlines. Probably, they are relics of a barrier beach complex.

Similar landforms are formed by the past sea-level oscillations during postglacial times.

During the maximum regressive stage the greatest part of the Pechora Sea represented a coastal plain cut by river valleys that was exposed to cryolithogenesis (Fig. 3 a-b). In this epoch the layer of dense clays underlying recent sediments was accumulated. Subsequent sea-level rise with stabilization at certain depths produced wave accumulative forms mainly composed by sands. A series of such landforms was found within the studied area. At present they are flooded and subjected to gradual destruction by the modern hydrodynamic processes.

Similar landforms corresponding to the ancient coastlines are located at the depths of 12-13; 14-16; 17-20, and 27-32 m.

Also, a series of small rounded depressions with a width of about 1 mile and relative depth of about 0.5-1.0 m was found in the studied area. These were probably thermokarst depressions. It should be stressed that these extremely

small-sized landforms were revealed due to detailed field investigations with the use of high-accuracy equipment. It is practically impossible to discover them with the help of navigation maps.

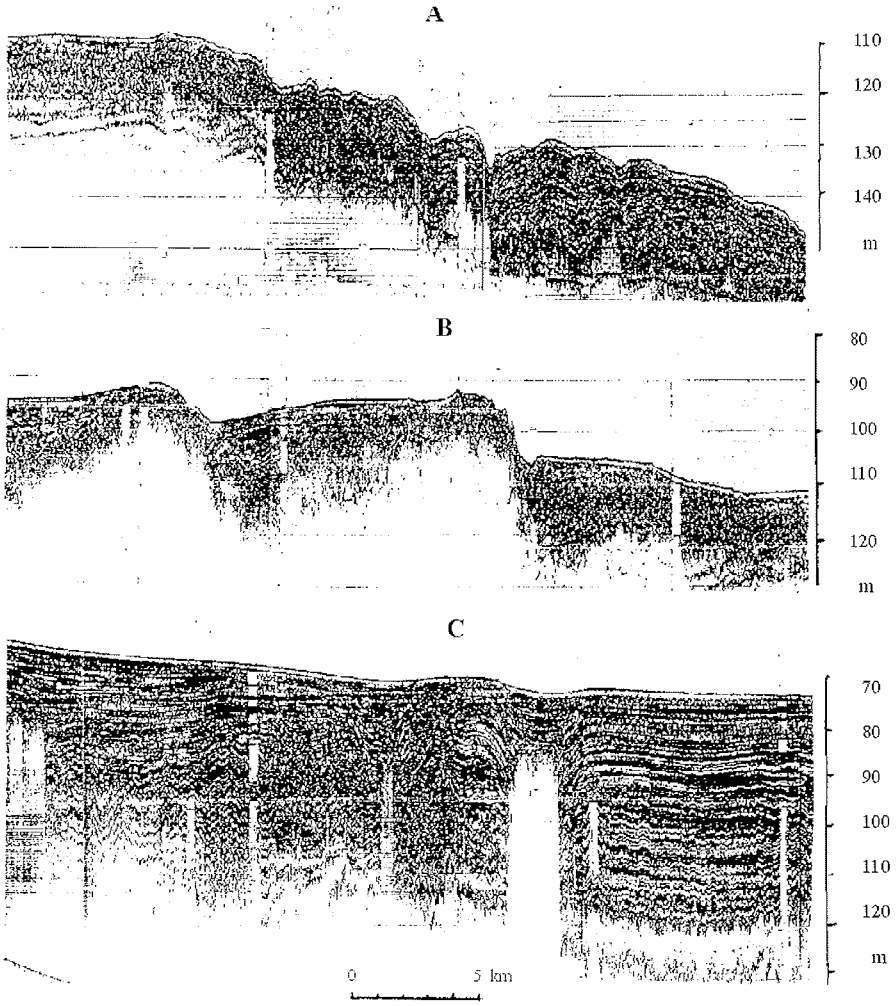

Fig. 3a

Within the limits of the Pechora Sea shelf, a number of large valley-like depressions could be traced, that are directed from the coastline to the SNZT. We identify them as paleovalleys of the following rivers (from the west to the east): Pyosha, Neruta, Pechora, More-Yu, and Korotaikha (Fig. 1). In the previously published materials only the location of the Korotaikha paleovalley agrees with our

data. Others are either mapped only partially or restricted to totally different places (Biogeotsenozy..., 1996).

This concerns even the biggest river of the region – the Pechora. We plotted the

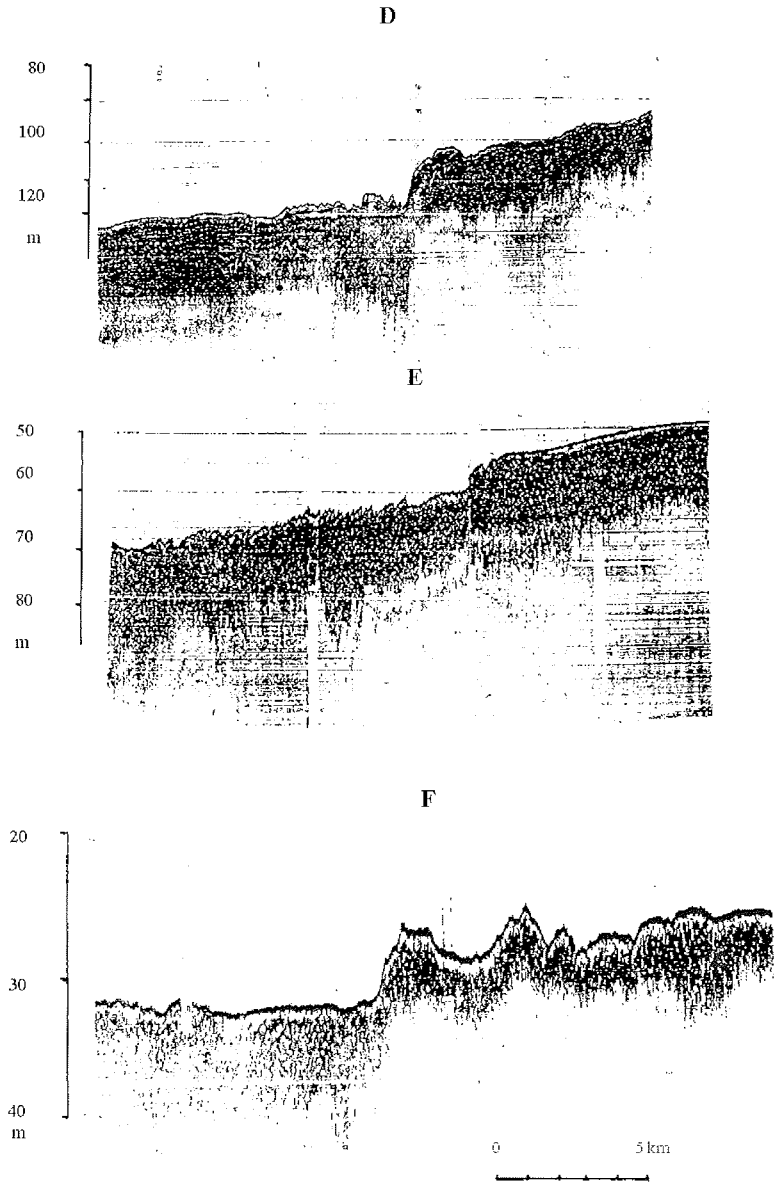

Fig. 3. Levels of submarine terraces on the Pechora Sea shelf (fragments of "Parasound" record):a) A- fragment terrace at the depth of 120 m (profile 1); B - fragment terrace at the depth of 105 m divided by listric faults (profile 1); C - fragment sea floor at the depth of 70-75 m with cryogenic deformations (profile 1); b) D - fragment terrace at the depth of 120 m (profile 2); E - fragment terrace at the depth of 60 m with surface sandy waves (profile 2); F - fragment terrace at the depth of 32 m (profile 2).

probable former direction of its runoff on the map published in the cruise report of the 13th cruise of r/v "Akademik Sergei Vavilov" in 1998 (Otchet..., 1998).

Besides big river valleys, numerous short hollows and depressions of different orientation cut the shelf. We consider them as ancient subaerial channels flowing either to the above mentioned big river valleys or the SNZT.

Since the problem of ancient river valleys demands special discussion, here we have restricted ourselves just to mentioning it.

Seismoacoustic profiling carried out during the 8th cruise of r/v "Professor Shtokman" and 11th (1997) and 13th (1998) cruises of r/v "Akademik Sergei Vavilov" ("Parasound" complex, accuracy 0.5 m for sedimentary sequence), and bathymetry analysis of navigation maps (scale 1:200000) revealed a series of submarine terraces. The terraces are arranged sub-latitudinally and have different elevations. Marine terrace is a subhorizontal or gently sloping surface of marine origin limited by slope discontinuities steeper than the surface inclination that was formed during previous epochs of sea level high- or lowstands. In the Pechora Sea, such surfaces were found at the depths of 25, 32, 40, 50-54, 60, 100-105, 110, 120 and 140 m, both within the limits of subhorizontal plain and in deeper parts of the SNZT. Among different terraces of the Pechora Sea, two terrace levels at the depths of 50-54 and 120 m are the most distinct and well-developed ones (Figs. 3-4), as evidenced by analysis of maps and 5 north-south seismoacoustic profiles obtained from the western, central, and eastern mid-shelf and the SNZT (see Pavlidis et al. "Submarine terraces...", this volume).

The best expressed form of bottom topography of the mid-shelf is the submarine terrace located north of the Pakhtusov shallow at the depth of 50-54 m. Here it is 16 km wide. In its central part, there are 5-m-deep buried erosional channels filled with modern laminated sediments. Some ancient coastlines are marked with specific morphosculptural landforms originated under considerable slowdown or stabilization of the sea-level rise. These include, for instance, a big accumulative form located northeast of the Kolguev Island. We identify it as an ancient river mouth bar. The river incorporated all inflows from the Timan coast of the Malozemel'skaya tundra. Bar length is 18 km, its width is 5 km, and the foot and top are located at -65 and -54 m water depth, respectively. This level (~-60 m) might be correlated with the coastline location at the beginning of the Holocene.

Detailed geological-geomorphological investigations using side-scan hydroradar AGPKS-300 were carried out on the Varandei mid-shelf area during the 13th cruise of r/v "Akademik Sergei Vavilov". They revealed linear heterogeneities of relief, that we consider as anthropogenic landforms (Fig. 5 A): traces of underwater cables or pipelines, swells and rectilinear furrows at the depth of about 18 m formed by anchor circuits of drifting vessels and by anchors themselves. Subparallel pairs of arcs are interpreted as traces of trawling. Small asymmetric sand swells with high backscatter coefficient are probably coarse debris dumps. The illustration of active intervention into the natural environment is a small ship lying on the seafloor and partly buried by sediments (Fig. 5 B). Anthropogenic landforms could be found not only in the Varandei area but also in many others, for example, near Kolguev Island, where an intensive exploitation of the coastal area is taking place. However, in order to detect these landforms, special high-accuracy equipment and thorough field investigations are needed.

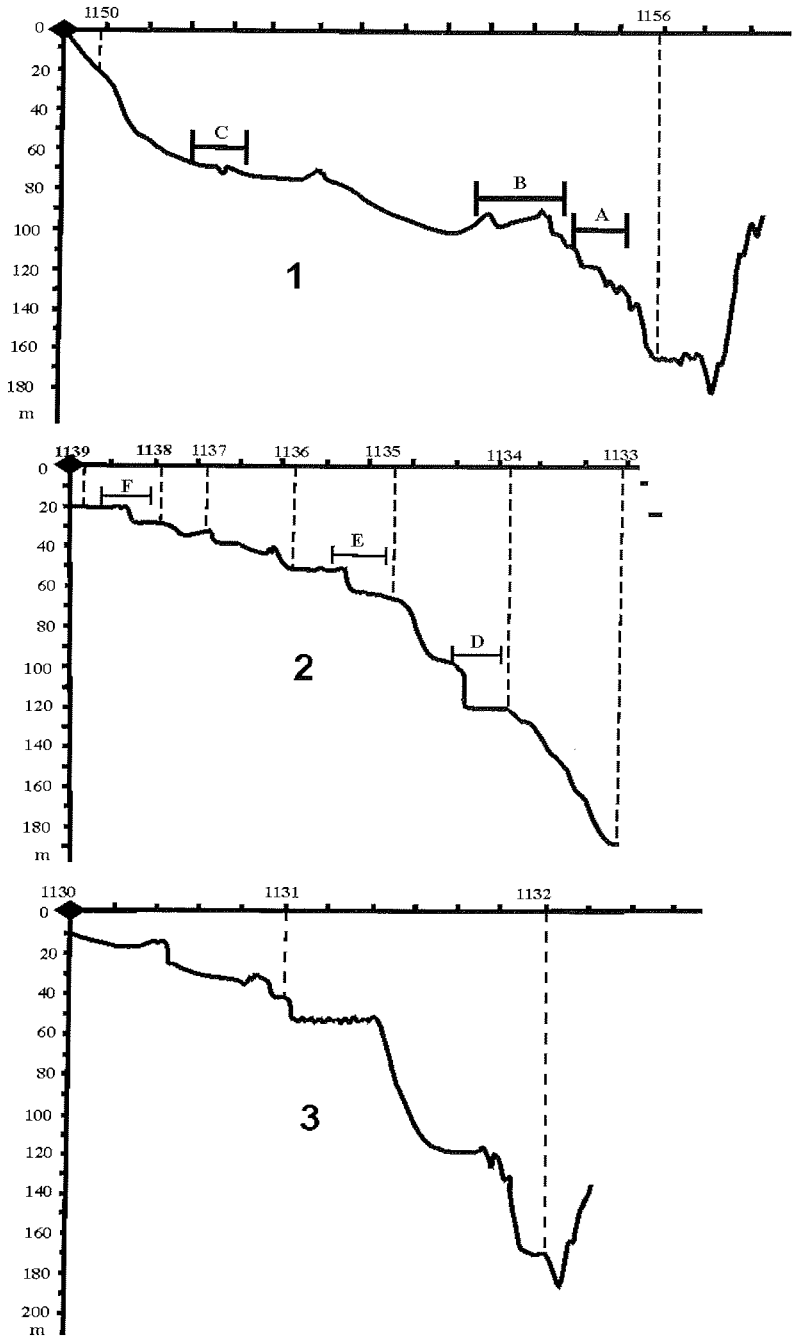

Fig. 4. Bottom profiles: 1 seismoacoustic profile 1; 2 seismoacoustic profile 2; 3 seismoacoustic profile 3. Letters A, B, C, D, E, F on profiles designate fragments of "Parasound" record (see Fig. 3).

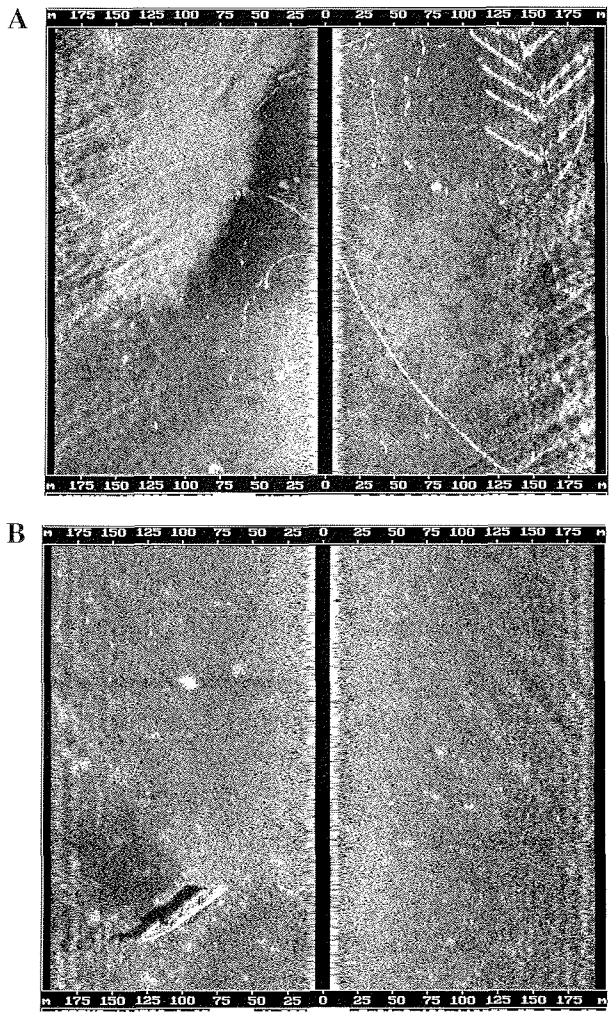

Fig. 5. Anthropogenous relief: ? - traces on sea floor formed by underwater cables or pipelines, swells and rectilinear cuts formed by anchors and anchor circuits, traces of trawling, sandy asymmetric swells probably a result of coarse material dumping; B - small ship partly buried under sediments.

Thus, the central Pechora Sea shelf could be referred to as a subhorizontal plain on the platform basement, located outside the zone of wave accumulation, with relic Late-Pleistocene-Holocene accumulative, abrasion, and erosional landforms, along with modern anthropogenic ones.

The Southern Novaya Zemlya Trough and Korotaikhinskaya depression are located in the northern part of the Pechora Sea.

The Korotaikhinskaya depression slopes are manifested by discontinuities at the depth of 26 m in its southern part and 45 m in the northern part. Its bottom lies at the depths of 70 to 96 m. The width of the slopes is 4-6 km, and the length is up to

70 km. The slopes represent a sloping plain with inclination angles of about 0.005-0.006. Compared to the slopes, the bottom of the Korotaikhinskaya depression is relatively flat and represents a gently sloping 4-km-wide and 35-km-long plain with inclination angles of about 0.001-0.003.

Distinct inclination at the depth of about 90 m marks the slopes of the SNZT. The bottom is located within depth range from 170 down to 210 m.

The slopes of the 20-50-km-wide and about 300-km-long trough represent a sloping plain with inclination angles of 0.003-0.007 composed by the thick sequence of Holocene, mainly pelitic, muds evidencing continuous sediment accumulation. It is confirmed by diverse data including the results of geological investigations carried out during the 13th cruise of r/v "Akademik Sergei Vavilov", when a 486-cm-long core was recovered at 169 m water depth (70°33' N, 52°48'E). The radiocarbon age dating of mollusk shells was carried out in the Labortoire des Sciences du Climat et de l' Environnement, France. The whole core is of Holocene age (see Pavlidis et al. "Sediment sequence...", this volume).

Our data are confirmed by palynological analysis (Rudenko, 2001). The upper 5 m thick layer of marine relatively deep-water deposits of Holocene age overlie denser deposits of similar lithology. Probably both sediment layers were accumulated in marine basin: during the Late Valdai cold epoch (the lower sediment layer) and subsequent Holocene warming.

If assuming that sedimentation rates in the SNZT remained nearly constant during the Late Valdai and Holocene, then the lower sediment layer with the same thickness as the overlying Holocene deposits should have been accumulated during the same time interval, i.e. 9-10 kyr. Thus, it might be assigned to the Ostashkov epoch of the Late Valdai. The total thickness of both layers equals 10-12 m. They have been accumulated during 18-20 kyrs. Hence, sedimentation rate in the SNZT during this period averaged 0.5 mm/year.

On the SNZT slopes a series of submarine terraces was revealed. The terraces are genetically correlated with similar formations on more shallow parts of the central shelf as confirmed by analysis of bathymetric maps of different scale and seismoacoustic "Parasound" profiles. At least three well-defined terrace levels are traced on the SNZT southern slope.

The lowermost terrace is located at the depths of 118 m (inner border) to 120 m (terrace cusp) (Figs. 3-4). Its nearly 2-km-wide surface is almost horizontal with a very small inclination (φ=0.001) to the trough thalweg. It has a rough surface with relative height range of about 1-3 m. The gentle 5-m-high bench separates the 120-m-high terrace from the second one located at the depth of 110 m. The latter has a convex wavy cusp and slightly concave (about 2 m) surface with a width of 4 km and a depth of 110 m. A 6-m-high gentle bench separates this terrace from the third terrace located within the southern SNZT slope at the depth of 105 m. Seismoprofiling record allows assuming accumulative origin of these terraces. The thickness of stratified deposits ranges from 15 to 20 m. The 105-m-high terrace is separated by a rather steep bench from the flat rise at the top of SNTZ border. The top of this rise is located at the depth of 91-92 m and is cut by the so-called listric faults. This surface and the rise itself mark a zone of slope discontinuity and transition to the central Pechora Sea shelf. The latter has a structural rise in the middle that represents a northwestern pericline of the Zakhar'inskii arch. The arch separates two depressions filled with stratified loose sediments. Maximum

sediment thickness in the depression located north of the arch determined by sounding reaches 35-40 m, while in the southern depression it exceeds 50 m.

We think that the 120 m terrace is the most interesting one from the paleogeographical point of view. Now it is commonly accepted that the glacioeustatic regression of the World Ocean during the last glacial maximum about 18-20,000 years ago reached depths of 110-130 m below the present sea level. Therefore, the terrace with morphological signs of the coastal landform stretching along the SNZT should have been formed during this epoch.

The fact that there was no ice cap on the exposed Pechora Sea shelf is evidenced by seismograms revealing fine-grained laminated deposits on the southern SNZT slope without any signs of glacioturbidites that appear due to melting of big ice masses. No morainic beds are recorded on the north-south transects. Also, no distinct continuous terrace levels could be formed under an ice cover.

Younger terraces were obviously formed at the final stage of the postglacial transgression. These are the terraces at the depths of 40, 32, and 25 m. It is possible that submarine terraces also occur on the northern SNZT slope, but right now no detailed geological-geomorphical data on this area are available.

In the eastern part of the SNZT, close to a sill in front of the Karskie Vorota Strait, the graben-like structure of the trough is clearly seen on the profiles. The structure appeared due to tectonic subsidence of the axial part of the trough along faults on its slopes.

Thus, the slopes of the SNZT and Korotaikhinskaya depression could be characterized as the sloping, structurally dependent, plains beyond the zone of wave accumulation, with a series of relic abrasion-accumulative wave-shaped landforms indicating the levels of sea-level oscillations during postglacial times.

The SNZT bottom has a gently sloping relief with inclination of about 0.0003-0.001 and small exogenous mesoforms. Their relative height is 2 m and their width reaches several hundreds of meters. Their origin is related to various modern geological-geomorphical processes: non-uniform consolidation of sediments, influence of constant bottom currents, nepheloid sedimentation, and smoothing of ancient structural elements by sediment accumulation.

The echo sounding record of sediment sequence displays several horizons. The upper layer with a thickness of 4-6 m was attributed the Holocene age, which was later confirmed by analysis of sediment cores. Therefore, the SNZT bottom represents the subhorizontal accumulative plain, with small modern exogenous mesoforms.

Thus, the Pechora Sea bottom relief is subdivided into the following major elements: 1 – inner shelf (underwater coastal slope), 2 – subhorizontal mid-shelf, and 3 – slopes and bottom of the Southern Novaya Zemlya Trough (SNZT) and the Korotaikhinskaya depression. The greatest part of the Pechora Sea shelf is located beyond the zone of modern wave accumulation and represents a combination of subhorizontal and sloping plains with different structural-dependent inclinations. The inner abrasion-accumulative part of the shelf (underwater coastal slope) occupies the nearshore shallow. Its structure depends upon the origin of the coast and its dynamics. Modern hydrodynamic processes shape this zone and produce small exogenous landforms of various origins. The Pechora Sea mid-shelf is a

subhorizontal plain on the platform basement not affected by wave activity, with relic Late-Pleistocene-Holocene accumulative, abrasion, abrasion-accumulative, erosional, and modern anthropogenic landforms. The biggest relic landforms are represented by submarine terraces at the depths of 25, 32, 40, 50-54, 60, 100-105, 110, 120, and 140 m. The most distinct ones are the terraces at 50-54 and 120 m water depth. The slopes of the SNZT and Korotaikhinskaya depression represent the structurally dependent sloping plain with flat bottom subjected to accumulation. In the regions of constantly increasing economic activity, anthropogenic landforms, that are already well defined in bottom topography, are of special interest.

References

Biogeotsenozy glyatsial'nykh shel'fov Zapadnoi Arktiki (Biogeocoenosis of the Western Arctic glacial shelves, 1996. Apatity, KNTs AN RAS, 166-170 (in Russian).

Gidrometeorologicheskie usloviya shel'fovoi zony morei SSSR (Hydrometeorological conditions of the shelf zone in the seas of the USSR). V. 6, Is. 1/2: Barents Sea, 1985. Leningrad, Gidrometeoizdat, 262 pp. (in Russian).

Ogorodov, S.A., 2001. Problems of environmental management and ecological vulnerability of coastal zone in the Varandei oil-gas area. In: Problemy razvitiya toplivno-energeticheskogo kompleksa: ekonomika, politika, istoriya (Problems in exploitation of energy park: economy, policy, history). Abstracts of the 2nd Intern. Scientific Practical Conf., Moscow, 111-114 (in Russian).

Ogorodov, S.A., Lugovoi, N.N., 2000. Technogenic factor in coastal dynamics of the Varandei industrial region. In: Geomorfologiya na rubezhe XXI veka (Geomorphology at the beginning of the XXI century). Abstracts of the 4th Shchukin's readings. Moscow, Geographical Faculty MSU, 432-436 (in Russian).

Otchet 13-go reisa NIS "Akademik Sergei Vavilov" (Cruise report of 13th cruise of r/v "Akademik Sergei Vavilov"), 1998. Deposited in the archive of IORAS (in Russian).

Polyak, L., Gataullin, V., Okuneva, O., Stelle, V., 2000. New constraints on the limits of the Barents-Kara ice sheet during the Last Glacial Wurm based on borehole stratigraphy from the Pechora Sea. Geology, 28, 7, 611-614.

Rudenko, O.V., 2001. Istoriya razvitiya rastitel'nosti barentsevomorskogo regiona v pleistotsene-golotsene (A history of development of vegetation in the Barents Sea region during the Pleistocene-Holocene). Abstract of PhD Thesis, MSU, 26 pp. (in Russian).

COASTAL MORPHOLOGY AND DYNAMICS OF THE PECHORA SEA

S.A. Ogorodov
Faculty of Geography, Lomonosov Moscow State University, Moscow, Russia

Abstract

Based on the geological and geomorphological structure of the Pechora Sea coasts and wind-energy calculations, the main types of the coasts and directions of sediment flows were determined. Ten morphodynamic regions were established with specific dynamic and morphological characteristics. Loose permafrost sediments exposed along a considerable portion of the Pechora Sea coastline favor formation of thermoabrasion and abrasion-denudation coasts. Because the dynamically active period is considerably longer than in the other Arctic seas and because of abundant sand deposits, big accumulative forms like barrier beaches are widespread in the coastal zone of the Pechora Sea.

Introduction

A common feature of all Arctic seas is the fact that permafrost exists in the coastal zone. Coastal systems in the cryolithozone are unstable (Geoekologiya Severa, 1992), which is especially evident in the areas of intensive resource exploitation including the Pechora Sea coast. The Pechora sector of the Barents Sea is distinguished by loose permafrost coasts. Under such conditions, technogenic impact activates destructive coastal processes that considerably complicate industrial development of the coastal zone and increase expenditures on elimination of negative environmental impact and regeneration of disturbed geosystems. In turn, natural morphodynamic processes, such as thermoabrasion, thermodenudation, thermoerosion, deflation and ice scouring, themselves could be the cause of economic losses. Hence, investigation of the morphology and dynamics of coasts in the Pechora Sea is important in terms of industrial development of this area.

Results and discussion

The shape of a modern coastal zone is the result of its evolution during the Late Pleistocene-Holocene under post-glacial sea-level rise and its subsequent stabilization. The modern-like coastal zone appeared in the Pechora Sea region about 6 ka (Kaplin, 1973; Tarasov and Alekseev, 1985) when the sea level reached its modern position. Since this time, it has experienced insignificant oscillations, and the main factors responsible for shaping the coast have been waves and thermal processes.

A modern morphodynamic scheme of the Pechora Sea coasts is shown in Fig. 1. To distinguish between different types of coasts we used genetic classification (Leont'ev, 1961) adjusted for Arctic coasts (Popov et al., 1988). Directions of sediment flows were determined through the use of geomorphological analysis (Morskaya..., 1980) and calculations of the wave energetic characteristics following the Popov-Sovershaev method (Popov and Sovershaev, 1982;

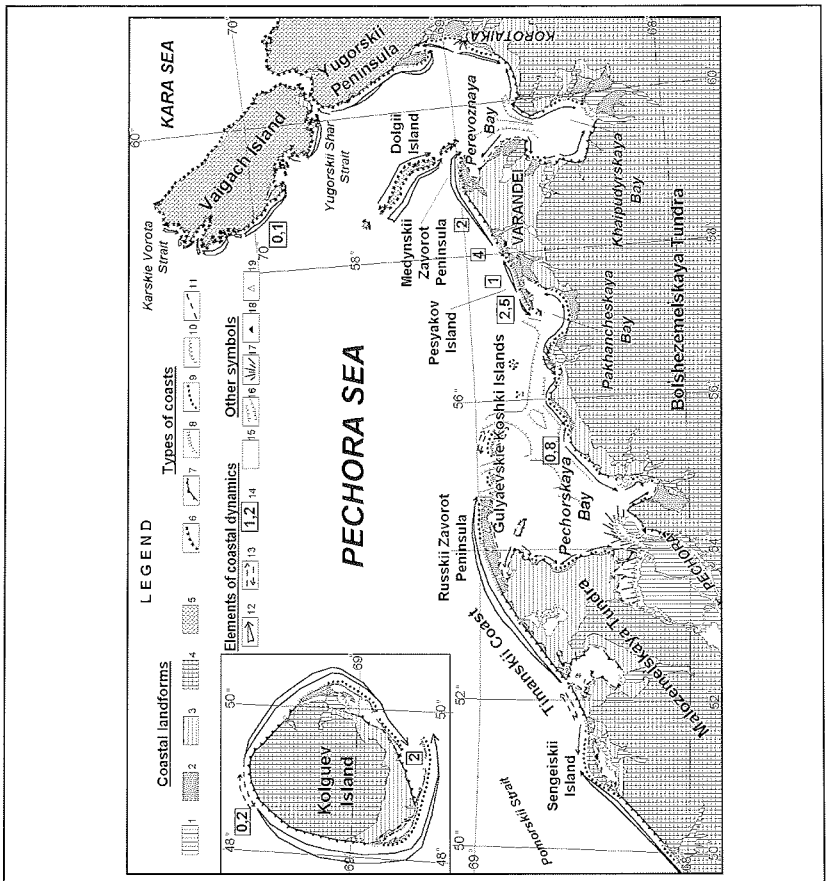

Coastal landforms: 1 - flood plains and river deltas (Q_{IV}); 2 - eolian-marine (up to 10 m high) and alluvial-lacustrine-marine (up to 3 m high) terraces (Q_{IV}); 3 -lacustrine-alluvial terraces up to 5-10 m high (Q_{III-IV}); 4 - denudation plains (Q_{II-III}) formed in loose glacial and glacio-marine sediments with fragments of high marine terraces; 5 - denudation plains (Q_{II-III}) formed in bedrocks with fragments of rock-defended marine terraces. Types of coasts: 6 - abrasion (cliffed) coasts with pebbly beaches; 7 - thermoabrasion and thermodenudation coasts with sandy-pebbly beaches or boulder benches; 8 - coasts with sandy (sandy-pebbly) beaches formed due to erosion of accumulative forms; 9 - accumulative coasts with sandy or sandy-pebbly beaches; 10 - deltaic coasts; 11 - coasts of lagoons and bays. Elements of coastal dynamics: 12 - alongshore fluxes of wave energy (arrow thickness proportional to drift-carrying force); 13 - coasts with bilateral drift migrations; 14 - coastal retreat rate, m/year. Other symbols: 15 tidal flats; 16 - fragments of flooded river valleys; 17 avandeltas; 18 - separate bedrock exposures; 19 - dune belts.

Fig. 1. Scheme of the morphology and dynamics of coasts in the Pechora Sea

Ogorodov, 2002). Zonation of the coasts is based on morphodynamic characteristics.

The southern Pechora Sea coast from Svyatoi Nos Cape to Khaipudyrskaya Bay lies within the Pechora plate composed of the Baikalian crystalline basement overlain by a thick sequence of Paleozoic-Mesozoic beds with a cover of Pleistocene-Holocene glacial, marine and lacustrine-alluvial deposits. Crystalline beds of the Cis-Ural depression are exposed only to the east of Dolgii Island.

Timan coastal region (Fig. 1) stretches from Svyatoi Nos Cape to the Russkii Zavorot Peninsula. The Svyatoi Nos Peninsula represents an accumulative form like tombolo fed from two sources – sediment drift originating from the abrasion coast in Indigskaya Bay and counter drift from Gornostal'ya Bay (Suzdal'skii, 1974). The tombolo connects the shore and the bedrock outlier. Farther northeastward a relatively straight shore section ("Timanskii bereg") stretches for more than 200 km. Abrasion-accumulative coast lies between Svyatoi Nos Cape and Sengeiskii Island. The shores of Gornostal'ya Bay are predominantly formed by thermoabrasion of the frozen sediments lying at the base of the 25-35 m high marine terrace. Farther eastward segments of accumulative coasts are present. The up to 50 m high Sengeiskii Island with bedrock exposures at the base probably represents a residue of a Middle-Late Pleistocene denudation plain. Eolian processes shape the surface of the island. Sand accumulations are related to sediment flows discharge in the zone of convergence. An up to 5-10 m high barrier beach of the Holocene age lies to the northeast of Sengeiskii Island. Under modern environmental conditions, the barrier beach is partly eroded. For instance, east of Kolokolova Bay, the 10-15 m high Late Pleistocene-Holocene lacustrine-alluvial terrace facing the sea, is eroded by thermoabrasion. No estimations of the coastal retreat have been carried out in this region, but according to the shore morphology it should be more than 1 m/year. The main direction of sediment flow is northeastern.

Pechora coastal region includes the accumulative forms Russkii Zavorot and Gulyaevskie Koshki (Popov et al., 1988) representing the Holocene barrier. As a continuation of the Russkii Zavorot Peninsula, a group of semi-submarine barriers and barrier islands called Gulyaevskie Koshki bound the Pechora (Pechorskaya) Bay from the north. The supposition that these forms are barriers is supported by the absence of a strong alongshore drift supplying sedimentary material and also by the presence of massive ice of subaerial origin (Velikotskii, 2001). The Russkii Zavorot Peninsula composed of fine-sorted sand is subjected to intensive eolian activity forming a dune belt. Both, the alongshore wave energy flux and the sediment flow are directed to the east (Fig. 1), and sediments are accumulated at the distal end of the peninsula.

The Gulyaevskie Koshki is a chain of 9 barrier islands subdivided into the Western and Eastern ones. The Western Gulyaevskie Koshki islands are bigger in size than the Eastern ones. They are moving to the south and east. Tides and drift currents form channel fans between them, while waves form spits at their ends. In general, these forms accumulating sedimentary material, derived from the seafloor and Pechora Bay, are relatively stable. Due to local hydrodynamic conditions, location and size of the Eastern Gulyaevskie Koshki islands are constantly changing (Suzdal'skii and Kulikov, 1997). These unstable forms cannot be used for long-term constructions. In the old Pomorian maps of the XVI-XVII centuries the Gulyaevskie Koshki Islands are bigger than their modern analogues, and also their number is greater. Probably, in former days the Russkii Zavorot Peninsula and Gulyaevskie Koshki Islands represented a single accumulative form.

Within Pechora Bay (Fig. 1), abrasion-thermodenudation coasts (worked out in the frozen postglacial marine, alluvial-lacustrine and biogenic deposits) intercalate accumulative coasts with laidas, beaches, bars and lagoons. The Pechora River Delta occupies the southern part of the bay. Morphologically it belongs to the type of multi-branch deltas.

Coasts with ancient abrasion bluffs and young lacustrine-alluvial-marine terrace (laida) are widespread in this area (Fig. 2). Laidas are formed behind barrier beaches and spits in coastal concavities and inner parts of the bays under the influence of storm surges up to 2.5-3.0 m high. Laidas are formed due to enhanced accumulation during the Holocene stabilization of the sea level following the period of Flandrian transgression when abrasion processes were dominant. Laidas are drained by streams and numerous laida channels formed by surges and tides. The laida channel network is rather complicated and usually has several outflows to Pechora Bay. Numerous lakes are located on the laida surface, especially where it is not protected from direct influence of surges by beaches and barrier beaches. These small lakes-puddles are formed by suffosion-erosion processes that are especially active during maximum surges and subsequent outflows, when fine-grained material is evacuated from the puddles (Romanenko, 1997). The puddles are often connected with each other by small channels, which serve as pathways for water running from one puddle to another.

Suzdal'skii and Kulikov (1997) estimated the average retreat of abrasion-thermodenudation shores in the southeastern part of the bay (in vicinity of the Vangurei settlement) as 0.8-1.2 m/year, and in the harbours as 0.4 m/year and less. Relatively low values of abrasion activity are due to a shorter dynamically active period as compared to the open coasts of the Pechora Sea, and, also, low wave energy in the semi-closed bay. The same authors approximately estimated the amount of sedimentary material supplied into the bay due to abrasion of coastal bluffs and submarine slope as 1000 m^3 that is 4.5 times less than the solid discharge of the Pechora River. The greatest part of sedimentary material is probably removed beyond the bay, also via the submarine Pechora paleovalley and numerous drainage channels worked out by surge waters. The height of tides in the Pechora Bay reaches 1.2 m. As a result, numerous tidal flats are formed in the coastal concavities and in the wave shadow of accumulative islands.

Sea ice is another important factor shaping coasts in the Pechora Bay. This is the area of the highest frequency of grounded ice ridges in the Pechora Sea. Therefore, a lot of ice gouges and wallows are left after ice melts. Close to the delta there could be numerous strudel scours known from the other arctic river mouths (Reimnitz and Kempema, 1983). Sea ice plays an important role in lithodynamics, removing sedimentary material during fast-ice break-up.

Varandei coastal region (Fig. 1) occupies an area between Pesyakov Island in the west and Medynskii Zavorot Peninsula in the east. Pesyakov and Varandei islands are sandy barriers of Holocene age similar to the Russkii Zavorot Peninsula (Popov et al., 1988). At present, central parts of the barriers are eroded (Fig. 3). Their distal ends are accumulative. To the east of Varandei Island, the thermoabrasion coast is represented by a 5-15 m high erosion terrace (Fig. 4). Here, the permafrost layer of the Middle Pleistocene boulder loams and clays is

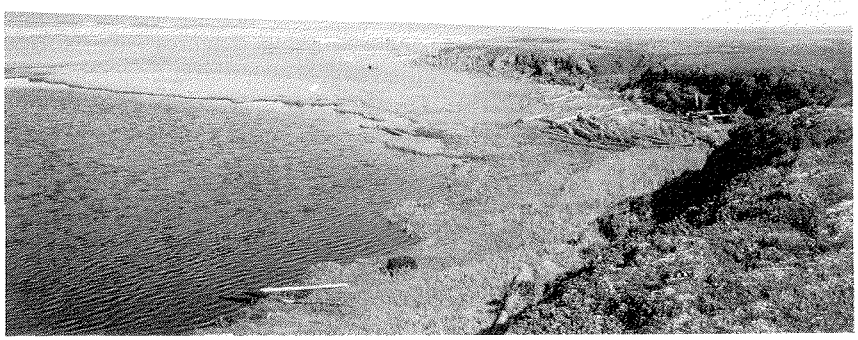

Fig. 2. Coasts with abandoned cliffs bounded with laida

Fig. 3. Erosion in the central part of the barrier beach on the Varandei Island

Fig. 4. Thermoabrasion coast, 30 km eastward from the Varandei settlement

abraded. The Medynskii Zavorot Peninsula has a complicated structure transitional from a spit to a barrier. In this region, alongshore wave energy fluxes of different directions are weaker than in the region of the Russkii Zavorot Peninsula. The zone of bilateral beach drifting is located in the central part of the described region. Only in the vicinity of the Medynskii Zavorot Peninsula the alongshore wave energy flux increases. Thus, the base of the peninsula is eroded, and sediments are accumulated at its distal end (Fig. 1).

Tidal flats and laidas occur behind barrier beaches and spits. Though the average height of tides in Pakhancheskaya and Perevoznaya bays is not high (0.8-1.2 m), extremely gentle slopes of landward and seaward parts of the barriers favor formation of these landforms. In Perevoznaya Bay the local counter drift of sediments exists in the wave shadow of the peninsula, where fine-grained material is accumulated. A big accumulative form stretches southward from Perevoznaya Bay to the entrance of Khaipudyrskaya Bay. It is evolving under the influence of wind-induced sea-level oscillations. Its supermarine part is represented by a vast laida cut by a network of channels, and its submarine part by a tidal flat.

Since 1987 the Laboratory of Geocology of the North, MSU, has carried out stationary observations in the Varandei region. Therefore, for this area the most reliable data on the coastal dynamics in the Pechora Sea are available. At the slightly technogenically altered coasts the rate of coastal retreat equals 1-2.5 m/year (Pesyakov Island; Ogorodov, 2001 a, b) and 1.8-2.0 m/year (thermoabrasion coast, Fig. 1; Novikov and Fedorova, 1989).

The island chain northeastward off the Varandei coastal region is of different origin. Matveev, Golets, Dolgii and Zelentsy islands (Fig. 1) form a single linear crystalline cusp eroded by waves and physical weathering. Abrasion, abrasion-accumulative and abrasion-bay coasts occur here. Inset and pocket beaches are composed of pebbles and rock debris. The height of the remaining beach ridges increases towards the center of Dolgii Island thus providing evidence for its tectonic uplifting. The presence of crystalline rocks and considerable height of the shores (10-18 m) make the islands, especially Dolgii Island, rather stable and suitable for economical development.

Nearly all types of coasts present in the southern Pechora Sea could be found in Khaipudyrskaya Bay. This variety is due to diverse morphogenetic complexes facing the sea (Fig. 1): from small river deltas to high marine terraces (up to 50-60 m). High (up to 50 m) abrasion-thermodenudation slopes border the bay from the south-southwest, while typical thermoabrasion coasts occupy the northern and western sectors. Accumulative coasts with beaches and deltas are present in the southeast. In the inner southern part of the bay, wave energy fluxes form a zone of convergence producing an elongated tidal flat.

Western-Yugorskii coastal region stretches from the Sin'kin Nos Cape to the Yugorskii Shar Strait (Popov et al., 1988). Unlike the other regions, the shores here are made of boulders, cobbles and pebbles with bedrock exposures in the northern part of the region. The zone of divergence of relatively weak wave energy fluxes causes erosion of the Sin'kin Nos Cape. The latter represents a bedrock cusp covered with loose coarse-grained debris. In the shore concavity to the east from the cape, accumulation predominates due to convergence of sediment drifts. A big alluvial cone, i.e. river avandelta, is formed near the Korotaikha River mouth.

Alongshore wave energy fluxes directed off both sides of the cone (Fig. 1) are responsible for removal of riverine sedimentary material. A zone of divergence of alongshore wave energy fluxes occurs at the entrance to the Yugorskii Shar Strait. One of these fluxes is directed to the south towards the Bel'kovskii Nos Cape and favors its growth. Another flux is directed inside the strait.

Novaya Zemlya and Vaigach islands are protrusions of the Ural mountain system and consist of rocks of Hercynian folding. Crystalline rocks form the western coasts of Yuzhnyi and Vaigach islands facing the Pechora Sea. The main fault running along western Vaigach and southern Novaya Zemlya is of coast-forming importance (Kaplin et al., 1991). The main faults are crossed by numerous transverse fractures occupied by river valleys. Glaciers reworked the valleys and formed troughs. Later their lower streams were transformed into fjords by transgressive sea (Kaplin, 1962). This is the case with the western part of Yuzhnyi Island. Strandflats of primarily abrasional origin (Kaplin, 1962) are widespread here. However, the Yuzhnyi Island coasts facing the Pechora Sea belong to the abrasion-bay type in the west and the fjord-skaren type in the south. The Yuzhnyi Island coasts cannot be referred to as indigenous coasts (Kaplin, 1962). Since this part of Novaya Zemlya is under the influence of a warm current and remains ice-free during the greatest part of the year, the coasts are affected by wave-induced abrasion and accumulation. A wide range of accumulative forms is formed including bay-bars, spits, crescentic bars and tombolos (Fig. 5).

Fig. 5. Novaya Zemlya Archipelago. Bay-bar in the inner part of the St. Anna Bay (photo by D.D. Badyukov)

The coasts of Vaigach Island are mainly represented by steep cliffs cut in Pre-Quaternary rocks. Insignificant dissection of the western and eastern coasts results from the fact that the coastline coincides with the regional strike. Cliffs are often surrounded by cobble beaches. Synclines and grabens in the west and northwest were flooded, and dissection of the coastline resembles that of the Dalmatian or fjord-like type (Kaplin et al., 1991). Where soft rocks are exposed, abrasion bays have been formed. Such coasts can be referred to as abrasion-bay ones. The zones of divergence of strong alongshore wave energy fluxes appear near capes. Sedimentary material released by abrasion is transported to the bays and shore concavities, where pebbly beaches and spits are formed. Since alongshore wave energy flux is directed to the south (Fig. 1), sediment drift moves towards the

Yugorskii Shar Strait. Due to the considerable strength of the rocks, the rate of abrasion does not exceed 0.1 m/year.

Location within the buried Kolguev-Pechora arch (Dibner, 1978), a platform structure of the Pechora plate cover, predetermines the structural-geomorphological position of Kolguev Island. No bedrock exposures have been found on the island. The northern part is uplifted and consists of sands, boulder loams and clays of glacial and glacial-marine origin. Abrasion terraces occur at the 20-30 and 40-70 m levels. Swamped lowlands formed by the Late Glacial and Postglacial sand deposits occupy the southern and eastern parts of the island. Thermoabrasion by the waves of northern rhumbs is active on permafrost coasts. The western, northern and northeastern coasts of Kolguev Island have steep cliffs 8 to 53 m high (Velikotskii, 1998). They are subjected to thermoabrasion (Fig. 6).

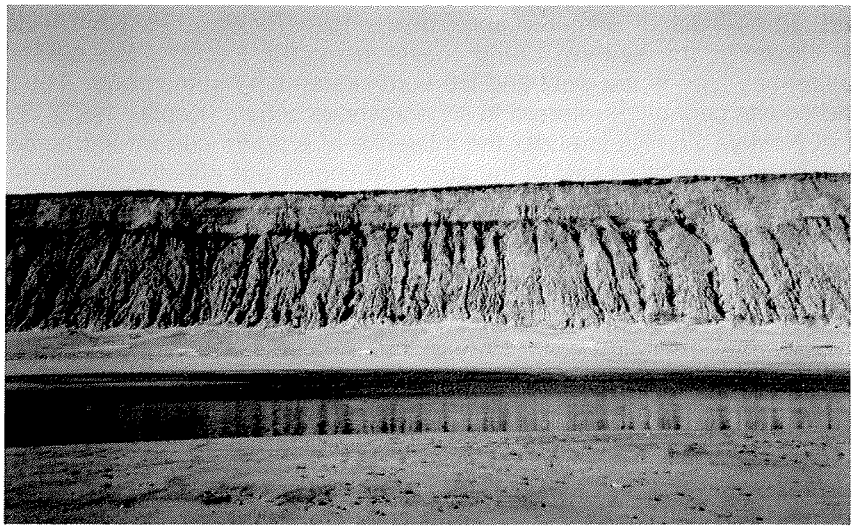

Fig. 6. Kolguev Island. Abrasion-thermodenudation cliff (22 m high), 1 km southward from the Velikaya River mouth (photo of G.A. Rzhanitsyn)

The highest cliffs are subdivided into two units. The lower unit up to 10-15 m is represented by boulder loams with low ice content. This part of the cliff is shaped by waves and thermoabrasion. The overlying unit (15-50 m) consists of ice-bearing sands and loams. It is shaped by thermodenudation. Such coasts are distinguished by a low rate of coast retreat equal to 0.1-0.2 m/year (Velikotskii, 1998). Abrasion here is suppressed by the presence of a boulder bench on the tidal flat and submarine slope and, also, accumulations of rock debris supplied by thermodenudation at the foot of the cliffs. This sector is characterized by the highest values of wave energy because of the maximum wave racing. When the height of the cliff decreases, the rate of abrasion grows up to 1-3 m per year (Suzdal'skii, 1974). The continental land massif protects the southern and southeastern parts of the island from direct wave impact.

At this part of Kolguev Island that is opposite to the main wave-inducing winds, the wave energy flux weakens, and sediment flows form accumulative landforms such as the Western and Eastern Tonkie Koshki spits and a big spit-barrier separating the Peschanaya lagoon from the sea.

Conclusions

The Pechora Sea coastal area can be subdivided into 10 morphodynamic regions with specific dynamic and morphological characteristics. Geomorphologically the Pechora Sea is distinguished by co-occurrence of big accumulative forms like barrier beaches and widespread thermoabrasion coasts.

References

Dibner, V.D., 1978. Morfostruktura shel'fa Barentseva morya (Morphostructures of the Barents Sea shelf). Leningrad, Nedra, 212 pp. (in Russian).

Geoekologiya Severa (Geoecology of the North), 1992. Solomatin, V.I. (ed.), Moscow, Izd. MGU, 270 pp. (in Russian).

Kaplin, P.A., 1962. Fiordovye poberezh'ya Sovetskogo Soyuza (Fjord coasts of the Soviet Union). Moscow, Izd. AN SSSR, 187 pp. (in Russian).

Kaplin, P.A., 1973. Noveishaya istoriya poberezhii Mirovogo okeana (The recent history of the World Ocean coasts). Moscow, Izd. MGU. 265 pp. (in Russian).

Kaplin, P.A., Leont'ev, O.K., Luk'yanova, S.A., Nikiforov, L.G., 1991. Berega (Coasts). Moscow, Mysl', 480 pp. (in Russian).

Leont'ev, O.K., 1961. Osnovy geomorfologii morskikh beregov (The basics of coastal geomorphology). Moscow, Izd. MGU, 417 pp. (in Russian).

Morskaya geomorfologiya. Terminologicheskii spravochnik. Beregovaya zona: protsessy, ponyatia, opredeleniya (Marine geomorphology. Reference book. Coastal zone: processes, terms and definitions), 1980. Zenkovich, V.P., Popov, B.A. (eds.), Moscow, Mysl', 280 pp. (in Russian).

Novikov, V.N., Fedorova, E.V., 1989. Destruction of coasts in the southeastern Barents Sea. Vestnik MGU, ser. 5, geografiya, 1, 64-68. (in Russian).

Ogorodov, S.A., 2001a. Morphology and dynamics of the Pechora Sea coasts. Proceedings of the Institute of Oceanology BAN, Varna, 3, 77-86 (in Russian).

Ogorodov, S.A., 2001b. Functioning of the Pechora Sea coastal systems under technogenic impact. In: Sedimentologicheskie protsessy i evolyutsiya morskikh ekosistem v usloviyakh morskogo periglyatsiala (Sedimentological processes and evolution of marine ecosystems under marine periglacial conditions). Apatity, Izd. KNTs RAN, 82-90 (in Russian).

Ogorodov, S.A., 2002. Application of wind-energetic method of Popov-Sovershaev for investigations of coastal dynamics in the Arctic. In: Rachold, V., Brown, J., Solomon, S. (eds.), Arctic Coastal Dynamics. Report of an International Workshop. Potsdam (Germany) 26-30 November 2001. Reports on Polar and Marine Research, 413, 37-42.

Popov, B., Sovershaev, V., 1982. Some features of the coastal dynamics in arctic Asia. Voprosy geografii, 119. Morskie berega (Sea coasts). Moscow, ysl', 105-116 (in Russian).

Popov, B.A., Sovershaev, V.A., Novikov, V.N., Biryukov, V.Yu., Kamalov, A.M., Fedorova, E.V., 1988. Coastal area of the Pechora-Kara Sea region. In: Issledovanie ustoichivosti geosystem Severa (Investigations of the geosystems stability in the North), Moscow, Izd. MGU, 176-201 (in Russian).

Reimnitz, E., Kempema, E.W., 1983. High rates of bedload transport measured from the infilling rate of large strudel-scour craters in the Beaufort Sea, Alaska. Continental Shelf Research, I, 3, 237-251.

Romanenko, F.A., 1997. Formation of lake depressions on the Arctic Siberian coastal lowlands. PhD Thesis summary, Moscow, 25 pp. (in Russian).

Suzdal'skii, O.V., 1974. Lithodynamics of the shallows in the White, Barents and Kara seas. Geologiya morya, Leningrad, Nedra, 3, 27-33 (in Russian).

Suzdal'skii, O.V., Kulikov, I.V., 1997. Landscape and lithodynamic scheme of the Pechora Bay. In: Voprosy kartirovaniya pribrezhnogo melkovod'ya Barentseva i Belogo morei (Problems of mapping in the shallow regions of the Barents and White seas), St. Petersburg, 72-83 (in Russian).

Tarasov, G.A., Alekseev, V.V., 1985. About sedimentation on the southern Barents Sea shelf. In: Geologiya i geomorphologiya shel'fov i materikovykh sklonov (Geology and geomorphology of shelves and continental slopes), Moscow, 112-117 (in Russian).

Velikotskii, M.A., 1998. Peculiarities of the modern coastal dynamics of the Kolguev Island. In: Dinamika arkticheskikh poberezhii Rossii (Dynamics of the Arctic coasts of Russia), Moscow, Izd. MGU, 93-101 (in Russian).

Velikotskii, M.A., 2001. About ice layers in sand spits of the Pechora barrier beach. In: Solomatin, V.I. (ed.) Problemy obshchei i prikladnoi geoekologii Severa (Problems of the general and applied geoecology of the north), Moscow, Izd. MGU, 148-154 (in Russian).

THE ROLE OF SEA ICE IN COASTAL AND SEA BOTTOM DYNAMICS OF THE PECHORA SEA

S.A. Ogorodov

Faculty of Geography, Lomonosov Moscow State University, Moscow, Russia

Abstract

The article deals with the morpho and lithodynamic role of ice in shaping the Arctic coasts. Taking the Pechora Sea as an example, the direct and indirect impact of ice on the seafloor and shores is described. The indirect impact of ice that blocks the coastal zone during the largest part of the year is considerable reduction of the overall energy of waves and currents. Direct impact means active ice scouring by ice ridges, ice-rafting of sedimentary material, formation of strudel scours and frozen rocks on shallows. Based on the performed analysis, the scheme was plotted showing zonation of the Pechora Sea according to the probable ice impact on shores and seafloor.

Introduction

As a zonal factor related to the high-latitude position of the Arctic seas, sea ice plays an important role in the evolution of the Arctic coastal zone. The currently available data on sea ice regime are especially important for navigation in the Arctic seas. Ongoing exploitation of oil and gas fields and related construction of engineering objects in the coastal and shelf areas of the Pechora Sea (navigation channels, water reservoirs, terminals, drill platforms, submarine pipelines) require a better understanding of the role of sea ice in coastal and bottom dynamics.

Analysis of the sea ice influence upon the Pechora Sea coast and seafloor consists of the following items: 1) protective role of fast ice and drift ice; 2) role of sea ice in evacuation of sedimentary material from shallows; 3) ice scouring of shores and seafloor; 4) local seafloor erosion due to specific sea ice conditions; 5) processes of fast-ice formation and sediment freezing in the nearshore zone.

Protective role of fast ice and drift ice

An indirect influence of sea ice on the Pechora Sea coast and seafloor dynamics is protection against waves and tides by fast ice and drift ice. Fast ice blocks the coastal zone during the largest part of the year thus regulating the influence of active hydrodynamic factors (Sovershaev, 1976; Kaplin, 1971; Are, 1980) and reducing the period of their activity down to 25-50% of the year. Hence, the dynamic age (Saf'yanov, 1978) of the coastal zone in the Pechora Sea is considerably younger compared to the seas of temperate and tropical latitudes.

The duration of the dynamically active period can be evaluated with the help of the ice-free period coefficient (Sovershaev, 1981), i.e. the ratio of the total multi-annual open-water period to the number of calendar days of the year expressed in percent. If considering the "adult" dynamic age of the modern coastline of ice-free seas as 6,000 years (the time when the global sea-level reached its present

position), then the dynamic age of the southeastern Pechora Sea is about 1.5-3.0 kyr.

In summer, when the largest part of the sea is free from ice, the latter is still able to indirectly affect coastal processes. Grounded ice ridges, which are preserved for a long time in the bays of the Pechora Sea, could prevent the waves from reaching the coast thus protecting it from their direct impact.

Also, blocks of fast ice (Fig. 1) and unconsolidated first-year ice accumulations on a beach are able to protect coastal cliffs from the direct destructive impact of waves (Are, 1980). However, this ice either quickly melts or is destroyed by waves.

Drift ice located in nearshore zone considerably decreases wave energy and sometimes also quenches them. Such events occur in the Pechora Sea during summer when drift ice from the Kara Sea enters it through the Karskie Vorota Strait (Fig. 2).

The evolution of the Pechora Sea shelf during post-glacial times was controlled by changes in sea-ice cover extent. Variations in the sea-ice extent and, hence, evolution of coasts were shown to be rhythmic. Periods of relatively high lithodynamic activity were replaced by periods of maximum "conservation" of the coastal zone (Sovershaev, 1982). A series of coastlines was formed in the course of the post-glacial transgression. Two of them, located at the depths of 28-30 and 12-15 m, were probably formed during the periods of the lowest ice extent. However, at the depths exceeding 50-60 m, fragments of Pre-Late Pleistocene landforms have been preserved due to the prolonged conservation of the coast by sea ice (Biryukov and Ogorodov, 2001).

The role of sea ice in evacuation of sedimentary material from shallows

Sea ice transports coarse debris from the nearshore zone to deeper regions (Sovershaev, 1981). In the course of the ice-rafting the natural sorting of bottom sediments is changed. The uplifting ability of sea ice is very high: one cubic meter of ice is able to transport from 100 to 300 kg of sediment load (Lisitzin, 1994). Sea ice transports sedimentary material of different sizes – from boulders more than 10 m in diameter to pelite particles. Several mechanisms of sediment entrainment into sea ice operate in the Pechora Sea: a) eolian transportation from land; b) accumulation of slope material falling from coastal bluffs; c) supply by flood waters; d) suspension entrainment at freeze-up; e) adfreezing of bottom sediments to the fast-ice surface in the zone of ice-sediment contact; f) dragging of bottom sediments by ice keels of drifting ice ridges; g) sediment accumulation on the fast ice during storms.

Mainly fine sand and silt-pelite particles are subjected to eolian transportation. Eolian accumulations are usually local because the plant cover on the Pechora Sea coast is patchy. Small thickness of snow cover and predominance of offshore winds predetermine considerable accumulations of eolian material on the surface of ice fields, especially in the areas of sand bars and spits (Pesyakov Island, Russkii Zavorot Peninsula).

The role of slope processes should not be overestimated, because during the largest part of the year coastal bluffs are frozen. However, during transitional seasons abundant sedimentary material falls on ice.

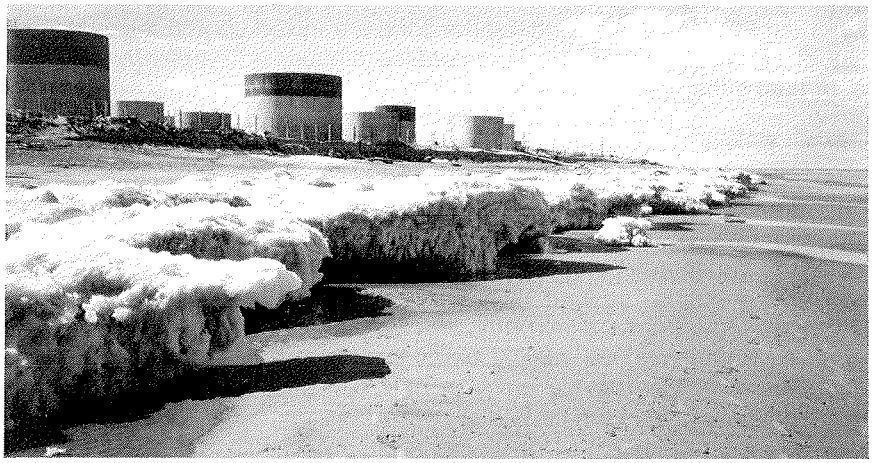

Fig. 1. Pechora Sea coast near the tank farm stock in Varandei settlement. Fast ice blocks pushed onshore protect coastal bluffs from waves

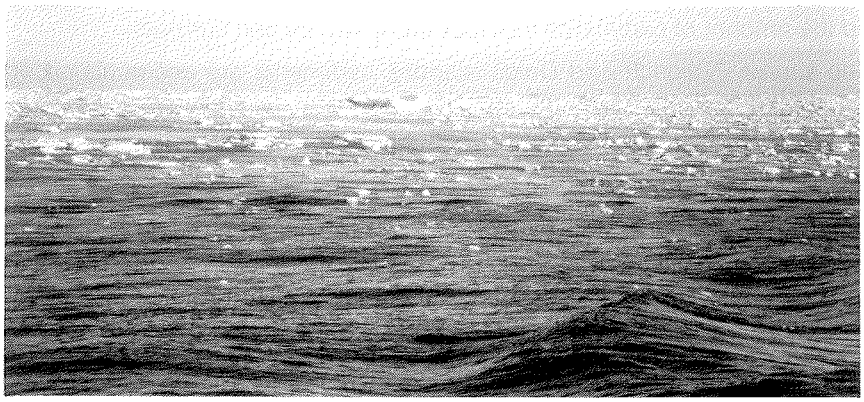

Fig. 2. The Pechora Sea, area around the Russkii Zavorot Peninsula. July 15, 2002. Drift ice from the Kara Sea nearly completely reduced the wave energy in the nearshore zone

Sedimentary material is also supplied to sea ice by rivers, primarily the Pechora River, and temporary streams during spring break-up, when floodwaters with a considerable amount of bed and suspended load overflow the fast ice surface (Sovershaev, 1981).

Another way of "contactless" incorporation of sediment load into ice is suspension freezing at ice freeze-up (Lisitzin, 1994). As a result of fall storms, fine-grained bottom sediments are partly re-suspended, and concentration of suspended particles in water reaches 1000 mg/l and even more (Kempema et al., 1989).

Further cooling causes formation of upward moving frazil ice grains that later adfreeze to each other.

The main source area for sediment entrainment into sea ice is adfreezing of bottom sediments to the fast ice surface at the ice-sediment interface. Seawater with a temperature close to freezing point is enriched in ice grains. During fall and winter storms, bottom sediments in the nearshore zone are mixed up with these ice grains (Reimnitz et al., 1985). Later, the sediment-ice mixture adfreezes to the fast-ice surface. In tidal seas, the process of adfreezing could be repeated several times, thus forming dirty-ice interlayers in the lower part of the fast ice (Archikov et al., 1989). Also, bottom sediments are pushed into tidal fractures, and sediment fragments adfreeze to the ice floes (Chuvardinskii, 1974). Sediments are also incorporated into fast ice by hummocks occurring directly above barrier bars. At steep gravelly shores (Vaigach and Dolgii islands) these phenomena are less pronounced. At the shores composed of fine sediments with the "fast ice-sea floor" contact zone reaching several kilometers (western part of Pechora Bay, Khaipudyrskaya Bay, Perevoznaya Bay) sea ice plays the leading role in sediment transportation. Sediments are mainly entrained by sea ice during freeze-up. In spring-summer, after the fast-ice cover is destroyed, ice floes drift offshore and loose their sediment load in the course of melting.

In the Pechora Sea, dragging of sediments by ice keels of drifting ice ridges has not yet been investigated. Big floebergs do not only scratch the sea floor, but also participate in the alongshore transportation of sediments. Within the water depth range of 10 to 15 m, the amount of sediment load transported by ice ridges could exceed the amount of sediments transported by waves and currents.

At steep shores (Vaigach and Dolgii islands), sediments are accumulated on the fast ice during storms. Here the fast ice formation takes a long time as it is interrupted by destruction during storms.

Ice scouring of shores and seafloor

Ice scouring means mechanical destruction of sediments by overlying ice. In the Pechora Sea, mechanical impact on the seafloor and shores is related to ice dynamics, ice activity and hummocking dependent on hydrometeorological factors and coastal relief. Ice scouring occurs in the coastal area from some meters above the sea level down to the depths of 15-35 m.

The shores are subjected to ice impact during both freeze-up in fall and break-up in spring. Gravelly beaches show traces of active bulldozing of sediments by ice. During fall - beginning of winter onshore winds or ice movements push the young 20-40-cm-thick ice onto the shore. The latter incorporates coarse debris and transports it landwards. We recorded accumulations of coarse fragments in the Pechora Bay just below the bank slope. In some cases, even the bank slope itself is scoured by ice. After fast ice has melted, the fragments on the beach become less sorted, while the size of fragments increases due to addition of fragments brought with ice from the underwater coastal slope (Fig. 3). Onshore movement is dangerous for engineering constructions including metallic ones (Fig. 4). On coastal lowlands overflooded during severe storms, ice floes can be brought as far inland as tens and hundreds of meters. Natives from Novyi and Staryi Varandei settlements told us that sometimes in winter fast ice moves onto the beach berm between these settlements for several hundreds of meters. Indirect evidence for such a phenomenon is the observation tower located 150 m onshore from the coastline, which has been bent at its base (Fig. 5).

Fig. 3. Pechora Sea coast near the tank farm stock in Varandei settlement. Gently sloping ridge of non-sorted debris was bulldozed onto the beach by fast ice

Small-scale ice scouring forms appear on sand beaches: furrows, scratches, wallows and also different ice-pushed ridges (Fig. 6). The depth of these forms does usually not exceed 0.5-1 m, and their length is about 50 m. Most ice scouring forms are transverse to the coastline. On sand beaches they are preserved for a very short period, just until the next summer storm.

Fig. 4. Pechora Sea coast near the constructed pipeline "Varandei sea". During the winter of 1999-2000 the offshore side of the barge-pontoon was destroyed by fast ice moving rapidly onshore

The mechanical impact of sea ice on the seafloor starts with freeze-up and lasts until the sea becomes completely ice-free. Young ice adfreezes to thesea floor in the nearshore zone, and the newly formed ice belt serves as a specific protection for the shore. Hummocks, closest to the coast (down to 3-5 m water depth), are

Fig. 5. Pechora Sea coast between Staryi and Novyi Varandei settlements. Observation tower destroyed by onshore moving fast ice

Fig. 6. Pechora Sea coast near Varandei airport. Small-scale ice scouring on the beach: ice furrows, ice-wallows and small ice-pushed ridges

formed above submarine bars. Since the water depth above bars is lower, they serve as the centers of hummocking and, hence, the number of ice ridges usually corresponds to the number of submarine bars. Ice gouges in this area are mainly transverse to the coastline due to onshore pushing impact of sea ice.

Farther offshore (stamukhi zone), location of hummocks becomes irregular being dependent on hydrodynamics, primarily the fast-ice edge location during severe storm winds. Storm winds destroy the fast-ice edge and form additional ice-ridge or single grounded hummocks. In this zone, ice gouges are either chaotic or parallel

to the coastline as a result of dominantly alongshore drift of ice ridges. At the fast-ice edge, where grounded ice ridges are constantly formed during winter, the impact on the seafloor is the highest.

The depth of ice gouges depends not only on the ice thickness (reaching about 1 m in the Pechora Sea by March) and shear stress, but also on the composition of bottom sediments. Investigations carried out by AARI and AMIGE have shown that the depth of ice gouges in dense clays and loams of Middle Pleistocene age reaches 0.5-1 m, while in loose mobile sands and loamy sands ice gouges are recorded quite rarely. Probably, the actual incision of ice gouges into sands and loamy sands reaches 1.0-1.5 m, but the gouges are quickly filled up under the influence of currents and waves.

Preservation of ice gouges depends on the water depth. In the shallow areas down to 7-8 m water depth, ice gouges can be recorded soon after the fast ice melts. Ice gouges less than 0.5 m deep usually disappear after the first strong summer storms. Thus, the age of ice gouges in the shallow nearshore zone does not exceed one year. Due to the active hydrodynamic regime these bedforms are quickly leveled. As a result, compared to the fast-ice edge zone, the gouge density here is low.

The highest gouge density is observed at the depths of 8-20 m (Rokos and Kostin, 1998). Within this depth range the most mobile hummocks and grounded ice ridges are formed. Compared to shallows, the hydrodynamic regime at these depths is considerably less active. That is the reason why ice gouges can be preserved here for several years, and, close to 20 m water depth, even for dozens of years.

In deeper areas (20-35 m) ice gouges do also occur, though ice ridges themselves are rather rare. This is the consequence of calm hydrodynamic environment and low sedimentation rates. Under such conditions, ice gouges, especially the biggest ones, can be preserved on the seafloor for years, i.e. low intensity of ice scouring is counterbalanced by fine preservation of gouges. This "piling-up" effect gives a wrong idea about the intensity of ice scouring.

All this shows that the intensity of ice scouring does not directly depend upon the gouge density. Besides this, the intensity of ice gouging and preservation of gouges considerably differ in the Arctic seas as they are directly dependent on such factors as bottom topography, sediment type, ice thickness, prevailing winds, temperature, waves, currents, duration of hydrodynamically active period, etc.

Not only is the process of ice gouging of particular interest, but also the form of gouges. The latter are morphologically different: U, V, W-shaped gouges, troughs, gouges of complicated morphology with symmetric and non-symmetric flanks. American scientists (Barnes et al., 1984) subdivide ice ridges into "multi-keeled" and "single-keeled" ones. The former produce a system of parallel gouges, while the latter leave only single gouges (Fig. 7). Ice gouges of all known types have been encountered in the Pechora Sea (Fig. 8).

Local seafloor erosion due to specific sea ice conditions

In Russia, such seabed forms as strudel scour depressions have not been investigated yet. According to foreign investigations (Reimnitz and Kempema, 1983), they represent craters up to several meters deep found on shallows. These forms appear in spring, when snow melts and floodwaters overflow fast ice.

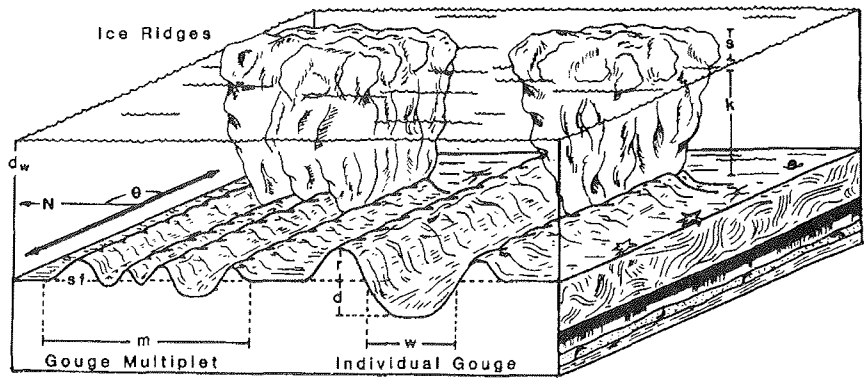

Fig. 7. Conceptual sketch of ice gouging and formation of the system of parallel "multi-keeled" and "single-keeled" gouges (Barnes et al., 1984)
Key: k keel depth; s sail height; d gouge depth; w gouge width;
r ridge height; m multiplet disruption width

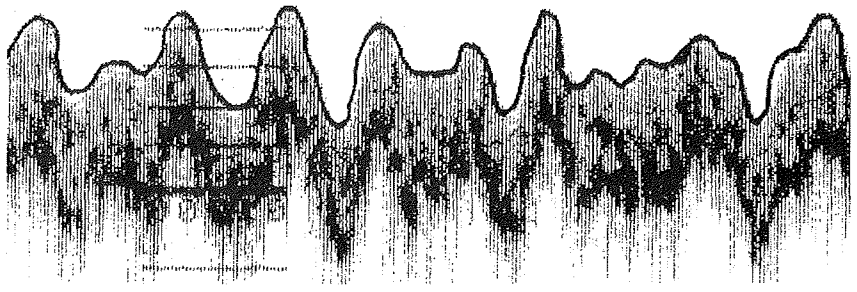

Fig. 8. Fragment of the echogram, Pechora Sea, 17-18 m water depth. Cruise of R/V "Ivan Petrov", 1999

Riverine and melt water jets flow downward through holes in the ice and scour the bottom formingwallows with swirls above them. Depending on hydrodynamic conditions, these wallows are infilled with sediments in 2-3 years on the open coasts or in several years in calm environments. No data are available on the strudel scour depressions in the Pechora Sea. However, favorable conditions exist off the deltas of Pechora, Chernaya and Korotaikha rivers.

Seafloor is locally eroded at the base of grounded hummocks and submarine pipelines. This is a well-known effect in the practice of bridge construction caused by increasing turbulence and velocity of currents flowing around seabed irregularities. Scouring of bottom grounds around pipelines is especially dangerous because the pipe protruding from the bottom could be destroyed by hummocks. Several times destruction of pipes has been recorded on Kolguev Island. Also, the pipeline in the vicinity of Varandei settlement is in a dangerous situation.

Processes of fast-ice formation and sediment freezing in the nearshore zone

Ice factor plays an important role in the heat balance of water masses and bottom sediments. In summer, floating ice reduces accumulation of solar radiation in the

upper water layer. In winter, it hampers the heat flux from below and alters temperature and mineralization of waters (including the bottom water layer, which is the main indicator of the temperature field of underlying bottom sediments). Long-living fast-ice cover causes continuous temperature fall and increasing mineralization of bottom water layer, thus favoring freezing of bottom grounds and preservation of relic permafrost (Zhigarev, 1997).

Fast ice is formed not only at continental shores and islands, but also on the shoals. It produces new permafrost sediment bodies through freezing of bottom grounds. This is typical for the shallow parts of the Pechora Sea bays. Freezing of beaches and shoals and formation of a thin ice film precede fast ice growth. The latter starts at the coastline in fall. Bottom fast ice stretches offshore to depths corresponding to the ice thickness. In this area submarine permafrost is formed (Zhigarev, 1997). As a result, in the contact zone between the shore and fast ice a "cap-peak" of frozen sediments is formed protruding offshore. Drilling in the Pechora Bay off the Dresvyanka River mouth revealed the presence of such a "cap-peak" of seasonally frozen layer down to the 1-m isobath.

Grounded hummocks also cause freezing of bottom sediments. When brought to shallow areas (water depth < 20 m), floating ice ridges adfreeze to the seafloor, become stable and turn into grounded hummocks. The latter are rapidly destroyed in summer by heat and waves. Even after ice ridges melt away, bottom sediments at the place of their grounding can remain frozen. However, their influence on the temperature field of bottom sediments is insignificant because of their low relative abundance, occasional settling and relatively small size of the hummock-bottom contact area (Zhigarev, 1997).

Chemical impact of sea ice, i.e. brine rejection due to fast ice formation, is evident at the shallows and lagoons. By the end of winter, when ice thickness reaches its maximum, these areas become nearly completely isolated from sea. Hence, a specific temperature and salt regime is formed that differs from that of the open sea. Since salinity is much higher than the average one, temperature falls below the freezing point, and a so-called cryopeg is formed. At the contact with cryopegs bottom grounds become salinized and turn into a seasonally supercooled state. Such conditions were recorded in the Pakhancheskaya, Perevoznaya bays, at the shoals of Khaipudyrskaya Bay and at some other shallows of the Pechora Sea.

Similar conditions favoring cryopeg formation exist in depressions between submarine bars in case growing ice adfreezes to the bars. Troughs between the bars become separated from the sea. Highly mineralized waters accumulating in these depressions protect bottom grounds from freezing.

Conclusions: zonation of the Pechora Sea according to the probable ice impact on the shores and seafloor

Zonation of the Pechora Sea according to the probable ice impact on the shores and seafloor (Fig. 9) is based on V.A. Sovershaev's model (Pririodnye usloviya..., 1997) taking into account local morpholithodynamic peculiarities. Several lithodynamic zones have been established with a characteristic number of factors determining the intensity of ice scouring.

Ice scouring is responsible for raking the seafloor below the fast ice during freeze-up and break-up. In winter, fast ice protects the seafloor from destruction. In the inner parts of the bays and on tidal flats ice scouring is insignificant due to stability

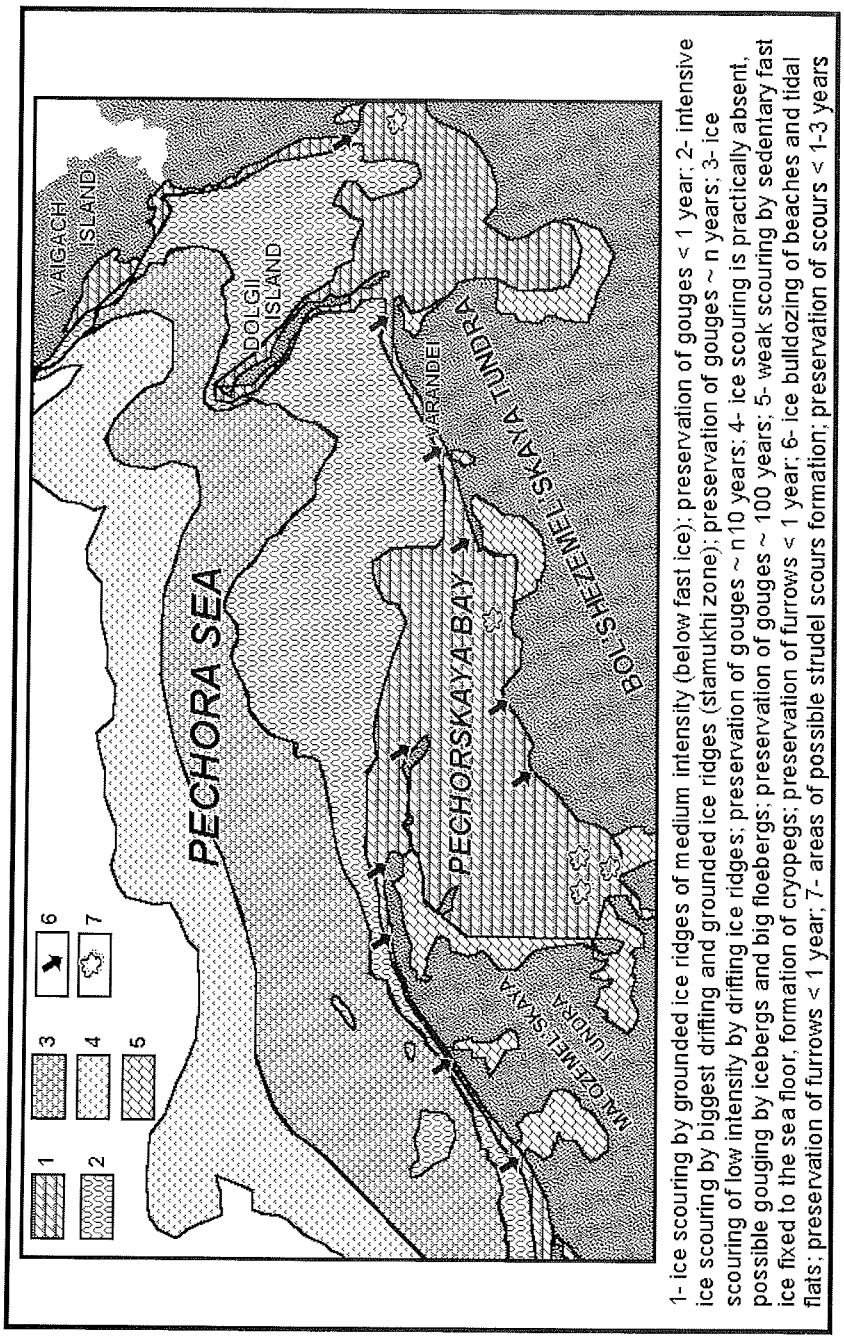

Fig. 9. Schematic map of the Pechora Sea zonation according to possible ice impact upon the shores and sea floor

of the fast-ice cover adfrozen to the seafloor. This is the area where cryopegs are formed. After fast ice melts, ice gouges become quickly infilled by waves and currents.

At the boundary between the fast ice and close floating ice at the depth of 18-22 m (stamukhi zone) ice scouring by the biggest drifting and deeply grounded ice ridges is intensive during the greatest part of the cold season. Here the deepest ice gouges are located, which are preserved for several years and sometimes for dozens of years.

At the depths of 20-35 m ice scouring is insignificant because big ice ridges with keels able to reach the seafloor are rare. However, due to calm hydrodynamic conditions ice gouges are preserved here for dozen years.

References

Archikov, E.I., Stepanova, L.E., Maiorov, I.S., 1989. Rol' ledovykh obrazovanii v razvitii beregovykh geosistem Okhotskogo moray (The role of ice in evolution of coastal ecosystems in the Sea of Okhotsk). Vladivostok, Izd. DVGU, 112 pp. (in Russian).

Are, F.E., 1980. Termoabraziya morskikh beregov (Thermoabrasion of sea coasts). Moscow, Nauka, 160 pp. (in Russian).

Barnes, P.W., Rearic, D.M., Reimnitz, E., 1984. Ice gouging characteristics and processes. In: Barnes, P.W., Schell, D.M., Reimnitz, E. (eds.) The Alaskan Beaufort Sea: ecosystems and environments, Academics Press Inc., Orlando, Florida, 185-212.

Biryukov, V.Yu., Ogorodov, S.A., 2001. Bottom topography of the Pechora Sea as a result of land-ocean interactions in the Pleistocene-Holocene. Abstracts of the XIV International School on Marine Geology, Vol. 2, Moscow, Izd. GEOS, 178-179 (in Russian).

Chuvardinskii, V.G., 1974. About the role of fast ice in accumulation of boulders, Kandalakshskii Bay as an example. In: Geologiya kainozoya severa Evropeiskoi chasti SSSR (Cenozoic geology of the northern European part of the USSR). Moscow, Nedra, 19-66 (in Russian).

Kaplin, P.A., 1971. Peculiarities of the dynamics and structure of coasts in the polar seas. In: Novye issledovaniya beregovykh protsessov (Recent investigations of coastal processes). Moscow, Nauka, 22-34 (in Russian).

Kempema, E.W., Reimnitz, E., Barnes, P.W., 1989. Sea ice sediment entrainment and rafting in the Arctic. J. Sediment Petrol., 59, 2, 308-317.

Lisitzin, A.P., 1994. Ledovaya sedimentatsiya v Mirovom okeane (Sea-ice sedimentation in the World Ocean). Moscow, Nauka, 448 pp. (in Russian).

Prirodnye usloviya Baidaratskoi guby. Osnovnye rezul'taty issledovanii dlya stroitel'stva podvodnogo perekhoda (Environmental conditions of the Baidaratskaya Bay. Main results of investigations for construction of submarine passage), 1997. Moscow, GEOS, 432 pp. (in Russian).

Reimnitz, E., Graves, S.M., Barnes, P.W., 1985. Beaufort Sea coastal erosion, shoreline evolution and sediment flux. U.S. Geological Survey. Open-File Report-380. 1-74.

Reimnitz, E., Kempema, E.W.,1983. High rates of bed load transport measured from the infilling rate of large strudel-scour craters in the Beaufort Sea, Alaska. Continental Shelf Research, I, 3, 237-251.

Rokos, S.I., Kostin, D.A., 1998. Ice gouges in the Barents, Kara and Pechora seas. Abstracts of the International Conference "Marine periglacial and glaciation of the Barents-Kara shelf in the Pleistocene", Apatity, 87-91 (in Russian).

Saf'yanov, G.A., 1978. Beregovaya zona okeana v XX veke (Coastal zone in the 20th century). Moscow, Mysl', 263 pp. (in Russian).

Sovershaev, V.A., 1976. The role of ice factor in coastal dynamics. Vestnik MGU, ser. Geogr., 4, deposited in VINITI, N 1777-76, 11 pp. (in Russian).

Sovershaev, V.A., 1981. The influence of sea ice upon evolution of the arctic shelf cryolithozone. In: Kriolitozona arkticheskikh morei (Cryolithozone of the Arctic seas), Izd. In-ta Merzl.SO AN SSSR, 70-83 (in Russian).

Sovershaev, V.A., 1982. Dynamics of marine glaciation and formation of coastlines on the arctic shelves. Vestnik MGU, ser. Geogr., 1, 88-90 (in Russian).

Zhigarev, L.A., 1997. Okeanicheskaya kriolitozona (Oceanic cryolithozone). Moscow, Izd. MGU, 320 pp. (in Russian).

SEDIMENT SEQUENCE OF THE SOUTHERN NOVAYA ZEMLYA TROUGH (PECHORA SEA): FACIAL AND STRATIGRAPHIC INTERPRETATIONS

Yu.A. Pavlidis, N.N. Dunaev, S.L. Nikiforov

Shirshov Institute of Oceanology RAS, Moscow, Russia

Abstract

The fine sediment structure in the Southern Novaya Zemlya Trough was carried out with the help of acoustic profiler "Parasound". This allowed establishing the facial dependence of deposits and sediment sequence in that part of the Pechora Sea, which remained a sea basin during the whole Late Pleistocene. Sediment sequence was subdivided into four stratigraphic horizons: 1 – Holocene (Q_4) marine deposits; 2 – Upper Valdai (Q_3^4) glacial-marine deposits; 3 – Middle Valdai (Q_3^3) marine deposits; 4 – Lower Valdai (Q_3^2) glacial-marine deposits.

Introduction

Paleogeographic environment of the Pechora Sea during the Late Valdai (Würm) epoch still remains largely unknown. Reconstructions of the present authors (Dunaev et al., 1995; Pavlidis and Polyakova, 1997; Pavlidis et al., 2001) and Velichko et al. (1998) have shown that during the Late Pleistocene glacial maximum the Southern Island of the Novaya Zemlya Archipelago, as well as the whole Pechora Sea, were not completely covered by an ice sheet.

With the use of a "Parasound" profiler we have recorded well-defined submarine terraces on the Pechora seafloor at the depths of 140, 120, 110, 100-104, 60, 50-54, 40, 32, and 25 m. The best preserved ones are the terraces at 120 and 50-54 m water depth. The 120-m-deep terrace is tentatively correlated with the Late Glacial sea-level lowstand, and the 50-54-m-deep one with pre-Holocene times (12-11 ka). The presence of submarine terraces on the Pechora Sea floor is inconsistent with the existence of a Late Valdai ice cap on the Pechora Sea shelf. These data were obtained in 1998 during the 13th cruise of r/v "Akademik Sergei Vavilov". One year before, during the 11th cruise of the same research vessel the data on the fine sediment structure were collected in the Southern Novaya Zemlya Trough (SNZT). The trough is located near the southern extremity of the Novaya Zemlya Island. It separates the island from the major part of the gently sloping terrace-bearing Pechora seafloor.

The applied procedure of seismofacial analysis (Dunaev, 1987) makes the relatively reliable reconstruction of the changing facial conditions on the basis of seismoacoustic record possible. In particular, we think that during the Last Glacial epoch sedimentary matter was brought to the trough by glacial meltwater and by separate glacial lobes flowing from the ice cap of the Northern Novaya Zemlya Island.

Materials and methods

The data were obtained during the 11th and 13th cruises of r/v "Akademik Sergei Vavilov" (1997 and 1998, respectively) with the help of acoustic profiler "Parasound". Based on these data we provide a first characterization of the fine sediment structure of the subsurface sediment unit (0-50 m) in the SNZT. The main acoustic profile obtained during the 11th cruise runs along the deepest axial part of the trough. Transects across the trough were retrieved in the 13th cruise. The ship moved at a speed of about 9 knots, hence it covered about 280 m in one minute. Minute and hour marks are given in the lower margin of the seismogram. In this record, the current water depth against the sea level is marked in the range of 50 m, less often, 100 m.

Results

The acoustic profile along the SNZT axis (Fig. 1) starts in the northwestern part of the Kostin Shar Strait (Belush'ya Bay) separating Mezhdusharskii Island from Novaya Zemlya. The profile extends further southward directly to the SNZT and around the southern extremity of Novaya Zemlya. In this article we deal with that part of the profile which is located directly in the trough (Fig. 2), i.e. approximately up to 56°30'E. During the cruise the profiling was carried out further eastward to the Karskie Vorota Strait.

At the beginning of the profile, in the outer part of the bay located between Mezhdusharskii Island and Gusinaya Zemlya Peninsula, we sounded stratified sediments filling the bedrock depression (Fig. 3). It is subdivided into three main units: upper unit with horizontal bedding, middle unit with wave bedding, and the lower one without bedding (acoustically transparent).

The upper sediment unit with a thickness of 8-12 m shows alternating light and dark interlayers parallel to the seafloor (fragment A on seismogram). A distinct reflecting boundary divides it into two layers: the upper, 4-5 m thick, and lower, up to 7 m thick. This unit unconformably overlies the middle sediment unit.

The thickness of the middle unit varies from 8 to 18 m. The unit consists of a series of discontinuous irregular layers resembling flat folds. However, this is not a result of plicative dislocation but manifestation of non-uniform pulsatory sedimentation. The upper border of the unit is distinct, while the lower one is less distinct. On the seismogram this unit is mainly shown as layers with acoustically dark record. Although the bedding is clearly expressed, a number of chaotic reflection boundaries were recorded in this unit.

The lower unit with a maximum thickness of 4-5 m represents deposits filling the deepest part of the depression. They are acoustically transparent. The unit overlies a rough surface of dense rocks forming a sill at the bay outlet. The sill closes the inner depression.

Further offshore there is a slope stretching towards the western part of the SNZT. It consists of three structural steps. Their edges resemble structural cliffs, while the inner parts are filled with poorly stratified deposits.

The SNZT bottom lies below 180 m water depth. At the foot of the structural block which lies farthest from Novaya Zemlya, we sounded a sedimentary sequence consisting of two units (Fig. 4, fragment B). The upper 10 m thick unit with fine

horizontal bedding is subdivided into two 5-m-thick layers. The lower unit is characterized by "coarse" irregular bedding and thinning out of certain layers. Its thickness is 18 m. Although its texture looks like fold one, it is, in fact, different.

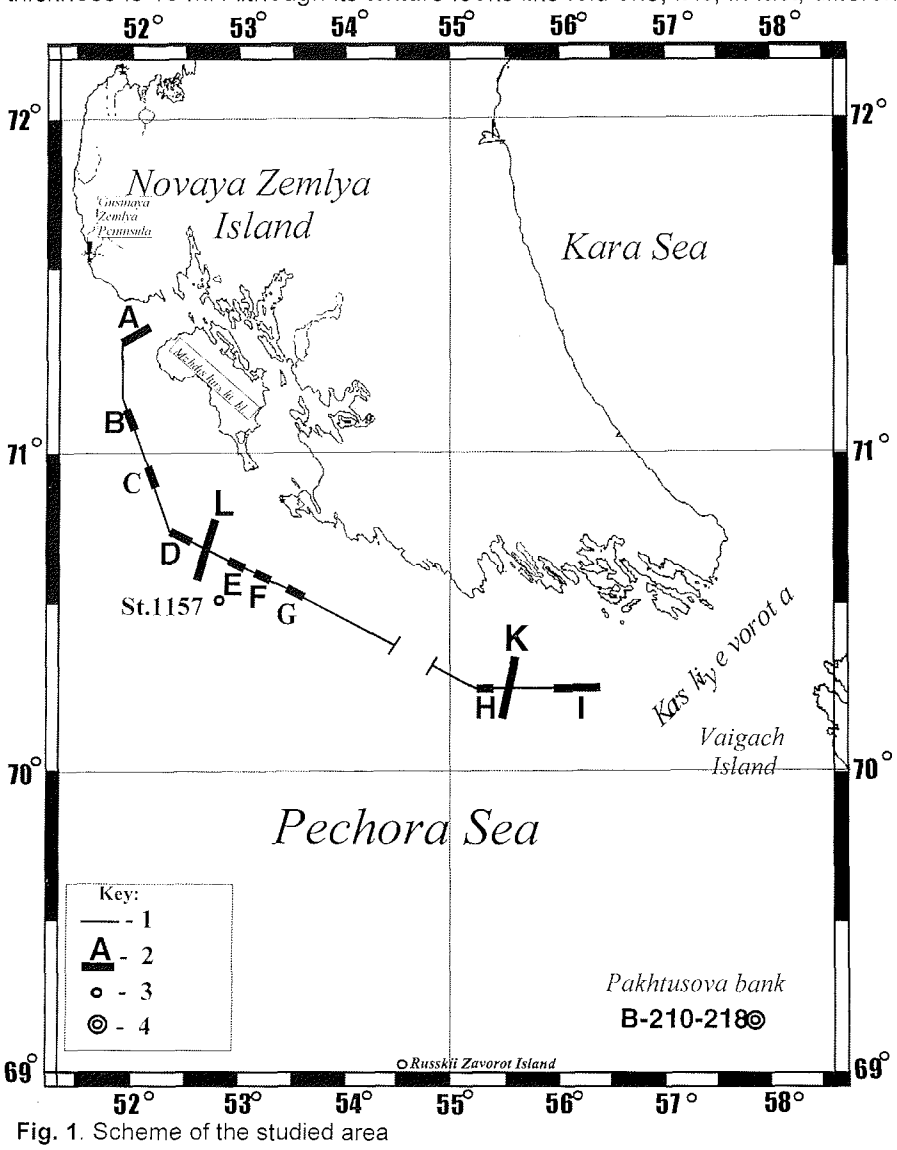

Fig. 1. Scheme of the studied area

Key: 1 acoustic profiling lines; 2 location of "Parasound" record fragments; 3 location of station 1157; 4 location of borehole 210-218.

These units, the upper two-layered horizontal-bedded and underlying irregular-bedded one, are traced along the whole SNZT axis where they overlie acoustically transparent deposits expressed as a layer with a wavy surface. At the slopes of a

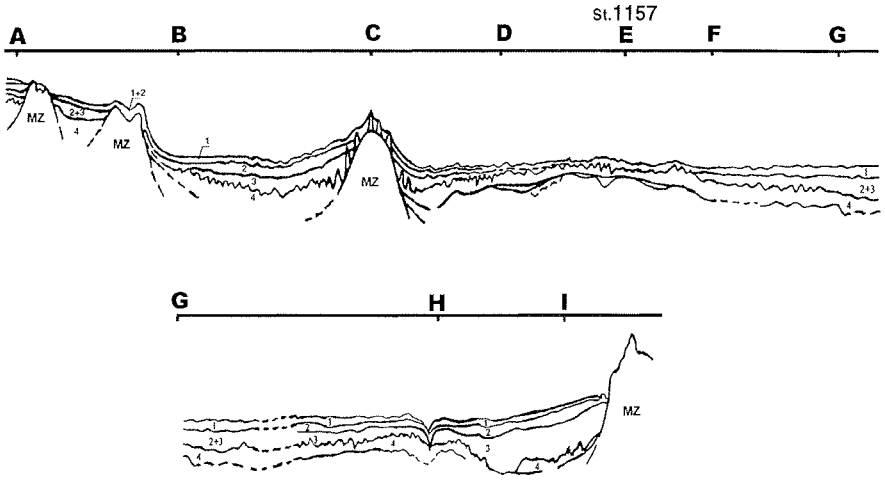

Fig. 2. Longitudinal acoustic profile along the trough thalweg.
Key: I location of acoustic record fragments; 1-4 numbers of sediment horizons.

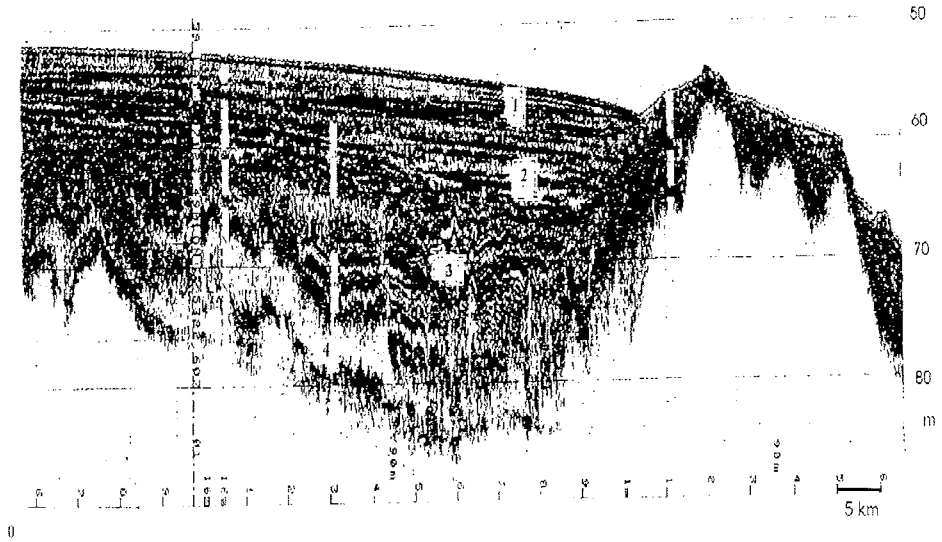

Fig. 3. Fragment A of acoustic longitudinal profile. Key: 1-4 numbers of horizons.

structural high (Fig. 5, fragment C), whose top rises from the trough bottom to the depth of about 160 m, this layer is expressed as separate swells with distinct foot, relative height of up to 10 m, and width at the base of 130-140 m. At the foot of its eastern slope these swells grow in size and become up to 12 m high and up to 300 m wide at the base.

Further to the east along the profile the lowermost acoustically transparent unit is traced as a continuous layer along the whole trough. Morphologically it looks like a series of ridges. Separate ridges remain up to 10-12 m high, and their width reaches several hundreds of meters. In some places this acoustically transparent

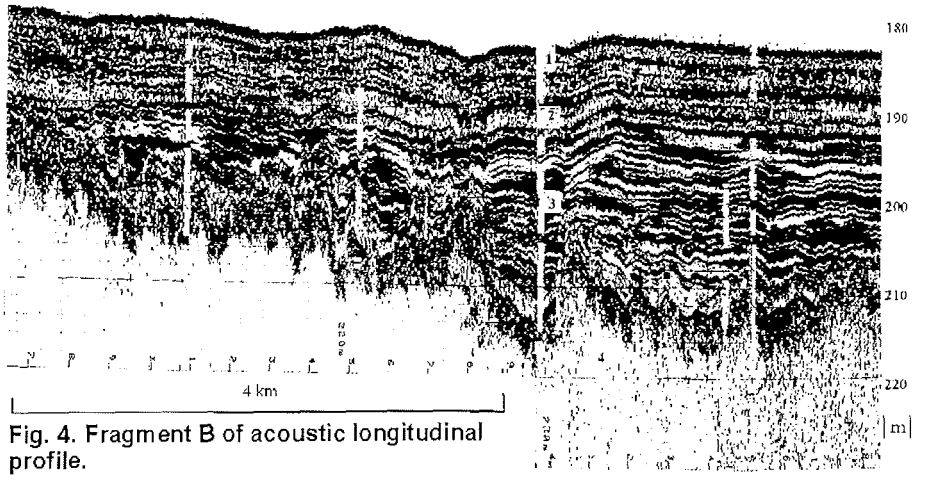

Fig. 4. Fragment B of acoustic longitudinal profile.

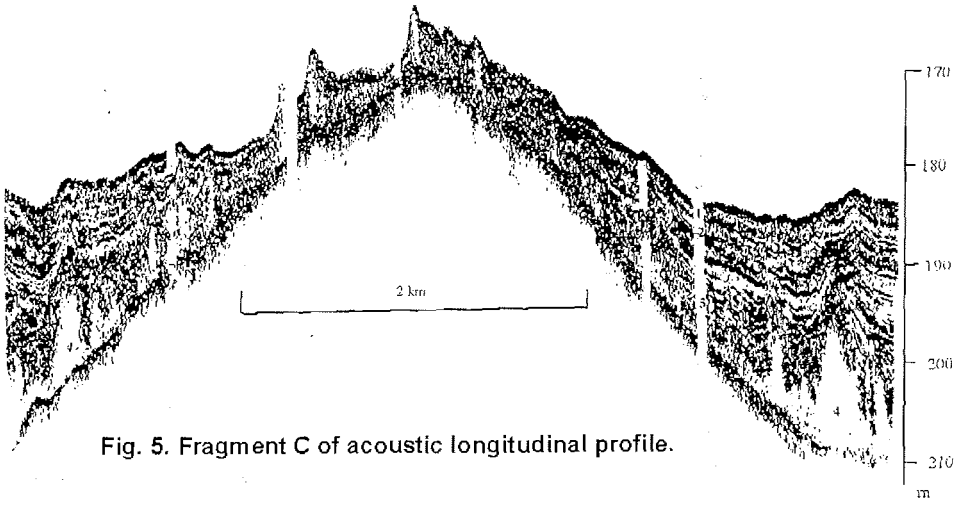

Fig. 5. Fragment C of acoustic longitudinal profile.

unit with wavy or ridge-like surface is underlain by one, and sometimes two-three, layers of also acoustically transparent deposits as seen in fragment D of the acoustic record (Fig. 6).

In the eastward direction the total thickness of the sounded sequence decreases to 10 m over the top of a gently sloping positive structural rise and then increases again. Approximately at the place where fragment _ (Fig. 7) was located, the lithological group of the shipboard scientific party of the 13th cruise of the r/v "Akademik Sergei Vavilov" (1998) recovered a 486-cm-long sediment core at water depth of 169 m (site 1157, 70°33'N, 52°48'E, Fig. 1). The following sediment layers were described (Fig. 8):

0-6 cm. Yellowish gray silty-pelitic terrigenous muds, homogeneous, semifluid. Gradual transition to the underlying layer.

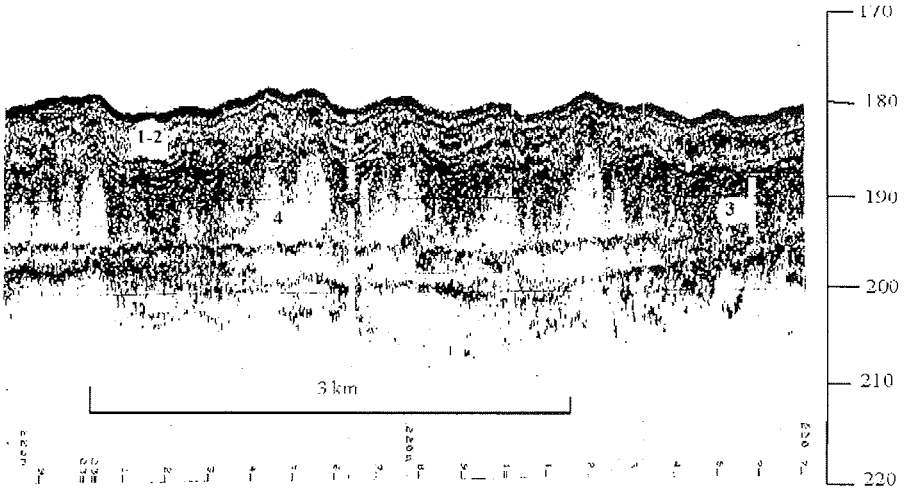

Fig. 6. Fragment D of acoustic longitudinal profile.

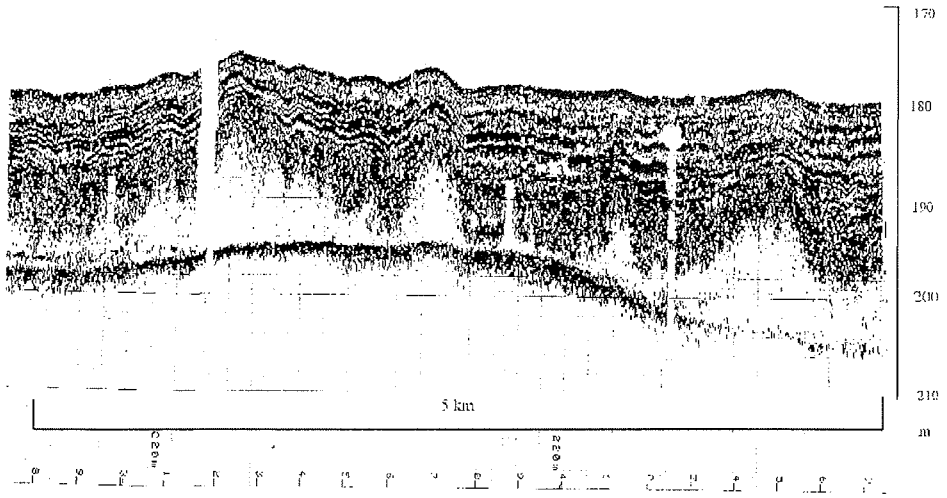

Fig. 7. Fragment E of acoustic longitudinal profile.

6-49 cm. Olive gray pelitic terrigenous muds, abundant black spots of hydrotroilite, strongly bioturbated, mollusc shells and shell debris. Lower boundary is sharp and uneven.

49-78 cm. Olive pelitic terrigenous muds, slightly bioturbated. Rare polychaete tubes and shell debris. Gradual transition to the underlying layer.

78-109 cm. Black pelitic terrigenous muds, strongly bioturbated. Polychaete tubes and shell debris. Lower boundary is sharp and uneven.

109-129 cm. Olive gray pelitic terrigenous muds, slightly bioturbated. Rare polychaete tubes. Gradual transition to the underlying layer.

129-258 cm. Black pelitic terrigenous muds, strongly bioturbated. Rare polychaete tubes and mollusc shells. Lower boundary is sharp and uneven.

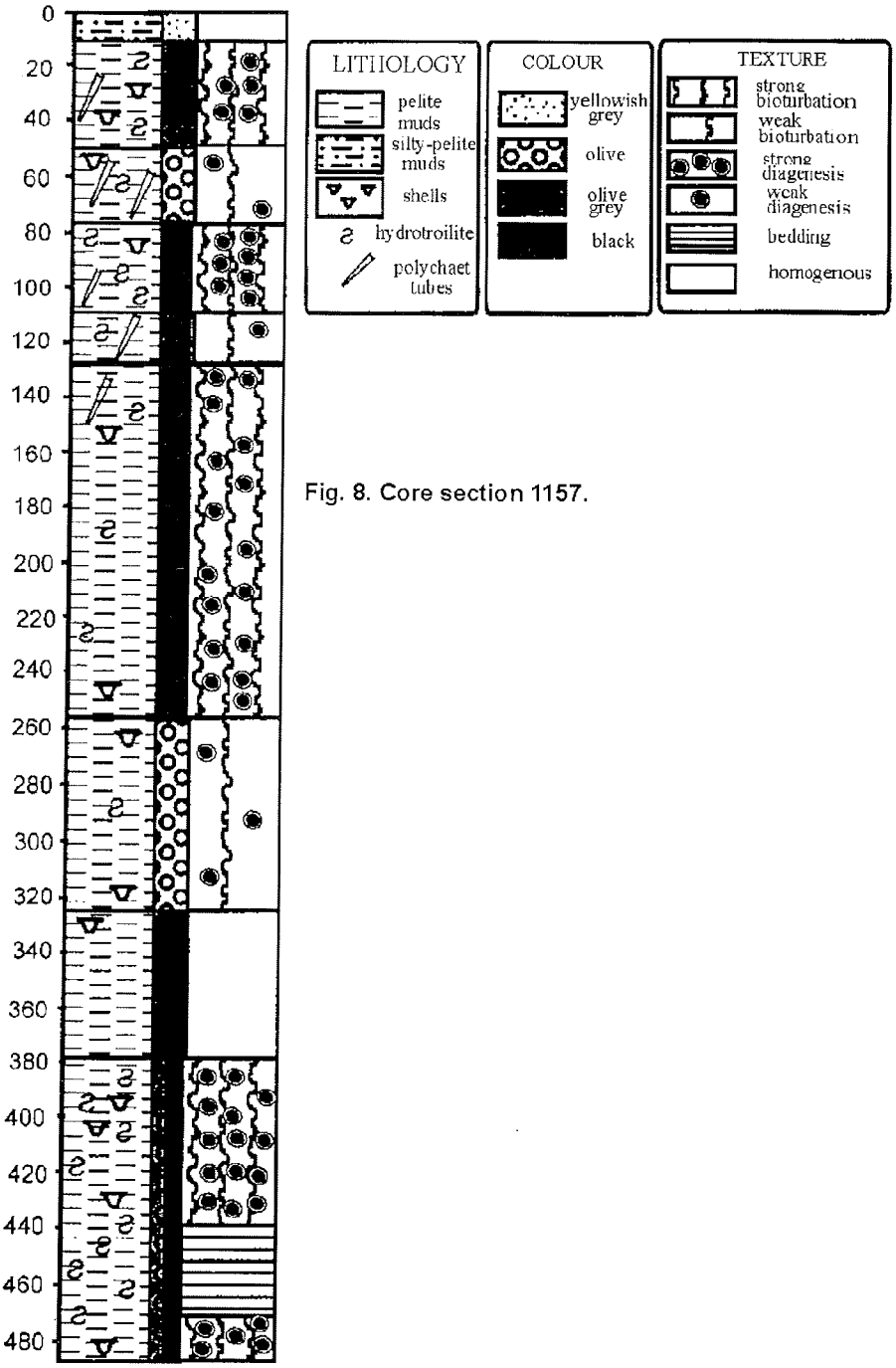

Fig. 8. Core section 1157.

258-324 cm. Olive pelitic terrigenous muds, poorly condensed, viscous, plastic. Shell debris. Gradual transition to the underlying layer.

324-379 cm. Olive gray pelitic terrigenous muds, condensed, plastic. Shell debris. Gradual transition to the underlying layer.

379-486 cm. Olive gray and black pelitic terrigenous muds, plastic, with textures of bioturbation and diagenesis. Shell debris.

Analysis of the absolute age datings from core 1157 allowed assigning the whole sequence to the Holocene epoch (M.A. Levitan, pers. comm.). In this place the upper seismoacoustic horizontal-bedded unit has a thickness of 4-5 m. Hence, on the whole profile it is possible to identify the upper unit as Holocene deposits.

Further eastward the thickness of the sounded sequence in the trough grows, and the layers become more contrasted. The thickness of the upper horizontal-bedded two-layered unit equals 8 m (Fig. 9, fragment F). The thickness of the underlying irregular-bedded layer underlying the Holocene deposits reaches 18 m. The lower acoustically transparent unit has the thickness of 4 to 14 m. Differences between the two upper units become more distinct when moving in eastward direction. Sometimes gas vents are clearly seen in the record (Fig. 10, fragment G). They form up to 1-m-deep craters on the seafloor. Since the sediments filling the SNZT are rich in hydrotroilite, this gas definitely is of subsurface origin, and most likely it is methane.

In this eastern part of the trough, the profile crosses a deeply incised depression, which is 20 m deeper than the surrounding seafloor (Fig. 11, fragment H). It is filled with laminated sediments, and cuts a layer of acoustically transparent deposits.

In the eastern part of the SNZT close to the sill in front of the Karskie Vorota Strait, the profiler was able to sound a thicker sediment sequence with less evident differences between units (Fig. 12, fragment I).

Transects through the trough reveal its distinct graben-like structure formed by tectonic subsidence of the axial part of the trough along the faults on its slopes. It is especially evident on the transect from the eastern part of the SNZT (Fig. 13, fragment K), where faults are clearly expressed. In this transect acoustically transparent unit is not traced, and only the two laminated units are distinguished. They follow the topography of acoustic base in the cross-section of the trough. Against this background the swell-like accumulative body is clearly seen. It is composed of relatively young sediments occurring on the northern trough slope adjacent to Novaya Zemlya.

The transect in the western part of the SNZT (Fig. 14, fragment L) displays swell-like accumulative forms below the laminated deposits. These forms consist of acoustically transparent deposits. We correlate them with unit 4 of the longitudinal profile, which forms the base of the sounded sequence. These swells unconformably overlie the rock surface broken by cracks produced by tectonic deformations. The swells are especially well-pronounced near the Novaya Zemlya slope, where their relative height reaches 15 m. Towards the opposite trough slope they become smaller and lower (down to 8 m), and on the southern trough slope unit 4 thins out at the depth of 160 m below the modern sea level. On this profile, overlying units are referred to as a single laminated sequence filling the trough bottom and lower part of its southern gentle slope. Two distinct terraces cut in pre-

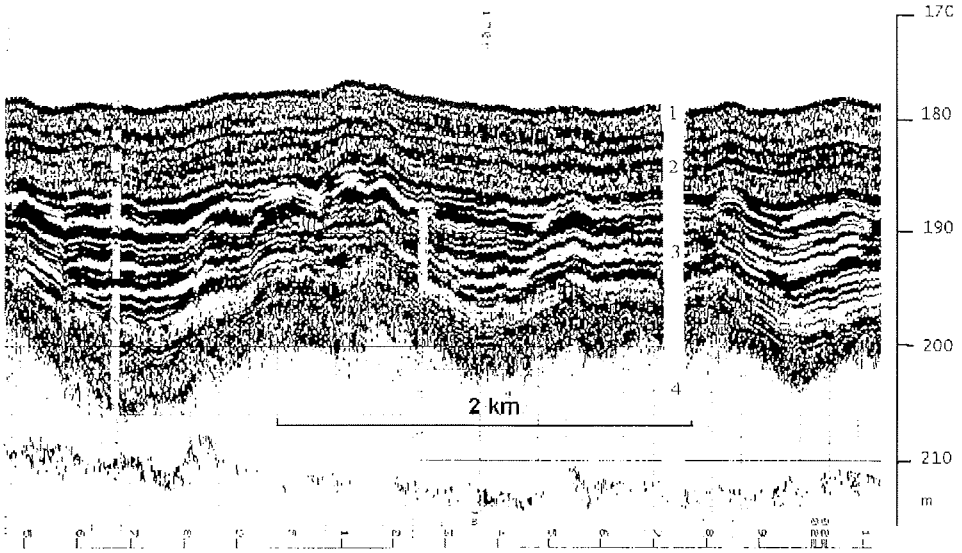

Fig. 9. Fragment F of acoustic longitudinal profile.

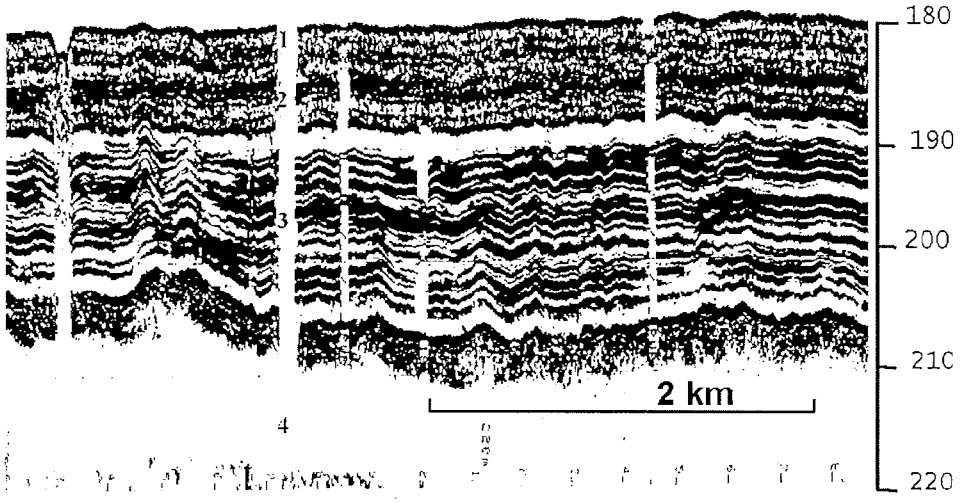

Fig. 10. Fragment G of acoustic longitudinal profile.

Quaternary sedimentary rocks are traced at the level of -120-130 m on the southern slope.

So, the SNZT seabed has a rather flat topography with only one big positive morphostructure (fragment C) resembling the Mesozoic bedrock scarps on the western part of the Novaya Zemlya slope at the outlet of the Belush'ya Bay. The seabed of the rest of the trough shows only small roughnesses with maximum relative height of 2 m and width of several hundreds of meters at the base. Their

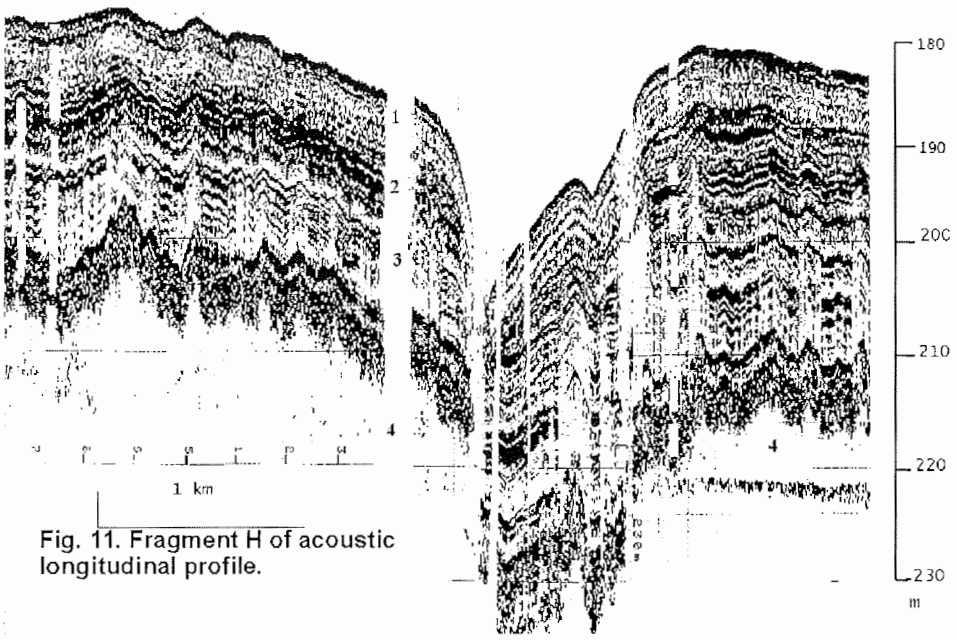

Fig. 11. Fragment H of acoustic longitudinal profile.

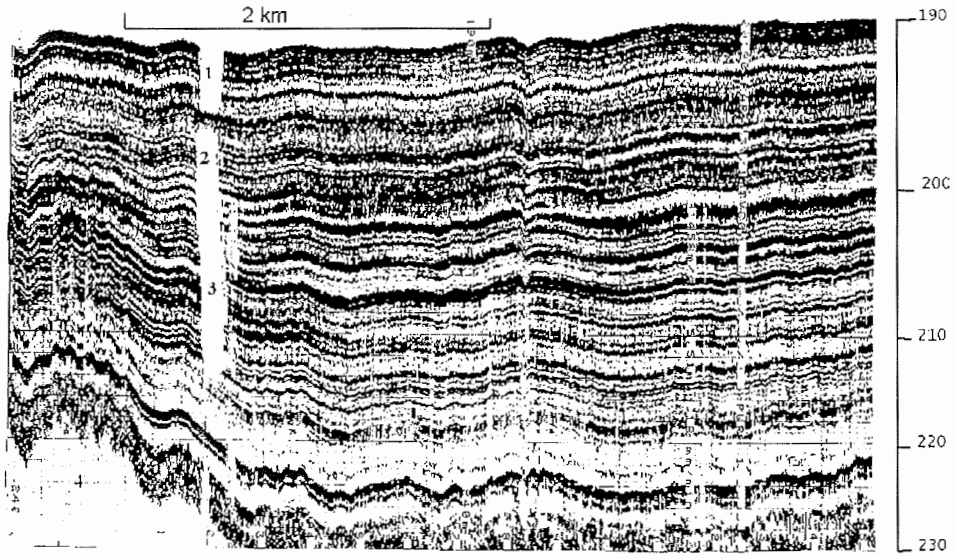

Fig. 12. Fragment I of acoustic longitudinal profile.

origin is probably related to different factors: non-uniform compaction of sediments, bottom currents, differences in sediment fluxes to various parts of the trough, and smoothening of older roughnesses by surface sediments. The sounded sediment sequence is subdivided into four units. The uppermost Holocene unit is 4-6 m thick. It conformably overlies the underlying sediments and is characterized by regular record of phase synchronism axes with dynamically moderate intensity.

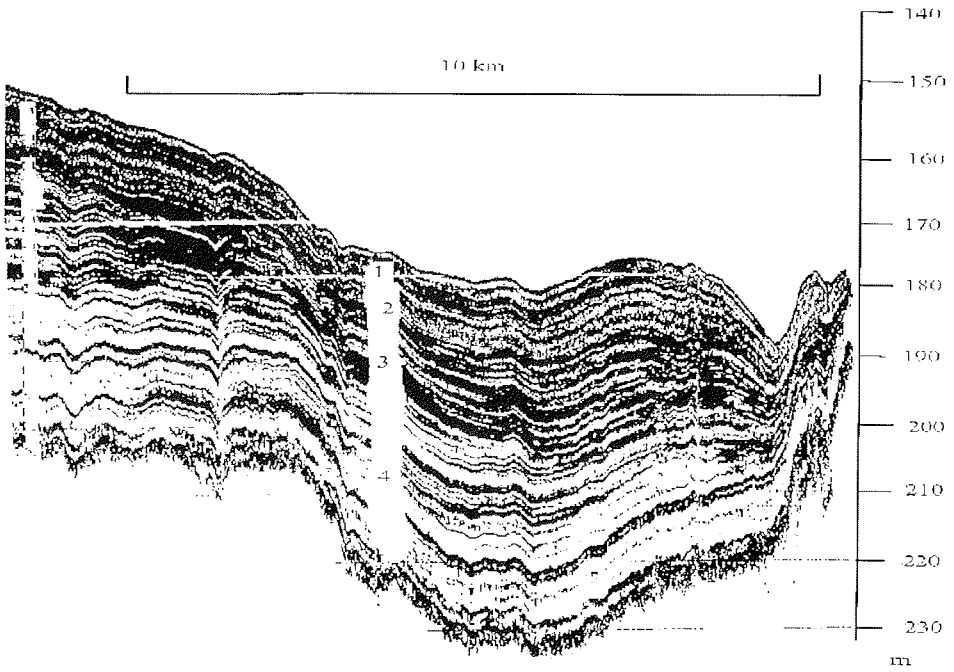

Fig. 13. Fragment K of acoustic eastern cross profile.

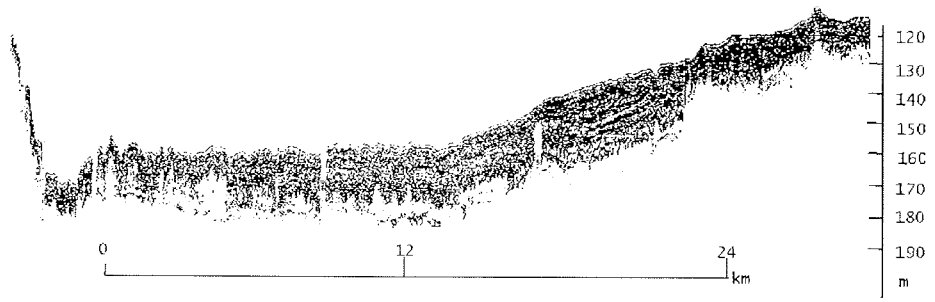

Fig. 14. Fragment L of acoustic western cross profile.

The second unit with a thickness of up to 6 m is of thin-laminated texture. It is distinguished by stronger dynamic expressiveness of phase synchronism axes and their regular record. The thickness of the third unit is up to 15 m, but increases up to 20 m in structural depressions. The unit is distinguished by intensive record of phase synchronism axes which are twice thicker in comparison with the records of over and underlying units. Finally, the fourth unit represents a 15-20-m-thick acoustically transparent sediment layer composing landforms that resemble hills and ridges.

Discussion

The study of the structure and stratification of sediment sequence in the SNZT based on seismofacial analysis allowed reconstructing a succession of paleoevents in the northern part of the Pechora Sea at the end of the Late Pleistocene and Holocene. The article of Pavlidis and coauthors (Submarine terraces..., this volume) describes the distribution of a series of marine terraces at the Pechora seafloor and provides paleogeographical analysis of their evolution. The lower terrace at -120 m water depth corresponds to global sea-level lowstand 18-20 ka, during the Last Glacial maximum. The presence of this terrace confirms our previous reconstructions (Pavlidis et al., 1997; 1998) showing that during this epoch the Pechora Sea shelf was occupied by Arctic tundra, and the SNZT represented a sea basin stretching along Novaya Zemlya as one of the Barents Sea bays.

Polyak et al. (2000) present the data on absolute age estimations of the Upper Quaternary deposits recovered by drilling in the Pechora Sea from board b/v "Bavenit". The deepest core (N 210-218), which received the greatest number of radiocarbon datings, is located in the southeastern nearshore part of the sea at the depth of 20 m (Fig. 1). The core section consists of Holocene sands (0-26 m) that yielded age estimation from 4.7 to 9.7 ka on the basis of 8 datings; underlying layer of varved clays (26-35 m) aging back to 23.6-28.3 ka; the layer of loams (35-63 m) dated at 35-36 ka; and the basal layer of dense clays (63-118 m) overlying the Mesozoic sedimentary rocks. The authors identify the clays as diamicton and consider them to be Middle Würm glacial deposits. The clays were only dated to 37.1 ka at the core depth of 100 m.

The data given in Polyak et al. (2000) show that there are no traces of the Late Valdai ice cap on the Pechora Sea shelf, and rather point to existence of subaerial environment.

The total thickness of the acoustically sounded sediment sequence in the trough is 50 m. Only for the uppermost 4-6 m thick Holocene layer, composition of sediments, their age, and origin are known. These are typical marine, relatively deep-water (for shelf environment) terrigenous laminated clayey muds, which correspond to unit 1 on our profile. Their maximum absolute age estimation is 9-10 ka. This layer conformably overlies similar, but denser, sediments, as evidenced by the absence of a distinct reflector in the upper part of unit 2. However, both layers represent a single sediment unit accumulated in the sea basin, which was covered with pack ice during the cold Late Valdai epoch, and by seasonal ice in the Holocene. At the lowest sea-level position, this basin located within the SNZT was 5-60 m deep, which is quite enough for normal sub-ice sedimentation.

If we assume that sedimentation rates in the SNZT remained nearly constant during the Late Valdai and Holocene, then accumulation of the lower sediment layer with the same thickness as the overlying Holocene deposits would have taken during the same time, i.e. 9-10 kyr. Thus, it might be assigned to the Ostashkov epoch of the Late Valdai. The total thickness of both layers equals 10-12 m. Their accumulation took 18-20 kyrs. Hence, sedimentation rate in the SNZT during this period averaged 0.5 mm/year.

These two marine sediment layers are underlain by layer 3. According to the seismoacoustic record, the latter was accumulated under irregular, pulsatory input

of sediments. As a result, a sediment layer with irregular, sometimes interrupted, sometimes gradational lamination was accumulated. There is no evident discontinuity between this layer and the overlying marine deposits. Therefore, we can conclude that accumulation of layer 3 directly preceded accumulation of the overlying layers, hence, it took place prior to the time of the Last Glacial maximum, i.e. already in the Middle Valdai. The thickness of this layer (15-20 m) allows assuming that its accumulation took at least 15-20 kyr. Sedimentation conditions were rather variable as demonstrated by the texture of sediments. Accumulation occurred in aquatic conditions. Thus, we consider these sediments as marine ones and correlate them with Mologa-Sheksna epoch of the Middle Valdai.

To determine the origin of layer 4 is the key task in order to reconstruct the paleogeography of this region. Acoustic record indicates that the layer is represented by fine-grained homogeneous sediments. These sediments form accumulative bodies with swell-like or wavy surface. The basal reflecting boundary of these bodies is distinct. Along the trough, layer 4 appears on the seismogram as a mainly continuous cover of varying thicknesses and hilly surface, as seen in the fragments of acoustic profile D, E, F (Figs. 6, 7, 9). In the cross profile (Fig. 14) layer 4 looks like separate hills and ridges, sometimes with contacting foothills. Notwithstanding the overlying cover of younger sediments, these hills and ridges express themselves in the modern bottom topography. The fact that on the longitudinal profile layer 4 looks like a layer with varying sediment thicknesses whereas on the cross profile it is ridge-like might be explained by the character of the ship's movement: when recording the longitudinal profile the vessel was moving along the strike of the ridges.

In the acoustic record layer 4 of the SNZT resembles accumulative depositions found in some parts of the Barents Sea, which we identify as glacial and glacial-marine deposits. These were found on seabed rises facing outlets of the Northern Norwegian fjords, where their glacial genesis is unquestionable; at the top of the Murmansk arch, where they form a large accumulative body produced by sediment release from the marine side of the ice shelf connected to the Scandinavian ice sheet; in the Sedov Trough between the Novaya Zemlya and Franz Josef Land archipelagos; on the Admiralty arch, and in other places (Pavlidis et al., 1997, 1998; Pavlidis and Polyakova, 1997). In most cases we dated these deposits by the Last Glacial maximum.

Acoustically transparent record of glacial deposits on the shelf results from their homogeneous and fine-grained composition. It should be realized that accumulation of these deposits at the ice-seawater interface differs from subaerial conditions of moraine accumulation. In most cases glacial-marine deposits on the shelf are formed of fine silt-clay material released directly into seawater from the melting sedentary edge of a glacier (ice shelf). Numerous boreholes, and also grab and box-core samples retrieved gray sandy-silty-pelites from the northern part of the sea, where they lie at the base of typical postglacial sediment sections. Unlike other researchers (Hald et al., 1999; Polyak et al., 1997) supposing these deposits to be glacial diamicton (moraine), we consider them to be glacial-marine sediments accumulated at the initial stage of ice caps destruction. Glacial-marine origin of these beds is evidenced by good preservation of planktic and benthic foraminiferal

tests, high pore-water salinity (Murdmaa et al., 1998), and granulometric spectrum of fine-dispersed sediment component dominated by fractions <0.01 mm.

It has been previously accepted (Dunaev, 1987) that morainic hills and ridges recorded on Arctic shelves by seismoacoustic investigations are characterized by the so-called "irregular record of axes of phase synchronism", i.e. chaotic record. The latter is caused by heterogeneity of granulometric composition of the sediments forming these accumulative forms. Such records are especially typical for moraines with abundant coarse debris, which are localized on the shelf, for instance, in the form of end moraines stretching along the outer slope of the Admiralty arch at the depth of 100-120 m below the sea level. The definition "acoustically transparent layer", therefore, is typical for glacial-marine homogeneous fine-grained deposits.

It is quite clear why glacial-marine deposits form such landforms as hills and ridges. Sediment release from marginal parts of glaciers, including ice shelves, is non-uniform. As a result such accumulative bodies are formed, which, in the SNZT, represent layer 4.

Thus, we can assume (until direct geological data by means of drilling and absolute age dating of deposits) that acoustically transparent layer 4 deposits at the base of acoustically sounded sediment sequence in the SNZT is of glacial-marine genesis, and was accumulated during the Kalinin (Zyryanka) glacial epoch of the Early Valdai period. In the other parts of the Barents Sea similar deposits are considered as Sartan beds. This does not contradict our paleogeographic reconstructions because at the places where glacial deposits on a shelf were referred to the epoch of the Last Glacial, paleoenvironmental conditions favoured their accumulation. In the SNZT, such conditions did not exist during the final stage of the Würm (Valdai) glacial epoch, since the area south of the trough was occupied by tundra, and north of it, on the Southern Island of Novaya Zemlya, ice caps were absent (Velichko et al., 1998).

Conclusions

At the Arctic coast of Eurasia the Late Pleistocene epoch is subdivided into four intervals: Mikulino (Kazantsevo), Kalinin (Lower Valdai, Zyryanka), Mologa-Sheksna (Middle Valdai, Karga), and Ostashkov (Upper Valdai, Sartan). Following this stratigraphic scheme, the acoustically sounded sediment sequence of the SNZT is subdivided into four stratigraphic units: 1 – Holocene (Q_4) marine deposits; 2 – Sartan (Upper Valdai) (Q_3^4) glacial-marine deposits; 3 – Karga (Middle Valdai) (Q_3^3) marine deposits; 4 – Zyryanka (Lower Valdai) (Q_3^2) glacial-marine deposits.

Our conclusions concerning the history and stratification of the Upper Quaternary deposits in the SNZT of the Pechora Sea are preliminary until drilling in the trough will be performed, absolute age will be estimated, and paleoenvironmental conditions will be reconstructed by the means of biostratigraphy.

References

Dunaev, N.N., 1987. Material-genetic interpretation of CSP seismograms in connection with seismostratigraphy. In: Problemy geofiziki okeanskogo dna (Problems of seabed geophysics). Moscow, Nauka, 1, 155-156 (in Russian).

Dunaev, N.N., Levchenko, O.V., Merklin, L.R., Pavlidis, Yu.A., 1995. Novaya Zemlya shelf in the Late Quaternary time. Oceanology (English Edition), 35 (3), 440-450.

Hald, M., Kolstad, V., Polyak, L., Forman, S.L., Herlihy, F.A., Ivanov, G., Nescheretov, A., 1999. Late glacial and Holocene paleoceanography and sedimentary environments in the Saint Anna Trough, Eurasian Arctic Ocean margin. Palaeogeogr., Palaeoclimatol., Palaeoecol., 146, 229-249.

Murdmaa, I.O., Ivanova, E.V., Pimenov, N.V., 1998. Marine periglacial sedimentation in the Barents Sea after glaciation. In: Morskoi periglyatsial I oledenenie Barentsevo-Karskogo shel'fa v pleistotsene (Marine periglaciai and glaciation of the Barents-Kara shelf in the Pleistocene). Apatity, KNTs RAS, 78-80 (in Russian).

Pavlidis, Yu.A., Dunaev, N.N., Shcherbakov, F.A., 1997. The late Pleistocene palaeogeography of Arctic Eurasian shelves. Quaternary International, 41/42, 3-9.

Pavlidis, Yu.A., Ionin, A.S., Shcherbakov, F.A., Dunaev, N.N., 1998. Arkticheskii shel'f. Pozdnechetvertichnaya istoriya kak osnova prognoza razvitiya (The Arctic shelf. Late Quaternary history as a basis for predicting future changes). Moscow, GEOS, 187 pp. (in Russian).

Pavlidis Yu.A., Murdmaa, I.O., Ivanova, _.V. et al., 2001. Were ice caps of the Novaya Zemlya and Franz Josef Land connected 18,000 years ago? In: Opyt sistemnykh okeanologicheskikh issledovanii v Arktike (Systematic oceanological studies in the Arctic). Moscow, Nauchnyi Mir, 456-467 (in Russian).

Pavlidis, Yu.A., Polyakova, E. I., 1997. Late Pleistocene and Holocene depositional environments and paleoceanography of the Barents Sea: evidence from seismic and biostratigraphic data. Marine Geology, 143, 189-205.

Polyak, L., Forman, S.L., Herlihy, F.A., Ivanov, G., Krinitsky, P., 1997. Late Weichselian deglacial history of the Svyataya (Saint) Anna Trough, northern Kara Sea, Arctic Russia. Mar. Geol., 143, 169-188.

Polyak, L., Gataulin, V., Okuneva, O., Stelle, V., 2000. New constrains on the limits of the Barents-Kara ice sheet during the Last Glacial Maximum based on borehole stratigraphy from the Pechora Sea. Geology, 28 (7), 611-614.

Velichko, A.A., Kononov, J.M., Faustova, M.A., 1998. New evidence on distribution and volume of the Earth's glaciation in the Last glacial maximum (18-20 thousand years ago). In: Glavneishie itogi v izuchenii chetvertichnogo perioda I osnovnye napravleniya issledovaniya v XXI veke (Major results in investigations of the Quaternary period and the basic trends for the 21st century). St. Petersburg, VSEGEI, 99 (in Russian).

CRYOGENIC PROCESSES AND PHENOMENA IN THE UPPER SEDIMENT LAYER OF THE PECHORA SEA

V.N. Bondarev[1], S.I. Rokos[1], G.A. Tarasov[2], D.A. Kostin[1], A.G. Dlugach[1], N.A. Polyakova[1]

[1] - GUP Arctic Marine Engineering-Geological Expeditions (AMIGE), Murmansk, Russia
[2] - Murmansk Marine Biological Institute, Kola Scientific Center RAS, Murmansk, Russia

Abstract

Unusual structures of the upper sediment layer and bottom relief forms were found in the northeastern Pechora Sea in the course of geological investigations. These forms represent pingo(bulgunnyakh)-like rises 20-60 to 100-130 m wide and 10-25 m high. The rises are prominent features of the generally gently sloping seafloor formed by ice-rich permafrost sediments. At the archs of diapir-like rises, permafrost sediments lie less than 0.5 m below the seafloor, and their thickness reaches 100 m and more. Between the rises, the top of 30 m thick permafrost sediments lies 15-20 m below the seafloor. The borehole drilled between the diapir-like rises revealed gas accumulation with excess pore pressure at the depth of 50 m below the seafloor.

Introduction

Recent investigations in the Pechora Sea revealed numerous diapir-like rises composed of ice-rich permafrost sediments and related gas accumulations with excess pore pressure. Morphologically these diapir-like rises resemble pingos (bulgunnyakhs), which are widespread on the adjacent land.

The region with diapir-like rises is located in the northeastern Pechora Sea (Fig. 1). It is restricted to the upper part of the slope dividing the deep Southern Novaya Zemlya depression and the gently sloping shallow area with depths less than 50 m that is the submarine continuation of the Pechora Lowland (Gritsenko, 1989). The rises occur in the overdeepened depression with relative descent of 15-20 m. Water depth within this depression is 50-75 m (Figs. 1, 2).

Drilling and seismic profiling carried out by GUP AMIGE in the eastern Pechora Sea in 1982-1996 unraveled the structure of the upper 100-150 m of sediment cover. The latter consists of the Holocene, upper, middle, and lower Pleistocene beds (Rokos, 1996). Up to 5-7-m-thick marine Holocene deposits are represented by sands and sandy-silty muds.

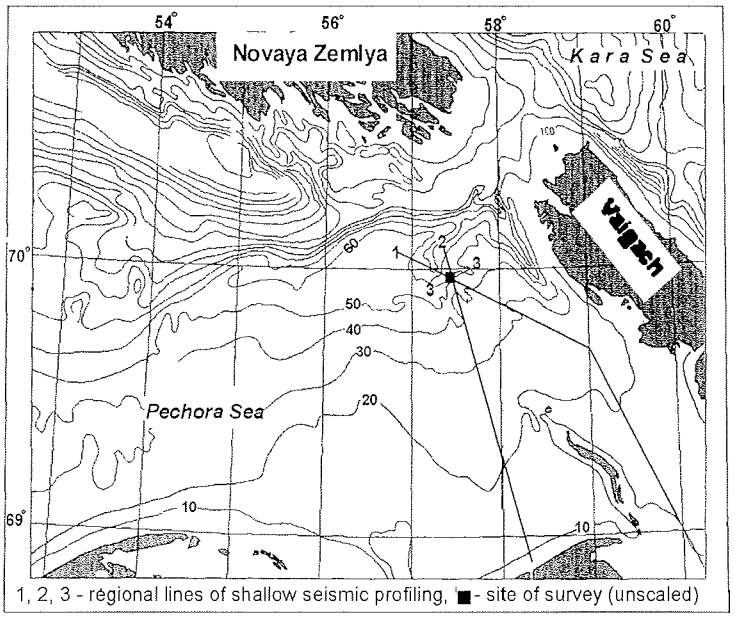

Fig.1 Map of the study area.

The underlying (upper Pleistocene) deposits are subdivided into three complexes. The upper complex corresponds to an acoustically stratified seismic unit with a thickness of 20-30 m and more. This complex is represented by marine laminated clays enriched in hydrosulphides. Its basal part consists of light fine sandy silts and sands with thin rhythmic bedding and peat inclusions. Coarser sediments occur at the top of the complex. The middle part is represented by fine plastic clays.

Similar deposits are widespread on the Barents, Pechora, and Kara shelves. Sediments at the top of the complex yield a radiocarbon age of 3,000-8,000 years. Amino acid dating of the basal layer gave the age of 18,000-25,000 years (Rokos, 1996). We correlate this complex with the up to 8-12-m-high first coastal terrace of the Pechora Lowland (Danilov, 1978) and continental upper Sartan deposits of West Siberia (mQ_{III}^4).

Underlying deposits consist of dusty sands with numerous plant remains and clayey interlayers. The thickness of sand layers averages 10-20 m. We correlate them with the lower Sartan deposits of the West Siberia (aQ_{III}^4). The sands overlie a thick (up to 20-50 m and more) clay formation. Clay deposits with interlayers of sands and thin peat interbeds are characteristic of the upper part of the sequence.

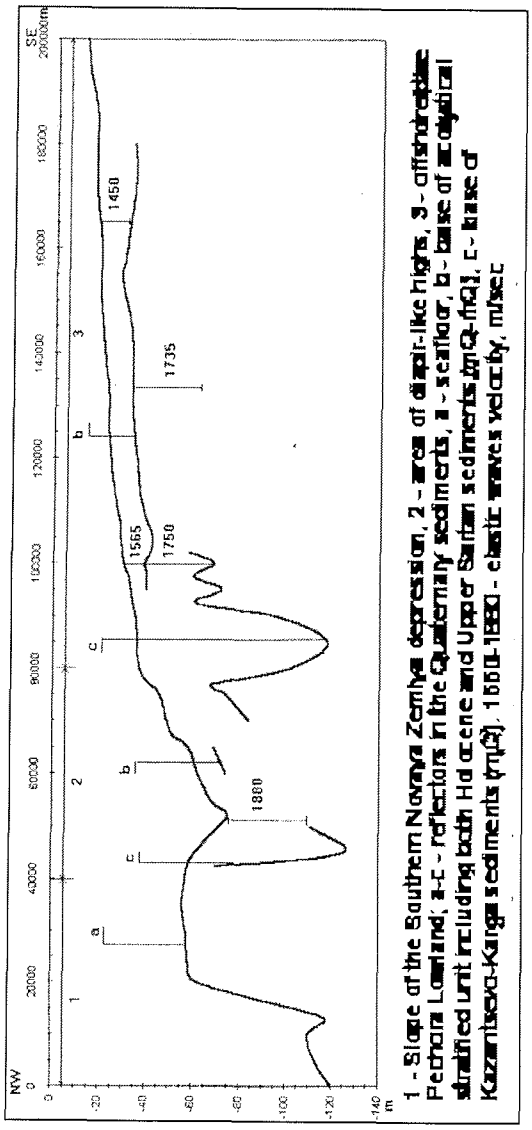

Fig.2. Seismostratigraphic interpretation along the regional line A-A'. Multichannel shallow seismic profiling

Downwards they are replaced by fine clays with interlayers of hydrosulphides and rare gravel inclusions. We correlate these deposits with marine sediments (mQ_{III}^{1-3}) on the adjacent Pechora Lowland and Kazantsevo-Karga deposits of West Siberia (Danilov, 1978).

The middle Pleistocene deposits are represented by 30-50-m-thick glacial or glacial-marine overthickened clays (g,gmQ_{II}). Sands of different composition predominate among the 20-50-m-thick lower Pleistocene alluvial-marine beds

(amQ_I). Thin-laminated clays occur in the upper part of the lower Pleistocene sequence. Their thickness ranges from 1-3 to 5-10 m. Drilling in the region with diapir-like rises has not revealed any lower or middle Pleistocene deposits.

Ice-rich permafrost sediments are characteristic of the shallow Pechora Sea shelf. They were found at water depths of 10-30 m (Gritsenko and Bondarev, 1994). The upper boundary of permafrost sediments runs 20-30 m below the seafloor. The established thickness of permafrost beds varies between 20 and 40 m. Ice-rich permafrost sediments have patchy distribution. Postcryogenic textures were reported at the areas with unfrozen grounds. These are disturbances in bedding related to melting of texture-forming ice and epigenetic freezing of sediments.

The permafrost sediments of the Pechora Sea were formed during regression under subaerial conditions. Considerable warming of permafrost grounds during the subsequent transgression resulted in their melting. It still persists today due to bottom waters with positive temperatures and the heat flux from the interior that equals 45-65 mW/m^2 in the study area.

The shallow Pechora Sea shelf is characterized by presence of free gas in acoustically stratified sediments. In the time sections of seismoacoustic profiling gas accumulations could be seen as the zones of complete or partial losses of seismic correlation and amplitude anomalies of the "bright-spot" type.

Saturation of the shallow Pechora shelf sediments with free gas probably results from degradation of submarine permafrost formed during the last Pre-Holocene regression (Bondarev et al., 1999). During regression, decomposition of the fossil organic material was suppressed by negative temperatures. Flooding in the course of the Flandrian transgression made the temperatures positive and initiated intensive melting of permafrost sediments. This, in turn, activated destruction of fossil organic remains, gas emissions, and, finally, saturation of the sediments with free gas.

Material

The diapir-like rises described in this article were first recorded in the regional seismoacoustic profile A-A' (Fig. 1) obtained by GUP AMIGE in 1988. Additional regional profiles B-B' and C-C' were executed in order to study these structures in more detail. Engineering drilling down to 15-100 m below the seafloor was carried out in the region with diapir-like rises in 1995. In 1996 GUP AMIGE performed detailed complex investigations within the 5x5 km area centered at the borehole site with recorded gas vents. The investigations included seismoacoustic profiling along the regular 50x50 m meshsize network together with echo sounding and side scan sonar observations. However, the 5x5 km area is not sufficient for mapping the area with diapir-like rises, which still remained improperly plotted.

Results

In the time sections retrieved with the help of electrospark generator (sparker) in the frequency range 300-1000 Hz, and high-frequency (2500 Hz) profiler, the sediment sequence is subdivided into two units. The upper unit has an acoustically transparent laminated structure (Figs. 3, 4). The thickness of the laminated unit varies from 1-5 to 30-50 m and more. The lower unit has a non-stratified and

acoustically reflective structure. Continuous interpretable inner reflectors are absent here. In the time sections the local seabed rises represent diapir-like structures cutting and deforming the overlying acoustically stratified sediments.

Drilling revealed the acoustically stratified unit to be composed of marine Holocene (mQ_{IV}) and marine upper Sartan (mQ_{III}^4) deposits (Fig. 3). The lower non-laminated unit includes the Kazantsevo-Karga deposits (mQ_{III}^{1-3}). The lower Sartan deposits can be part of both the upper acoustically stratified and lower reflective units. In case these deposits are either frozen or saturated with free gas, they are reflected in time sections as acoustically reflective non-stratified deposits and are included in the lower unit. If the sediments are unfrozen and gas-free, they are reflected as acoustically stratified deposits and are included in the upper unit.

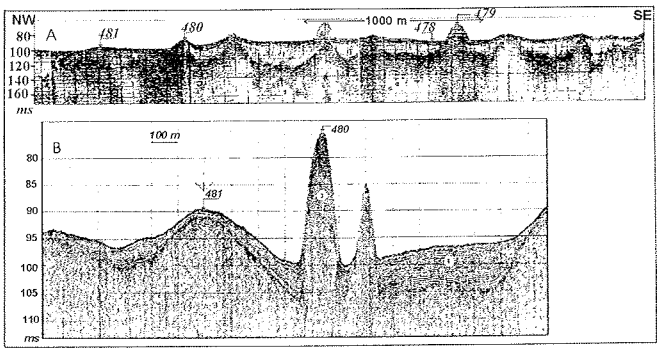

A - a fragment of time section along the line 1-1 (sparker, 200-500 Hz)
B - time section of detailed survey in the vicinity of bor location 480 and 481 (high resolution boomer, 2500 Hz)
C - interpretation based on bor (1-8 - lithologic log: 1- sand, 2 - lean clay, 3 - clay, 4 - clayey sand, 5 - gas accumulations with excess pore pressure, 6 - segregation ice, 7 - top of permafrost, 8 - shallow bore-hole).
Diapir-like structure on sparker (300-1000 Hz) time sections (below) and sonograms of side scan sonar DF-1000 survey (top).

Fig. 3. Time sections of shallow seismic profiling (A-B) and their interpretation (C).

Diapir-like rises are separated by depressions filled with acoustically stratified Holocene (mQ_{IV}), and upper and lower Sartan deposits (mQ_{III}^4 and aQ_{III}^4, respectively). The observed thickness of stratified deposits in these depressions is 50 m and more (Figs. 3, 4). Also, many diapir-like structures intruding the acoustically stratified sediments do not reach the seafloor. In the bottom topography they are seen as gently sloping rises.

More than 50 diapir-like rises were found in the study area with side-scan observations and echo sounding. In the sonograms they are well manifested as rounded positive forms rising above the flat monotonous seafloor surface (Fig. 4). Besides single rises, we also recorded twin and triple diapir-like rises divided by saddles. No regularities were discovered in the spatial distribution of diapir-like rises by sonar survey within the 5x5 km area.

In the time sections, the boundary between the acoustically transparent stratified deposits and underlying acoustically reflective beds is laterally discontinuous. It could be traced in sharp changes in the structure of the wave record (Figs. 3, 4). It is often related to amplitude anomalies producing modes of multiple reflections.

As a whole, the boundary has a heterogeneous character (Fig. 3, 4). Bore data show this heterogeneity to be related to changes either in geological structure or physical properties of the sediments. The boundary could be correlated with the top of the Kazantsevo-Karga beds (mQ_{III}^{1-3}) or free gas accumulations in the lower Sartan sands (aQ_{III}^4) or topmost permafrost layer.

During summer 1995 two boreholes were drilled. They showed that ice-rich permafrost grounds are widespread within the study area. The borehole, located at the arch of one of the diapir-like rises, recovered frozen Kazantsevo-Karga clays ($mQ^{1-3}{}_{III}$) with high ice content (more than 70% of the volume) from the depth of 0.4 m below the seafloor. Another borehole drilled at the foot of the same diapir-like high revealed frozen sands of the lower Sartan age at the depth of 27 m below the seafloor. Ice content in the sands was about 35%.

Two additional boreholes were drilled in the fall of 1995. One of them located at the top of a diapir-like rise, recovered frozen ice-rich Kazantsevo-Karga clays (mQ_{III}^{1-3}) from the depth of 0.5 m below the seafloor (Fig. 5a). The whole core sequence (observed thickness 100 m) consists of plastic-frozen Kazantsevo-Karga clays (mQ_{III}^{1-3}) with numerous schlieren of freshwater ice. The borehole did not reach either the base of the Kazantsevo-Karga deposits or the permafrost base, because they both lie at depths exceeding 100 m below the seafloor. The upper part of the core section down to the depth of 50 m below the seafloor is distinguished by high ice content (50-90% of the volume). Downcore the ice content decreases down to about 30%.

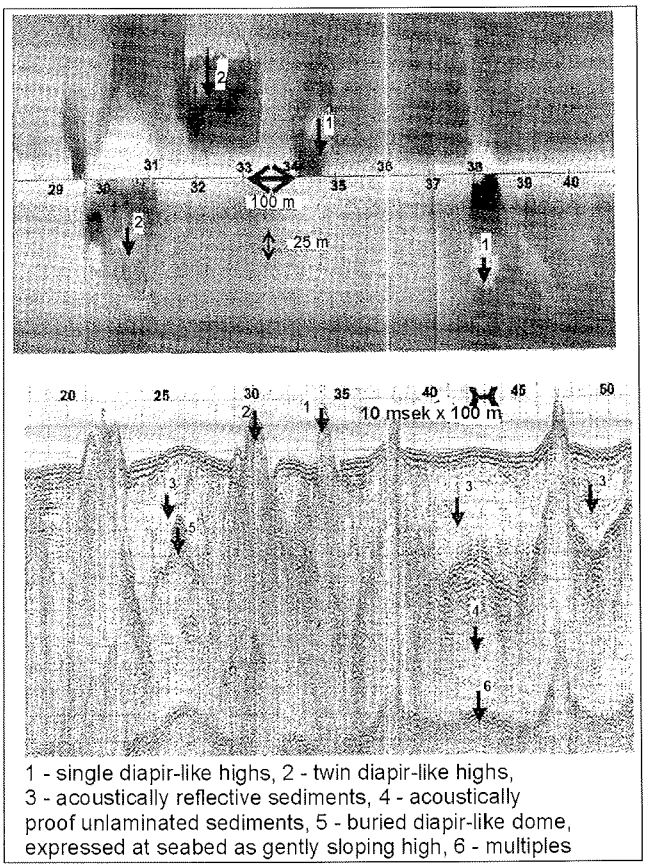

1 - single diapir-like highs, 2 - twin diapir-like highs, 3 - acoustically reflective sediments, 4 - acoustically proof unlaminated sediments, 5 - buried diapir-like dome, expressed at seabed as gently sloping high, 6 - multiples

Fig.4a. Single and twin diapir-like highs, separated by lenses of acoustically reflective sediments

from the depth of 0.5 m below the seafloor (Fig. 5a). The whole core sequence (observed thickness 100 m) consists of plastic-frozen Kazantsevo-Karga clays (mQ_{III}^{1-3}) with numerous schlieren of freshwater ice. The borehole did not reach either the base of the Kazantsevo-Karga deposits or the permafrost base, because they both lie at depths exceeding 100 m below the seafloor. The upper part of the core section down to the depth of 50 m below the seafloor is distinguished by high ice content (50-90% of the volume). Downcore the ice content decreases down to about 30%.

Another borehole located on the gentle slope of a buried diapir-like structure (Table 1, Fig. 5b) is 51 m deep.

Table 1: Sediment description of Borehole 481

Interval (m)	Sediments
Holocene sediments (mQ_{IV})	
0.0-0.6	Mud, dark grey, silty, uniform.
Upper Sartan complex (mQ_{III}^{4})	
0.6-8.5	Sandy clays, dark grey, fluently soft-plastic, non-uniform, with inclusions and interlayers of sand.
Lower Sartan complex (aQ_{III}^{4})	
8.5-27.8	Sand, grey, dusty, loose, water-saturated. In places is replaced by plastic silty sands. Below 20.2 m sediments are frozen, with massive cryotexture.
Kazantsevo-Karga complex (mQ_{III}^{1-3})	
27.8-47.0	Clays and sandy clays, dark grey slightly brownish, plastic and semi-dense consistence, frozen, with fine horizontal bedding marked by thin layers of dusty sand along bedding plane. Horizontal and vertical microfractures, schlieren, and interlayers of transparent freshwater ice.
47.0-51.0	Sediment was not recovered. Probably this section is represented by gas- and water-saturated sands. When the borehole reached the depth of 49.5 m, a blow-out of gas-water mixture occurred.

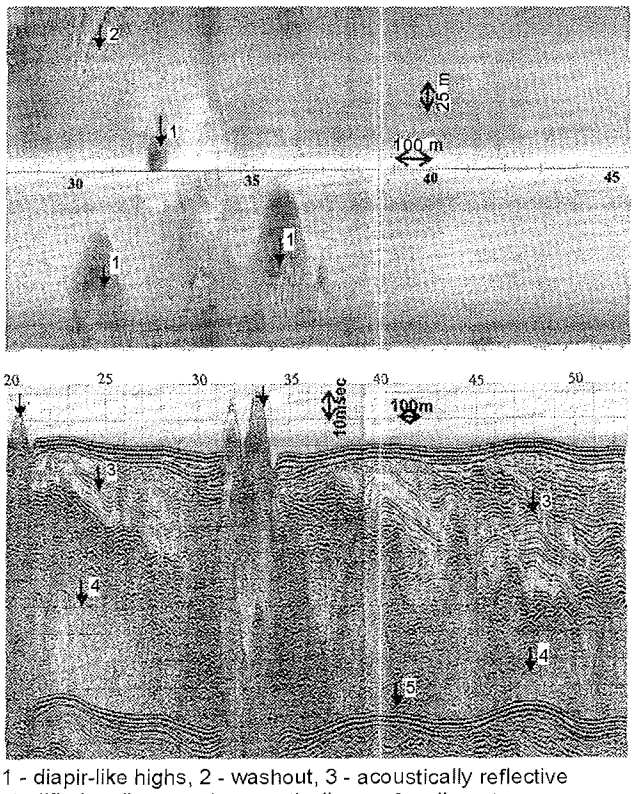

1 - diapir-like highs, 2 - washout, 3 - acoustically reflective stratified sediments, 4 -acoustically proof sediments, 5 - multiples

Fig. 4b. Diapir-like structures and sedimentary section. Dislocations and inner unconformities within the acoustically stratified sediments are clearly distinguished.

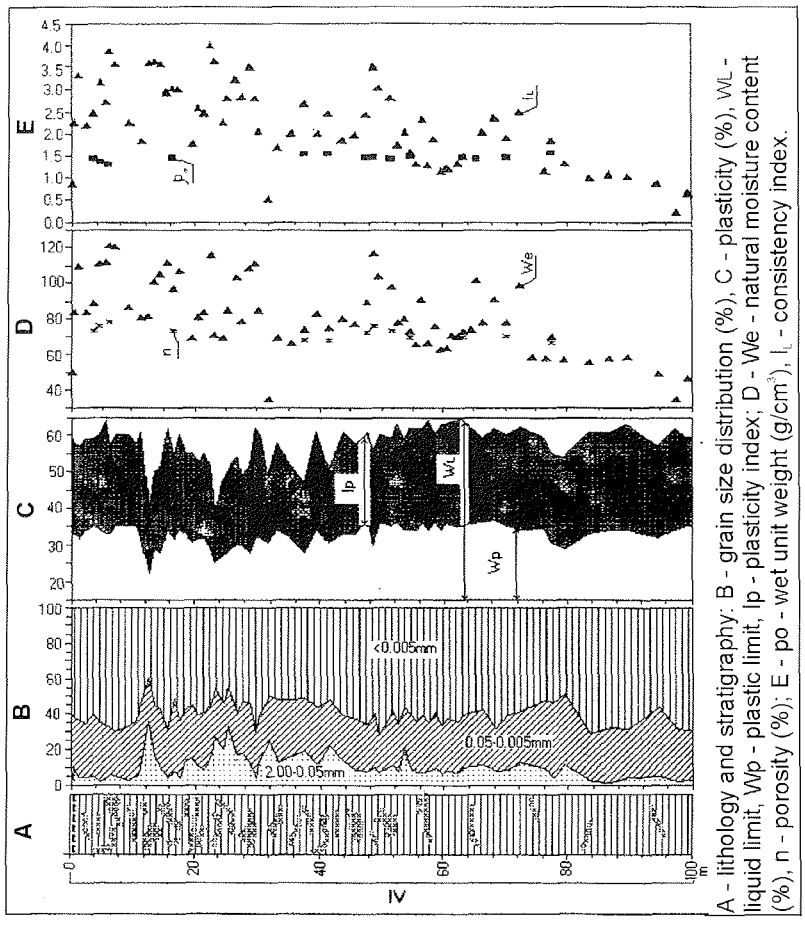

Fig. 5a . Downhole log of the boreholes 480 and 481. Soil properties and grain size distribution

At the depth of 49.5 m the core penetrated the zone of excess pore pressure. As a result, an intensive gas blow-out occurred (Fig. 6), and a "boiling kettle" was formed on the sea surface with diameter of 100-200 m. Inside the kettle, water with distinct gas bubbles and suspended sediment particles was roughing. No traces of liquid hydrocarbons (oil, gas condensates, etc.) were observed. Due to the gas blow-out and sharp changes in seawater properties the hydracoustic system of the drilling vessel positioning was destroyed. Ingress of gas into the cooling system of the drilling vessel caused slowdown of the main and, later, pilot engines of the vessel. The vessel got a distinct 5-7° tilt over. At the last strokes of the engine the vessel managed to leave the danger zone. Because of the emergency situation no measurements were carried out, and no gas samples were taken. However, the extent of the phenomenon allows supposing the gas pressure in the penetrated "pocket" to be at least several dozens of atmospheres.

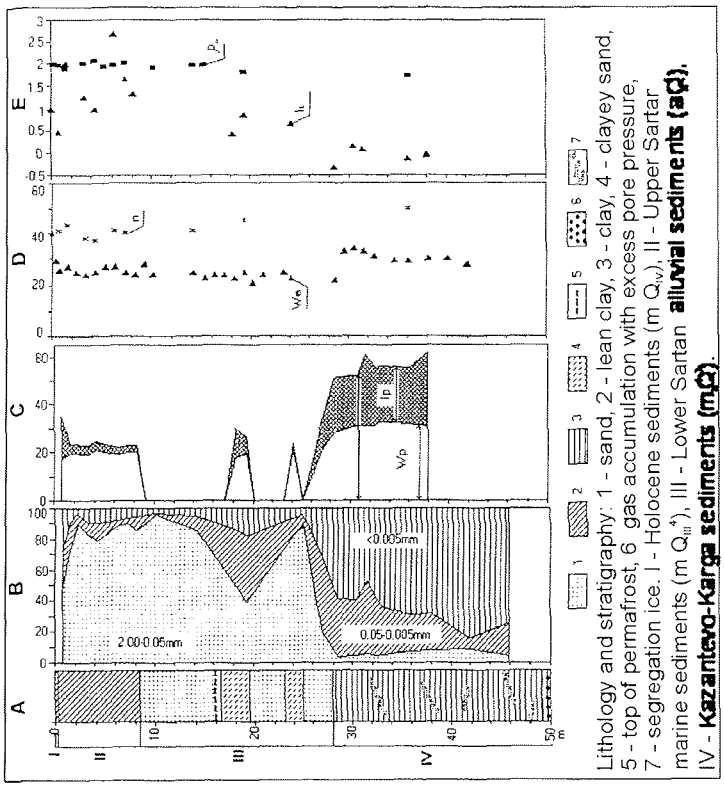

Fig. 5b. Downhole log of the boreholes 481. Soil properties and grain size distribution

Discussion and conclusions

It is obvious that accumulations of gas with excess pressure are related to the existence of the thick permafrost layer. This layer plays the role of a specific protection cover that is practically impenetrable for biogenic gas accumulated in the underlying sediments. Thus, being accumulated at the base of the permafrost layer biogenic gas forms local gas "pockets" (Fig. 3). Based on the bore data, one could suppose that they occur between the diapir-like structures on the relatively gently sloping parts of the seafloor. Probably, distribution of gas "pockets" in the sediment sequence is rather uneven, as evidenced by bore results.

Gas accumulations with excess pore pressure seem to be restricted to the lenses of melt sands underlying the permafrost. Due to their high permeability they serve as collectors. However, the origin and structure of diapir-like rises are not clearly understood. It should be mentioned that American and Canadian scientists found similar structures in the Beaufort Sea (Marine..,1987; Shearer et. al., 1971) and named them pingo-like structures (PLF). As in the Pechora Sea, they consist of ice-rich clays. However, no gas emissions have been recorded there, probably because of the insufficient boring depth.

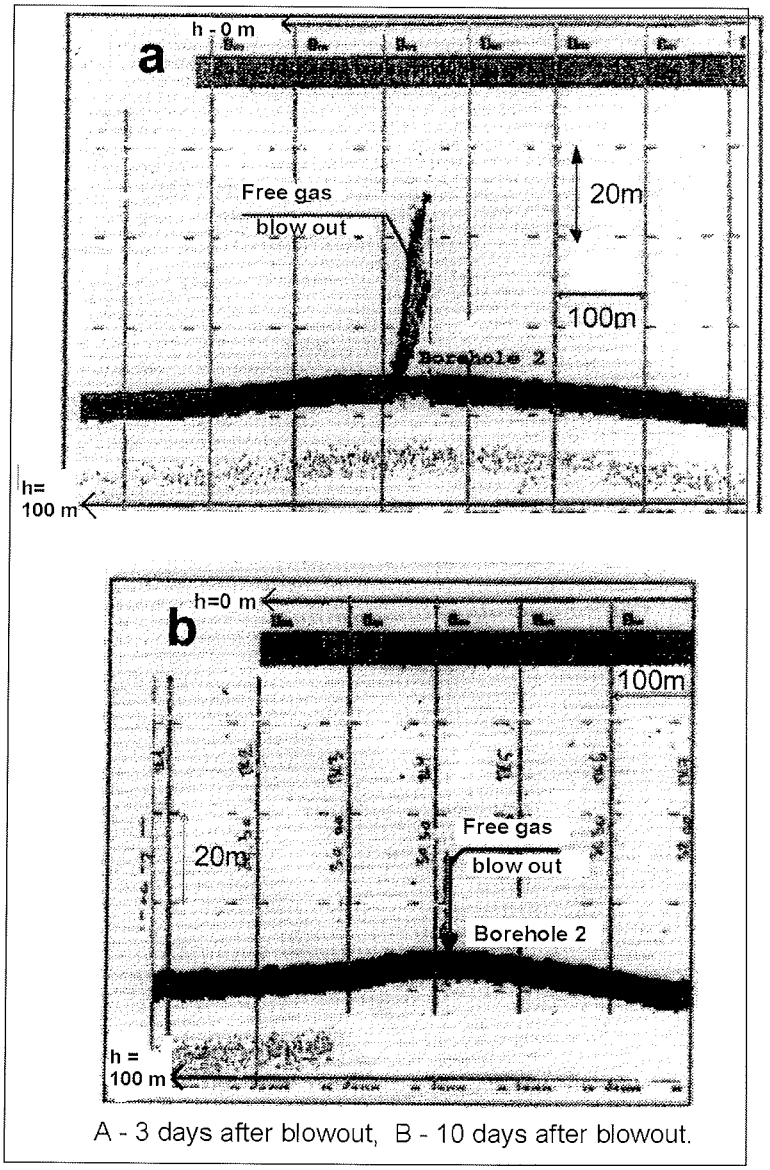

A - 3 days after blowout, B - 10 days after blowout.

Fig.6. Seafloor echograms in the area of bore-hole 481. Echograms show a gas vent in the bore-hole location.

American and Canadian scientists worked out two alternative hypotheses for the genesis of these structures. According to the first hypothesis, the ice-rich diapir-like rises are relic forms like bulgunnyakhs or pingos formed during the Pre-Holocene regression. However, paleogeographical reconstructions and observations of the ongoing abrasion of the coasts allowed concluding that pingos should have been inevitably destroyed during the Holocene transgression. The second hypothesis seems to be more reliable. It suuposes that the ice-rich diapir-like rises of the Beaufort Sea have been formed recently in the course of the subaquatic freezing of

slightly mineralized sediments under the influence of bottom seawater with negative temperatures (Shearer et al., 1971).

Turning back to the genesis of the diapir-like structures in the Pechora Sea, it will be remembered that there exist gas accumulations with excess pore pressure. The latter might be the main factor in the formation of diapir-like structures. We suppose that the pressure at the patches between scattered gas "pockets", where the base of permafrost clays penetrates deeply into the sediment sequence, produces lateral compression and subsequent squeezing out of permafrost sediments to the seafloor. The most ice-rich sediments, primarily segregation ice with relatively high plasticity, are the first to be involved in this process. Therefore the upper parts of the diapir-like structures become enriched in ice, as is clearly manifested by the drill cores. No gas blow-outs occur during formation of the diapir-like rises. At least, no free gas emissions have been recorded acoustically.

We suggest the following scheme for the formation of diapir-like structures:

1. During the Pre-Holocene regression the study area was occupied by a lake. Sediments that accumulated in this lake were water-stained and enriched in organic matter. It must be kept in mind that the diapir-llike structures occur within relative lows. At present, such territories on the Yamal Peninsula and Pechora Lowland are usually full of lakes because of low evaporation under arctic climatic conditions.
2. Prior to the beginning of the Flandrian transgression, the lake, being a rather ephemeral formation, turned into boggy lowland, and the sediments became frozen.
3. During the Flandrian transgression the territory was inundated. It is well-known that the sea-level rise was very rapid. Combination of the rapid inundation and gentle relief protected the permafrost sediments from destruction.
4. During the Holocene, degradation of the basal permafrost layer went on under the warming influence of the heat flux from the interior. It was accompanied by intensive emission of biogenic gas by organic-rich lacustrine sediments. It is likely that degradation of the upper permafrost layer was either absent or slow because of the cooling influence of the cold Kara Sea current. At present, the bottom water temperature in the study area is negative.
5. Ongoing accumulation of biogenic gas produced a considerable gas "pillow" below the permafrost. Most probably it was uneven in size. At the same time, the ice-rich permafrost layer served as a protecting cover making the gas pressure higher than the lithostatic one.
6. When the gas pressure reached certain (but unknown) values, deformation of the sediments started that caused changes in bottom relief in the "slackening zones". These zones could be related to the regions of decreased permafrost thickness, tectonic and lithologic contacts, etc. First of all, deformations occurred in the most plastic sediments – plastic frozen clays with ice schlieren. It is evident that the main direction of sediment-mass displacement was the vertical one.
7. Under the influence of gas pressure, the permafrost cover was destroyed in the most slackening places, and diapir-like structures were formed that are composed of clayish ice-sediment mixture. The presence of ice at small depths

(from 0.5 m below the seafloor) might be due to negative bottom water temperatures and, also, possible "reactance" effect.

8. Diapir-like rises of the other type are less evident in the modern bottom topography than the above described structures and represent the penultimate stage in the evolution of the diapir-like clayey structures, prior to destruction of the permafrost cover. At this stage, the gas pressure reaches its highest values.

Thus, the studied diapir-like rises are the consequence, result, and reflection of the processes operating in the subsurface part of the sediment cover. The presently available data do not allow evaluating the intensity of the processes of growth or destruction of the diapir-like structures. This demands additional investigations including repeated echo sounding, side scan observations, and seismoacoustic profiling along a special system of fixed profiles. The changes revealed in the course of repeated profiling will provide insight into development of these structures.

As a whole, it might be concluded that independently of their genesis, the ice-rich diapir-like structures and subsurface gas accumulations with excess pore pressure threaten the exploitation of oil and gas fields in the Pechora Sea. It is obvious that the phenomena described above have still been insufficiently studied, and it is necessary to carry out additional investigations in order to clarify their origin and estimate the threat.

References

Bondarev, V.N., Dlugach, A.G., Rokos, S.I., Kostin, D.A., Lisunov, V.K., 1999. Acoustic facies of the postcryogenic environments of the shallow Pechora and Kara seas. Razvedka i okhrana nedr (Prosperity and protection of natural resources), 7-8, 10-14 (in Russian).

Danilov, I.D., 1978. Pleistotsen morskikh subarkticheskikh ravnin (The Pleistocene of the subarctic marine lowlands). Moscow, Izd. MGU, 198 pp. (in Russian).

Gritsenko, I.I., 1989. Distribution of the Upper Cenozoic deposits in the Barents Sea Region and the modern morphostructures. In: Problemy kainozoiskoi paleogeografii I paleoekologii arkticheskogo basseina (Problems of the Cenozoic paleogeography and paleoecology of the Arctic basin). Apatity, Kola Branch of the Acad. Sci. USSR, 14-16 (in Russian).

Gritsenko I.I., Bondarev V.N., 1994. Subsea permafrost, gas hydrates and gas pockets in Cenozoic sediments of the Barents, Pechora and Kara Seas. Preprint 4-th World Petroleum Congress, topic 6, Stavanger.

Marine Science Atlas of the Beaufort Sea, 1987. Geology and geophysics, Geological Survey of Canada, Canada, Cartographic Information and Distribution Centre.

Rokos, S.I., 1996. Stratigraphy and geochronology of the Quaternary deposits in the shallow Pechora and Kara seas based on engineering drilling data. Proceedings of the International Conference "Evolution of biological processes and marine ecosystems under marine periglacial conditions, Murmansk, 22-23 (in Russian).

Shearer, J.M., Macnab, R.F., Pelletier, B.R., Smith, T.B., 1971. Submarine pingos in the Beaufort Sea, Science, 174, 4011, 816-818.

QUATERNARY PALYNOSTRATIGRAPHY OF THE PECHORA SEA

O.V. Rudenko[1], Ye. I. Polyakova[2]

[1] – Orel State University, Orel, Russia
[2] – Faculty of Geography, Lomonosov Moscow State University, Moscow, Russia

Abstract

By combining the lithologic, original palynologic and published micropaleonthological data we reconstructed paleogeographical events on the Pechora shelf during the Younger Dryas and Holocene time. Our paleoenvironmental reconstructions are based on the regularities in formation of pollen-and-spores assemblages in the surface sediments of the Pechora Sea. The main stages in paleogeography of the Pechora Sea during the Late Pleistocene were emphasized. The Late Valdai sediments in the Pechora Sea region were accumulated under the influence of fluvioglacial flows probably from the melting ice cap on Kolguev Island and, also, coastal glaciers. Climate deterioration considerably changed coastal vegetation as reflected in the depleted taxonomic and quantitative composition of palynospectra. The pollen data suggest that open steppe-like plant communities with *Artemisia, Poaceae, Asteraceae* and *Caryophyllaceae* dominated dry ecotopes on watersheds, whereas tundra-like communities with *Betula nana*, arctic *Salix, Dryas, Saxifraga, Carex* and *Brassicaceae* were common in more humid coastal lowlands.
The overlying silts and loamy sands are believed to have been accumulated during early deglaciation, i.e., Older Dryas and Alleröd. During this phase the glacial sedimentation was rather rapidly replaced by a glaciomarine deposition. Progressive climate warming caused prominent changes in coastal vegetation. Discontinuous treeless tundra-steppe associations were replaced by dwarf and shrub ernik tundra. A "complex vegetation cover" of forest-tundra apparently existed in the northern part of the Kola Peninsula and in the Northern Dvina Lowland. By the end of the Alleröd alder-bushes and horsetails occupied riverbanks, and spruce occurred in the forest-tundra communities on the adjacent hinterland.

Introduction

The Arctic is highly sensitive to climate variations and, consequently, it is an important region for understanding present and past climate changes. The Pechora Sea, which occupies the southeastern part of the Barents Sea shelf, is one of the key areas in the Eurasian Arctic for solving some cardinal problems of Quaternary stratigraphy and paleogeography. So far, existing conceptions about the Late Cenozoic stratigraphy of the Pechora Sea are based mainly on still debatable seismoacoustic profiling data (Gritsenko and Krapivner, 1989; Musatov, 1992; Lavrushin et al., 1985; Samoilovich et al., 1993) and scarce drilling data (Pavlidis et al., 1998; Polyakova, 1997; Lebedeva and Ivanova, 1987) and, thus, make detailed biostratigraphic investigations necessary. Among other biostratigraphic methods palynology is one of the most effective for this region, because of extremely low abundance of other microfossils in bottom sediments noted by many scientists (Polyakova, 1997; Kagan, 1989; Pogodina, 1994, among others).

However, implementation of this method for investigating marine and glaciomarine sediments demands special approaches dealing with regional peculiarities of aerial transportation of pollen and spores, transportation with rivers, and hydrodynamic conditions of sea basins. Nevertheless, the results of methodical investigations of subfossil

palynospectra from surface sediments of the Barents Sea (Rudenko, 1999; Rudenko and Polyakova, 2001) and published data on the Laptev Sea (Naidina and Bauch, 1999), and Canadian Arctic (Mudie, 1982) show that the average composition of subrecent palynospectra gives an overview of zonal and even subzonal types of coastal vegetation.

The main goals of our investigations presented in this paper are:
1) to reveal downcore changes in taxonomic composition of spore-and-pollen spectra;
2) to carry out palynozonal subdivision of the Quaternary sequences;
3) to determine the local peculiarities in paleoenvironmental evolution of the Pechora Sea region.

Modern setting

The Pechora Sea occupies the southeastern part of the Barents Sea. Its western boundary runs along the Kolguev Island, its eastern boundary along Vaigach Island, and the northern one along Novaya Zemlya (Fig. 1). Within these bounds its total area is nearly 90,000 km^2. Southward from 70°N the Pechora Sea shelf represents a gently northward sloping submerged plain with maximum depth not much more than 80 m (Matishov, 1984). Processes of abrasion and accumulation together with currents control bottom topography down to the depth of 45-60 m (Pogodina and Tarasov, 2001). Silty sands and sandy silts predominate among surface sediments within the 50 m isobath contour.

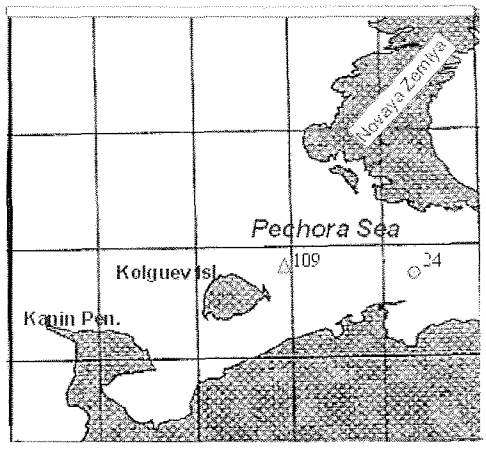

Fig. 1. Overview map of the Pechora Sea with investigated sites

The thickness of the Quaternary sediments in the Pechora Sea area exceeds 100 m (Gritsenko and Krapivner, 1989). Modern drilling and seismic data in the Pechora Sea revealed that deposits of the upper unit of Pleistocene sequence are represented by dark-greyish vaguely laminated sandy siltstone with abundant foraminifers, molluscs and ostracods in its upper part (Gritsenko and Krapivner, 1989; Epshtein et al., 1983). These sediments are regarded to be correspondent to the period of deglaciation of the Pechora Sea shelf (time span of 39-35 Ka according to Polyak et al., 2000). These modern data are in a good correlation with the results of radiocarbon dating of postglacial sediments of the Pechora Plain (Mangerud et al., 1999).

The Pechora Sea is distinguished by severe climatic conditions formed under the strong

influences of Arctic anticyclone, while the impact of warm Atlantic air and water masses is negligible. The coastal areas are ice-covered from October until July. During a short summer season freshwater mainly belonging to the Pechora River supplies the marine basin with a huge amount of dissolved and suspended material including both spore and pollen grains and chlorophyte algae cysts (Tarasov et al., 2000).

According to the Russian traditional scheme of the high-latitudinal vegetation zonation (Yurtsev et al., 1978), the waterlogged coastal area lies within the northern moss-lichen-shrub tundra subzone. Vegetation covering most part of the Southern Novaya Zemlya Island as well as Kolguev Island and Kanin Peninsula corresponds to the subzone of southern arctic tundra dominated by polar shrubs – dwarf birch and polar willow. Berry-fields of cloudberry, bilberry and others are also widespread. Riverbanks are occupied by alder and horsetails. *Valeriana capitata* and other motley grass species are abundant among tundra plants of Novaya Zemlya.

Material and methods

The Late Glacial and Holocene stratigraphy and paleogeography of the Pechora Sea presented in this paper are based on the spore-and-pollen analysis of sediments from piston core 24 recovered by Marine Arctic Geologic-Research Expedition (MAGE) during cruise aboard RV "Professor Kurentsov" in 1994 and core 109 obtained by drilling vessel "Kimberlit" belonging to the Arctic Marine Geotechnical Expedition (AMIGE) in 1982 (Fig. 1, Table 1).

Table 1. Position and core length of piston core 24 and core 109

Core No.	Coordinates		Core length, m	Water depth, m
	Latitude	Longitude		
24	68º 40E	55º 56N	1.0	15
109	69º 20E	52º 22N	41.6	21

The piston core was sampled for palynological investigations with 5 cm intervals, and core 109 with 100-150 cm intervals. From every sample 100-200 g of sediment were taken for treatment. Standard heavy-liquid separation method of V.P. Grichuk (1966) without acetolysis and subsequent glycerin mounts was used to process samples and to extract pollen and spores.

Spore and pollen grains were examined under "Biolam R-15" microscope with x450 and x900 magnification. The first 300 specimens encountered in each representative sample were identified, and species abundance was converted to percentages. In some non-representative samples we did not count percentages, but used only quantitative registration. Spore-and-pollen percentages were calculated based on the total sum of registered grains. Pollen zonation is based on the changes in relative abundances of spores and pollen, and relative abundances of the main tree-line groups. Finally, palynozones established in diagrams were correlated with all-Europe Blitt-Sernander climate-stratigraphic scale (Mangerud et al., 1974; Khotinskii, 1977) and with Timan-Pechora regional biostratigraphical scale (Yakhimovich and Zarkhidze, 1993).

Results

Spore-and-pollen spectra from the surface sediments

The surface layer of the Pechora Sea bottom sediments contains numerous palynomorphs: subfossil and redeposited pollen and spores, freshwater algae (*P. kawraiskii, P. boryanum*), dinoflagellate cysts, foraminifera linings, plant and coal debris, and others (Table 2).

Table 2. Total percentages of different microfossils in the Pechora Sea surface sediments

Microfossils	Total percentage	
	Piston core 24	Borehole 109
Redeposited pollen and spores	18.2	28.7
Subfossil pollen and spores	68.7	60.7
Freshwater chlorococcalean algae	2.6	1.8
Dinoflagellate cysts	6.1	5.0
Diatom algae	1.3	1.0
Foraminifera linings	3.1	2.8

Satisfactorily preserved pollen of modern terrestrial plants dominates palynospectra at both sites. Pollen concentrations are low ranging from 50 to 150 grains per gram. All registered pollen grains were subdivided into local pollen and spores of coastal tundra zone and long-distance transported components. Long-distance transported components include mainly arboreal and shrub pollen, primarily *Alnus, Pinus, Picea, Abies, Betula*, as well as easy-floating spores of *Sphagnum* and *Polypodiaceae*. These long-distance transported components comprise more than 50% of the "pollen rain" (Table 3, Fig. 2).

Table 3. Averaged spore-and-pollen associations in surface sediments

Taxonomic composition	%	Taxonomic composition	%
Arboreal and shrubs		*Herbs*	
Pinus silvestris	20	Poaceae	2
P. sibirica	4	Cyperaceae	2
Picea obovata	6	Artemisia sp.	5
Abies sp.	2	Asteraceae	2
Betula sect. Albae	2	Ericales	2
Betula sect. Nanae	14	Varia (total sum)	5
B. sect. Fruticosae	4	*Spores*	
Alnus sp.	3	Polypodiaceae	7
Alnaster sp.	1	Lycopodiaceae	6
Salix glauca + S. polaris	2	Sphagnum	9
Carpinus sp.+ Corylus sp.	1	Bryales	2

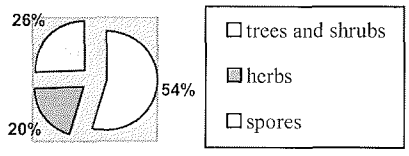

Fig. 2. Averaged total spore-and-pollen percentage composition in surface sediments

The major local pollen producers are *Cyperaceae, Poaceae, Salix, Asteraceae* (including *Artemisia), Saxifragaceae* and *Betula nana.* Other pollen types are found only occasionally, or, if counted, are not very abundant. However, in spite of the fact that well-floating pollen of conifers dominates palynospectra, local components are registered in such amounts that they might adequately reflect zonal and subzonal vegetation type. Re-deposited associations of the Pechora Sea surface sediments include pollen and spores of Quaternary, Paleogene-Neogene, Mesozoic and Paleozoic plants. Most of the re-deposited forms are poorly preserved; grains are crumpled, flattened, crushed and sometimes undeveloped. Among all re-deposited microfossils, only spores of Paleogene-Neogene plants are well preserved and have the specific orange color. Average percentage of re-deposited pollen and spores amounts to 28.7% of the total recorded palynomorphs. Their taxonomic composition is diverse and usually numbers 30-50 species in case the association is representative. Palynospectra are mainly represented by the Early Cretaceous and Triassic forms *Matoniaceae, Aratrisporites, Nevesisporites, Marattiaceae, Sphagnum, Gleichenia, Leiotriletes, Schizaeaceae* and pollen of *Cupressaceae, Pinus, Podocarpus,* and *Picea.* Single Permian forms include *Striatolebachiites,* and *Vittatina.* Ancient-looking pollen of angiosperms from the Upper Cretaceous-Paleogene beds (*Aquillapollenites, Mancicorpus, Oculopollis globosus, Trudopollis* and rare representatives of the Arctic-Tertiary flora – *Rhus, Nyssa, Carya, Pterocarya, Moraceae, Myricaceae)* were also found.

The group of aquatic palynomorphs is dominated by dinoflagellate cysts (mainly *Brigantedinium simplex, Algidasphaeridium minutum* and *Spiniferites*) and foraminifera linings thus indicating marine environments. At the same time, the presence of freshwater chlorococcalean algae (*Pediastrum cawraiskii, P. duplex* and *P. simplex*) provides evidence for considerable river runoff, mainly due to the Pechora River.

Distribution patterns of pollen-and-spore spectra in the Quaternary sequences

Borehole 109

Borehole 109 is located in the deltaic part of the submarine valley eastward from the Kolguev Island (Fig.1). It penetrated a 5-m thick unit of clays and silts overlying the 36-m thick unit of loams and loamy sands with abundant gravel, pebbles, rock debris, and coal interlayer (core interval 24.5-24.6 m). The dark grayish color of the uppermost sediment layers indicates anoxic conditions.

Table 4. Spore-and-pollen assemblage zones (PAZ) in borehole 109

PAZ	Depth (m)	Description
1	0.8-3.3	Dwarf and shrub birch zone with AP (pine, spruce and alder) admixture
2	3.3-5.0	Dwarf and NAP zone with arctic-type clubmosses

Two upper units composed of clays and silts contain representative palynospectra, where pollen and spores of Quaternary age are dominant. Spore-and-pollen diagram of this part of the borehole is subdivided into two spore-and-pollen assemblage zones (PAZ) as shown in Table 4.

Taxonomic and quantitative composition of pollen and spores in PAZ 1 and PAZ 2 is rather poor. Dwarf *Betula* pollen is abundant in almost all spectra (>20-40%). Besides Hypoarctic species *Betula nana*, other taxonomic groups, including Boreal (*Vaccinium sp.*), Arctic (*Dryas octopetala, Rumex sp.*), and Arctic-Alpine ones (*Saxifraga sp., Lycopodium appressum*) are identified. Almost all registered spore-and-pollen spectra contain grains of long-distance transported wind-blown pollen from the taiga zone (*Pinus s/g Haploxylon, Picea*) – up to 15% in total. Alder, shrub alder (usually called *Alnaster*), and polar willow pollen grains are extremely rare. Water-drifted pollen of exotic broad-leaved plants, such as oak, hornbeam, and elm, are also scarce. Spores of *Sphagnum* mosses and *Polypodiaceae* ferns dominate the spore group.

Predominance of *Artemisia* pollen in NAP composition and occurrence of single *Ephedra* pollen indicate dry ecotopes and provide evidence for prominent climate amelioration in coastal regions. The floristic composition of non-arboreal pollen (NAP) is very diverse: in addition to pure periglacial taxa (*Ranunculus arcticus, Minuartia cf.arctica*), pollen of more thermophilic plants (*Polygonum viviparum, Polemonium boreale* and others) and different cereals is also present. At the same time, quantitative composition of NAP group is unrepresentative.

Core interval 5.0-11.0 m represented by moraine-like loams with numerous pebbles, gravel and rock debris is characterized by only sporadic occurrence of pollen and spores of the Quaternary age (mainly *Betula nana* and *Sphagnum*) contrary to abundant reworked pollen of Mesozoic conifers and Paleozoic spores of formal genus.

Laminated loamy sands and silts underlie moraine-like loams. This sediment unit does not contain any spores and pollen of the Quaternary age but only heterochronous Paleozoic-Mesozoic palynospectra dominated by Early Cretaceous *Classopollis,* pollen of different conifers (*Protopodocarpus, Pseudopicea* spp., *Pinus* spp. *Lebachia* sp. etc.) and spores (*Schizaeaceae* with typical Barremian-Aptian *Cicatricosisporites, Pilosisporites* as well as *Klukisporites, Aequitriradites, Sphagnum, Gleicheniaceae).* Sediments with Early Cretaceous palynospectra occur on the Pechora Sea coast (Gryazeva, 1980) and correlate with the above-described unit. These sediments were accumulated in aerial-subaerial environments.

Piston core 24

Piston core (PC) 24 was recovered at the base of the submarine coastal slope from 15 m water depth. Core section consists of 0.25 m of sandy silt underlain by an 0.55-m-thick layer of sandy-silty pelite, and ends with 0.2-m-thick layer of dense clayey silt with gravel and pebbles.

The percentage diagram of piston core 24 shows few changes in the abundance of pollen and spore taxa during the time of sedimentation and is subdivided into four pollen assemblage zones (PAZ) (Table 5, Fig.3).

Table 5. Spore-and-pollen assemblage zones (PAZ) in piston core 24

PAZ	Depth (m)	Description
1	0.0-0.25	Modern-like moss-lichen-shrub tundra zone
2	0.25-0.5	Sparse birch-wood zone with spruce, fir, pine and forester mosses
3	0.5-0.8	Dwarf-birch and polar willow zone with alder and humid motley grass
4	0.8-1.0	Dwarf and NAP tundra-steppe zone with arctic-type clubmosses

Pollen concentrations are lower than in the borehole section and decrease downcore. The *Betula sect. Nanae* curve in the percentage diagram shows maximum values in the lower part of the core (28%). Cool and dry climate conditions are reflected in considerable amounts of *Artemisia* and *Chenopodiaceae* pollen (up to 20 % in total) as well as xerophilous motley grass pollen: *Brassicaceae, Ephedra, Plantago* sp., and *Rumex* sp. The admixture of long-distance transported pollen from the taiga zone (*Pinus, Picea, Abies*) is negligible.

Palynospectra of PAZ-4 reflect an extremely unfavorable environment at a time when only sparse forest tundra with extensive open fields of dry-steppe communities were able to exist in the coastal zone. PAZ-4 closely resembles those recorded in adjacent areas: Sartan PAZ of the Taimyr Lowland (Andreev et al., 2002), and Younger Dryas PAZes of the Southern Novaya Zemlya Island (Serebryannyi et al., 1998), South-Western Barents Sea shelf (Okuneva and Stelle, 1986; Stelle et al., 1989) and Kolguev shelf (Baranovskaya et al., 1976; Veinbergs et al., 1995).

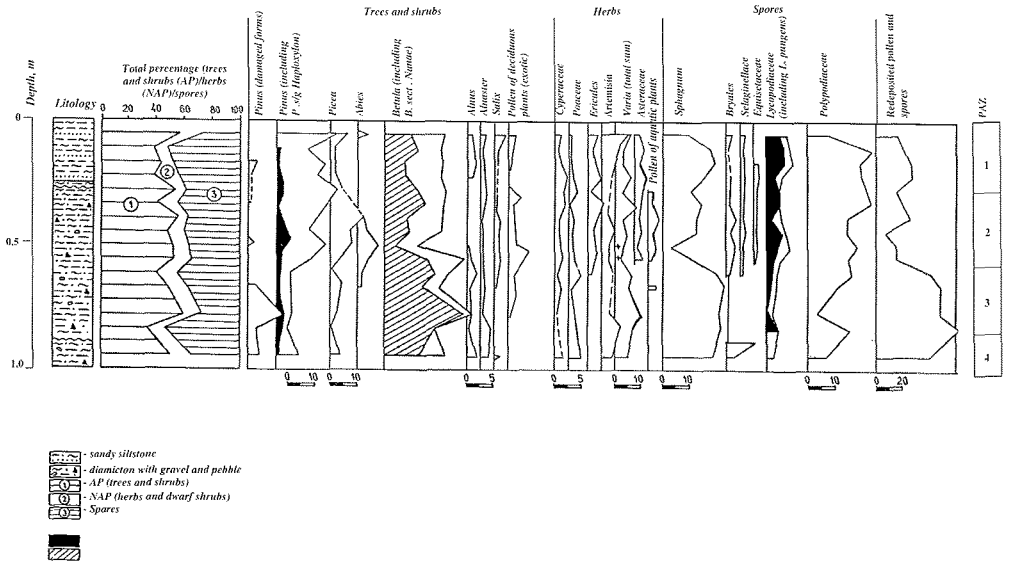

Fig. 3. Percentage spore-and-pollen diagram of piston core 24

PAZ-3 is characterized by increase in pollen concentration and considerable changes in

spore-and-pollen composition, primarily, dramatic decrease in herb pollen percentage, especially steppe and tundra taxa (e.g. *Artemisia, Dryas, Poaceae, Asteraceae* and some others). In contrast, significant increase in *Betula sect. Nanae, Alnaster, Ericales* content as well as long-distance transported *Pinus* and *Picea* is noticeable.

PAZ-2 is distinguished by maximum percentages of conifer pollen. *Abies* and *Picea* percentages rise up to 10 and 14%, respectively, in 0.35-0.45 m interval. The peak in *Pinus s/g Haploxylon* percentage (5%) and considerable decrease in Hypoarctic elements percentage are recorded. Another peculiarity of PAZ-2 is presence of pollen belonging to thermophillous aquatic and nearshore aquatic plants such as *Typha latifolia, Alisma* sp., and *Potamogeton* sp. A visible increase in *Ericales* and herbs pollen percentage in the upper part of PAZ-2 and simultaneous dramatic decrease in conifer pollen suggest significant climate cooling during the final phase in sandy-silty pelite layer accumulation.

PAZ-1 reflects environmental deterioration in the area during the time of sandy silt accumulation. The Hypoarctic, Arctic, and Arcto-Alpine taxa dominate specta thus indicating modern-type vegetation of moss-lichen-shrub northern tundra. We consider *Betula* sect. *Nanae, Salix polaris, S. glauca, Polygonaceae* (including *Oxyria*), *Saxifragaceae, Cyperaceae, Sphagnum* and *Bryales* to be the main local producers of pollen and spores. It should be mentioned, however, that the long-distance transported conifers in association with arboreal *Betula* sect. *Albae* comprise more than 45% of palynospectra.

Climatostratigraphic interpretation

Unit 1

Bedrock recovered from borehole 109 is represented by 20-m-thick laminated loamy sands and silts with a coal interlayer at core depth of 24.5-24.6 m. According to palynological data, this unit was determined to be of the Early Cretaceous age, and its terrigenous lacustrine genesis was confirmed by geological and geomorphological data (Lavrushin et al., 1985). The depleted foraminiferal assemblages represented by Pre-Cenozoic species redeposited from continental sections (Kostin et al., 1988) are correlative to those studied in the northern Pechora Plain (Gryazeva, 1980) and in the area eastward from the Kolguev shoal (Baranovskaya et al., 1976).

Unit 2

The Early Cretaceous bedrock in borehole 109 section is unconformably overlain by 6 m thick moraine-like loam (core interval 5.0-11.0 m). According to our palynological and foraminiferal data (Kostin et al., 1988), the age of moraine-like loams was determined as the Late Valdai. We suppose that this unit was accumulated under the influence of fluvioglacial flows, perhaps, from the melting ice cap on Kolguev Island and, also, coastal glaciers. Glacial bottom sediments of this kind are widely spread at the periphery of the Barents and Pechora seas (Pavlidis et al., 1998; Tarasov et al., 2000; Samoilovich et al., 1993). They are characterized by extremely low concentrations of foraminifer tests and diatom valves (less than 20-50 specimens). The damaged shape of the valves suggests that they have been reworked from more ancient interglacial sediments. Numerous unvegetated areas on adjacent land formed by cryogenic processes could be possible sources for the reworked material. Diatom assemblages are dominated by sublittoral species – *Paralia sulcata, Diploneis subcincta, D. interrupta,* and *Trachineis aspera.* Such assemblages provide evidence for low surface water temperatures and low productivity of

phyto- and zooplankton (Polyakova, 1997; Druzhinina and Musatov, 1992; Gudina, 1976; Pogodina, 1994; Polyak, 1985).

Climate deterioration considerably changed coastal vegetation as reflected by depleted taxonomic and quantitative composition of palynospectra. Such distribution pattern is quite typical for Late Glacial sediments (Rudenko, 1999; Polyakova, 1997; Sharapova, 1996; Baranovskaya et al., 1976; Lebedeva and Ivanova, 1989; Okuneva and Stelle, 1986; Serebryannyi et al., 1998; Andreev et al., 2002). One possible explanation for extremely low pollen concentrations might be low pollen productivity of plants in coastal areas due to extraordinarily severe climate conditions. Plant cover of the coastal areas was undoubtedly discontinuous and existed mainly in refuges. The pollen data suggest that open steppe-like plant communities with *Artemisia, Poaceae, Asteraceae* and *Caryophyllaceae* dominated dry ecotopes on watersheds, whereas tundra-like communities with *Betula nana*, Arctic *Salix, Dryas, Saxifraga, Carex* and *Brassicaceae* were common in more humid coastal lowlands.

Unit 3

The overlying silts and loamy sands with a thickness of 5 m are supposed to have been accumulated during early deglaciation in oceanic periglacial environments of the Older Dryas and Alleröd. Considerable climate warming resulted in rapid degradation of glaciers. During this phase the glacial sedimentation was rather rapidly replaced by glaciomarine sedimentation (Tarasov et al., 2000; Matishov, 1984). This unit is characterized by considerable increase in abundance of foraminifers. The relative abundance of the dominant species *Retroelphidium clavatum* is more than 80% (Kostin et al., 1988). This species is able to survive considerable freshening. The ecological structure of the foraminiferal assemblage with arctic and arctic-boreal *Elphidiella arctica, E. tumida, Retroelphidium hyalinum, Cassidulina barbara,* and *Islandiella norcrossi* provides evidence for extreme environments. At the same time, the remaining low total concentration of diatom valves as well as dinoflagellate and chlorophyte cysts allows assuming that this unit was accumulated under unfavourable environmental conditions with oscillating sea level and unstable hydrodynamic conditions.

Progressive climate warming caused prominent changes in coastal vegetation. Discontinuous treeless tundra-steppe associations were replaced by dwarf and shrub ernik tundra. Appearance of plants characteristic for waterlogged areas such as *Carex, Equisetum arvense* manifests some climate humidification. At the same time, steppe associations with *Artemisia, Ephedra, Chenopodiaceae* and *Poaceae* were still widespread. In northern Taimyr, Andreev et al. (2002) reconstructed such a "mixed" vegetation structure for the Alleröd epoch. "Complex vegetation cover" of forest-tundra apparently existed in the northern part of the Kola Peninsula (Rudenko, 1999; Sharapova, 1996) and in the Northern Dvina Lowland (Pleshivtseva, 1983). We suppose that by the end of the Alleröd alder-bushes and horsetails occupied riverbanks, and spruce occurred in the forest-tundra communities.

Unit 4

The Pleistocene-Holocene boundary corresponds to the core depth of 0.8 m in piston core 24. It is marked by considerable changes in composition of spores, pollen, foraminifers, and diatoms (Fig. 3).

Conclusions

By combining the lithologic, original palynologic and published micropaleonthological data we reconstructed paleogeographical events on the Pechora shelf during the Younger Dryas and Holocene. The main conclusions are as follows:

1) The Late Valdai sediments in the Pechora Sea region were accumulated under the influence of fluvioglacial flows, perhaps, from the melting ice cap on Kolguev Island and, also, coastal glaciers. Climate deterioration considerably changed coastal vegetation as reflected in depleted taxonomic and quantitative composition of palynospectra. The pollen data suggest that open steppe-like plant communities with *Artemisia, Poaceae, Asteraceae* and *Caryophyllaceae* dominated dry ecotopes on watersheds, whereas tundra-like communities with *Betula nana*, arctic *Salix, Dryas, Saxifraga, Carex* and *Brassicaceae* were common in more humid coastal lowlands.

2) The overlying silts and loamy sands are supposed to have been accumulated during early deglaciation in oceanic periglacial environments of the Older Dryas and Alleröd. During this phase the glacial sedimentation was rather rapidly replaced by glaciomarine sedimentation. Progressive climate warming caused prominent changes in coastal vegetation. Discontinuous treeless tundra-steppe associations were replaced by dwarf and shrub ernik tundra. "Complex vegetation cover" of forest-tundra apparently existed in the northern part of the Kola Peninsula and in the Northern Dvina Lowland. By the end of the Alleröd alder-bushes and horsetails occupied riverbanks, and spruce occurred in the forest-tundra communities on the adjacent hinterland.

References

Andreev, A.A., Siegert, C., Klimanov, V.A., Derevyagin, A.Yu., Shilova, G.N., Melles, M., 2002. Late Pleistocene and Holocene vegetation and climate on the Taymyr Lowland, Northern Siberia. Quarternary Research, 57, 138-150.

Baranovskaya, O.F., Grigorjev, M.N., Malyasova, Ye.S., 1976. Late Cenozoic stratigraphy of Kolguev Island. In: Kainozoi shel'fa i ostrovov Sovetskoi Arktiki (Cenozoic of the shelf and islands of the Soviet Arctic), Leningrad, Nauka, 83-90 (in Russian)

Danilov, I.D., 1978. Pleistotsen morskikh subarkticheskikh ravnin (Pleistocene of marine subarctic plains). Moscow, Uzd. MGU, 280 pp. (in Russian).

Druzhinina, N.I., Musatov, E.E., 1992. New data on stratigraphy of the upper Cenozoic deposits of the Barents Sea. Problems of Cenozoic Paleoecology and paleogeography of the Arctic seas. Abstracts of III All-Union Conference, Apatity, 27 (in Russian).

Epshtein, O.G., Lavrushin, Yu.A., Valpeter, A.P., 1983. Quaternary sediments of the southeastern part of the Barents Sea and adjacent paleoshelf. Doklady AN, 242, 1. 180-183. (in Russian)

Grichuk, V.P., 1966. Glacial flora of the Russian Plain. In: Grichuk, V.P. (ed.), Znachenie palinologicheskogo analiza dlya stratigrafii i paleofloristiki (Importance of palynological analysis for the purposes of stratigraphy and paleofloristic). Moscow, Nauka, 189-196 (in Russian)

Gritsenko, I.I., Krapivner R.B., 1989. Late Cenozoic sediments of the southwestern Barents Sea region: sedimentary seismostratigraphic units and their substantial composition. In: Sovremennye osadki i paleogeografiya severnykh morei (Modern sediments and paleogeography of the northern seas). Apatity, Izd. KolaSC RAS, 28-45 (in Russian).

Gryazeva, A.S., 1980. Stratigraphy of the Lower Cretaceous sediments of the Pechora Basin based on palynological analysis. In: Mikrofitofossilii v neftyanoi geologii (Microphytofossils in oil geology). Leningrad, izd. VNIIO, 96-112 (in Russian).

Gudina, V.I., 1976. Morskie pleistotsenovye foraminifery, stratigrafiya I paleozoogeografiya Severa SSSR (Marine Pleistocene foraminifers, stratigraphy and paleozoogeography of the USSR North). Novosibirsk, Nauka, 125 pp. (in Russian).

Kagan, L.Ya., 1989. Diatom analysis of the late Cenozoic deposits of the Arctic seas. In: Noveishie otlodzeniya i paleogeographiya severnykh morei (Recent deposits and paleogeography of the northern seas). Apatity, Izd. KolaSC RAS, 64-66 (in Russian).

Khotinskii, N.A., 1977. Golotsen Severnoi Evrazii (Holocene of the Northern Eurasia). Moscow, Nauka, 198 pp. (in Russian).

Kostin, D.A., Skorobogat'ko A.V., Borovaya, O.V., 1988. Otchet po geologicheskoi s'emke shel'fa Barentseva morya v masshtabe 1:1000000 (Report on the state geological survey of the Barents Sea shelf on a scale 1:1000000). Murmansk, Izd. Murmanskoi Morskoi Geologicheskoi Ekspeditsii, 234 pp. (in Russian).

Lavrushin, Yu.A., Golubev, Yu.K., Gritsenko, I.I., Epshtein, O.G., 1985. The structure and composition of shallow-water sediments of the glacial Kolguev shelf. In: Problemy chetvertichnoi paleoekologii I paleogeografii morei Barentseva I Belogo (Problems of Quarternary paleoecology and paleogeography of the Barents and White seas). Murmansk, Izd. MMBI, 78-81 (in Russian).

Lebedeva, R.M., Ivanova, L.V., 1987. Results of complex biostratigraphic analysis of bottom sediments in the Pechora Sea. In: Problemy chetvertichnoi paleoekologii I paleogeografii morei Severnogo Ledovitogo okeana (Problems of the Quarternary paleoecology and paleogeography of the Arctic Ocean seas). Apatity, Izd. KolaSC RAS, 50-52 (in Russian)

Mangerud, J., Andersen, S.A., Berlund, B.E., Donner, J.I., 1974. Quaternary stratigraphy of Norden, a proposal for terminology and classification Boreas, 3, 3, 109-126.

Mangerud, J., Svendsen, J., Astakhov, V., 1999. Age and extent of the Barents and Kara ice sheets in Northern Russia. Boreas, 28, 46-80.

Matishov, G.G., 1984. Dno okeana v lednikovy period (The Seabed in the Glacial period). Moscow, Nauka, 176 pp. (in Russian).

Mudie, P.J., 1982. Pollen distribution in recent marine sediments, eastern Canada. Can. J. Earth Sci., 19, 729-747.

Musatov, E.E., 1992. Seismostratigraphy and mapping of the Neogene-Quarternary sediments of the Barents-Kara Shelf. In: Geologicheskaya istoriya Arktiki v mezozoe i kainozoe (Geologic history of the Arctic in the Mesozoic and Cenozoic), book 2. St. Petersburg, Izd. VNIIO, 38-47 (in Russian).

Naidina, O.D., Bauch, H.A., 1999. Distribution of pollen and spores in surface sediments of the Laptev Sea. In: Kassens, H.A. et al. (eds.), Land-Ocean system in the Siberian Arctic, Berlin, Springer-Verlag, 577-586.

Okuneva, O.G., Stelle, V.Ya., 1986. New data on biostratigraphic investigations of geotechnical boreholes at the East Kolguev Coast. In: Inzhenerno-geologicheskie usloviya shel'fa i metody ikh issledovaniya (Geotechnical conditions of the shelf and methods of their investigations). Riga, Zinatne, 8-12 (in Russian).

Pavlidis, Yu.A., Ionin, A.S., Shcherbakov, F.A., Dunaev, N.N., Nikifirov, S.L., 1998. Arkticheskii shel'f: Pozdnechetvertichnaya istoriya kak osnova prognoza razvitiya (Arctic shelf: Late-Quaternary history as the basis for forecast of the future development). Moscow, GEOS, 187 pp. (in Russian).

Pleshivtseva, E.S., 1983. Palynological characteristic of the Late Glacial and Postglacial sediments of the Northern Dvina Lowland. In: Palinologiya golotsena i marinopalinologiya (Holocene palynology and marine palynology). Moscow, Nauka, 23-26 (in Russian).

Pogodina, I.A., 1994. Micropaleontologic investigations of the Late Quaternary sediments in the Barents Sea. In: Foraminifery Barentseva morya (Gidrobiologiya i chetvertichnaya paleoekologiya (Foraminifers of the Barents Sea (hydrobiology and

Quaternary paleoecology). Apatity, Izd. Kola SC RAS, 71-83 (in Russian).
Pogodina, I.A., Tarasov, G.A., 2001. Some peculiarities of the Pleistocene-Holocene sedimentation processes in the Pechora Sea. In: Sedimentologicheskie protsessy I evolyutsiya morskikh ekosistem v usloviyakh morskogo periglyatsiala (Sedimentological processes and evolution of marine ecosystems marine periglacial conditions). V. 2., Apatity, Izd. Kola SC RAS, 13-19 (in Russian).
Polyak, L.V., 1985. Foraminifers of the Barents and Kara seas bottom sediments and their stratigraphic importance. Abstract of Candidate Dissertation. Leningrad, 22 pp. (in Russian).
Polyak, L., Gataullin, V., Okuneva, O., Stelle, V., 2000. New constraints on the limits of the Barents-Kara ice sheet during the Last Glacial Maximum based on borehole stratigraphy from the Pechora Sea. Geology, 28, 7, 611-614.
Polyakova, Ye.I., 1997.Arkticheskie morya Evrazii v pozdnem kainozoe (Eurasian Arctic Seas in the Late Cenozoic). Moscow, Nauchnyi Mir, 146 pp. (in Russian).
Rudenko, O.V., 1999. Several regularities in distribution of redeposited palynomorphs in Upper Cenozoic sediments of the Barents Sea. In: Geology of seas and oceans. V.1. Moscow, GEOS, 97-98 (in Russian).
Rudenko, O.V., Polyakova, Ye.I., 2001. Peculiarities of the spore-and-pollen spectra in surface sediments of the Barents Sea. In: Sedimentologicheskie protsessy I evolyutsiya morskikh ekosistem v usloviyakh morskogo periglyatsiala (Sedimentological processes and evolution of the marine ecosystems in the conditions of marine periglacial). V. 1. Apatity, Izd. Kola SC RAS, 111-120 (in Russian).
Samoilovich, Yu.G., Kagan, L.Ya., Ivanova, L.V., 1993. Chetvertichnye osadki Barentseva morya (Quaternary sediments of the Barents Sea). Apatity, Izd. KolaSC RAS, 72 pp. (in Russian).
Serebryannyi, L., Andreev, A., Malyasova, E., Tarasov, P., Romanenko, F., 1998. Late glacial and early-Holocene environments of Novaya Zemlya and the Kara Sea Region of the Russian Arctic. Holocene, 8, 323-330.
Sharapova, A.Yu., 1996. Paleoekologicheskii analiz chetvertichnoi pyl'tsy iz donnykh osadkov Barentseva morya (Paleoecological analysis of Quaternary pollen assemblages from the bottom sediments of the Barents Sea). Apatity, preprint, 44 pp. (in Russian).
Stelle, V.Ya., Savvaitov, A.S., Yakubovskaya, I.Ya., 1989. Biostratigraphy of the Late-Quarternary sediments from the East Barents Sea deep-shelf zone. In: Inzhenerno-geologicheskie usloviya neftegazonosnykh raionov shel'fa (Engineering-geologic conditions of the prospective oil-and-gas shelf areas). Riga, Zinatne, 51-71 (in Russian).
Tarasov, G.A., Pogodina, I.A., Khasankaev, V.B., Kukina, N.A., Mityaev, M.V., 2000. Protsessy sedimentatsii na glatsial'nykh shel'fakh (Processes of sedimentation on glacial shelves). Apatity, Izd. Kola SC RAS, 473 pp. (in Russian).
Veinbergs, I.G., Stelle, V.Ya., Savvaitov, A.S., Yakubovskaya, I.Ya., 1995. Late Cenozoic history of the Pechora Sea coast. In: Svitoch, A.A. (ed.), Korrelyatsiya paleogeograficheskikh sobytii: kontinent-shel'f-okean (Correlation of the paleogeographical events: continent-shelf-ocean). Moscow, Izd. MGU, 106-113 (in Russian).
Yakhimovich, V.L., Zarkhidze, V.S., 1993. Stratigrafiya neogena Timano-Ural'skoi oblasti (Neogene stratigraphy of the Timano-Ural region). Ufa, Izd. BNS UrO AN SSSR I BYChK, 27 pp. (in Russian).
Yurtsev, B.A., Tolmachev, A.I., Rebristaya, O.V., 1978. The floristic delimitation and subdivision of the Arctic. In: Yurtsev, B.A. (ed.), Arkticheskaya floristicheskaya oblast' (The Arctic Floristic Region). Leningrad, Nauka, 9-66 (in Russian).

THE LATE QUATERNARY HISTORY OF THE PECHORA SEA

G.A. Tarasov[1], I.A. Pogodina[1], G.G. Matishov[1], H.A. Bauch[2], N.A. Kukina[1]
[1] – Murmansk Marine Biological Institute, Kola Scientific Center RAS, Murmansk, Russia
[2] – Mainz Academy of Sciences, Humanities and Literature, Germany

Abstract

More reliable reconstructions of the Late Quaternary glacial history of the Pechora Sea have been carried out due to new radiocarbon datings. The bulk of evidence favors the view that complete deglaciation of the Pechora Sea occurred in the middle Valdai epoch, about 35-40 ka. After a short interstadial period with normal marine conditions, sea-level fall gave rise to establishment of continental environments. In the late Valdai, the Novaya Zemlya ice sheet occupied only the northernmost Pechora Sea and did not reach the Pechora Lowland. In the course of the subsequent Holocene transgression, the shelf was abraded. Modern lithodynamic conditions in the Pechora Sea determine accumulation of sandy-silty deposits.

Introduction

Though the Quaternary history of the North American and Eurasian arctic margins has been adequately studied the extent of the Pleistocene ice sheets in the Barents Sea area, and, in particular, in the Pechora Sea, is still a point open to question. In this area, the Quaternary deposits form a single more than 1000 m thick terrigenous formation unconformably overlying the Paleozoic and Mesozoic rocks. One group of scientists (Gritsenko and Krapivner, 1989; Danilov, 1982) considers these deposits to have been accumulated under marine conditions during the whole Pleistocene and even Neogene. Another group of scientists is of the opinion that this formation includes thick glacial beds, and the youngest preserved glacial layers are of the Valdai age (Gataullin et al., 1993; Polyak et al., 2000).

Material and discussion

As a result of analysis of the sediment core data (Fig. 1), deposited and published materials, and new radiocarbon datings (Table 1), it became possible to reconstruct the evolutionary history of this region on a higher scientific level.

The Quaternary deposits of the Pechora Sea shelf were formed under the influence of global sea-level oscillations and repeated changes in environmental conditions from marine to continental ones. The latter were distinguished by development of thick ice sheets. As a result, shelf sediment sequence represents an extremely complicated intercalation of Pleistocene moraines and interglacial beds overlain by Holocene marine sediments. Age estimation of the morainic beds is rather difficult, but the presence of ice sheets on the Pechora Sea shelf during the early-middle Pleistocene is beyond question, because several cores were drilled into morainic beds overlain by the Mikulino marine deposits (Tarasov et al., 2000).

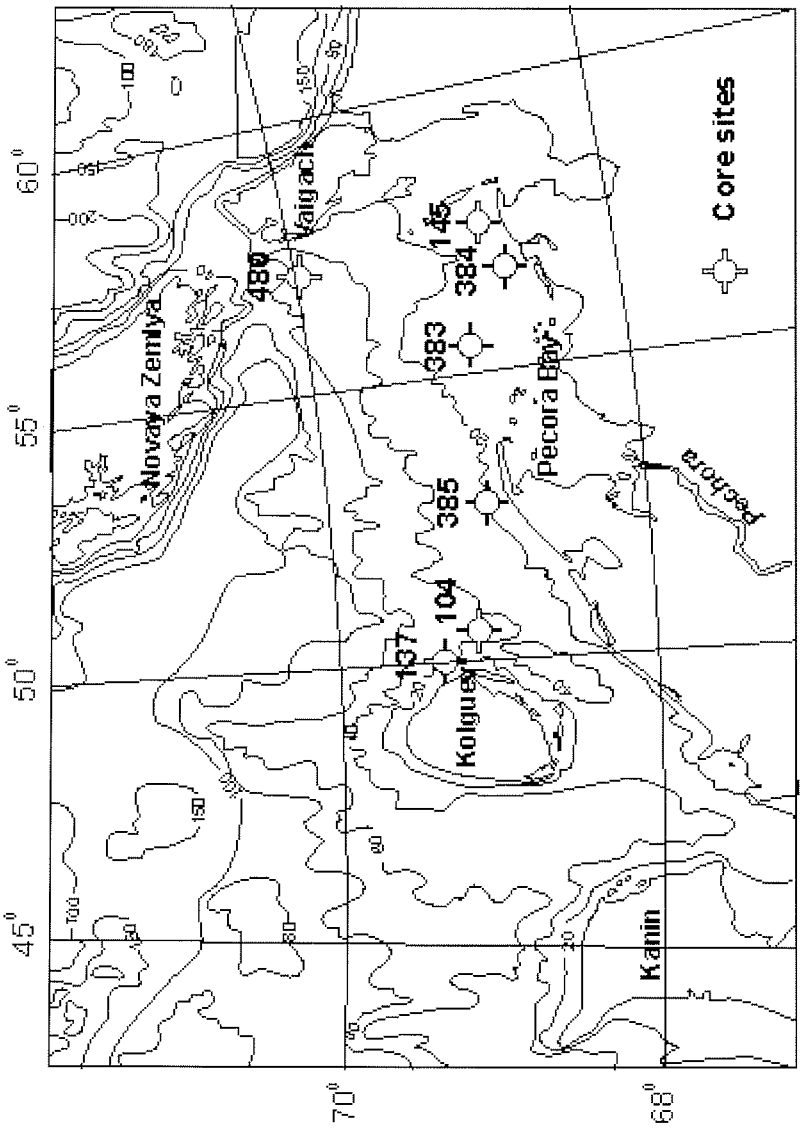

Fig. 1. Location map of the studied cores

During the Mikulino epoch, North Atlantic water flowed into the Barents and Pechora seas considerably farther eastward than at present, as documented by composition of foraminifers in the Mikulino horizon in core 145 recovered in the Varandei area, central part of the Medynskii arch (Figs. 2, 3).

Table 1. Accelerator mass spectrometer ^{14}C dates

Lab. no.	Core no.	Depth in core (m)	Material	Mass (mg)	Uncorrected age (yrs. B.P.)
KIA 16840	137	1.4-1.5	*Montacuta maltzani*		5360±30
KIA 16841	137	9.4-9.5	*Montacuta maltzani*		5390±30
KIA 16843	137	35.0-35.1	shell detritus		>52900
KIA 16844	137	42.0-42.1	shell detritus		>52900
KIA 16845	480	2.0	plant detritus	0.5	22390±420/-400
KIA 16846	480	19.5	plant detritus	2.8	27560±210
KIA 16847	480	41.8	plant detritus	1.4	26110±260
KIA 16848	480	73.2	plant detritus	2.2	26170+210/-200
KIA 16849	480	82.4	plant detritus	2.9	28460+220/-210

The foraminiferal assemblage, found in the dark grey clays with rare pebbles and interlayers of fine well-sorted sand, does not have any analogs in the modern fauna of the Pechora Sea. High species diversity, considerable portion of boreal species, and absence of any traces of dissolution on foraminiferal tests provide evidence for normal marine salinity and hydrochemical regime of bottom and pore waters, which favored preservation and burial of tests. The palynological association dominated by arboreal pollen indicates interglacial conditions (Sharapova, 1996).

The early Valdai cooling gave rise to thick ice sheets, which covered the Pechora Sea and Pechora Lowland. Glacial streams reworked a considerable portion of the marine Mikulino sediments. The early Valdai deposits are represented by dense dark grey loams with coarse-grained material and single faunistic remains of definitely allochthonous origin. No spores and pollen of the Quaternary age were reported from these beds.

Revision of the drill and seismoacoustic data with the help of modern chronostratigraphic methods (Polyak et al., 2000) has shown that the Pleistocene loams of the southeastern Pechora Sea are overlain by indistinctly laminated dark grey silt. The lower 10 m of this silt are enriched in foraminifers, molluscs, and ostracods indicative of marine interglacial conditions. Palynological spectra include a considerable portion of arboreal pollen. The sediments yield radiocarbon age estimations of 39-35 ka. It can be concluded, therefore, that the Pechora shelf became considerably deglaciated in the middle Valdai epoch.

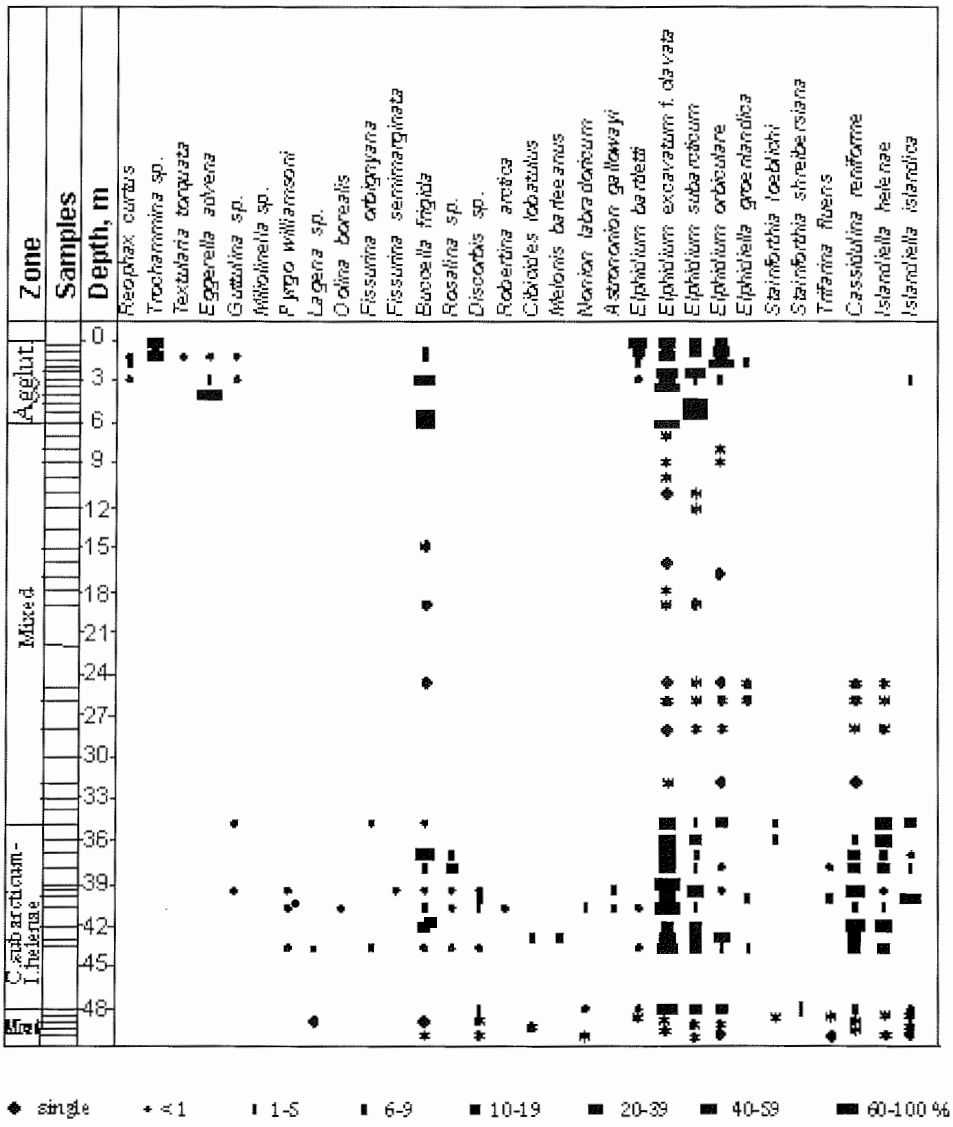

Fig. 2. Relative abundance (%) of ***Foraminifera*** species in core 145

These data are in accordance with radiocarbon and thermoluminescence datings of the post-glacial deposits on the Pechora Lowland and Yamal Peninsula (Mangerud et al., 1999; Forman et al., 1999). Micropaleontological investigations of the Pleistocene sections on the Kola Peninsula (Gudina and Evzerov, 1973) have provided evidence for a vast transgression during the Karga epoch (40-35 and

30.7-24.1 ka). The Karga transgressive waters flooded coastal lowlands and estuarine parts of the rivers. However, the Karga basin was considerably smaller in size than the Mikulino and, probably, the modern basins. We assume that the southeastern shelf was exposed. In core 145 located farther south than the cores studied by Polyak et al. (2000), marine layers enriched in fossils have not been found. Marine faunistic assemblages of the Karga and Mikulino beds are different. Paleofaunistic assemblages of the Karga age are composed of arctic species that inhabited a cold modern-like sea basin.

Due to the subsequent sea-level fall, the short interstadial period with normal marine conditions was replaced by the period with continental environments. In the southern part of the sea, the Pleistocene loams are overlain by grey, regularly laminated, silts practically devoid of faunistic remains. Spore and pollen spectra of these deposits are dominated by herbaceous pollen, mainly wormwood (*Artemisia*). Absence of microfauna and increasing percentage of herbs mark the transition to shallow-water marine, prodeltaic conditions due to sea-level fall and close location to coastline. A considerable part of the Pechora Sea was exposed and represented coastal marine, alluvial-marine, and alluvial-lacustrine plains subjected to active cryogenic processes and permafrost formation (Avenarius and Dunaev, 1999). In the northern Pechora Sea, near the Karskie Vorota Strait, a thick clayey sequence was accumulated (Fig. 4). The studied core 480 displays a 100-m-thick series of dark grey plastic-frozen clayey sediments without any visible lithological boundaries (Fig. 4). Temperature of the sediments does not show any gradient and equals –1.0 to -1.5°C. Ice content is the highest in the upper part of the core (up to 60%) and decreases downcore (down to 5-10%). Ice schlieren are usually angular and reach 3 cm in size. Ice is clean and transparent without any visible inclusions. Thin clay interlayers (up to 30 cm thick) with preserved net-like cryostructure occur throughout the whole core section. Micropaleontological analysis of the sediments revealed abundant plant debris and single microscleres of tetractinellid sponges. Radiocarbon age estimations (Table 1) evidence high sedimentation rates. The age reversal could be a result of strong dislocation due to sediment freezing. Thus, during the late Valdai epoch, the Novaya Zemlya ice sheet occupied only the northernmost Pechora Sea and did not reach the Pechora Lowland.

Later, in the course of the Holocene transgression, the shelf underwent intensive abrasion by the advancing sea. Holocene sediments are present all over the Pechora Sea. They overlie the eroded surface of the Pleistocene beds, and the contact is often marked by a layer of pebbles and gravel. The thickness of Holocene sediments varies from several meters to 50 m (Skorobogat'ko, 1992; Polyak et al., 2000). Increasing thickness is observed in neotectonic depressions. Core 104 recovered near the eastern coast of Kolguev Island (Fig. 1), reveals a 44.2-m-thick Holocene sequence represented by sands underlain by silts and clays. Similar deposits were recorded in the core 137, recovered nearly (Fig. 5), with a thick sandy-clayey unit that has been accumulated extremely rapidly. The radiocarbon age of the *Montacuta maltzani* bivalve shells is 5390±30 years (KIA-16841) for the sample from 9.4-9.5 m interval, and 5360±30 years (KIA-16840) for the sample from 1.4-1.5 m interval. Therefore, the sedimentation rates in this part of the shelf during the middle Holocene were avalanche-like.

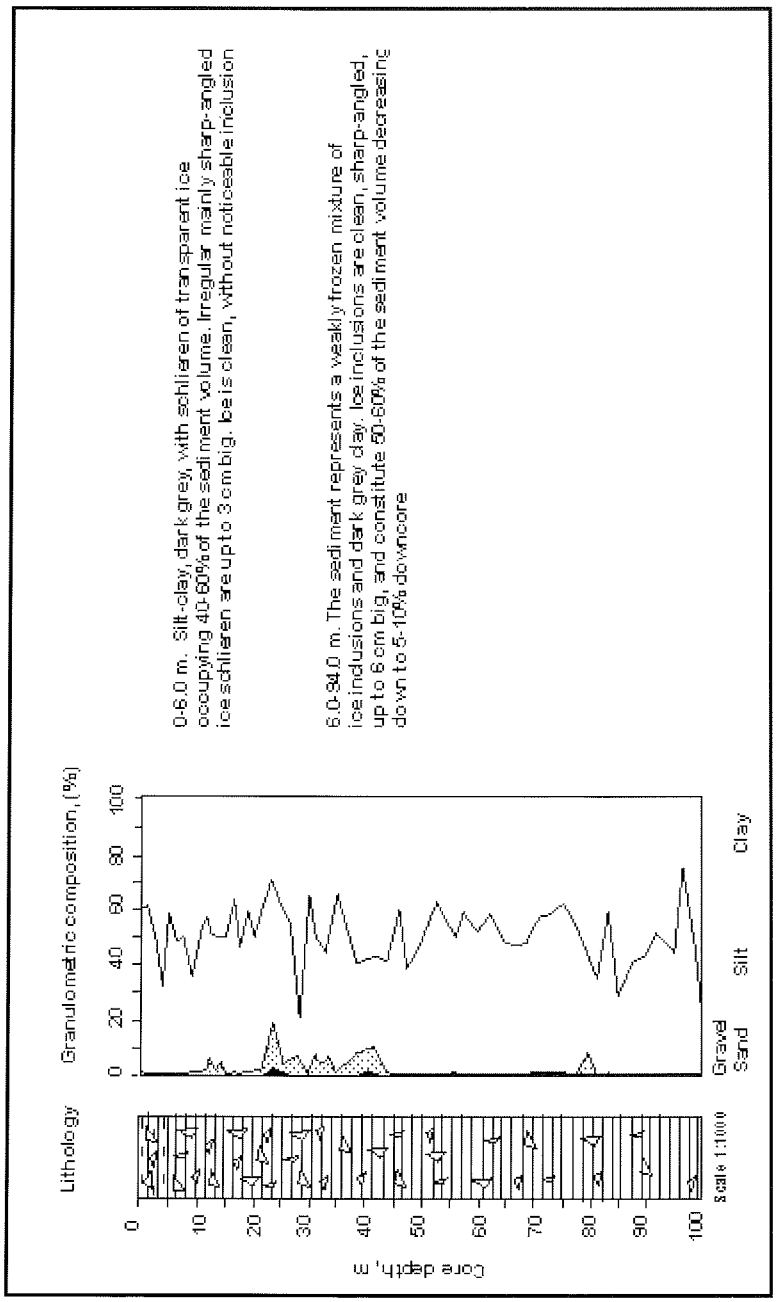

Fig.4. Lithology and granulometric composition of sediments in core 480

From the lithodynamic point of view, it is interesting to investigate the area with elevated thickness of the Holocene sediments stretching in sub-latitudinal direction from 52° and 58° E. Here, the thickness of the Holocene sediments exceeds 5 m,

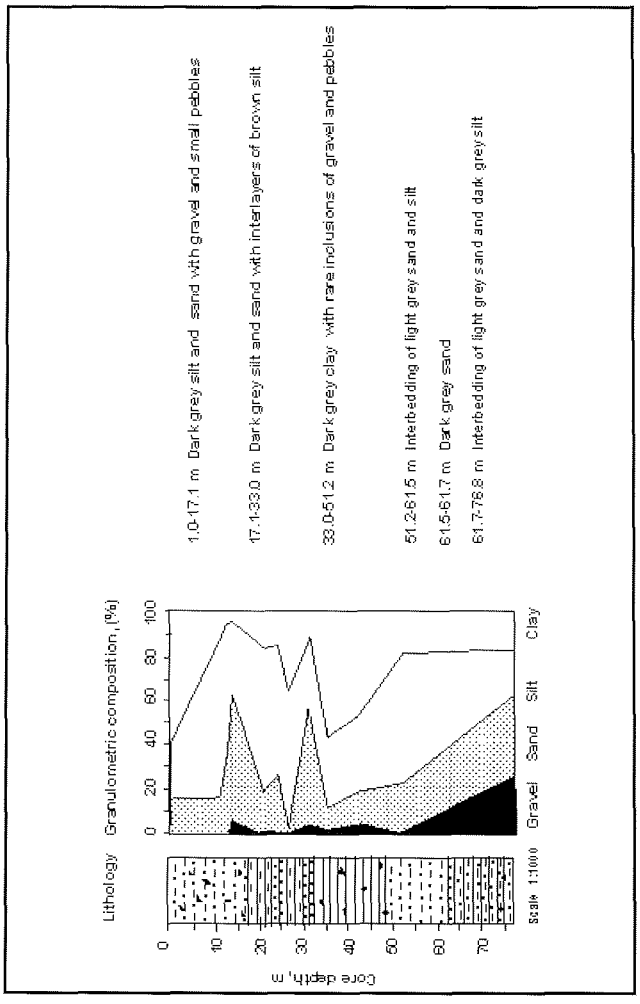

Fig. 5. Lithology and granulometric composition of sediments in core 137

and at two sites even 10 m. It decreases with water depth. It should be mentioned that this area is oriented across the strike of the known neotectonic structures. The elevated thickness of the Holocene sediments in this area, which is restricted to water depths between 35 and 55 m might be attributed to decreasing wave impact on bottom sediments and, thus, active accumulation of sediment particles. On the other hand, the prevailing currents are only capable to carry suspended load. Thus, a big accumulative sediment body is being formed here. However, it is not well defined in the bottom relief. The mechanism of its formation resembles that of a submarine bar.

Accumulation of the fine-grained fossiliferous sediments in the southern Pechora Sea started 9.5-8 ka. Complex analysis of organic remains and sediment structure revealed a river-affected shallow environment.

The Holocene sequence is subdivided into three units: transgressive sands accumulated about 10-8 ka; marine clay with microfossils dating back to approximately 8-5 ka; and marine sands enriched in molluscan shells that have been accumulated since 5 ka. Microfaunal assemblage allows distinguishing the layers corresponding to the Holocene optimum (Fig. 6). Three units of the Holocene sequence could be traced in most studied and age-constrained core sections (Samoilovich et al., 1993; Mel'nikov and Spesivtsev, 1995; Kupriyanova, 1999; Levitan et al., 2000; Polyak et al., 2000).

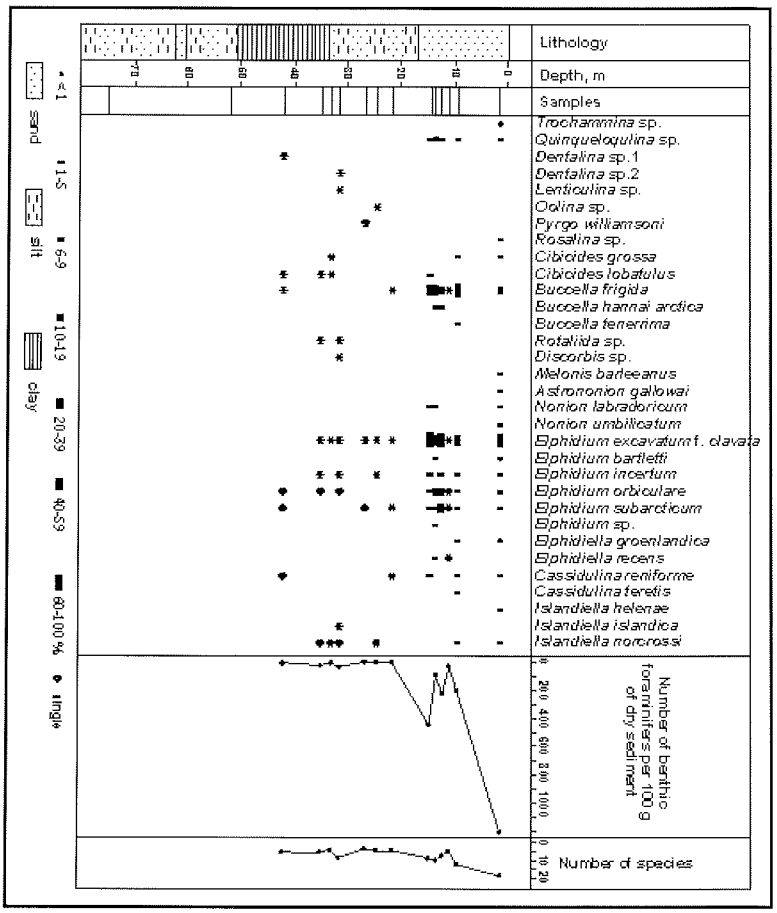

Fig. 6. Relative abundance (%) of Foraminifera species in core 137

Conclusions

In the Pechora Sea region, the Mikulino interglacial was the warmest period of the Quaternary epoch. Climatic parameters of this epoch considerably differ from the Holocene. During the Mikulino interglacial, the forest boundary shifted northward, and hydrological characteristics of water masses were different. The early Valdai cooling gave rise to thick ice sheets, which covered the Pechora Sea and reached

the Pechora Lowland. Deglaciation of the Pechora Sea region was completed in the middle Valdai, about 35-40 ka. During the Karga warming climatic conditions were temperate cool, i.e. similar to the modern ones. Sea-level fall after this short interstadial period gave rise to establishment of continental environments. The Pechora Sea floor was exposed and represented coastal marine, alluvial-marine, and alluvial-lacustrine plains subjected to active cryogenic processes and permafrost formation. In the late Valdai, the Novaya Zemlya ice sheet occupied only the northernmost Pechora Sea and did not reach the Pechora Lowland. In the course of the subsequent Holocene transgression the shelf was abraded by the advancing sea. The modern lithodynamic conditions in the Pechora Sea determine accumulation of sandy-silty deposits.

References

Avenarius, I.G., Dunaev, N.N., 1999. Some aspects of the relief development in the eastern Barents Sea and adjacent land during the late Valdai time. Geomorfologiya, 3, 57-62 (in Russian).

Danilov, I.D., 1982. The problem of correlations between glaciations and marine transgressions in the Late Cenozoic. Vodnye resursy, 3, 119-135 (in Russian).

Forman, S.L., Ingolfsson, O., Gataullin, V., Manley, W., Lokrantz, H., 1999. Late Quaternary stratigraphy of Marresale, Yamal Peninsula, Rossia: New constraints on the footprint of the Eurasian ice sheet . Geology, 27, 807-810.

Gataullin, V., Polyak, L., Epstein, O., Romanyuk, B., 1993. Glacigenic deposits of the Central Deep: a key to the Late Quaternary evolution of the eastern Barents Sea. Boreas, 22, 47-58.

Gritsenko, I.I., Krapivner, R.B., 1989. Recent deposits of the southern Barents Sea region: sediment seismostratigraphic complexes and their composition. In: Noveishie otlozheniya i paleogeografiya severnykh morei (Recent deposits and paleogeography of the northern seas), Apatity, Izd. KNTS RAS, 28-45 (in Russian).

Gudina, V.I., Evzerov, V.Ya., 1973. Stratigrafiya i foraminifery verkhnego pleistotsena Kol'skogo poluostrova (The upper Pleistocene stratigraphy and foraminifers of the Kola Peninsula), Novosibirsk, Nauka, 145 pp. (in Russian).

Kupriyanova, N.V., 1999. Biostratigraphy of upper Cenozoic sediments of the Pechora sea by ostracodes. Berichte zur Polarforschung, 306, 62-79.

Levitan, M. A., Kuptsov, V. M., Romankevich, E. A., Kondratenko, A.V., 2000. Some indications for late Quaternary Pechora River discharge: results of vibrocore studies in the southeastern Pechora Sea. J. Earth Sciences, 89, 533-540.

Mangerud, J., Svendsen, J.I., Astakhov, V.I., 1999. Age and extent of the Barents and Kara ice sheets in Nothern Russia. Boreas, 28, 46-80.

Mel'nikov, V.P., Spesivtsev, V.I., 1995. Inzhenerno-geologicheskie i geokriologicheskie usloviya shel'fa Barentseva i Karskogo morei (Engineering-geological and geocryological conditions of the Barents and Kara shelves), Novosibirsk, Nauka, 198 pp. (in Russian).

Polyak, L., Gataullin, V., Okuneva, O., Stelle, V., 2000. New constraints on the limits of the Barents-Kara ice sheet during the Last Glacial Maximum based on borehole stratigraphy from the Pechora Sea. Geology, 28, 7, 611-614.

Samoilovich, Yu.A., Kagan, L.Ya., Ivanova, L.V., 1993. Chetvertichnye otlozheniya Barentseva morya (Quaternary deposits of the Barents Sea), Apatity, Izd. KNTS RAS, 75 pp. (in Russian).

Sharapova, A.Yu., 1996. Paleoekologicheskii analiz chetvertichnykh palinokompleksov iz donnykh otlozhenii Barentseva morya (Paleoecological analysis of the Quaternary palynoassociations from the Barents Sea bottom sediments), Apatity, Izd. KNTS RAS, 44 pp. (in Russian).

Skorobogat'ko, A.V., 1992. Genetic types of marine Holocene deposits of the Eastern Kolguev region of the Barents Sea shelf. In: Problemy kainozoiskoi paleoekologii i paleogeografii morei Severnogo Ledovitogo okeana (Problems of the Cenozoic paleoecology and paleogeography of the Arctic seas), Moscow, Nauka, 53-60 (in Russian).

Tarasov, G.A., Pogodina, I.A., Khasankaev, V.B., Kukina, N.A., Mityaev, M.V., 2000. Protsessy sedimentatsii na glyatsial'nykh shel'fakh (Sedimentation processes on glacial shelves), Apatity, Izd. KNTS RAS, 473 pp. (in Russian).

EVOLUTION OF BARRIER BEACHES IN THE PECHORA SEA

S.A. Ogorodov, Ye.I. Polyakova, P.A. Kaplin, O.B. Parunin, E.E. Taldenkova
Faculty of Geography, Lomonosov Moscow State University, Moscow, Russia

Abstract
The article discusses the main results of the complex investigations of barrier beaches in the Pechora Sea including coastal dynamics and accompanying exogenous processes (eolian transportation), lithological and micropaleontological studies of the sediment sequence and radiocarbon dating. We were the first to reconstruct sedimentation conditions and evolution of these big accumulative forms in the Pechora Sea. Stationary observations on coastal dynamics and the rate of eolian sedimentation allowed estimating the rate of barrier retreat. The mechanism of formation and evolution of dune belts on these barriers is described. Composition of diatom associations and lithological data provide evidence for facial-genetic conditions of sedimentation during accumulation of barriers. Radiocarbon datings corroborate the "young" age of the modern avandune ridges of the barrier beaches.

Introduction

Coastal accumulative landforms (spits, barriers, bay-bars) are widespread in the Pechora Sea, among them big barrier beaches and barrier islands – Varandei Island, Pesyakov Island, Gulyaevskie Koshki Islands (Popov et al., 1988). These landforms are thought to have been accumulated during the period of climatic optimum at the final stage of the Holocene transgression, when both duration of dynamically active period and hydrodynamic activity were the highest (Zenkovich, 1957; Badyukova and Kaplin, 1999). Clastic material from the upper shelf involved into onshore movement was accumulated in big coastal landforms. Where the wave resultant is nearly normal to the coastline, the typical barrier beaches and barrier islands were formed. Other accumulative forms of the Holocene age, like the Russkii and Medynskii Zavorot peninsulas, are usually referred to by specialists as barriers-spits (Popov et al., 1988). Besides transversal movement of load, alongshore sediment flow also plays an important role in their formation. Further lengthening of barrier-spits results from decrease in the alongshore wave energy flux and corresponding sediment discharge.

Where the waves are high enough to overflow the coastal accumulative forms, the latter are lower than 2.5-3.0 m. Over considerable stretch of shoreline, eolian processes have built a thick dune belt (avandune) over barrier beaches and barriers-spits. Their absolute height averages 4-7 m, but some dunes are up to 10-12 m high. Some researchers take the average height of the dune belt as the height of the ancient coastal ridges formed during the maximum Holocene (Flandrian) transgression (Avenarius, 2001). Based on this assumption, the Middle Holocene sea-level highstand is estimated as 5-6 m above its present position, and the high fragments of accumulative forms are referred to as the Middle Holocene ones (Avenarius et al., 2001; Avenarius and Repkina, 2001). Therefore, according to this hypothesis, the dune belt partially represents "fragments of paleo-barriers", which could hardly be a justified assumption.

Detailed geological and geomorphological investigations of Varandei and Pesyakov islands carried out by the authors included observations on coastal dynamics and accompanying exogenous processes (eolian transportation), lithological and micropaleontological studies of the coastal sections and radiocarbon dating. This allowed us to carry out the first reconstructions of sedimentation conditions and evolution of big coastal accumulative forms in the Pechora Sea.

Results and discussion

The barriers of Varandei and Pesyakov islands have a similar structure (Fig. 1). The shoreface of these accumulative forms is covered with the dune belt (avandune) up to 4-10 m high. In the zones of divergence of wave energy, an abrasion bluff formed on the marine slope of avandune, evidences a relatively high rate of coastal retreat. At the places of sediment transit, marine slope of avandunes is relatively gentle (about 20-50°) due to less intensive wave activity and the influence of slope processes. However, during the years of extremely strong storms it could become steeper for a period of time due to abrasion. A relatively narrow beach (20-100 m) leaning against the marine slope of avandune gradually turns into the tidal flat.

At the distal parts of the barriers, the avandune becomes lower and is replaced by a series of inactive coastal ridges marking certain stages in evolution of accumulative landforms. Coastal ridges have been considerably reworked by eolian processes. Where the storm surge overwashes the barrier, the well-developed active coastal ridge is formed.

Laidas or high-water surge berms occupy the inner part of the barrier beach behind the dune belt. They are located at 2.5-3.0 m asl. Two morphological levels correspond to wind surges of low and high recurrence (Fig. 1).

In general, barrier beaches of the Pechora Sea relatively rapidly move onshore because of shoreface abrasion, wave and eolian transportation of sand from the windward to leeward slope. Field observations on the coastal dynamics from 1969 till 2000 showed that the coastal retreat rates on Pesyakov Island which is practically unaffected by human activity, equaled 0.5-2.5 m per year (Ogorodov, 2001b). As a result, the so-called "fragments of paleo-barriers" with widths of 50 to 350 m must be completely reworked during 100-400 years. Thus, they could hardly be of Middle Holocene age even if assuming that the rates of coastal retreat have increased during the past century. Radiocarbon dating of wood (MSU-1585) from the lower part of the "peat-grass pillow" of the laida exposed in the basal part of coastal bluff (Figs. 1, 2) corroborates the extremely "young" age of the overlying sand layer.

Eolian processes play an important role in formation and evolution of barrier beaches in the Pechora Sea. This role has been previously underestimated. In case wind speed exceeds 12 m/s fine-grained sand material is evacuated from beaches and tidal flats. Observations revealed that during one storm the 3-5 cm thick sand layer could be blown away from the open beach surface (Ogorodov, 2001a; Fig. 3). During the dynamically active period, deflation removes not less than 1 m^3 of sediments from one square meter of beach surface. The greatest part of eolian material removed from beaches and tidal flats is accumulated within the

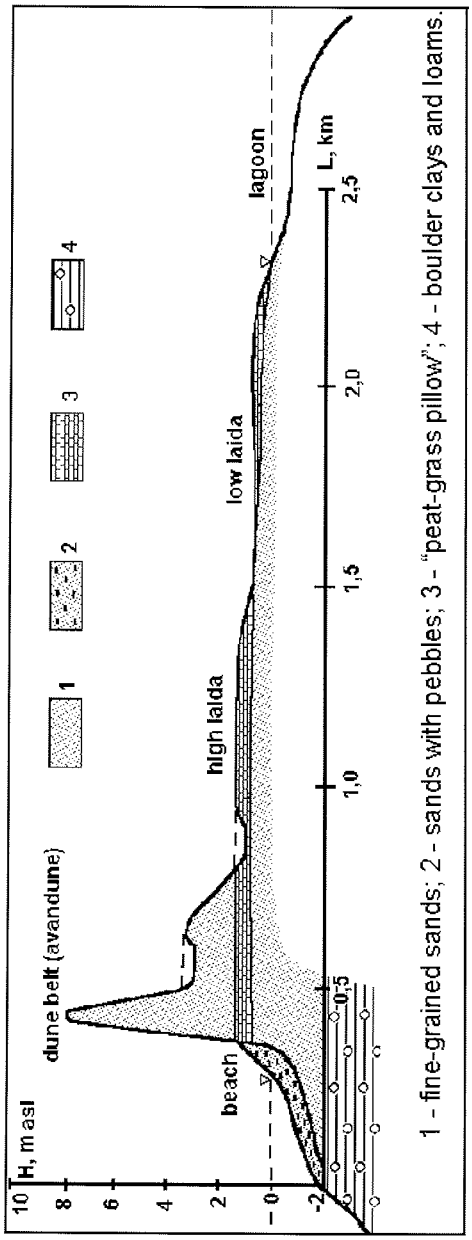

Fig. 1. Geologic-geomorphologic transect of the barrier beach, Pesyakov Island (opposite the pyramide "Middle Tower" of GUGK).

dune belt (avandune). Specific vegetation growing on avandunes protects it from deflationand favors intensive accumulation of eolian material. It should be noted

that the extent of the opposite eolian transportation – from the dune belt to the beach and tidal flats – is considerably smaller due to high anti-deflation stability of the dune belt.

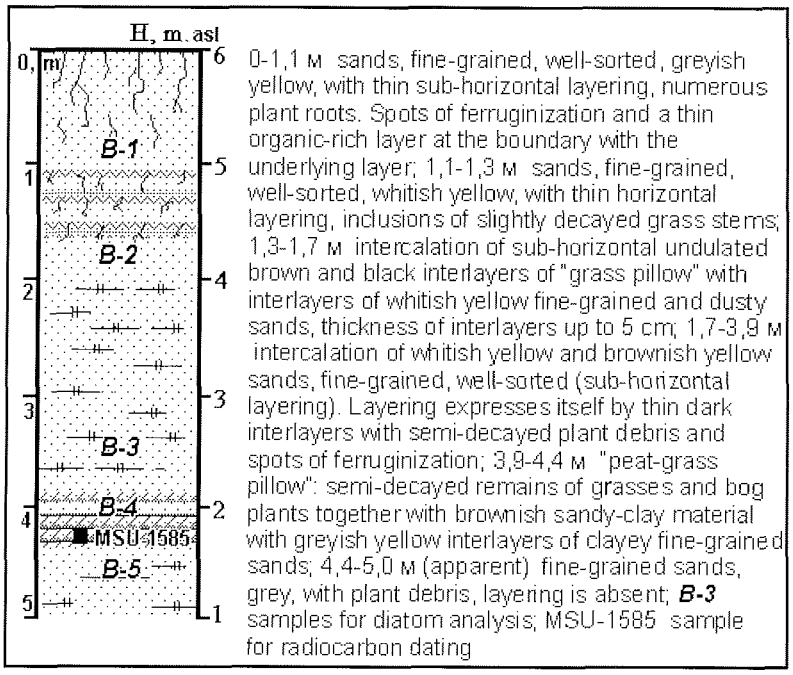

Fig. 2. Composite section of the barrier beach, Varandei Island

During fieldwork in 2000 we measured the rates of eolian sedimentation at the specially equipped monitoring stations. Averaged data on repeated measurements carried out at more than 50 reference marks showed that the sand layer, accumulated during the two summer months, ranged from 3-16 cm at a distance of 10 m from the avandune edge to 0.5-4 cm at 100 m distance. These high rates of eolian accumulation are responsible for considerable height and width of the dune belt previously mistaken for "fragments of paleo-barriers".

Actually, the sediment sequence exposed in coastal bluffs of the barriers above 1.0-2.0 m is entirely represented by subaerial complex (Fig. 2): fine-grained sands with abundant grass remains and traces of soil processes. They are devoid of any pebbles, gravel and other coarse-grained debris. On the contrary, deposits of beaches, active coastal ridges and high-water surge berms in the Pechora Sea consist of less sorted sands with numerous pebbles, gravel, rock debris and single bivalve shells. Coarse-grained material originates from numerous exposures of boulder clays and loams on the submarine coastal slope (Fig. 1). No coarse debris was found in the barrier beach sediments from the cores recovered at considerable distance from the coastal bluffs. Laida deposits with characteristic peat-grass pillow are usually exposed below the 1-2 m level. Laida deposits, accumulated in the inner parts of barriers under the influence of storm surges up to 2.5-3.5 m high, do

not provide evidence either for higher than modern sea-level position or the Middle Holocene age of the overlying sand unit.

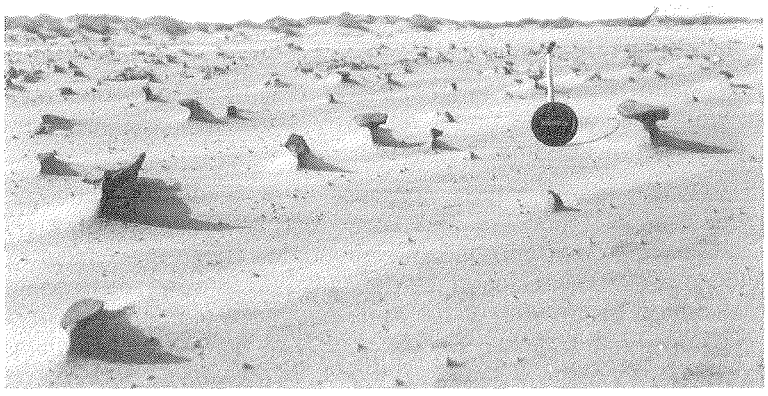

Fig. 3. Beach surface after severe storm wind, Pesyakov Island (photo N.N. Lugovoi)

Diatom analysis of the barrier beach sequence from Varandei Island (Fig. 2) revealed the gradual succession of fossil associations indicating changing sedimentation conditions.

Fine-grained grey sands with grass remains exposed at the base of coastal bluff (**sample B-5**) contain ecologically diverse diatom association including both marine and freshwater species. Taxonomically diverse marine benthic diatoms inhabiting littoral and sublittoral zones of the arctic seas (*Diploneis interrupta, D. bombus, D. smithii, D. litoralis, Paralia sulcata)* along with euryhaline species *(Achnanthes delicatula v.hauckiana, A. lemmermannii, Fragilaria pinnata)* typical of the arctic brackish waters (Polyakova, 1997) predominate in this association (~ 80%). Freshwater diatoms are rare. They are represented by species dwelling in bottom sediments and on overgrowths in the Arctic inland basins (*Navicula bacillum, Pinnularia leptostauron, P. microstauron, P. viridis)*. Composition of diatom associations allows assuming that sedimentation went on either in the inner sublittoral or littoral zone under changing marine and subaerial conditions.

The overlying peat-grass layer (**sample B-4**) is distinguished by the highest species diversity and abundance of diatoms. Like in the underlying layer, diatom association includes different species in terms of salinity preferences with predominance of typical freshwater lacustrine-bog forms primarily of *Eunotia, Pinnularia* and *Cymbella* genera. Halophobic species are also present. *Pinnularia microstauron, P. divergentissima, P. viridis, P. subcapitata, P. borealis, P. stomatophora, Eunotia fallax, E. praerupta, E. pectinalis, Cymbella hilliardii, Encyonema minutum, Neidium bisulcatum* dominate the association. However, species diversity of halophiles and brackishwater species is also high. These include *Nitzschia hybrida, Diploneis interrupta, D. bombus, D. litoralis, Amphora ovalis, Navicula cryptocephala, Cavinula pseudoscutiformis*. Their presence gives evidence for possible infiltration of seawaters or periodic flooding of the swamped coastal lowland during high tides or wind surges.

The abundance and diversity of diatoms sharply decrease in the overlying, mainly fine-grained, sands (**sample B-3**). Diatom association is represented by freshwater species typical of the bottom grounds of the northern shallow water basins *(Pinnularia viridis, P. molaris, P. streptoraphe, Neidium bisulcatum, Navicula importuna, N. semen)*. Rare freshwater planktic and rheophile species *(Stephanodiscus hantzschii, Luticola mutica)* are present, as well as fragments of marine Paleogene diatoms. Composition of diatom associations suggests the sediments were accumulated under relatively active hydrodynamic environment, probably, in temporary streams.

Upward the section (**sample B-2**), composition of diatom associations changes. Planktic and rheophile species disappear, but aerophile diatoms (*Hantzschia amphioxys, Navicula contenta)* become abundant. These are typical for edaphic (soil) coenoses of diatoms. Subsurface deposits (**sample B-1**) represented by fine-grained well-sorted sands with grass roots contain a diatom association entirely dominated by subaerial bog-soil species, mainly of *Eunotia* and *Pinnularia* genera *(P. brevicostata, P. microstauron, Eunotia parallela, E. lunaris, Hantzschia amphioxys* and others).

Thus, composition of diatom associations indicates changes in sedimentation environment during accumulation of the barrier beach – from nearshore marine, littoral, probably marshes, to swampy laida and, finally, subaerial avandune. Temporary streams played an important role in formation of the lower part of subaerial unit lying above 2.0 m asl. These streams redistributed abundant eolian material and supplied plant debris into shallow lakes and puddles during flood. The plant debris was accumulated in the form of thin interlayers. At present, similar conditions exist in the inner part of the dune belt between the avandune ridge and laida (Fig. 1). The uppermost part of the subaerial unit was accumulated due to active eolian-soil sedimentation typical for the topmost part of the dune belt on the barrier beach.

Conclusions

As a result of the complex investigations we came to the following conclusions. Barriers of the Pechora Sea were formed in the coastal zone by accumulation of coarse debris derived from the submarine coastal slope. In the course of coastal evolution, the barriers were moving onshore overlapping coastal laidas formed behind them. Eolian processes played an important role in shaping the shores. Eolian transportation of sand from beaches resulted in accumulation of big dune ridges. The latter rework and overlap barriers. That is why absolute height of the barriers in the Pechora Sea could not serve as an indicator of the sea-level position in the Holocene. Diatom associations evidence upward changes in sedimentation environments during formation of coastal accumulative forms in the Pechora Sea, from nearshore marine, littoral, probably marshes, to swampy laida and, finally, subaerial avandune. According to radiocarbon datings, the modern avandune in the studied region began to form not earlier than 350-400 years ago.

Acknowledgements: This study was supported by INTAS project 99-1489 and by the Russian Foundation for Basic Research (project 02-05-65105).

References

Avenarius, I.G., 2001. Coastlines of the second half of the Holocene as a model for the coastal zone evolution under the global sea-level rise. In: Chelovechestvo i beregovaya zona Mirovogo okeana v XXI veke (Mankind and the coastal zone in the 21st century). Moscow, GEOS, 266-274 (in Russian).

Avenarius, I.G., Repkina, T.Yu., 2001. Paleogeography of the Varandei area in the Late Valdai – Holocene (Barents Sea). In: Geologiya morei i okeanov (Geology of seas and oceans). Abstracts of the XIV International School in Marine Geology, Vol. 2, Moscow, 4-5 (in Russian).

Avenarius, I.G., Ermolov, A.A., Myslivets, V.I., Repkina, T.Yu., 2001. Relief and some aspects of the Late Valdai – Holocene paleogeography of the Varandei Island. In: Sedimentologicheskie protsessy i evolyutsiya morskikh ekosistem v usloviyakh morskogo periglyatsiala (Sedimentation processes and evolution of marine ecosystems under marine periglacial conditions). Vol. 1, Apatity, KNTs RAN, 135-147 (in Russian).

Badyukova, E.N., Kaplin, P.A., 1999. Coastal barriers. Geomorfologiya, 3, 3-13 (in Russian).

Ogorodov, S.A., 2001a. Morphology and dynamics of the Pechora Sea coasts. Proceedings of the Institute of Oceanology BAN, Varna, Vol. 3, 77-86 (in Russian).

Ogorodov, S.A., 2001b. About formation and evolution of coastal barriers in the Pechora Sea. In: Geologiya morei i okeanov (Geology of seas and oceans). Abstracts of the XIV International School in Marine Geology, Vol. 2, Moscow, 202-203 (in Russian).

Polyakova, Ye.I., 1997. Arkticheskie morya Evrazii v pozdnem kainozoe (Arctic Eurasian seas in the Late Cenozoic). Moscow, Nauchnyi Mir, 145 pp. (in Russian).

Popov, B.A., Sovershaev, V.A., Novikov, V.N., Biryukov, V.Yu., Kamalov, A.M., Fedorova, E.V., 1988. Coastal area of the Pechora-Kara Sea region. In: Issledovanie ustoichivosti geosystem Severa (Investigations of the geosystems stability in the North), Moscow, Izd. MGU, 176-201 (in Russian).

Zenkovich, V.P., 1957. About the origin of barrier beaches and lagoon coasts. Proceedings of the Institute of Oceanology AN SSSR, Vol. 21, 5-32 (in Russian).

TECHNOGENIC IMPACT ON THE COASTAL DYNAMICS IN THE VARANDEI REGION, PECHORA SEA

S.A. Ogorodov

Faculty of Geography, Lomonosov Moscow State University, Moscow, Russia

Abstract

The geoecological situation in regions of intensive industrial exploitation on the Pechora Sea coast, particularly Varandei area, is nearly critical. Technogenic impact causes intensification of eolian and slope processes, thermoerosion and thermokarst. Stability of coasts decreases, and the rate of their retreat increases. Industrial exploitation results not only in destruction of natural environments, but also in considerable material losses. Several housing estates and industrial constructions have already been destroyed in the course of abrasion cliff retreat. The damage will increase every year following the cliff retreat towards the center of Varandei settlement. Oil terminal, airport and other industrial objects are endangered.

Introduction

Under natural conditions, the Pechora Sea coasts are relatively stable, but are rapidly destroyed under technogenic impact (Geoekologiya..., 2001). The case in point is the Varandei industrial where expeditious measures on protection of industrial and residental buildings are necessary. Technogenic impact on the Varandei area activates abrasion because of improper exploitation, which does not take into account peculiarities of coastal relief and dynamics (Novikov and Fedorova, 1989; Ogorodov, 2001a, b; Sovershaev et al., 2001). Coastal erosion of the Varandei area poses a threat to settlement, oil terminal and airport. Therefore, it is necessary to thoroughly analyze coastal morpholithodynamic schemes before the natural environments are disturbed.

Results and discussion

Two main morphogenetic complexes (Fig. 1) are distinguished within the studied area. The latter stretches for 90 km from the western extremity of Pesyakov Island to the eastern extremity of the Medynskii Zavorot Peninsula.

The first complex represents a young marine accumulative terrace with the average height of 3-5 m formed during the Holocene transgression. The terrace occupies the Pesyakov and Varandei islands (that are, in fact, barrier beaches), Peschanka River mouth and Medynskii Zavorot Peninsula. Its width reaches 2-6 km. The terrace is formed by fine sand unit underlain by a peat-grass pillow. Cryogenic structure of the terrace sediments is characterized by small ice volume, 5-10% (Novikov and Fedorova, 1989). The frontal, seaward, part of the terrace is covered by an avandune (dune belt of the barrier beach) reaching 5-12 m asl (Fig. 2). At the distal parts of the barrier beaches, the avandune turns into a series of ancient and young barrier ridges corresponding to different stages in evolution of the barrier beaches and barriers-spits.

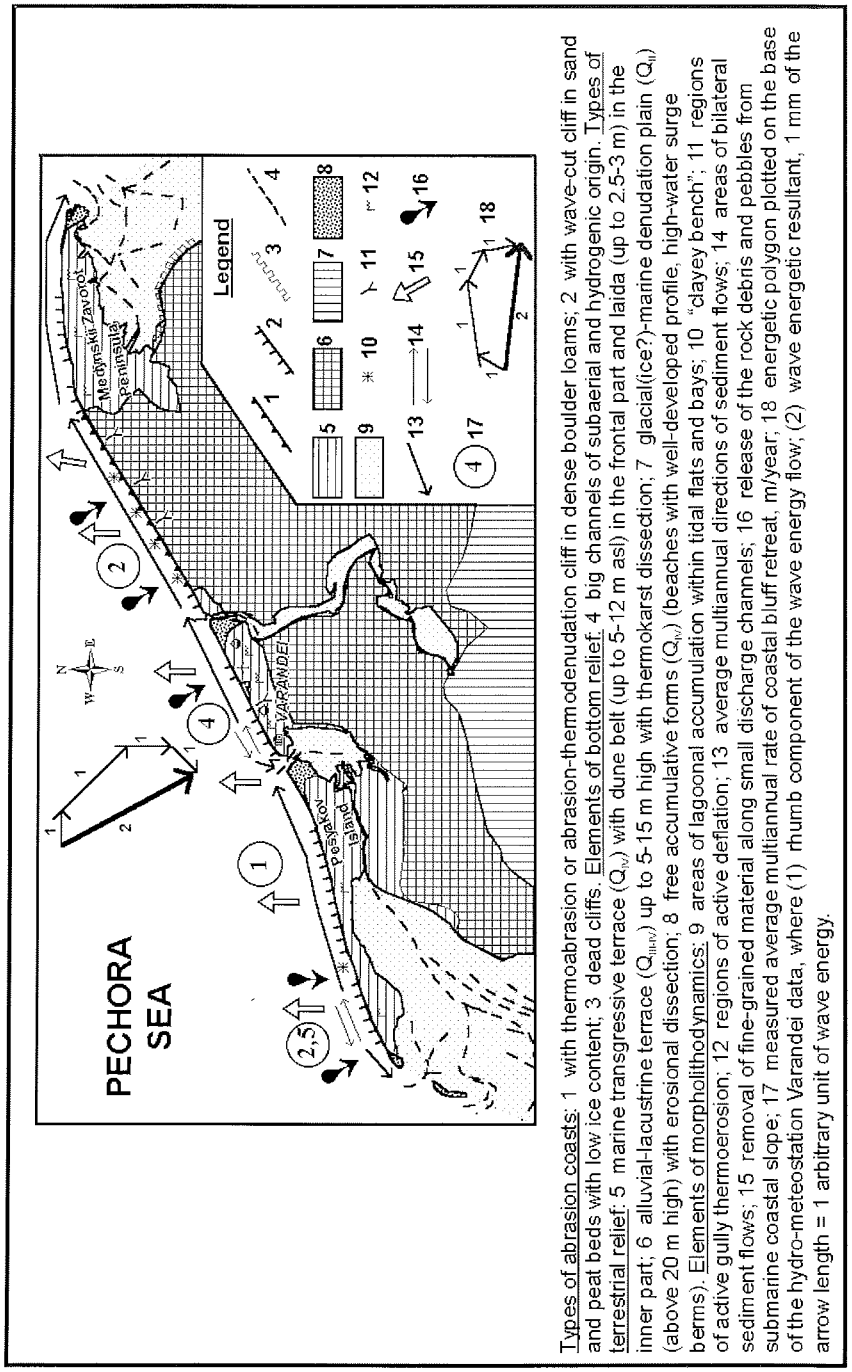

Fig. 1. Morpholithodynamics of the Pechora Sea coasts near Varandei settlement

Fig. 2. Dune belt on the barrier beach separating laida from the sea, Pesyakov Island (photo of N.N. Lugovoi).

The barrier ridges have undergone considerable reworking by eolian processes. The inner parts of the terrace behind the dune belt represent a laida up to 2.5-3 m high with two levels corresponding to the surges of low and high recurrence.

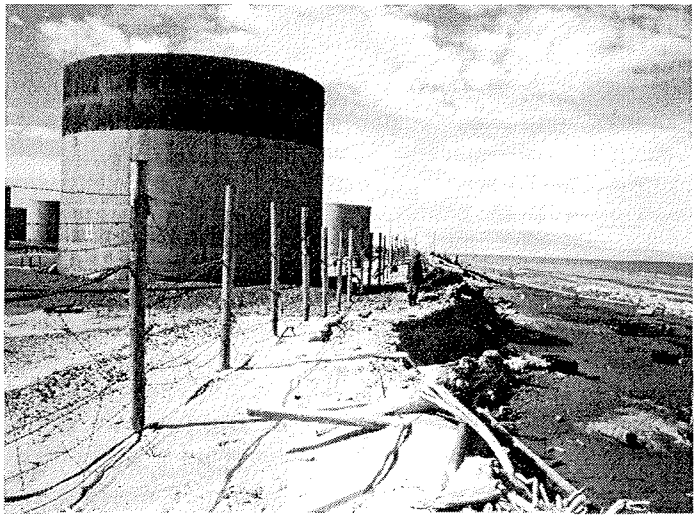

Fig. 3. Wave-cut cliff near the Varandei oil terminal.

At present, under natural conditions, the greatest part of the Holocene terrace is being eroded at a rate of 1.0-2.5 m per year (Ogorodov, 2001 a, b; Fig. 1). The abrasion coast (Fig. 3) has an erosion scarp cut in eolian-marine fine sands. Its height ranges from 1 to 6 m. Close to the zones of wave energy divergence, where the rate of abrasion is higher, the coastal bluff is well pronounced and remains nearly perpendicular during the greatest part of the year. In the regions of sediment transit, due to denudation, deflation and slope processes the coastal slope is relatively gentle, about 20-50°. However, during the years with extraordinarily strong fall storms the slope is eroded and becomes steeper for a short period of time. Thermoabrasion does, in fact, not erode slopes of the Holocene terrace. The

latter is destroyed due to relatively high average annual ground temperatures, small ice volume and considerable thickness of the layer of seasonal melting. Coastal erosion is determined by a combination of different factors including deficit of coarse-grained beach-forming material (discrepancy between the grain size and hydrodynamic conditions), not well developed profile of the submarine coastal slope, and high gradient of the avandune slopes. Sediment material released due to erosion is accumulated at the distal parts of the Pesyakov and Varandei islands and Medynskii Zavorot Peninsula, where the wave energy flow decreases. Here, the young beach ridges and high-water surge berms are formed (Fig. 1).

The second morphogenetic complex is represented by the 5-15 m high gently rolling lacustrine-alluvial (?) plain with numerous lakes (Fig. 1) usually referred to as the First terrace of the Late Pleistocene-Holocene age (Novikov and Fedorova, 1989). The origin of this terrace has long been debated (Danilov, 1978), but there is still no concrete evidence for its genesis. Also, the age of the terrace is still uncertain. Though this terrace occupies the greatest part of the territory, it reaches the coastline only between the Peschanka River and the base of the Medynskii Zavorot Peninsula. The surface of the terrace is covered with frost polygons and bogs. The base of the terrace is composed of dense ice(glacial?)-marine loams and clays with inclusions (3-5%) of strongly weathered boulders, blocks, rock debris and gravel (3/4 of the section). The layer of sands and peat represents the upper 1/4 part of the terrace section. The terrace sediments include ice wedges and massive ice beds.

Where the First terrace reaches the sea, the thermoabrasion coast (Fig. 4) has a cliff worked out in frozen dense boulder loams. The height of abrasion cliff ranges from 3 to 10 m. Unlike the Holocene terrace, here thermoabrasion plays the main role in coastal erosion. At some places, the typical thermoabrasion niches are present. Thermodenudation processes (thermoerosion, solifluction, slumping, suffosion) considerably affect the coastal dynamics supplying sediment material to the coast basement (Fig. 4). The abrasion cliff is surrounded by a narrow (10-20 m) pebbly-sandy beach that gradually turns into abraded tidal flat (Fig. 5) – the so-called "clayey bench". Due to specific granulometric composition of the sediments, the amount of beach-forming material produced by thermoabrasion is insufficient. Presence of landslides and mud-flows, as well as small beach width give evidence for relatively low resistance of the coasts. The average rate of thermoabrasion coast retreat was estimated at 1.8-2.0 m per year (Novikov and Fedorova, 1989).

About 300×10^3 m^3 of fine sand material are supplied to the coastal zone every year due to erosion of the Holocene terrace (Ogorodov, 2001a). Also, the thermoabrasion coast supplies 130×10^3 of sand, 5×10^3 of coarse debris, 25×10^3 of peat and 120×10^3 of clay to the coastal zone. Part of the sand and all clay material are accumulated below the 10 m isobath. All coarse debris and part of the sand material are incorporated into alongshore drift and form beaches and beach ridges at the distal ends of barriers and spits. In course of eolian transportation fine-grained fraction is partly evacuated from the beaches towards the barriers and settles within the dune belt.

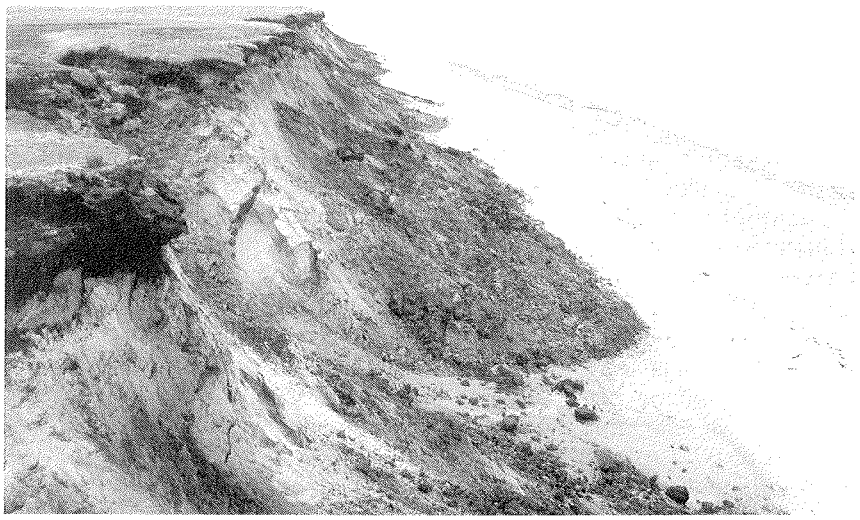

Fig. 4. Thermoabrasion coast 30 km to the east-northeast of Varandei settlement (photo of N.N. Lugovoi).

Fig. 5. Abrasion surface of tidal flat ("clayey bench"), 30 km to the east from Varandei settlement.

Coastal retreat is accompanied by erosion of submarine coastal slopes and tidal flat due to abrasion (including thermoabrasion) (Fig. 5). This results in increasing water depths. As mentioned by Mel'nikov and Spesivtsev (1995), presence of permafrost and, hence, thermoabrasion of submarine coastal slope are typical only

for thermoabrasion coasts. As a rule, permafrost is absent on the submarine coastal slope of barriers and spits. In the Varandei coastal region, the submarine coastal slope is mainly composed by the same clayey sediments (with inclusions of coarse grained material – 3-5%) that are exposed at the thermoabrasion part of the coast. The thin layer of sands in places overlying boulder loams is unable to protect the submarine coastal slope from abrasion during strong storms. Practically no beach-forming material is produced due to abrasion of the submarine coastal slope. Discharge and rip currents evacuate clay particles, that move downslope in the form of suspension flows. The currents are restricted to numerous troughs that cut the lower part of the submarine coastal slope at the depths of 5-10 m. Coarse-grained material washed out from loams is mainly accumulated *in situ* forming a pebbly pavement at bottom swells. Where the shifting force of waves is sufficiently great, some fragments reach the coastline and take part in beach formation. For instance, pebbly beaches at the western extremity of Pesyakov Island and eastern extremity of Varandei Island were formed through this mechanism (Fig. 6). Coastal bluffs of these beaches are formed of fine sands solely. Using the method of Shuiskii (1986), we estimated the average layer of effective abrasion of submarine coastal slope at 0.02 m/year. It slightly increases at tidal flats. As a result, the amount of sediment material supplied to the coastal zone is nearly equal to the amount of sediments released in the course of coastal erosion. However, as shown above, the amount of beach-forming material in this zone is extremely small.

Fig. 6. Pebbly beach on the eastern end of Varandei Island

Active exploitation of the Varandei industrial area started in the seventies. Varandei Island was subjected to the strongest technogenic impact. Here, the main industrial base was formed, and Novyi Varandei settlement for 3,500 inhabitants was built. The well-drained dune belt of the Holocene terrace (first morphogenetic complex) composed of sand beds with low ice content was chosen as a place for the settlement, oil terminal and storehouses because it seemed to be more stable from the engineering-geological point of view than the surrounding swampy tundra lowland (second morphogenetic complex).

Construction of residential and industrial buildings was held practically at the edge of the abrasion cliff and demanded repeated withdrawals of sand and sand-pebble sediments from the avandune and beach. This is absolutely unallowable for the zones of wave energy divergence (Fig. 1) (Popov et al., 1988), especially in the zones that have been eroded before.

Within the zone of industrial exploitation, the coastal bluff and the coastal zone experienced considerable mechanical deformations of the landforms because of

transport ramps, mechanical leveling of coastal declivities and other technogenic disturbances (Novikov and Fedorova, 1989; Sovershaev et al., 2001). Systemless use of transport and construction technique including caterpillars caused degradation of soil and plant covers of the whole dune belt of Varandei Island. Under conditions of deep seasonal melting, the dune belt formed of fine sands is subjected to deflation, thermoerosion and thermokarst. The extent and rate of these processes are so great that in places the surface of the island became 1-3 m lower than before the period of exploitation (Fig. 7). Deflation hollows and thermokarst depressions became widespread. Numerous deflation-thermoerosional gullies were formed in the abrasion cliff. As a result, the cliff becomes lower, its homogeneity is disturbed, the amount of sediments supplied to the coastal zone decreases and, finally, the coasts become less stable, and the rate of their retreat grows.

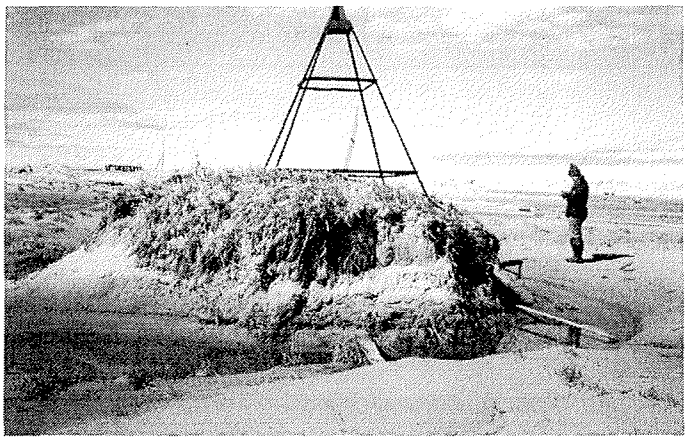

Fig. 7. During the period of exploitation, the surface of barrier beach on Varandei Island became 1-3 m lower due to deflation, thermoerosion and thermokarst.

During the 2000 field season we measured the rates of deflation and thermoerosion on the specially equipped stations (Ogorodov, 2001b). The averaged data of repeated measurements at more than 50 reference squares have shown that the thickness of the sand layer blown away by wind was 10 to 14 cm at technogenically-deformed territories. At the same time, eolian accumulation took place in the areas that are not affected by human activity. At the "erosional" station, we observed formation of a big gully (up to 4 m deep) in the coastal bluff. Up to 400 m^3 of sand were removed from the gully itself and from its catchment area during the two weeks of snow melt in June.

Coast protection in the area close to Novyi Varandei settlement (the region of wave energy flow divergence and, correspondingly, formation of sediment flows) caused decrease in sediment supply to the adjacent areas and, hence, their erosion.

After the earth-dam and bridge across the Promoi River branch were constructed in the eastern part of Varandei Island, the height of storm surges increased. The latter is an important factor of coastal dynamics. Previously, during high surges corresponding in time with tides water was partly flowing into the Promoi branch and then to the Varandeiskii Shar channel, thus lowering the surge height and

decreasing its influence upon the coast.

Under existing conditions of intensive technogenic impact, the abrasion rate considerably increased in the middle-late seventies. In some years it was up to 7-10 m/year. The rate of coastal retreat slightly decreased, down to 1.5-2 m/year, after the coastal protecting construction was built near Novyi Varandei settlement. However, it remained high in the adjacent areas. Recent measurements during 1987-2000 (Fig. 8) have shown that the rate of coastal retreat in the region around the settlement increased and reached 3-4 m/year, which is twice as high as in the regions that are not affected by human activity.

Conclusions

The geoecological situation on Varandei Island is nearly critical. Industrial exploitation of the territory resulted not only in destruction of the natural coastal system, but also in considerable material losses.

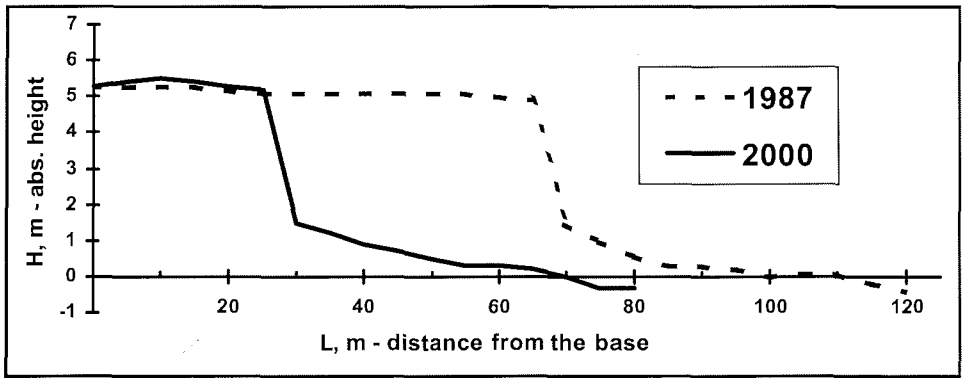

Fig. 8. Dynamics of the coast near Varandei settlement

Due to rapid retreat of the abrasion cliff, several industrial and residential buildings were destroyed by October 2000. With further retreat of the coastal cliff towards the center of the settlement, the losses will increase from year to year. The oil terminal is endangered because the distance between the coastal bluff edge and the nearest oil storage tank is less than 6 m (Fig. 3).

Active industrial exploitation of the Pechora region demands a well-developed strategy of territory development and finding of proper areas for new constructions. The negative example of the Varandei region requires a well-developed ecologically grounded approach to further exploitation of coastal regions.

After many years of investigations in the Pechora Sea region, the Research Laboratory of the Geoecology of the North, MSU, has worked out a unique methodology of morpholithodynamic research and has created a database on the coastal morpholithodynamics of this area, that will be a basis for solving both fundamental and applied problems arising in the course of coastal reclamation.

References

Danilov, I.D., 1978. Pleistotsen morskikh subarkticheskikh ravnin (The Pleistocene of the subarctic marine lowlands. Moscow, Izd. MGU, 198 pp. (in Russian).

Geoekologiya Severa (Geoecology of the North), 2001. Solomatin, V.I. (ed.), Moscow, Izd. MGU, 270 pp. (in Russian).

Mel'nikov, V.P., Spesivtsev, V.I., 1995. Inzhenerno-geologicheskie i geokriologicheskie usloviya shel'fa Barentseva i Karskogo morei (Engineering-geological and geocryological conditions of the Barents and Kara shelves). Novosibirsk, Nauka, 197 pp. (in Russian).

Novikov, V.N., Fedorova, E.V., 1989. Destruction of coasts in the southeastern Barents Sea. Vestnik MGU, ser. 5, geografiya, 1, 64-68 (in Russian).

Ogorodov, S.A., 2001a. Morphology and dynamics of the Pechora Sea coasts. Proceedings of the Institute of Oceanology BAN, Varna, vol. 3, 77-86 (in Russian).

Ogorodov, S.A., 2001b. Functioning of the Pechora Sea coastal systems under technogenic impact. In: Sedimentologicheskie protsessy i evolyutsiya morskikh ekosistem v usloviyakh morskogo periglyatsiala (Sedimentological processes and evolution of marine ecosystems under marine periglacial conditions). Apatity, Izd. KNTs RAN, 82-90 (in Russian).

Popov, B.A., Sovershaev, V.A., Novikov, V.N., Biryukov, V.Yu., Kamalov, A.M., Fedorova, E.V., 1988. Coastal area of the Pechora-Kara Sea region. In: Issledovanie ustoichivosti geosystem Severa (Investigations of the geosystems stability in the North), Moscow, Izd. MGU, 176-201 (in Russian).

Shuiskii, Yu.D., 1986. Problemy issledovaniya balansa nanosov v beregovoi zone morei (Problems in investigations of sediment balance in the coastal zoneof the seas). Leningrad, Gidrometeoizdat, 239 pp. (in Russian).

Sovershaev, V.A., Ogorodov, S.A., Kamalov, A.M., 2001. Technogenic factor in development of coasts in the Varandei industrial area. In: Solomatin, V.I. (ed.) Problemy obshei I prikladnoi geoekologii Severa (Problems of the general and applied geoecology of the North). Moscow, Izd. MGU, 126-134 (in Russian).

GEOECOLOGICAL SITUATION IN THE "PRIRAZLOMNOE" OILFIELD AREA (PECHORA SEA)

N.N. Dunaev, S.L. Nikiforov, Yu.A. Pavlidis, N.V. Politova
Shirshov Institute of Oceanology RAS, Moscow, Russia

Abstract

Exploitation of shelf oilfields requires a fair estimation of its impact upon marine ecosystems.Using the "Prirazlomnoe" oilfield as example the existing geoecological situation is analyzed as a background level prior to intensive anthropogenic influence. It is concluded that exploitation of the "Prirazlomnoe" oilfield itself will not have a major negative effect on the environment.

Introduction

One of the primary tasks in exploiting natural resources on the Russian Arctic shelf is development of the "Prirazlomnoe" oilfield located in the shallow Pechora Sea northwest of Varandei Island. Exploitation demands minimization of the negative ecological consequences of human activities. Nature protection has to be based on the knowledge of the modern geoecological situation in the area in order to forecast possible environmental changes.

During the IO RAS expedition in 1998, a study area was chosen close to the "Prirazlomnoe" oilfield where complex investigations were carried out. They included detailed analysis of bottom topography in combination with gravity core sediment sampling down to 175 cm (Fig. 1). Sediment core evidence and geomorphological data together with hydrological and climatic information about the area are used to characterize the modern geoecological situation in the study region and to forecast its future changes under technogenic impact.

By the term "geoecology" we mean the branch of science studying the properties and functions of lithospheric component of ecosystems in its interaction with living organisms. It is worth noting that any territory as an element of geological environment (including lithosphere and related landforms, fluids, geophysical fields, endogenous and exogenous processes) provides a habitat for benthic life concentrated in sub-surface horizons. Studying the geological environment in terms of stability, dynamics, intensity and direction of geological processes gives an idea how ecological properties of lithospheric components influence the functioning of ecosystems and their self-regulating ability under changes caused by anthropogenic impact.

In the seas, the most evident negative biotic changes occur at the "water – air" and "water – bottom" interfaces. That is why geoecological research is primarily aimed at the study of geological-geomorphological factors indicative of ecological stress upon the investigated area. "Ecological" characteristic of the lithosphere could be accessed through such parameters as relief, sediments, tectonic structure etc., both separately and in any combination. It is often convenient to analyze neotectonic structure as the most stable and long-living component of ecosystems giving them, similarly to a skeleton, a fixed position and a certain spatial autonomy. Neotectonic structural forms predetermine the basic features of bottom relief,

transit conditions of particulate matter fluxes, degree of porosity, relief of strain, and also activity of exogenous processes. Thus, they predetermine the location of the zones of pollutant removal, transit, or accumulation.

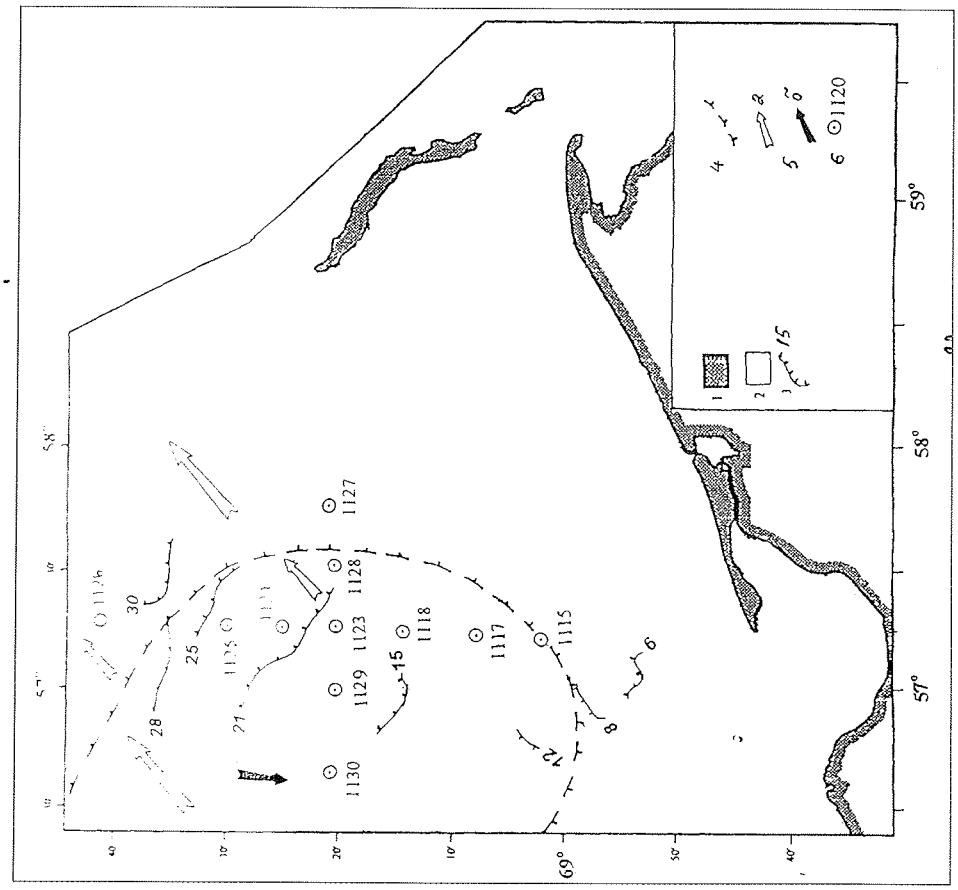

Fig. 1. Location of coretop sampling sites in the Prirazlomnoe area.
Key: 1 land boundary; 2 submarine abrasion-accumulative plain (Q_4) with fragments of subaerial erosion-denudation relief (Q_3^4); 3 submerged coastlines (Q4) and their modern depth; 4 boundary of recent uplift; 5 lateral transportation of bottom sediment material: a general, b local; 6 geological sampling sites and their numbers.

Study area

The study area is located in the subarctic climatic zone in the region of the northeastern Kolguev-Pechora current formed over the Northern Kanin bank in the Barents Sea as a branch of the Nordcap coastal current of the Gulf Stream. Its waters have relatively low salinity and constantly keep negative temperature near the bottom as a result of cooling in the Pechora Sea. Surface current velocity

averages 40 cm/s, but may reach one knot. Bottom current velocity changes from place to place and is about 50 cm/s in the vicinity of "Prirazlomnoe". The velocity of northwestern and submeridional tidal currents is about 40-50 cm/s growing up to 150-200 cm/s in straits. Tidal currents are produced by transformation of the southeastern front of the Atlantic tidal waves. The height of the syzygy tide reaches 1 m, and that of the neap tide 0.6 m. Storm activity in the region is reduced in comparison with the western Barents Sea, but, nevertheless, the height of wind waves may reach 8 m (Danilov and Efremkin, 1998). Ice formation starts in the last decade of October, or at the end of November, and finishes in March or April - July. Therefore, the duration of the ice-covered season ranges from 130 to 270 days. Northerly winds are dominant.

Particulate matter supply to the sea is low due to the climatic conditions which cause physical weathering to prevail on the adjacent hinterland, to long winters, plain relief, and the weak river system.

From the geomorphological point of view the study area is located within 14-32 m water depth range on the northeastern slope of the Pakhtusov shallow belonging to the gently northward sloping (0.0003-0.0008) abrasion-accumulative shelf plain. The slope has irregular inclinations (0.00035-0.001) and several 4-7 km-wide flats (Fig. 2), obviously produced by irregular sea-level rise during the Holocene transgression. During periods of slowdowns flats were developed, and subsequent increases in the rate of sea-level rise formed more abrupt or gentler slopes. A similar relief is usually formed at the stage of passive flooding of subsiding accumulative coastal lowlands. If assuming flats and adjacent slopes to be formed simultaneously, back junctions of flats could be considered as ancient coastlines, which are located at water depths of 21, 25 and 28 m. Relief formation dates back to the Early Holocene. The modern geomorphological stage of the area's development is close to a dynamic balance. Basic geomorphological processes are related to the specificity of subarctic submarine exogenesis and general subsidence of the territory.

Geotectonically the study area is located within the limits of the positive structural form stretching in a northwestern direction on the East Pechora step on the Epibaikalian Pechora plate. In publications it is identified either with the Sorokin arc stretching landward, or only with a submarine rise called Kolvinskoe or Gulyaevskoe. It is possible, that the rise is a more active and, accordingly, better-expressed part of the Sorokin arc. The prevailing neotectonic process in the region is downwarping. Background amplitudes of descending movements for the recent tectonic stage (P_3-Q) range from -100 to -200 m with lower values locally, from zero to -100 m (Musatov, 1990). Therefore, this positive structural form represents a relative height on the seafloor. Taking into account proximity to the coast, which subsides at a rate of up to 3 mm/year (Nikonov, 1978), it is possible to assume the positive structural form to subside at a rate slightly smaller than subsidence rate of surrounding seafloor. This allows it to manifest itself in the bottom topography as a local shallow with specific morphosculptural features. The modern bottom topography is a result of the plate-like character of the Pechora Region tectonic structure, Late Quaternary sea-level history, and modern lithodynamic processes.

From the seismic point of view the area is quiet. Its potential seismotectonic danger is estimated as lower than the magnitude value 3.9, the lowest one among closely located seismic stations (Assinovskaya, 1994).

The uppermost sediment unit in the region is represented by a thin layer of postglacial transgressive deposits underlain by the Pliocene-Quaternary transgressive-regressive basal complex consisting of marine, glacial-marine and periglacial deposits. Taking into account the Late Quaternary paleogeography of the region (Avenarius and Dunaev, 1999) and shallowness of the study area, it might be assumed that, depending on local lithodynamic conditions, there should be either a thin layer of marine Holocene deposits or a layer of periglacial Late Valdai deposits slightly reworked by waves.

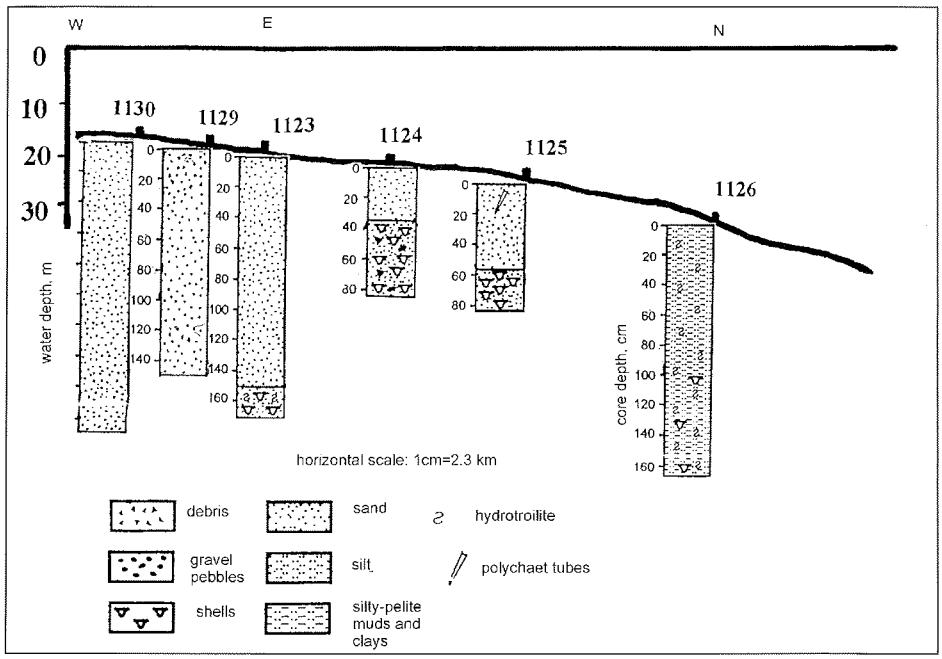

Fig. 2. Geological characteristic of bottom sediments in the Prirazlomnoe area.

Gravity coring has shown that, besides the deepest station 1126, bottom sediments are represented by terrigenous, mainly fine-grained, sands, grayish green or olive, with the observed thickness of up to 170 cm (Fig. 2). The maximum thickness might exceed 2 m as evidenced by the deep core 384 recovered slightly northward from the "Prirazlomnoe" oilfield area.

The modern wave activity at such depths does not exceed the first ten centimeters, and there are no possible sources of sand material. So, we can conclude that the bottom sand layer was formed during the period of the Holocene transgression as a result of re-washing of the basal sediments represented by intercalating loams and sands. Material input from the mainland was impossible in this area because of its remoteness and specificity of bottom relief and hydrological conditions. Therefore, it is possible to assume, that the modern lithodynamic conditions of the study area are characterized by either removal of pre-Holocene sands or their transit from the above-mentioned positive structural form with possibly partial or

permanent accumulation. Clearly expressed gravitational (from suspended matter) accumulation takes place only in the deepest part in the north of the study area (st. 1126).

Presence of fine-grained deposits evidences quiet lithodynamic conditions. Occurrence of coarse silts and fine-grained sands characterizes unstable sediment balance. Coarse material and, in particular, the absence of or locally low thickness of modern deposits (the first decimeters) point to active lithodynamic conditions.

Evaluation of the geoecological situation

The given review of natural background conditions in the study area allows us to analyze its geoecological state. As mentioned above, complex methods were applied. Based on the data on recent tectonics, regional geomorphology, and climatic and hydrological conditions we assume that under the environmental conditions of the study area it is unlikely that hydrocarbon pollutants resulting from oilfield exploitation accumulate here.

It is known that bottom sediments are not only accumulators but also pollutants of the environment. Therefore, their analysis demands special attention. Concerning sedimentation regime, the most geoecologically sensitive areas are those of fine-grained material accumulation through precipitation from the water column. The most geoecologically stable regions are those of sediment transit and bottom erosion. From the lithologic point of view geoecological danger decreases with growing particle size, from clay and pelite muds to coarse-grained sands and pebbles.

Bottom current velocities in the "Prirzlomnoe" oilfield area suggest that findings of coarse sands on the seafloor characterize unstable sediment balance conditions. The presence of fine sands reflects removal and transit (active removal of fine sand starts at a current velocity of 20-22 cm/s). Core evidence shows that sedimentation conditions have remained constant at least since the Late Holocene. Hence, we may assume that accumulation of pollutants is possible only at the northern boundary of the studied area where water depths exceed 25 m.

The given complex data allow us to conclude that the background geoecological conditions in the study area are safe, and the possibility of hydrocarbon accumulation during the oilfield exploitation is insignificant. Besides, it is known that the state of benthic organisms and, above all, echinoderms is the most important indicator in terms of pollution. We know from publications (Pogrebov, 1998) that bioproductivity in the "Prirazlomnoe" area is low, which is also favorable for diminishing the influence of technogenic interference within the environment.

Acknowledgements: This research is supported by the Department of Industry and Science (FCP "World Ocean", projects 5.10, 5.11) and INTAS (project No. 99-1489).

References

Assinovskaya, B.A., 1994. Seismichnost' Barentseva moray (Seismicity of the Barents Sea). Moscow, Nation. Geophys. Com. RAS, 128 pp. (in Russian).

Avenarius, I.G., Dunaev, N.N., 1999. Some aspects of the evolution of relief in the eastern Barents Sea and an adjoining land during the Late Valdai. Geomorphology, 3, 57-62 (in Russian).

Danilov, A.I., Efremkin, I.M., 1998. Natural-climatic conditions in the area of oil-gas fields on the Arctic shelf. In: Osvoenie shel'fa arkticheskikh morei (Reclamation of the Russian Arctic seas shelf). Saint-Petersburg, A.N. Krylova CRSI, 479-487 (in Russian).

Musatov, E.E., 1990. Neotektonika Berentsevo-Karskogo shel'fa (Neotectonics of the Barents-Kara shelf). Geologiya i razvedka, 20-27 (in Russian).

Nikonov, A.A., 1978. Vertical movements of coasts of the polar seas. Priroda, 6, 16-22 (in Russian).

Pogrebov, V.B., 1998. Development of biota in marine ecosystems in the Pechora Sea and Pechora Bay in relation to the future exploitation of coastal and shelf oilfields. Abstracts of the Second Inter. Confer. "City in polar regions and environment". Syktyvkar, State Com. of the North of the Russian Federation, 325-327 (in Russian).

POSSIBLE SEA-LEVEL CHANGES AT THE BEGINNING OF THE THIRD MILLENIUM

Yu.A. Pavlidis
Shirshov Institute of Oceanology RAS, Moscow, Russia

Abstract

Possible scenarios of transgression development at the beginning of the third millenium based on analysis of sea-level rise during the past 2,000 years are the concern of the present article. The next stabilization of the transgression is predicted for the XXII century. Only by this time can the sea-level have risen by 1 m compared to the modern one. Apparently, stabilization at this level will be similar to that which occurred in the XVI and XIX centuries. This stabilization will possibly be accompanied by a regressive shift followed by slow sea-level rise until it reaches its maximum by 2500 equal to 1.5 m above the modern one.

Introduction

Forecast of the future evolution of the coastal zone and shelf should be based on certain preconditions. These are, primarily, global climate warming and sea-level rise. Estimations of the global sea-level rise range from 0.5 to 4.5 m per 100 years. However, all these estimations are mainly declarative. They were presented to the scientific community as "alternative" scenarios by the Intergovernmental Commission of Experts on Climate Change (ICECC), which was founded by the World Meteorological Organization (WMO) and the United Nations Organization Environmental Program (UNEP) in 1988. According to the so-called "Usual practice" scenario, the global sea level should have risen by 1 m by the end of the next century. Simultaneously the ICECC task group developed a more "moderate" scenario suggesting that the global sea-level rise by the end of the XXI century will reach 0.65 m. All these scenarios start from the assumption of climate warming with different degrees of intensity related to the greenhouse effect, i.e. caused by technogenic impact. We share the opinion about climate control on sea-level rise, but disagree with the theory of "anthropogenic" warming. We consider natural environmental changes to be dominant.

The forecast of such a multifactor process as sea-level rise (Kaplin, 1989) is always conventional and can be considered only as a working hypothesis. Our reasoning about possible changes will be based on "the good old" geographical method of comparative analogies using the data on sea-level changes in the Late Holocene and historical time. We need a theoretical (even hypothetical) basis for carrying out several research projects including RFBR No. 00-05-64077 "Shelf and coastal zone of Russian seas in the XXI century", FCP "World Ocean" № 5.10. "Creation of a general forecast model of the shelf and coastal zone evolution in the Russian Arctic seas necessary for ecological substantiation of economic activities" and No. 5.11. "Forecast of the Russian Arctic coasts evolution in the XXI century", INTAS No 1489 "The Pechora Sea – Late Pleistocene paleogeography, present state of the shelf and coastal zone and forecast for the 21st century".

Final stage of the Flandrian transgression and global sea-level changes between 5 and 2 ka

The postglacial "Flandrian" transgression terminated about 5-6,000 years ago, when in some regions the sea level was 1 to 3 m higher than the modern one. By "modern sea level" we mean a "zero depth" mark established by tide-gauges observations during the last decade of the XX century. Prior to reaching its maximum height the global sea level was rising non-uniformly. As shown by numerous investigations of this process including our data, during the past 15,000 years stabilizations and even sea-level falls occurred several times as evidenced by relevant signs at different levels.

The study of the global sea-level variations (Kaplin, 1989) is substantiated by thousands of radiocarbon datings of the ancient coastlines. Despite numerous regional differences related to tectonics, glacioisostasy, geodynamics, etc., the general global trend of the transgression was established. Systematization of the datings for the past 6,000 years in 500-years intervals allowed producing a global curve of sea-level variations (Kaplin et al., 1982).

The final stage of the postglacial transgression is distinguished by transgressive-regressive sea-level oscillations: after achieving its maximum at the end of the Atlantic period, the level fell down to -2 m in the Subboreal and remained there until the beginning of the Subatlantic.

Reliable data on sea-level changes in the second half of the Holocene were obtained in studies of ancient coastlines, nearshore sediment facies, and low coastal terraces in the equatorial-tropical zone of the World Ocean. We dated Cuban mangrove peats, which reliably preserve records of sea-level positions (Ionin et al., 1997). These results were used for the construction of the sea-level curve (Fig. 1).

In order to reconstruct the last stage of the postglacial transgression, it is especially important to investigate low coastal terraces, which frequently border coasts in the equatorial-tropical zone, primarily those of the coral islands. These terraces consist of cemented carbonate clastic material, including coral fragments. The first (lower) terrace formed in the Late Holocene is especially widely distributed. In Cuba it was named "seboruko" terrace. We suggest using this name for similar terraces in other parts of the World Ocean.

The "seboruko" terrace has a beach-like profile. Its upper part consists of cemented fragments of massive corals and big shells of molluscs, for example, *Strombus gigas*. Its lower unit is represented by slightly cemented coral-shell sand. At the southeastern Cuban coast, at the foot of the Sierra-Maestra mountains, in particular near the rivers mouths, the "seboruko" terrace deposits often include pebbles and even small boulders of crystal rocks. On some islands along Cuba's northern coast (Romano, Coco, Santa Maria, etc.), on the southern coast of the Pinos Island, on Cajo Largo Island and other islands of the Los-Canarreos Archipelago forming the southern boundary of Batabano Bay, the "seboruko" terrace mainly consists of oolitic sandstones.

The structure of the "seboruko" terrace, its contours, profiles, sediment composition and lamination, allow to assume that the terrace represents a coastal accumulative form preserved by cementation. It is formed of coral fragments, mollusc shells and

sand thrown by waves from the seabed to the coast. Coral fragments are rounded. This evidences that they spent a certain time in the surf zone.

According to radiocarbon datings, the age of the "seboruko" terrace and its analogues in the Indian (Geographiya..., 1990) and Pacific (Nikiforov, 1975) oceans ranges from 2 to 4 ka (Table 1). Thus, the "seboruko" terrace and its analogues were formed at the end of the Atlantic/beginning of the Subboreal period of the Holocene, when the global sea level had reached its modern position. However, it was not absolutely stable. As shown by our investigations in Cuba, the sea level was slightly above the zero level between 4 and 3 ka and fell again at about 2 ka (Fig. 1).

Table 1. Radiocarbon datings of the "seboruko" terrace

Laboratory index or relevant reference	Material	Sampling place	Absolute height (m)	Age, years
MGU-417	Corals	Cuba, Cape Guanos, "seboruko" terrace	+2	2240±150
MGU-418	Corals	The same	+2	2230±130
MGU-419	Shells	The same	+2	1980±120
GIN-510	Shells	Cuba, Mariel, "seboruko" terrace	+5	3889±130
GIN-511	Shells	Cuba, Oriente, "seboruko" terrace	+5	2290±110
GIN-513	Shells	Cuba, Cape Seboruko, "seboruko" terrace	+5	2090±100
MGU-1097	Bioaccumulated limestone	Indian Ocean, Amirante shoal, Resource Island	+2	2070±220
MGU-1092	Corals	Indian Ocean, Farquare Island	+2	2160±230
MGU-689	Coral fragments	Indian Ocean, Seychelles, Bird Island	+2	2200±460
MGU-980	Mollusc shells	Indian Ocean, Amirante shoal, African Island	1,5	3020±300
MGU-972	Mollusc shells	Indian Ocean, Seychelles, Deny Island	+2	2880±200
Bellair,1996	Coral fragments	Pacific Ocean, Cocos Islands	+4	5500

Due to the sea-level rise above the ordinary level, the tops of coral reefs were also "elevated" to this high level. When the sea level fell, the tops of reefs became exposed to intensive destruction by waves. Coral fragments and other carbonate clasts were transported to the coast and preserved in the coastal accumulative forms. Shortly after, these forms composed of carbonate biogenic breccia were cemented, cut from the coast by abrasion, and the scarp of "seboruko" terrace was formed.

Datings of Cuban mangrove peats revealed a sea-level lowstand at 2 m below its modern position at about 2 ka (Ionin et al., 1997).

Badyukov (1982) has shown that the sea-level curve for the period between 8 and 2 ka at the Atlantic coast of Northern America generally coincides with our curve for the Caribbean region.

Sea-level variations during the past 2,000 years

In the Late Holocene, climate fluctuations were almost synchronous to the changes in the rate of global sea-level rise. The American scientists who studied this problem (Thomas and Varekamp, 1991; Varekamp et al., 1992; Nydick et al., 1995) have shown that during the past 1500 years the sea level continued to rise, at least in the North Atlantic, but at a different rate. The data were obtained in the course of investigating sections of the coastal marches and their level-by-level radiocarbon dating. It was taken into consideration that in coastal marches sedimentation rate is comparable with the rate of relative sea-level rise. In such a way, the data on sea-level position against the modern "zero depth" at the eastern US coast and the eastern coast of England were obtained. An amazingly good agreement between the sea-level curves (Fig. 2) allows to consider the transgression as a common one for the whole Atlantic Ocean, or at least its northern part. About 1500 years ago, i.e. at the beginning of the Subatlantic period, the sea level was approximately 2 m below its modern position, which is in good accordance with our "eustatic curve" based on the data from Cuba. Apparently, after this time the current stage of sea-level rise began. The period between 1000 and 500 years ago is characterized by a rate of sea-level rise of about 1 mm/year. The subsequent period of sea-level stabilization or even small regressive shift by 1 m between 1650 for 1500 corresponds to the Little Ice Age (Monin and Shishkov, 1979; Selivanov, 1996). Later the sea level continued to rise at the rate of 2.5 mm/year. The relatively cold XIX century was marked by a new stabilization, and at the beginning of the XX century the sea level started to rise again. At present the gradually growing rate of sea-level rise equals 1.5-2 mm/year and will possibly continue to increase (Klige et al., 1998).

Possible sea-level variations in future

As has already been noted, estimations of the average global sea-level rise during the next 100 years differ by more than an order and range from 10-20 cm to 4 m. It is thought (Selivanov, 1996; Razvitie..., 1997) that the principal reason of these essential differences in estimations is the complexity of forecasting possible environmental changes, primarily, the response of the Antarctic and Greenland ice sheets to the global warming.

During the whole Quaternary the global sea-level experienced certain periodic oscillations. These were, first, periodic changes of "glacial" and "interglacial" levels. These high and lowstands are estimated to have had a duration of 10-100 millenia, and their amplitude to reach 10-200 m. This is the *first order* periodicity. Secondly, these were fluctuations covering thousand-year time intervals (*the second order* periodicity). Thirdly, there were fluctuations lasting for one-two centuries (*the third order* periodicity). Existence of shorter fluctuations is also doubtless, since every "eustatic" curve demonstrates such periodicity. We are interested in periodicity in sea-level oscillations during the so-called "interglacial" highstands. During the previous, Riss-Würm, interglacial the sea level reached at least three maxima. Bylinskii (1996) defines the transition from the glacial to interglacial epoch and vice versa by the sea-level passage through the –25 m mark. Accordingly, the modern

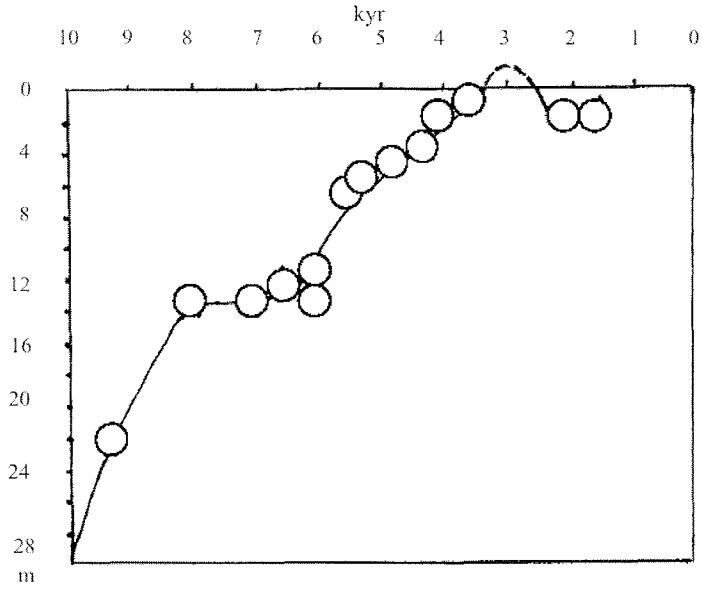

Fig. 1. Holocene sea-level changes near the coast of Cuba from 8 to 2 kyr (Kaplin, 1986).

interglacial epoch started about 8-10,000 years ago, i.e. at the beginning of the Holocene, and will possibly last, by analogy with the previous interglacial, for another 30-40,000 years. During this interglacial, the only sea-level maximum was observed 5-6,000 years ago. Sea-level minimum occurred about 2,000 years ago. It is not improbable that at present the sea level is tending to reach the next maximum. Against the background of these millennial fluctuations with an amplitude of several meters, the transgressive or regressive runs of sea-level curve exhibit small oscillations with an amplitude of tens of centimeters and a duration of several hundreds of years. The latter approximately correspond to the so-called "centennial" cycles of solar activity. According to the hypothesis of Charles Sonnet (Arizona University, USA), a quiet phase of solar activity in the XVII century corresponds to climate cooling and glacier advance – the Little Ice Age. At the end of the XVIII century the sun reached its maximum activity, replaced in the XIX century by another cycle of low activity and temporary re-establishment of cold conditions. At present the Earth is experiencing another period of increasing solar activity.

The most intensive climate warming started in the seventies of the XX century. Budyko (1971) established a correlation between the global sea level and air temperature anomalies in the zone between 17 and 90° N (Fig. 3). According to this dependence, increase in Δt° by 0.5°C results in the sea-level rise by 50 cm.

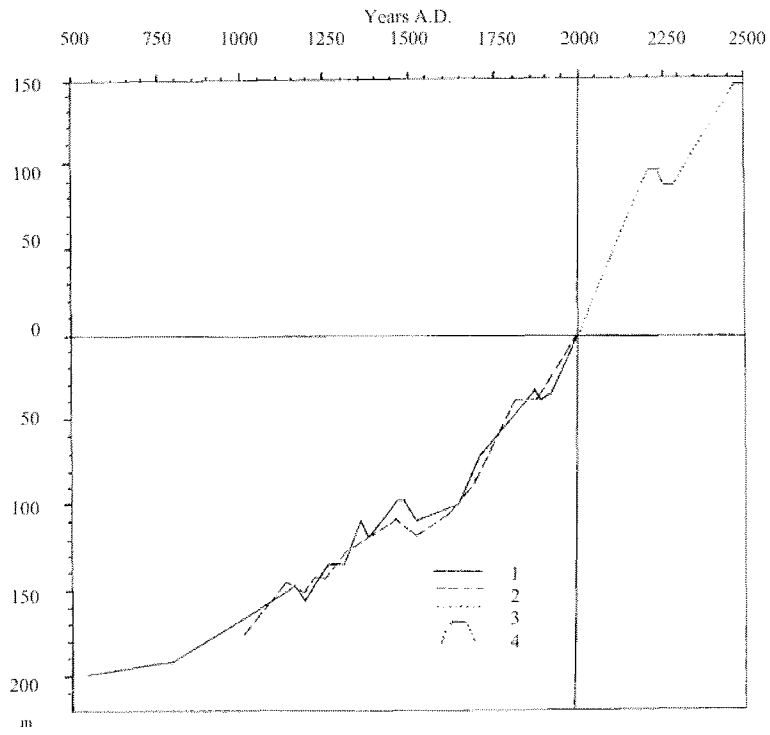

Fig. 2. Sea-level rise in the Atlantic Ocean near the coasts of the USA and England over the past 1500 years (Razvitie..., 1997; Klige et al., 1998; Monin and Shishkov, 1979; Nikiforov, 1975) and possible development of this process in the next centuries. Key: 1 – curve based on ^{14}C dating of deposits near Long-Island (USA); 2 – the same curve for the eastern coast of England; 3 – anticipated sea-level change at the beginning of the third millenium.

Within 25 years, from 1975 until 2000, the positive ground air temperature anomaly on Earth reached approximately 0.3°C. Hence, the sea level should have risen by 30 cm. However, in the North Atlantic, according to the above-mentioned data from American scientists, the sea-level rise was not more than 10 cm, and according to the data from Klige and co-authors (see in Kaplin, 1986) only 5 cm. This discrepancy could be explained by considerable delay in sea-level rise compared to the growth of positive temperature anomalies. Calculations of Kalinin et al. (1975) show that climate warming causes an annual reduction in the global volume of continental and gletcher ice by approximately 250 km^3. This, in turn, results in water inflow to the World Ocean and an average sea-level rise of 1.5-2 mm/year. The most intensive sea-level rise is observed in the Arctic Ocean (2.6 mm/year), whereas in the Atlantic Ocean it is about 2 mm/year, in the Pacific Ocean 1 mm/year, and in the Indian Ocean 0.6 mm/year. The constructed mutual correlation functions between the levels of separate oceans have shown that the level rise in the Arctic Ocean is 3 years ahead of the rise in the Atlantic Ocean, 6 years ahead of the rise in the Indian Ocean, and 8 years ahead of the rise in the Pacific Ocean. Therefore, the dependence established by Budyko seems to be overestimated. When forecasting the future sea-level changes in the North Atlantic

and Arctic Ocean, we use the value of 25 cm per 50 years, recognizing considerable increase in mountain glacier melting and reduction of the Greenland ice cover. This is evidenced by satellite images showing enlargement of coastal ice-free areas during the past 25 years (Fig. 4). Such correlation corresponds to interpolation of the North Atlantic sea-level curve for the last 100 years (Fig. 2).

Recently the website of the US Geological Survey (USGS) published the data on possible global sea-level rise due to melting of various glaciers (Table 2). It turned out that melting of all glaciers without those of Antarctica and Greenland can add such an amount of water to the World Ocean that will cause a 0.45 m rise of its level. If Antarctic ice shelves melt away, no real sea-level rise will be observed. Peripheral Greenland glaciers that are actively melting now can produce only a 5 cm sea-level rise. It is hardly probable that Antarctic and Greenland ice caps will actively melt in the nearest geological future. Due to partial melting of Antarctic outlet glaciers the total increase of sea level will reach 11 cm. Hence, it is rather hasty to predict a 1 m sea-level rise during 100 years.

Table 2. Area of glaciers, ice volume, and maximum possible global sea-level rise

Geographical region	Area, km^2	Volume, km^3	Maximum possible sea-level rise, m
All glaciers except Antarctica and Greenland	680 000	180 000	0,45
Greenland, central ice cap	1 736 095	2 600 000	6,50
Greenland, peripheral glaciers	48 599	20 000	0,05
Antarctica, ice cap	13 586 400	30 109 800	73,44
Antarctic Peninsula	446 690	227 100	0,46
Ross ice shelf	536 070	229 600	0,01
Other Antarctic ice shelves and outlet glaciers	532 200	351 900	0,11

The second order periodicity in sea-level fluctuations is characteristic for the past 6,000 years. During this interval the sea level has fallen from the maximal Holocene elevations (1-3 m above the modern one) observed 3-2 ka to about 2 m below the modern sea level. Later, at approximately 500 AD the modern sea-level rise started. Supposing an approximately equal duration of the periods of sea-level fall and rise, the present sea-level rise will continue for another 500 years.

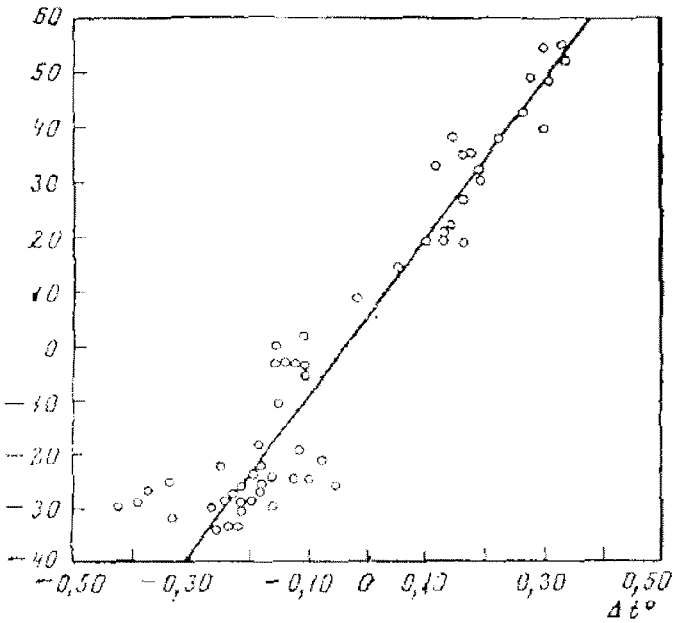

Fig. 3. Correlation between global sea-level variations and anomalies of air temperature in the Northern Hemisphere.

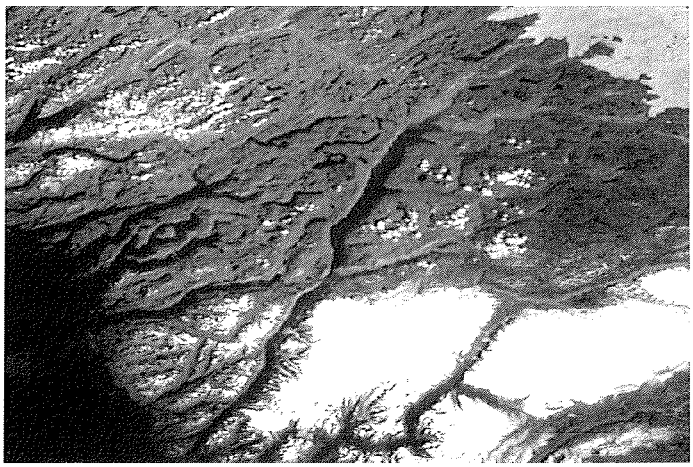

Fig. 4. Ice-free area at the Atlantic coast of Greenland (space image). http://www.usgs.gov/

As mentioned above, against the background of the 2,000-year-long continuous sea-level rise in the North Atlantic, stabilizations and regressive shifts occurred in the XVI and XIX centuries. Interpolating this succession in the future we should

expect another sea-level stabilization in the XXII century similar to those of the XVI and XIX centuries. Only by this time the sea level may rise by 1 m against the modern position. It might be accompanied by a regressive shift, which will give way to a slow sea-level rise until the next maximum will be reached by 2500. This will be the end of the 2,000-year-long transgressive cycle. Probably, stabilization will take place at the sea level 1.5 m higher than the modern one.

Already in the seventies Nikiforov (1975) wrote that the modern relative stabilization of the global sea level is an insignificant episode in the Holocene history of the Earth, and might be replaced by a new climate warming with another climate optimum and sea-level highstand.

References

Badyukov, D.D., 1982. The influence of geoid form change and deformations of the solid Earth under water load on the Late Glacial sea-level changes. In: Kolebaniya urovnei morei i okeanov za 15000 let (Sea-level fluctuations during the last 15 000 years). Moscow, Nauka, 51-77 (in Russian).

Budyko, M.I., 1971. Klimat i zhizn' (Climate and life). Leningrad, Gidrometeoizdat, 250 pp. (in Russian).

Bylinski, E.N. 1996. Vliyanie glyatsioizostazii na razvitie rel'efa Zemli v pleistotsene (Influence of glacioisostasy on development of the Earth's relief in the Pleistocene). Moscow, Izd. Natsional'nogo Geofizicheskogo Komiteta RAS, 212 pp. (in Russian).

Geografiya Seishel'skikh ostrovov (Geography of the Seychelles), 1990. Kaplin, P.A., Kosmynin, V.N., Nikiforov, L.G. (eds.), Moscow, Izd. MGU, 267 pp. (in Russian).

Ionin, A.S., Pavlidis, Yu.A., Avel'o-Suares, O., 1977. Geologiya shel'fa Kuby (Geology of the Cuba shelf). Moscow, Nauka, 215 pp. (in Russian).

Kalinin, G.P., Breslav, E.I., Klige, R.K., 1975. Some peculiarities of the modern sea-level variations. In: Kolebaniya urovnya Mirovogo okeana i voprosy morskoi geomorfologii (Global sea-level oscillations and problems of marine geomorphology). Moscow, Nauka, 5-12 (in Russian).

Kaplin, P.A., 1986. Types of sea-level changes. Geomorphologiya, 3, 16-22 (in Russian).

Kaplin, P.A., 1989. Coastal zone of World Ocean. Zemlya i Vselennaya, 3, 12-17 (in Russian).

Kaplin, P.A., Badyukov, D.D., Selivanov, A.O., 1982. Study of coastlines over the last 15 thousand years (a review). In: Izmeneniya urovnya okeana (Sea-level variations). Moscow, Izd. MGU, 5-16 (in Russian).

Klige, R.K., Danilov, I.D., Konishchev, V.N., 1998. Istoriya gidrosfery (A history of the hydrosphere). Moscow, Nauchnyi Mir, 568 pp. (in Russian).

Monin, A.S., Shishkov, Yu.A., 1979. Istoriya klimata (A history of climate). Leningrad, Gidrometeoizdat, 407 pp. (in Russian).

Nikiforov, L.G., 1975. Postglacial eustatic sea-level rise and its role in evolution of seacoasts. Kolebaniya urovnya Mirovogo okeana i voprosy morskoi geomorfologii (Global sea-level oscillations and problems of marine geomorphology). Moscow, Nauka, 12-40 (in Russian).

Nydick, K.R., Bidwell, A., Thomas, E., Varekamp, J.C., 1995. A sea-level rise curve from Guilford, CT. Marine Geology, 124, 137-159.

Razvitie morskikh beregov Rossii i ikh izmeneniya pri vozmozhnom pod"eme urovnya Mirovogo okeana (Evolution of the seacoasts of Russia and their changes at the possible global sea-level rise), 1997. Kaplin, P.A., Selivanov, A.O. (eds.). Moscow, Izd. MGU, 304 pp. (in Russian).

Satellite Image Atlas of Glaciers of the World. Chapter A: Introduction (U.S. Geological Survey Professional Paper 1386-A). Richard S. Williams, Jr., Jane G. Ferrigno (Eds.). http://www.usgs.gov/

Selivanov, A.O., 1996. Izmeneniya urovnya Mirovogo okeana v pleistotsene-golotsene I razvitie morskikh beregov (Global sea-level oscillations in the Pleistocene-Holocene and evolution of seacoasts). Moscow, 267 pp. (in Russian).

Thomas, E., Varekamp, J.C., 1991. Paleoenvironmental analyses of marsh sequences: evidence for punctuated sea-level rise during the latest Holocene. J. Coastal Research, special issue, 11, 125-158.

Varekamp, J.C., Thomas, E., van de Plassche, O., 1992. Relative sea level rise and climate change over the last 1500 years. Terra Nova, 4, special issue, Global Change (ed. Wezel), 293-304.

EVOLUTION OF THE SOUTHERN PECHORA SEA COASTS DURING THE PRESENT CENTURY AS EXPECTED FROM FUTURE CHANGES IN CLIMATE AND SEA-LEVEL

P. A. Kaplin , A. O. Selivanov, V.M. Sobolev
Faculty of Geography, Lomonosov Moscow State University, Moscow, Russia

Abstract

Global and regional climate changes during the present century including sea-level rise will inevitably affect the Pechora Sea coasts. Principal factors of adverse impact include retreat and degradation of various types of the coasts. Main attention is paid to depositional coasts prevailing in the study area. Semi-quantitative models based on the Zenkovich-Bruun Rule to quantify coastal retreat are proposed and their applicability is discussed. Several development series of coastal responses under the influence of various factors, namely nearshore bottom slope, sediment supply, and rate of sea-level rise, are presented. A possible influence of storm surges and tidal movements on coastal evolution is discussed. The authors' comprehensive methodology for prediction of evolution of various coastal types is briefly presented. General patterns of future coastal evolution of the southern Pechora Sea are demonstrated. Depositional coastal barriers and ice-rich coastal escarpments will suffer from global and regional changes to the greatest extent. Additional influence of extreme events such as storm surges and high tides is discussed.

Introduction

Accumulation of carbon dioxide, methane, chlorofluorocarbons, and some other "greenhouse gases" in earth's atmosphere is amongst the most important, inevitable consequences of man's activities. It results in an increase of air temperatures, melting of continental glaciers, thermal expansion of ocean water, and changes in precipitation and water supplies in continental areas. All of these processes tend to replenish the ocean and to raise global sea level. The globally averaged surface air temperature is projected to increase by 1.4-5.8°C over the period 1990 to 2100 (Summary..., 2002). This increase is very likely (90-99%) without precedent during at least the past 10,000 years. Estimates of global sea-level rise in the next century range from 0.1-0.2 meters to about 4.0 meters and there is no reliable corroboration to favor one estimate over the other. The official Third Assessment Report of the Intergovernmental Panel on Climate Change states the 0.09-0.88 m global mean sea-level rise during the present, 21st, century; the best estimate is thought to be 0.33 m (from 0.31 to 0.45 m) (Summary..., 2002). Global sea-level rise over one meter during the next century, therefore, is unlikely (10-33% chance), but cannot be totally excluded as yet. In any case, a strong possibility exists for significant acceleration of sea-level rise in the near future in comparison with the 0.10-0.15 m rise in global mean sea level during the past century (Klige, 1990; Emery and Aubrey, 1991; Gornitz, 1993). Moreover, even a rise in global sea level of 0.1-0.5 m would have substantial negative impacts on a worldwide scale. Storm surges would increase in their

frequency above critical inundation levels and saltwater intrusions to estuaries and coastal aquifers would cause problems in water supply and coastal ecosystem survival. Passive inundation would occur only at a few low-lying coastal segments, e.g. in small semi-enclosed bays and along very gently sloping coasts where wave and tidal energy is much reduced at the coastline. Modification, landward retreat, and general erosion of coastal morphological features (cliffs, barriers, bars, lagoons, marshes, mangroves, coral reefs, etc.) would become the most expressive and significant impact of sea-level rise.

Coastal zones will experience the substantial economic and environmental damage due to shoreline retreat and changes in the environmental conditions at the preserved part of land areas due to underground flooding and other related processes, which will be especially intensive in areas at present dominated by permafrost. In addition to the direct loss of property, many industrial facilities will need reconstruction or change of their specialization. Unique ecosystems will not be able to survive.

Predictive principles for coastal morphological responses

Mapping of coastal inundation for different sea-level rise scenarios remains the most popular activity in this field. There is a positive experience of such a kind for the United States (Barth and Titus, 1984; Giese and Aubrey, 1987; Pilkey and Davis, 1987), Canada (Eddington and Andrews, 1989) and certain areas in Western Europe (Tooley and Jelgersma, 1992). Some of these studies include corrections for tectonic deformations and estimates of increase in storm surge elevations due to sea-level rise.

Nevertheless, passive coastal inundation will occur only on few coasts: in small semi-enclosed bays and on very gently sloping coasts, i.e. where wave energy does not reach the shoreline. In most cases an active reformation of "land edge" will be inevitable. During sea-level rise, shoreward slopes of coastal accumulative features, usually steeper than the nearshore bottom surface, become part of the wave-active zone. The steeper the surface, the higher is the wave energy to erode a shoreface. Sediments from the shoreface are cast to the nearshore bottom slope thus causing the shoreline and the accumulative feature as a whole to move inland, onto the shoreface or the lagoon behind it. The above model, put forward by Vsevolod Zenkovich and his successors, was applied to different coastal areas (Zenkovich, 1967; Kaplin, 1973). American and European scholars investigating related problems denominate this model as the Bruun Rule (Schwartz, 1967) after the pioneering studies of Per Bruun (1962). The Zenkovich-Bruun Rule (ZBR) postulates the equality of sediments eroded on a coast during sea-level rise to their deposition in the nearshore, as well as preservation of the transverse profile shape. According to this rule, a shoreline retreat R is proportional to the change U of relative sea level and width, B, of wave-induced bottom zone, and inversely proportional to its depth, D:

$$R = U \bullet B/D = U \bullet \tan \alpha \quad (1)$$

where R = surface inclination of an underwater coastal slope. However, this simple model adequately describes coastal evolution only for the narrow boundary conditions:

(a) slow sea-level rise in comparison with shoreline retreat, i.e. $R \approx U$;
(b) general availability of sediments to maintain an equilibrium profile;
(c) exclusively shoreline-transverse sediment movement by waves in a seaward direction;
(d) existence of a seaward limit of sediment movement by waves or any other factor ("lower limit of an underwater coastal slope", or "wave base").

Therefore, determination of the "wave base" becomes an important problem and depends on wave parameters. According to different authors, the "wave base" varies from 1.5 to 3.5 times the height of 5% of the waves beyond the breaking zone (Zenkovich and Popov, 1980; Bruun, 1988). Generally, over 90% of longshore sediment transport occurs above this "wave base" (Bruun, 1988).

To account for the possible variety of the parameters mentioned in (b)-(d), as well as for other processes involved in reformation of the coastal zone, different modifications of the BR were developed.

Field studies reveal that under special conditions the coastal evolution pattern can differ significantly from the above model. The Caspian Sea serves as an excellent "natural laboratory" for studying sea-level rise impacts: the water level fluctuated by 3 m or even more during the past century. Since 1978 it has risen by 2.5 m, i.e. at a rate of over 10 cm/year. Investigations in this region show that during sea-level changes sediments can either be cast ashore and washed inland to an accumulative feature or be moved downslope. The latter portion can be drawn into a longshore current or moved down the bottom slope to the depths where waves do not act. Field observations demonstrate not only strong dependence of shoreline retreat values on nearshore slopes, as was postulated by ZBR, but differences in the very patterns of coastal evolution according to the nearshore surface slope (Ignatov et al., 1993; Kaplin, 1989; Kaplin and Selivanov, 1995, 1999; Selivanov, 1997) (Fig. 1). This is probably due to the fact that nearshore slope values determine not only the position of the wave-breaking zone, but also the character of the breaking process.

Moreover, to assume an equilibrium pattern for all coastal modifications limits the application of ZBR most strongly. Possible sea-level rise in the next century can reach significant rates and turn coastal evolution to essentially disequilibrium patterns. Shoreline migration would lag behind sea-level rise. SCOR Working Group members (1991) believe the time lag to be the primary reason for the fact that single storm-induced shoreline migration values are usually 3 to 6 times lower than those predicted by ZBR.

Essential problems arise if one tries to predict shoreline migrations for erosional coasts with cliffs. Extrapolation of historical trends usually involved the studies in this field (Barth and Titus, 1984; Leatherman, 1989; etc.) does not correspond to the possible shift in patterns of future coastal evolution due to the acceleration of sea-level rise.

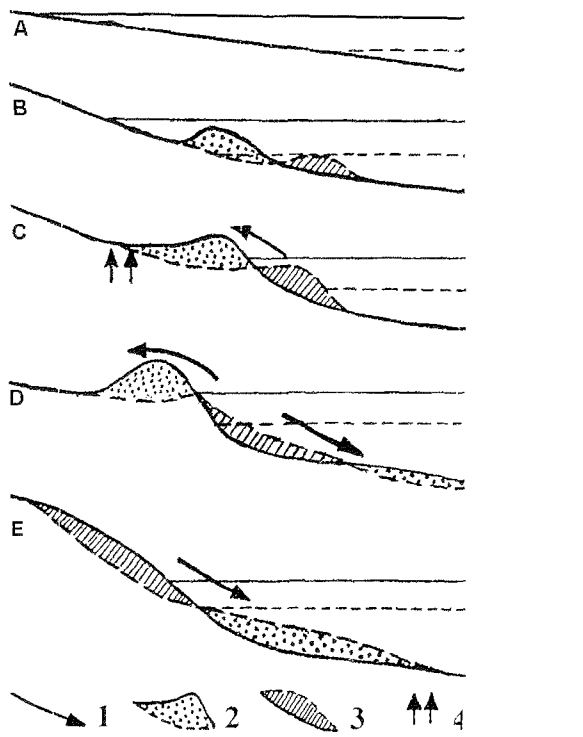

(A) "passive inundation" of low-lying land edge; (B) landward movement of sediments and coastal depositional bodies; (C) landward movement of sediments and coastal depositional bodies
barriers and formation of lagoons behind the barriers; (D) alternative landward and seaward movement of sediments and increase in nearshore gradients; (E) seaward sediment movement;(1) direction of transverse sediment movement; (2) deposited part of the profile; (3) eroded part of the profile; (4) groundwater table rise and lagoon formation.

Fig. 1. Different types of coastal evolution during the sea-level rise depending upon the gradient (tan) of the nearshore bottom slope (on the basis of Kaplin, 1989; Ignatov et al., 1993; Kaplin & Selivanov, 1995, modified)

In order to estimate relative sea-level change U where intensive tectonic movements occur, recent vertical deformation trend p obtained from tide-gauge records should be incorporated into the global sea-level rise value A:

$U = A + p \bullet t$ (2),

where t is a prediction time interval in years. In the vast majority of the studied coasts, the tectonic correction is less than 15-20 percent of global sea-level

change, but for the area under study it can be as much as 50-70% because of an intensive tectonic submergence of several coastal segments, especially in river mouths.

Genetic series of coastal responses under the influence of various factors

Depositional coasts. According to our studies, principal factors of their evolution include inclination of underwater (nearshore) coastal slope, sediment budget of the specific coastal segment, rate of sea-level rise (annual and decadal), intensity of short-term, namely tidal, storm-surges and other types of sea-level fluctuations.

In general, during water-level rise, shoreward slopes of coastal accumulative features, usually steeper than nearshore bottom surface, come into the wave-active zone. The steeper the surface, the higher is the wave energy to erode a shoreface. Sediments from the shoreface are cast to the nearshore bottom slope thus causing the shoreline and the accumulative feature as a whole to move inland, onto the shoreface or the lagoon behind it.

Our analysis demonstrates fairly well that, as first stated by Kaplin (1989), the nearshore bottom slope determines not only shoreline retreat values but also the very patterns of coastal evolution (Fig. 1). This may be due to differences not only in the position of the wave-breaking zone, but also in the type of wave breaker. The boundary values between the response types depend on the grain size of nearshore slope sediments. The approximate values cited below represent medium and fine sands.

On very gentle coasts (tan α < 0.0005) wave energy is dissipated long before reaching the shoreline and a "passive inundation" of the low-lying land edge occurs (Fig. 1A). On steeper coasts, the higher the nearshore slope, the closer is the breaking zone to the shoreline. The wave breaking process causes erosion of shorefaces and of seaward slopes of emerged coastal depositional features. Simultaneously, where the nearshore slope values are relatively low (approximately tan $\alpha \approx 0.0005 \div 0.001$), a rising sea level results in a landward movement of the crests of coastal depositional bodies. However, substantial deformation of general morphological features does not occur (Fig. 1B). In many coastal segments of this type a submerged ridge (or series of such ridges) exists on the underwater coastal slope and acts as a main breaker for storm waves. If sediment supply from rivers, erosional scarps, or onshore aeolian transport is extremely high, shorelines may possibly advance with the water-level rise.

A steeper nearshore zone (tan $\alpha \sim 0.001 \div 0.005$) causes waves to break close to the shoreline eroding the shoreface and seaward slope of the beach. The beach ridge, thus, is raised by washovers whereas at the shoreface a seaward movement of sediments prevails. The beach ridge increases in size, its crest moves landward, and simultaneously seawater infiltrates across the ridge, while the lagoon, as it forms, receives freshwater from streams and the rising groundwater table (Fig. 1C). During the sea-level rise, the beach ridge may evolve to become a giant coastal barrier. However, where land behind the barrier is not low-lying, a lagoon does not form.

Where nearshore slopes reach values of tan $\alpha \approx 0.005 \div 0.01$, both landward and seaward sediment movements occur resulting in a relative stability of coastline position with increasing amplitude of elevations in the coastal zone (Fig. 1D). Principal erosion is typical of the zone exactly near the shoreline.

At those depositional coasts where the nearshore slope is very steep (usually tan $\alpha < 0.01$), the largest portion of sediments moves seaward and accumulates in the lower nearshore under the breaker zone (Fig. 1E). General erosion of the beach occurs and cannot be described by any of the existing semi-quantitative models.

Deltaic coasts, which are dependent in their evolution on the relative importance of fluvial and marine processes, primarily an intensity of sediment discharge from a river and sediment redistribution by waves and tides, also demonstrate different response patterns to water-level changes depending on the nearshore and offshore bottom slope. The steeper the delta-front surface subjected to submergence during the water-level rise, the more rapid is upstream deposition in deltaic channels and at the delta surface. However, progressive decrease in sediment discharge of most rivers, as a consequence of anthropogenic factors, suppresses deposition in river deltas under the water-level rise.

Erosional coasts are not well studied in their response to sea-level changes. Naturally, the slope of the shore platform affects the evolutionary pattern of the specific erosional coastal segment. Steeper shore platforms need more time to be covered at the cliff foot by a water layer significant for intensification of cliff retreat. However, the structural features of both shore platform and coastal cliff govern the type and intensity of their destruction under sea-level rise (see Selivanov, 1996 for the review). However, all existing models for this coastal type have an empirical nature and can only be applied regionally. Therefore, these models still have to be clarified.

Quantification of shoreline movement

It appears to be rather difficult to evaluate coastal zone reformation under sea-level rise. The main problem is to collect the necessary data covering at least several decades.

Depositional coasts. Based on our data, we can only propose a comprehensive methodology to estimate shoreline migration induced by sea-level rise on depositional coasts. Any analogues of this model do not exist. The slope-dependent model (Fig. 1) can be used as a first approximation. The very gently inclined coasts (tan α lower than 0.0005) will possibly exert passive inundation (Fig. 1A). To evaluate an intensity of this process, one can take necessary data on coastal morphology from topographic maps, coastal inventories and sailing directions. Mean annual position of shoreline should be used as a primary parameter. Lacking reliable predictions of storm surge elevations under rising sea level, we could not take their changes into account.

Shoreline retreat on relatively gently sloping coasts (tan α approx. $0.001 \div 0.005$) with submerged coastal ridges (Fig. 1B) may be evaluated using ZBR (Eq. 1) if one includes parameters of a seaward slope of the ridge into the equation (Dubois, 1990). It is worth noting, that, in contrast to our previous views, in several cases of excessive sediment supply, submerged ridges may emerge

above the water surface and show the same features as typical coastal ridges (Kaplin and Selivanov, 1995; 1997). Steeper coasts (tan α 0.005÷0.01) are usually characterized by coastal dunes or depositional barrier features that isolate lagoons (Fig. 1C). Sedimentary exchange between shoreface and backshore can be indirectly taken into account if a height e of coastal dunes is included into the traditional ZBR equation (Weggel, 1979):

$$R = U \bullet B/(e + D) \quad (3).$$

The so-called "generalized" ZBR (Dean and Maurmeyer, 1983) allows us to account for sediment washover to the lagoon:

$$R = U \bullet (B + W + B1)/[(D + h) - (D1 + h1)] \quad (4),$$

where h is the height of a beach berm, B1, D1, and parameters of a landward (lagoon) slope of the barrier island, and W its width.

Portion S of suspended material (less than 0.005 mm), usually carried out to an open sea, and a quantity L of material, brought/carried away by longshore currents, should also be evaluated. Then, a tentative equation for retreat of depositional shorelines is the following:

$$R = U \bullet B/D \bullet (1-S) \pm L \quad (5).$$

This approach is of the highest importance for the case of both landward and seaward transverse sedimentary movement (Fig. 1D) and for the steepest coastal slopes (Fig. 1E), which behave generally according to ZBR itself (Eq. 1).

The rate of shoreline movement at depositional coasts strongly depends on the pattern of shoreline response. In several cases, a sea-level rise may result in a seaward shoreline movement and vice versa because of the sediment budget of the specific coastal segment (Selivanov, 1996).

The rate of sea-level change is among the principal factors influencing the response patterns for depositional coasts. In general, the faster the sea-level rise, the higher the possibility of drowning and destruction of the coastal depositional body. The faster the sea-level fall, the more probable is the preservation of depositional bodies above the retreating sea, e.g. in the form of beach ridges and coastal dunes. The sediment budget of a coastal zone serves as another primary factor governing coastal responses. Under excessive sediment supply, the shoreline may advance to sea even during the sea-level rise. This phenomenon, called depositional regression, is common on many coasts (Dolotov, 1992). In the conditions of intensive lateral sediment movement a coast may react differently to the successive periods of sea-level rise (Selivanov, 1996). We analyzed sediment sequences at several sea coasts of Russia as well as data of direct observations of coastal changes under the water-level changes. These studies resulted in the construction of two genetic series of coastal evolutionary patterns under the accelerating sea-level rise for the conditions of substantially excessive and insufficient sediment supply, respectively (Selivanov, 1996) (Fig. 2). Under excessive sediment supply (Fig. 2A) on a primary graded coastal profile, slow sea-level rise (usually less than 2

mm/year for sand beaches) causes formation of a beach ridge and, in extreme cases, depositional regression. A moderately accelerating sea-level rise (5-10 mm/year) usually results in a landward translation of a coastal depositional body by overwash processes. No significant transformation of coastal morphology occurs. Faster sea-level rise (over 10 mm/year) results in a transformation of the depositional body, namely increase of its elevation, steepening of the landward slope, etc. An extreme acceleration causes flooding of the coastal depositional body by the rising sea level and formation of an overlapping sediment sequence. Under insufficient sediment supply (Fig. 2B), mobilization of existing scarce sediments on a primary graded coastal slope results in formation of a poorly expressed depositional body. With an accelerating sea-level rise, this body moves landward in a translational manner and undergoes erosion of its seaward slope. The latter process causes partial or total destruction of the coastal body under the very rapid sea-level rise. The extreme acceleration may bring in situ flooding of the depositional body and overstepping of the shoreline. Grading of the coastal profile is also possible.

The patterns distinguished by conditions of excessive sediment supply may be interpreted in terms of quasi-equilibrium evolution under relatively slow sea-level rise (up to 5 mm/year). With the accelerating sea-level rise, the possible intensity of coastal reformation becomes insufficient to keep pace with the rising sea level. Disequilibrium evolution becomes total under extremely fast sea-level rise. Following the terminology proposed for evolution of coral reefs under sea-level rise at various rates (Neumann and MacIntyre, 1985; Spencer, 1993), the response patterns for the conditions of excessive sediment supply can be termed as keep-up, catch-up and give-up respectively.

An alternative approach to morphological prediction for depositional coasts based on numerical simulation has been described by Kaplin and Selivanov (1997).

However, numerical simulation requires extensive information on wave and sediment movement parameters and is not yet applicable for long-term prediction.

Erosional coasts. The most natural way to predictive estimates of shoreline migration on erosional coasts is to use one or another empirical equation. It becomes a commonplace in analysis of shoreline retreat on depositional coasts as a function of the rate of level rise. The linear character of this function is commonly assumed in prediction surveys (Barth and Titus, 1984; Kay, 1990). However, statistical analysis proved this assumption to be true only for depositional coasts composed of loose sediments and unconsolidated rocks, where only poor beaches exist at the foot (Shuiskii, 1986).

A more adequate model of sea cliff retreat and beach lowering based on hydrodynamic analysis of consolidated rock destruction was put forward by Esin and his colleagues (Esin et al, 1980; Esin and Kuklev, 1992). The model allows for wave parameters and directions, the morphology of the nearshore, rock strength, cliff height, intensity of bottom sediment erosion, and sediment budget. The model is represented by the system of second-order differential equations. It is assumed that the shallow nearshore maintains a straight-line profile, whereas its slope changes.

If sea level rises at a constant rate u, after an infinitely long time, the model has an asymptotic amplification for cliff retreat rate v(x):

$(x) = u \bullet (\tan \alpha)$ (6),

where a is the slope of the nearshore breaking zone. One can easily see that Eq. 6 is similar to the Bruun Rule, thus confirming its reliability for equilibrium processes.

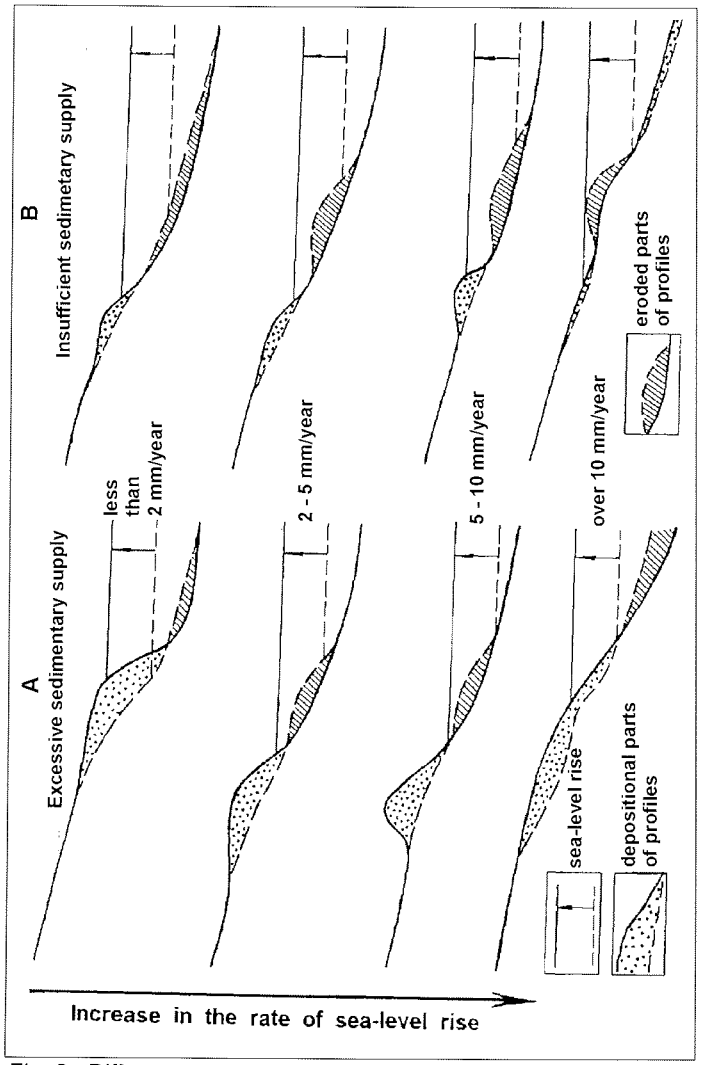

Fig. 2. Different types of depositional coast response to sea-level rise under the conditions of excessive (A) and insufficient (B) sedimentary supply depending upon the rate of sea-level rise

Eq. 6 corresponds well to the instrumental time series on erosional coast retreat for the Sea of Azov eastern coast. Moreover, the rate of cliff retreat, both for condensed and weak rocks, depends on the volume of sediments to be eroded from each meter of the cliff width, Le on its elevation H (Esin et al., 1980). The simple model (5) remains valid only for the conditions of slow uniform sea-level rise when the equilibrium cliff retreat process can be maintained. One of the necessary premises but not a sufficient one for this is the relative weakness of sediments composing the cliff. The latter value should be sufficient to allow the bench to reform, adapting the sea-level rise. It depends on the rate of rise u and the rate of bench lowering v(y), which can be obtained from instrumental data, where available, or from theoretical estimates of erosion intensity for certain rock types.

Bearing in mind the above-mentioned regularities, we have put forward the step-by-step scheme for evaluation of shoreline retreat on erosional coasts. Where u exceeds v(y), shoreline retreat will maintain the present rate, or even decelerate, because erosional processes will not keep pace with the sea-level rise. During the possible future sea-level rise at a rate up to 1-2 cm per year this evolutionary pattern will become widespread on erosional coasts composed of crystalline and metamorphic rocks, conglomerates, schists, etc. Where u is lower than v, retreat of erosional shoreline can be calculated according to Eq. 6 with the observed maximum rate of this process for certain types of rocks used as an upper limit. The empirical coefficient Kl should be also included in several cases to allow for slope processes. The value of the coefficient K2 depends upon morphology, lithology and position of the cliff to dominant waves. Moreover, one can consider also for the longshore sedimentary movement L. The final equation for the horizontal retreat C of sea cliff in equilibrium conditions becomes the following:

$$C = Kl \bullet K2 \bullet u \bullet dt/H \bullet (\tan \alpha) +/- L \quad (7).$$

A variety of factors interacting in coastal response to sea-level rise makes us to calculate a shoreline retreat in any given coastal segment as a probabilistic value. It can be expressed in the following form:

$$S = [s + k(s)] \bullet t, \quad (8)$$

where s is the predicted mean rate of shoreline retreat, (s) its standard deviation, K the reliability coefficient of the forecast, which is a function of reliability of prediction in percent.

General character of future coastal evolution of the southern Pechora Sea

Our predictive methodology of sea coast evolution under accelerated sea-level rise includes analysis of morphology of backshore and nearshore zones, their slopes, supplies of beach-forming material in the coastal zone itself and from neighbouring rivers, lithology of sea cliffs, etc. (Selivanov, 1996; Kaplin and Selivanov, 1997, 1999). As a first step, we attribute the future evolution of each coastal segment to one (or more) "primary" coastal process, i.e. passive

inundation, reformation of accumulative coastal features, and/or retreat of erosional scarps (sea cliffs). Deltaic, meso- and macrotidal, glacial and some other coastal types were attributed to the special evolutionary types. Further, a quantitative estimate for each coastal segment is proposed based on models presented above in Eqs. 1-8.

Bearing the existing data in mind, we will concentrate our attention in the present publication on the southern coast of the Pechora Sea (see Ogorodov, this volume, for the general morphological sketch of the area). Depositional coasts of this area are represented by Pleistocene and Holocene glacio-marine, marine and alluvial plains, which have partly emerged through neotectonic and glacioisostatic movements to elevations of 180-220 m (see Danilov, 1978; Kaplin and Selivanov, this volume, for details). Because of high ice content, these fine-grained silt and fine sand sediments are, to a large extent, subjected to various kinds of temperature-dependent erosional processes. Under the present, relatively slow, warming some coasts of the area retreat by over 10 m during extremely warm years. This is especially true for the southern coasts of Arctic islands such as Kolguev and Vaigach islands in the study area (Selivanov, 1996; Kaplin and Selivanov, 1999). According to the instrumental data, several segments of southern coasts of Arctic islands retreat by 40-50 m/year (Are, 1988, 1996; Zhigarev, 1997).

According to the Third Assessment of the Intergovernmental Panel on Climate Change, in northern East Europe and Asia the warming during the 21st century will exceed the global mean values by more than 40% (Summary..., 2002). Therefore, mean yearly temperature will be 2-8°C higher in 2100 than it is nowadays. This will inevitably result in an intensification of thermoabrasion, thermoerosion and related processes. General thawing of permafrost inland will contribute to the process. However, an inevitable increase in sediment discharge of the largest rivers of the area will activate depositional processes in peri-deltaic zones. These processes will be especially important for the Pechora Bay, adjacent to the Pechora River deltaic area. Prevailing shoreward movements of sediments in the Pechora Bay will favour depositional processes in it.

On the other hand, the Pechora River delta, as well as other deltaic areas of the region, undergoes an intensive submergence at a rate of up to 3-4 mm/year and does not emerge seaward under the present relatively slow sea-level rise (van Eerden, 2000). Preliminary estimates by one of the authors clearly demonstrate the highest probability of the preservation of a general balance between deposition and erosion in the Pechora River delta by the 2040s-2050s and accelerated delta degradation beyond this time period. The intricate balance can be damaged by the possible anthropogenic decrease of both water and sediment discharge into the Pechora River delta due to inevitably increasing water consumption for industry and population. Growing oil and gas industry in the upstream area is the important reason for this process.

Anyway, other rivers of the southern Pechora Sea (Neruta, Chernaya, More-Yu, Peschanka, Korotaikha and others) do not bring enough sediment material to significantly influence the erosional/depositional regime of the coastal zone. The lower reaches of these rivers will be inevitably destroyed under the accelerating sea-level rise. Rapid degradation during this century is inevitable for outer

reaches of the Korovinskaya Bay in the Pechora River deltaic channels presently drying up (Fig. 3).

Another process preventing an extreme shoreline retreat is the progressing deposition of eroded material on the flat beach and underwater coastal slope. In several decades, it will result in deceleration of shoreline retreat. However, this effect is rather difficult to quantify.

Because of these factors, significant degradation will occur on the so-called "buffer zones", namely sand and mud tidal and surge flats. The width of these zones exceeds 2-3 km in the Pechora and Khaipudyrskaya bays and 1-1.5 km in Kolokolkova and Pakhancheskaya bays. In these areas an increase of tidal prism (the amount of water entering/leaving bays during the tidal cycle) with the mean sea-level rise is expected. This process will cause an increased transport of fine-grained material down an underwater coastal slope. Therefore, buffer zones will possibly degrade and high-water depths will increase in these areas, especially in the Khaipudyrskaya and Pakhancheskaya bays where sediment discharge from rivers is relatively low.

Prevailing alongshore sediment movement in the southern Pechora Sea results in a formation of eastward-oriented spits in the north of the Kolokolkova, Pechora and Khaipudyrskaya bays. At present they are all represented by a series of sandy depositional barrier islands. These forms will inevitably suffer full degradation during the next decades even under the present sea-level regime. Acceleration of sea-level rise can contribute to the partial restoration of Gulyaevskiye Koshki Islands in the northern Pechora Bay by the 2020s-2030s (Fig. 3). However, beyond this date the archipelago will share the fate of other similar islands and totally disappeared by the 2060s-2080s.

The exceptional westward-oriented Pesyakov (Bezyakov) Island in the northeastern part of the Pakhancheskaya Bay will possibly survive because of the increasing alongshore sediment supply from the eroding Varandei coastal area (Fig. 3). Oppositely, Sengei Island with its presumably transverse bottom supply will inevitably suffer from the sea-level rise. It will possibly totally disappear in the next 30 to 50 years.

Erosional coasts are relatively rare on the coast under study. They are represented by high (30-50 m) escarpments composed of fine sand, loams and silts with high ice content (30-50% and up to 80% in some coastal stretches). These coastal segments at the Timan and Varandei coasts alternate with the above-mentioned alongshore spit-like depositional forms.

According to our comprehensive analysis, the shoreline retreat value for the southern coasts of Kolguev Island will be as much as 200-250 m and up to 100-150 m on Vaigach Island by the end of the 21st century.

Discussion

Coastal morphological evolution strongly depends not only on the mean (annual and decadal) sea-level changes but also on the short-term and extreme events represented in the southern Pechora Sea presumably by storm surges superimposed by high tides.

Even presently, storm surges and high tides strongly influence coastal evolution. Their combined elevation above mean sea level varies from 120-150 cm in the outer part of the Pechora and Khaipudyrskaya bays to over 300 cm in the Kolokolkova Bay, the inner part of the Pechora Bay and in several segments of the Khaipudyrskaya Bay (Fig. 4).

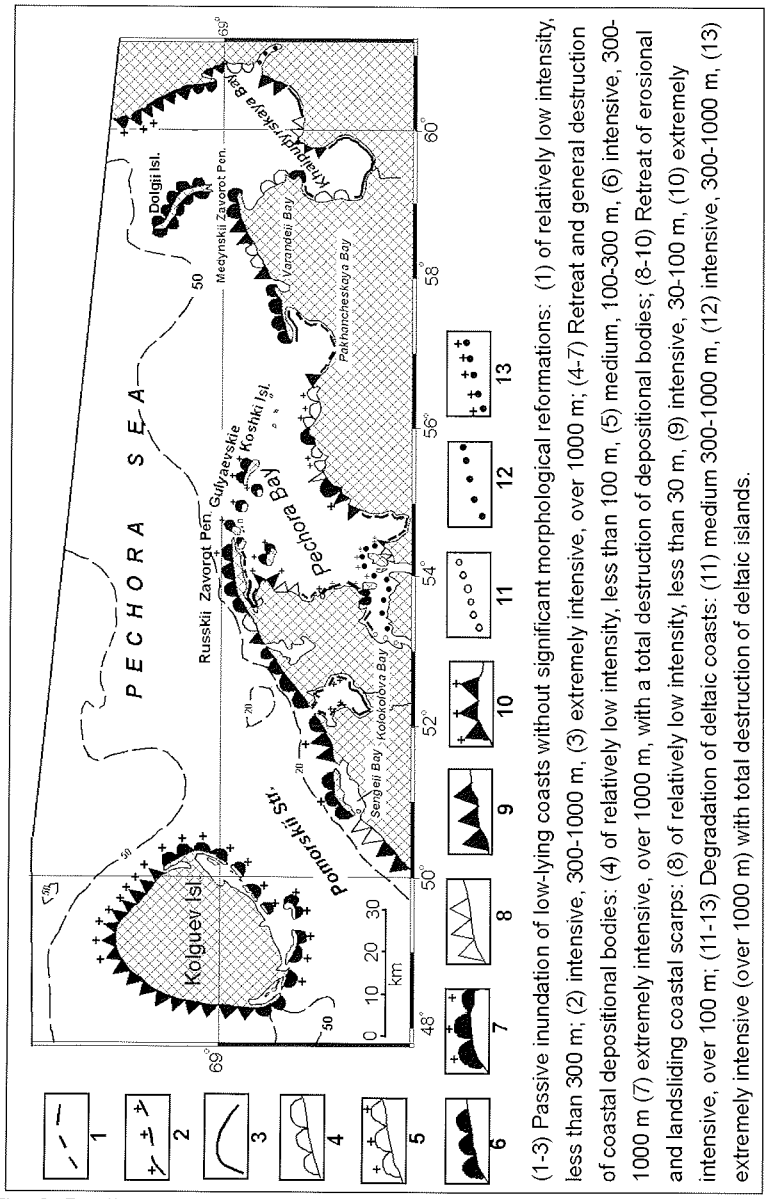

Fig. 3. Predictive map of coastal evolution for the southern Pechora Sea under the anticipating climate changes and sea-level rise during the 21st century

During the high-water periods, the sea inundates surge and tidal flats and adjacent beaches, and reaches the bases of coastal escarpments in icy loose Quaternary sediments, which suffer intensive degradation. Several terrace edges retreat by over 5-6 m during a single event (Are, 1988; Selivanov, 1996; Kaplin and Selivanov, 1999).

The intensity of storm surges depends primarily upon waves at open coasts of the area whereas inner parts of tidal embayments suffer much from high tides. It is problematic to quantitatively predict coastal variations under these short-term sea-level changes.

However, under sea-level changes tidal variations will affect reformation of depositional coasts even if the present tidal heights, elevations and periods will remain stable. Under conditions of high nearshore gradients, which are rarely observed in the study area (Fig. 1E), per square unit energy of tides will decrease with rising sea level (Selivanov, 1996). It will generally favor deposition in the intertidal zone. This phenomenon will be typical of several open stretches of eroding permafrost coastal scarps with narrow beaches such as Varandei Peninsula and most coasts of the Pomorskii Strait.

Lower nearshore gradients will favor an increase of per square unit energy during the tidal cycle thus resulting in a more intensive landward movement of coastal depositional bodies and general nearshore bottom erosion according to the examples shown in Fig. 1C and Fig.1D.

This contrast to wave bottom speed, rates of bottom currents, including tidal ones, are in general proportional to bottom gradients and their dependence on the latter factor is stronger than that of microtidal coasts.

Shallow tidal flats, including those in deltaic areas, are widely spread in the area. A close correlation of sea-level rise and sedimentation rates is of major importance for this type of coast. The predicted general increase of tidal range along with other factors (lower sediment discharge from rivers; degradation of vegetation, etc.) will inevitably result in intensified erosion of tidal flats.

This process will be aggravated in U-type tidal embayments where the entrance is equal in width to or narrower than the inner part of the bay (Carter and Woodroffe, 1997). Most tidal bays of the area, such as Sengei, Kolokolkova, Pechora, Pakhancheskaya and Khaipudyrskaya bays, belong to this type. Relative increase of ebb currents will cause tidal flats to intensively erode. Barrier islands in the outer parts of these bays are doomed to partial degradation. This can cause Sengei, Russkii Zavorot, Varandei and Medynskii Zavorot peninsulas/islands, among others, to degrade in several decades, i.e. faster than according to the predictions for non-tidal regime.

This process can be extreme in Sengei Bay where the tidal range will inevitably increase. Degradation of the barrier separating this bay from the sea is inevitable (see above). However, all the above effects are yet to be quantified.

Moreover, recurrence time of certain extreme events under the possible sea-level rise during this century may, possibly, become less than the corresponding relaxation time in many coastal segments, thus turning coastal evolution to essentially disequilibrium patterns. In some cases shoreline migration can lag

behind equilibrium evolution under sea-level rise, whereas in others it may be more than equilibrium estimates by several times (Pilkey et al., 1993; Selivanov, 1996). The general tendency to the prevalence of coastal erosion over deposition will be amplified by a drastic anthropogenic decrease in river sediment discharge.

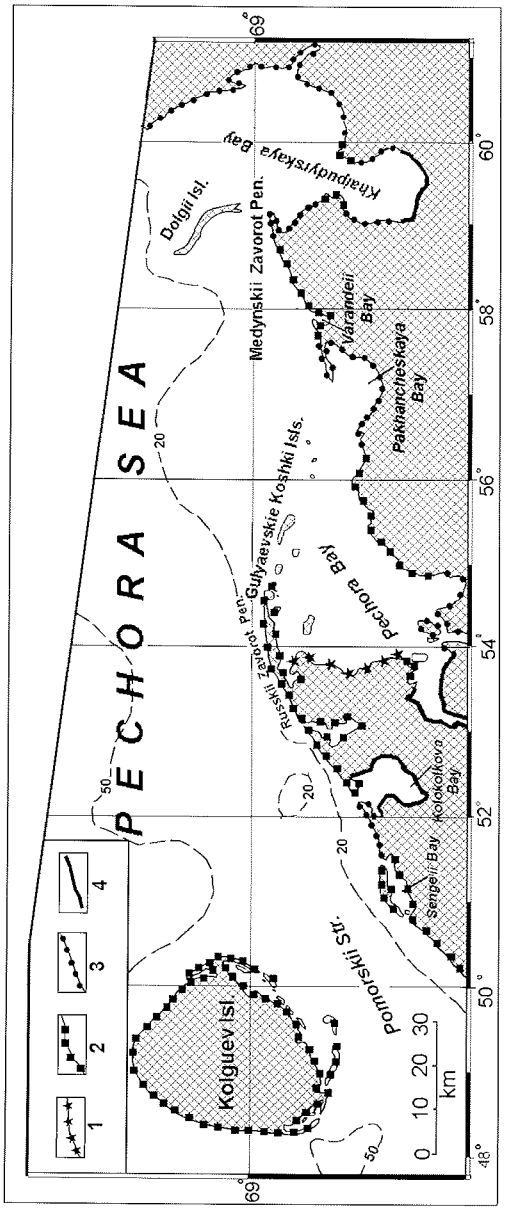

Fig. 4. Map of maximum observed high water elevations in the Pechora Sea (southern coast): (1) less than 150 cm; (2) 150-200 cm; (3) 200-300 cm; (4) over 300 cm

This will be especially true for the Pechora River, which suffers from decreased river runoff at present (van Eerden, 2000). The idea of "southern river transfer" from the Russian Arctic to the Middle Asia revived during the past couple of years can seriously aggravate this problem.

Boundary conditions for a shift of coastal response to the disequilibrium pattern will obviously vary from one coastal type to the other. Coastal barrier islands, spits, and similar detached depositional bodies represent specific coastal features that would certainly be among the most sensitive ones under the anticipated sea-level rise. Our data independently prove the ideas of many other authors that only slow sea-level changes (lower than 2-2.5 mm/year) favor the formation of depositional coastal barriers (Kaplin and Selivanov, 1995; Selivanov, 1997). However, according to the above-mentioned predictions, in the next decades the rate of greenhouse-induced regional and local sea-level rise may possibly become as high as 5-10 mm/year.

Therefore, strict analytical prediction of coastal response to accelerated sea-level rise is yet to be calculated. Analysis of every response pattern of depositional coasts to sea-level changes requires a specific modification of the ZBR. However, these equations should be regarded only as the means to estimate an order of magnitude of shoreline retreat or advance. In many cases these equations cannot be 'assimilated' by coastal morphology (Pilkey et al., 1993). Morphological influence of waves, tides and other marine factors on sea coasts will possibly intensify under the sea-level rise, owing both to direct increase of nearshore depths and higher intensity of wind-induced storms. Therefore, the minimum predictive time of ZBR-based equations will also increase. ZBR-based estimates become meaningless for future shoreline retreat over seasons or successive years under a possible acceleration of sea-level rise. Moreover, more frequent recurrence of certain wave heights requires higher values of a wave base to be included into the equations with other conditions being equal.

Conclusions

Global and regional climate changes during the present century including sea-level rise will inevitably affect many of the Pechora Sea coasts. Principal factors of adverse impact include retreat and degradation of various types of the coasts. Main attention is paid to depositional coasts prevailing in the study area. Semi-quantitative models based on the Zenkovich-Bruun Rule to quantify coastal retreat are proposed and their applicability is discussed. Several genetic series of coastal responses under the influence of various factors, namely nearshore bottom slope, sediment supply, and rate of sea-level rise, are presented. A possible influence of storm surges and tidal movements on coastal evolution is discussed. Our comprehensive methodology for predicting evolution of various coastal types allows us to quantitatively present future coastal evolution of the southern Pechora Sea. In contrast to some investigations of the Arctic littoral zone of Eurasia and adjacent sectors of North America where only estimates of "passive inundation" were achieved to evaluate shoreline retreat under the anticipated global and regional sea-level rise, we are the first to attempt to estimate coastal zone deformations, as well as shoreline position changes. Depositional coastal barriers and ice-rich coastal escarpments will suffer from global and regional changes (warming and mean sea-level rise) to the highest

extent. Additional influence of extreme events such as storm surges and high tides will superimpose annual and decadal changes and can overwhelm them in several areas such as the upper parts of tidal bays.

Acknowledgements: This study was supported by INTAS project 99-1489 and by the Russian Foundation for Basic Research (projects 01-05-64181 and 02-05-65105). The paper is a contribution to the International Geological Correlation Programme (IGCP) Project 437 "Coastal Environmental Change During Sea-Level Highstands".

References

Are, F.E., 1988. Thermal Abrasion of Sea Coasts. Polar Geography and Geology 12. V.H.Winston and Sons. 157 pp.

Are, F.E., 1996. Dynamics of the littoral zone of Arctic seas (state of the art and goals). In: Polarforschung, 64 (3), 123-131.

Barth, M.C., Titus, J.G., 1984. Greenhouse effect and sea level rise: a challenge to this generation. New York, Van Nostrand Reinhold, 325 pp.

Bruun, P., 1962. Sea level rise as a cause of shore erosion. J. Waterways and Harbour Division, ASCE, 88 (WW1), 117-130.

Bruun, P., 1988. The Bruun rule of erosion by sea-level rise: a discussion on large-scale two- and three-dimensional usages. J. Coast. Res., 4, 4, 627-648.

Carter, R.W.G., Woodroffe, C.D. (eds.), 1997. Coastal evolution: Late Quaternary shoreline morphodynamics. Cambridge Univ. Press, 517 pp.

Danilov, I.D., 1978. Pleistotsen morskikh subarkticheskikh ravnin (Pleistocene of marine Subarctic plains). Moscow, Izd. MGU, 198 pp. (in Russian).

Dean, R.G., Maurmeyer, E.M., 1983. Models for beach profile responses. In: Komar, P.D. (ed.), Handbook of coastal processes and erosion, CRC Press, Boca Raton, 151-166.

Dolotov, Yu.S., 1992. Possible types of coastal evolution associated with the expected rise of the World's sea level caused by the greenhouse effect. J. Coast. Res., 8, 719-726.

Dubois, R.N., 1990. Barrier-beach erosion and rising sea level. Geology, 18, 11, 1150-1152.

Eddington, P.A., Andrews, J.T., 1989. Sea level are changing. Geos, 18, 15-22.

Emery, K.O., Aubrey D.G., 1991. Sea levels, land levels, and tide gauges. N.Y. e.a., Springer-Verlag, 237 pp.

Esin, N.V., Kuklev, S.B., 1992. Mathematical model of shoreline retreat under sea-level changes. In: Aibulatov, N.A., Lukyanova, S.A. (eds.), Coastal Evolution Under the Global Sea Level Rise, Moscow, Inst. Oceanol. RAN, P. 25-31 (in Russian).

Esin, N.V., Savin, M.T., Zhilayev, A.P., 1980. Abrazionnye protsessy na morskikh beregakh (Erosional processes on sea coasts). Leningrad, Gidrometeoizdat, 200 pp. (in Russian).

Giese, G.S., Aubrey, D.G., 1987. Loosing coastal uplands to relative sea-level rise: 3 scenarios for Massachusetts. Oceanus, 30, 16 -22.

Gornitz, V., 1993. Sea-level rise: recent past and future trends. Abstr. 3rd Int. Geomorphol. Conf. Hamilton, Canada, August 1993,147.

Ignatov, E.I., Kaplin, P.A., Lukyanova, S.A., Soloviova, G.D., 1993. Influence of the recent transgression of the Caspian Sea on its coastal dynamics. J. Coast. Res., 9 , 1, 104-111.

Kaplin, P.A., 1973. Noveishaya istoriya poberezhii Mirovogo okeana (Recent history of the World Ocean coasts). Moscow, Izd. MGU, 265 pp. (in Russian).

Kaplin, P.A., 1989. Shoreline evolution during the twentieth century In: Ayala-Castanares, A., Wooster, W., Yaner-Arancibia, A. (eds.), Oceanography'1988. Mexico, Autonomous Univ.Press, 59-64.

Kaplin, P.A., 1995. L'evolution future des cotes arctiques de la Russie. Norois, 42, 165, 37-48.

Kaplin, P.A., Selivanov, A.O., 1995. Recent coastal evolution of the Caspian Sea as a natural model for coastal responses to the possible accelerated global sea-level rise Marine Geology. 124, 1/4, 161-175.

Kaplin, P.A., Selivanov, A.O. (eds.), 1997. Razvitie morskikh beregov Rossii i ikh izmeneniya pri vozmozhnom pod'eme urovnya Mirovogo okeana (Evolution of sea coasts in Russia and their changes under possible global sea-level rise). Lomonosov Moscow, Izd. MGU,. 307 pp. (in Russian).

Kaplin, P.A., Selivanov, A.O., 1999. Izmeneniya urovnya morei Rossii i razvitie beregov: proshloe, nastoyashchee, budushchee (Sea-level changes and coasts of Russia: past, present, future). Moscow, GEOS, 299 pp. (in Russian).

Kay, R., 1990. Assessing the risks to the UK coastline from greenhouse-gas-induced sea-level rise. In: Littoral'1990: Compt. rend. Symp.int. Assoc. europ. EUROCOAST, Marseille, 325-329.

Klige, R.K., 1990. Influence of global climatic processes on the hydrosphere regime. In: Paepe, R., Fairbridge, R.W., Yelgersma, S. (eds.), Greenhouse effect, sea level and droughts, Dordrecht e.a., Kluwer, 165-181.

Leatherman, S.P., 1989. Response of sandy beaches to sea-level rise. In: Scott, D.B. et al. (eds.), Late Quaternary sea-level correlations and applications. Dordrecht, Kluwer Acad. Publ., 57-69.

Neumann, A.C., Macintyre, I.G., 1985. Reef response to sea level rise: keep-up, catch-up, or give-up. In: Proc. 5th Int. Coral Reef Symp., v.3, 105-110.

Pilkey, O. H., Davis, T. W., 1987. An analysis of coastal recession models: North Carolina coast. In: Nummedal, D., Pilkey, D.H., Howard, J.D. (eds.), Sea-level fluctuation and coastal evolution. S.E.P.M. (Society for Sedimentary Geology) Special Publication, 41, Tulsa, Oklahoma, 59-68.

Pilkey, O.H., Young, R.S., Riggs, S.R., Smith, A.W.S., Wu, H., Pilkey, W.D., 1993. The concept of shoreface profile of equilibrium: a critical review. J. Coast. Res., 9 , 1, 255-278.

Reimnitz, E., Graves, S.M., Harper, J., 1990. A review of beach nourishment from ice transport of shoreface materials, Beaufort Sea, Alaska. J. Coast. Res., 6, 439-470.

Schwartz, M.L., 1967. The Bruun theory of sea-level rise as a cause of shore erosion. J. Geol., 75, 76-91.

SCOR Working Group'89, 1991. The response of beaches to sea-level changes: A review of predictive models. J. Coast. Res., 7, 4, 895-921.

Selivanov, A.O., 1996. Izmeneniya urovnya Mirovogo okeana v pleistotsene-golotsene i razvitie morskikh beregov (Global sea-level changes during the Pleistocene-Holocene and evolution of sea coasts), Moscow, Schwartz, 267 pp. (in Russian).

Selivanov, A.O., 1997. Coastal modifications on the Caspian Sea and other Central Asian lakes as natural models for coastal responses to the global sea-level rise. Bol. geofisica. teor. ed appl., 38, 3-4, 255-266.

Shuiskii, Yu.D., 1986. Problemy issledovaniya balansa nanosov v beregovoi zone morei (Problems of studies of sediment budget in marine coastal zones). Leningrad, Gidrometeoizdat, 240 pp. (in Russian).

Spencer, T., 1993. Geomorphology of coral reefs: response to the sea-level rise in the past, present and future. In: Abstr. 3rd Int. Geomorphol. Conf. Hamilton, August 1993, 102.

Summary for policymakers: A report of working group I of the intergovernmental panel on climate change, 2002. Den Hague, 20 pp.

Tutus, J.G. (ed.), 1988. Greenhouse, sea level rise and coastal wetlands. Wash., D.C., Environ. Protect. Agency, 152 pp.

Tooley, M.J., Jelgersma, S., 1992. Impacts of sea-level rise on European coastal lowlands. Oxford et al., Basil Blackwell, 450 pp.

van Eerden (ed.), 2000. Pechora delta: Structure and dynamics of the Pechora delta ecosystems (1995-1999). Inst. Inland Water Management and Wastewater Treatment. 367 pp.

Weggel, R.J., 1979. A method for estimating long-term erosion rates from a long-term rise in water level. In: Coastal Eng. Techn. Aid, 79-2, 80 pp.

Zenkovich, V.P., 1967. Processes of coastal development. Edinburgh, Oliver and Boyd, 738 pp.

Zenkovich, V.P., Popov, B.A. (eds.), 1980. Morskaya geomorphologiya. Beregovaya zona: terminologicheskii slovar' (Marine geomorphology. Coastal zone: Terminological glossary). Moscow, Mysl', 210 pp. (in Russian).

Zhigarev, L.A., 1997, Okeanicheskaya kriolitozona (Oceanic cryolithozone). Moscow, Izd. MGU, 320 pp. (in Russian).

MODELING THE SEDIMENTARY EVOLUTION OF THE PECHORA SEA COAST

I.O. Leont'ev

Shirshov Institute of Oceanology RAS, Moscow, Russia

Abstract

This work uses morphodynamic modeling to predict the long-term evolution (over the next 100 years) of typical sedimentary coasts in the Varandei region situated in the southeastern part of the Barents Sea, called the Pechora Sea. The model takes into account not only short-term processes (storm events) but also long-term factors (for example, changes in sea level, interannual variations in gross sediment flux, lack or excess of sediment supply). It is revealed that under the given environmental conditions the morphological evolution is strongly influenced by storm surges and associated wind-driven circulation. The water level gradient created by a surge generates a seaward flow at the bottom. This outflow is shown to be an important destructive mechanism contributing to the erosion and recession of Arctic coasts. The rate of change is found to depend on coast elevation above sea level. Lower cliffs ($\leq$ 5 m height) are expected to recede by as much as 300-500 m over 100 years, while higher cliffs (8-10 m height) can be eroded by only about 60-80 m. It is concluded that the expected relative sea-level rise (up to 1 m over the next 100 years) is non-crucial for the future coastal evolution since erosional activity is already considerable.

Introduction

Coasts composed of unconsolidated easily movable sediments (mainly sands) occur in all seas of the Russian Arctic (also along the Alaskan and Canadian Arctic margin) and occasionally serve as a basis for economic activity in neighboring territories. At present, processes of erosion and recession predominate at most Arctic shores. Coastal erosion may result in destruction of nearshore structures and pipelines for oil and gas recovered from the continental shelf and adjacent land. Developing effective models for quantitative prediction of coastal change in the Arctic environment can significantly enhance engineering design and coastal management practice.

The present work attempts to predict the evolution of some typical sedimentary coasts of the Varandei region (Fig. 1) in the Pechora Sea during the next 100 years. The method employed is numerical modeling of nearshore morphodynamics. Previously developed models of large-scale coastal behavior have allowed successful hindcast (and forecast) of long-term morphological changes of the coasts of Holland (Stive and De Vriend, 1995) and Southeast Australia (Cowell et al., 1995). The model used in the present study differs somewhat in the manner of aggregating short and long-term variables. Besides, it involves additional variables playing an important role in the coastal zone of the shallow Arctic seas.

Most Arctic coasts are influenced by various high-latitude processes, such as thermal erosion, thaw subsidence, retrogressive thaw failure, thermal niching (Are, 1985; Forbes and Taylor, 1994). These phenomena, however, are beyond the scope of the present work concentrating on coasts whose dynamics is primarily controlled by wave and wind-induced sediment transport mechanisms and only to

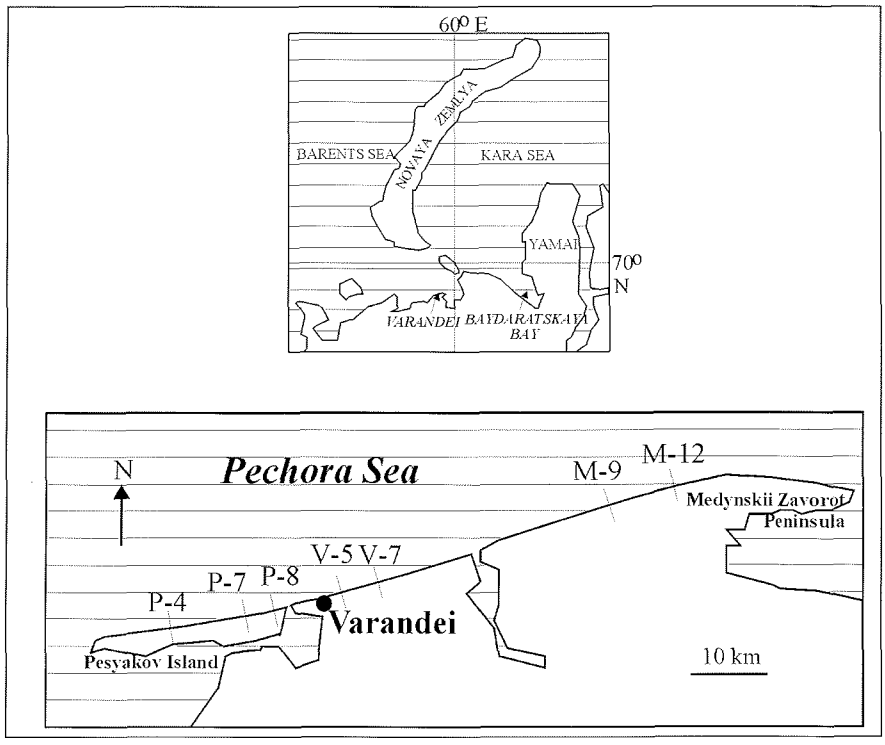

Fig.1. Disposition of reference coastal profiles in studied region of the Barents Sea

a minor extent by thermal factors. In particular, such environmental conditions occur in the Pechora Sea.

Morphological changes in polar regions may also be caused by sea-ice impact on the shore and nearshore bed. But this factor has not yet been included in the present model.

The causes and mechanisms behind the observed recession of Arctic coasts are non-transparent in many cases. Modeling helps to reveal additional mechanisms responsible for this phenomenon.

Environmental conditions

An important factor influencing the recent and future behavior of Arctic coasts is a global sea-level rise due to both ice melting and thermal expansion of the ocean surface layer as a result of global warming. The latest consensus on the mean sea-level rise from 1990 to 2100 is between 0.09 and 0.88 m with an average value close to 0.5 m corresponding to a rate of rise of about 0.005 m/year (Church et al., 2001).

Changes in relative sea level may also be due to tectonic motions in the lithosphere. In accordance with available data (Kaplin et al., 1991), the continental platform in the region of interest subsides at a rate of 2-5 millimeters per year. That

is quite comparable with the above-mentioned value due to global warming. Therefore, a representative rate of the relative sea-level rise in a given region can be around 0.01 m/year. This value will be used henceforth.

Global warming may also lead to a decrease in the total area of drifting ice fields and an increase in the ice-free water area near the coast in summer (Anisimov et al., 2001). Thus, the extent of wind action becomes greater and, moreover, surface waves can be generated in deeper water. As a result, the height and energy of storm waves attacking the shore will increase with time, and so will the height of storm surges. These trends are most important for the central and eastern Russian Arctic coasts, where the most severe ice conditions now exist. In the western Russian Arctic the drift ice edge at present is observed at a relatively large distance from the coast in summer. So, possible changes in wave parameters would be comparatively insignificant. It seems that the first-step predictions of coastal evolution in the chosen Arctic regions may be based on the assumption that wave activity is kept at recent levels. It should be noted that due to increasing duration of the open-water season, the probability of severe wave and surge events might also increase. Estimating this influence, however, is the task of future studies.

A noticeable feature of the Pechora Sea is its shallowness. Relatively small depths occur far offshore and restrict the heights and lengths of waves generated in the open sea. Besides, a very gentle bed slope (usually less than 0.01) leads to a gradual decay of the incoming waves. Approaching the coast, they tend to become more uniform in height. As a consequence, near the shire wave heights vary in a relatively narrow range, while the open-sea storm conditions are much more variable.

Due to the gradual dissipation of wave energy, the radiation stress gradients in the nearshore zone are small, and wave-driven mean currents are relatively weak. At the same time, environmental conditions are favorable for the development of storm surges reaching 1.5-2 m. Associated water level gradients induce a seaward flow near the bottom, which balances the onshore mass flux created by wind shear stress at the free surface. Such a return current or outflow is found to be comparable in strength to the wave-induced mass transport at the bed (see Appendix). Hence the wind-generated outflow can work as an additional offshore sediment transport mechanism, which should be incorporated into morphodynamic modeling (Hequette et al., 2001).

Morphodynamic model

Existing approaches to modeling shoreface profile evolution are grouped into two classes depending on the temporal and spatial scales of processes investigated. The short-term or *event scale* morphological changes are simulated by involving the whole chain of elementary driving mechanisms (waves, currents and sediment transport) responsible for local deformations of a given cross-shore profile (Nairn and Southgate, 1993; Leont'ev, 1999). On the contrary, models of coastal behavior at *engineering or geological scales* operate with long-term morphodynamic factors (sea-level rise, deficit or excess in lateral or cross-shore sediment supply and others) while incorporating only the aggregated contribution of short-term primary mechanisms (Stive and De Vriend, 1995, Cowell and Thom, 1995, De Vriend, 1997).

Combining these two approaches, the author (Leont'ev, 2001) has proposed a hybrid-type model that allows simulating coastal profile behavior at temporal scales ranging from days (*event scale*) to tens of years (*engineering scale*). The model is based on the sediment conservation equation, to which the short-term and long-term constituents contribute as follows:

$$\frac{\partial d}{\partial t} = \frac{\partial q_x}{\partial x} + \frac{q_{AEOL} + \Delta Q / \Delta y - q_*}{l_*} + w \qquad (1)$$

During a given storm event, the principal contributions to the mass balance over the shoreface profile are the gradients of cross-shore sediment transport rates q_x, created by waves and currents (axis *OX* is directed onshore, *d* is the still-water depth, *t* is the time). Sediment balance at temporal scales of years and decades is mainly controlled by alongshore gradients of the bulk shore-parallel sediment flux $\Delta Q / \Delta y$, and also the factors q_{AEOL} (eolian transport) and q_* determining the long-term sediment discharges across the upper and the lower limits of the active zone, respectively. If needed, the contributions of other possible sediment sources or sinks may be included. All long-term contributions are averaged over the length of the profile active zone, l_*, where the bed deformations are most pronounced. Besides, changes in depth may be due to long-term variations in relative sea level (caused by climate changes or tectonic motions) and those are characterized by the rate *w*.

Influences of long-term variables result in gradual changes in reference levels of water surface $\overline{z_0}$ and bed $\overline{z_b}$,

$$\overline{\Delta z_0} = w \Delta t, \qquad \overline{\Delta z_b} = -\frac{q_{AEOL} + \Delta Q / \Delta y - q_*}{l_*} \Delta t \qquad (2)$$

The value of $\overline{\Delta z_b}$ expresses the averaged thickness of the sediment layer (positive or negative) deposited or eroded during the time lapse Δt, in the order of years. The magnitude of $\overline{\Delta z_0} / \Delta t$ in accordance with the above mentioned estimation is taken as 0.01 m/year.

A flow chart of the model is shown in Fig. 2. Numerical procedure includes two cycles providing the calculations of short and long-term morphological changes. Within the inner cycle the process-based morphodynamic model is employed to simulate the development of coastal profile under storm conditions occurring once per year (also taking into account the corresponding surge height). These conditions are assumed to be able to determine the principal shoreface profile geometry. Consequences of more frequent weak storms are supposed to be mainly shoreline oscillations and migrations of longshore bars (if those exist).

At each time step of the inner cycle, at first the wave shoaling, refraction and dissipation are computed. Then the near-bed currents (wave-induced mass transport and wind-generated outflow) and sediment transport rates are determined (see details in the next section). Finally, the new depths are derived from the Eq. (1) in which only the first term on the right-hand part is involved. Calculations continue until the coastal profile stabilizes. The time t_e needed to form a quasi-equilibrium beach profile (under a steady storm) amounts usually to about 10-20 hours (Leont'ev, 2001).

It should be noted that the model is capable of simulating an avalanche, if the local

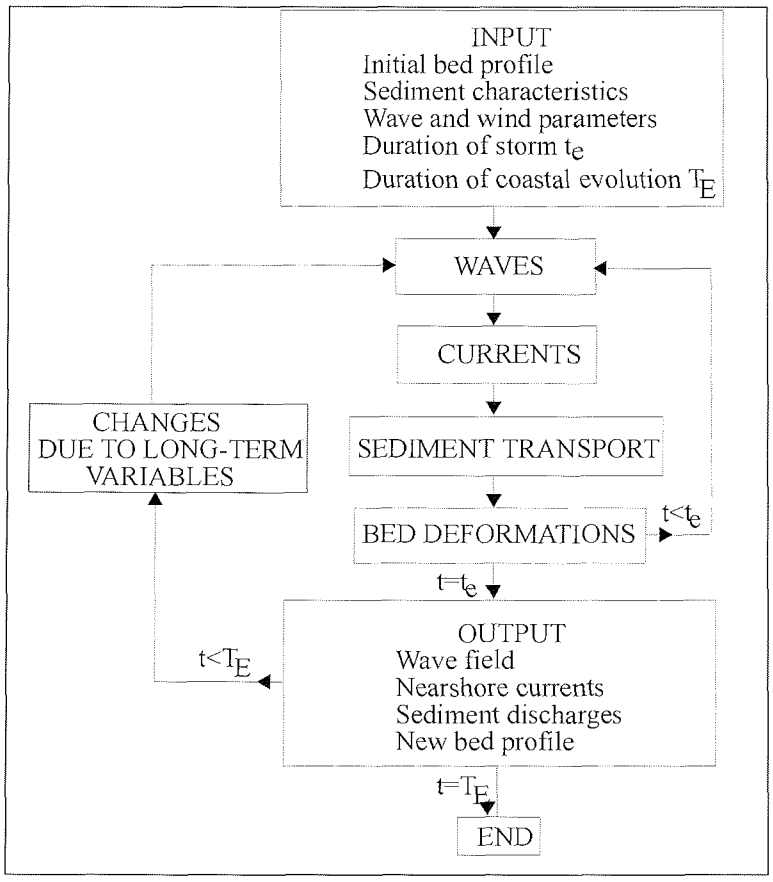

Fig.2. Flow chart of the morphodynamic model

depth gradient would exceed the threshold of slope stability (Leont'ev, 1996). Avalanche causes perturbations in profile also above the run-up limit, and the model allows reproducing morphological changes over the whole cliff height.

Within the outer cycle of numerical procedure computed depths are adjusted in response to long-term influence by inclusion of quantities $\overline{\Delta z_0}$ and $\overline{\Delta z_b}$. The resulting profile serves as the initial one at the next stage of calculations. In a given case the period of interest, T_E, is one century, and with Δt taken as 1 year the total number of time steps in the outer cycle is 100 for each run.

As to the length of the profile active zone l_*, that model parameter is to be determined empirically. For the Arctic coasts with a very gentle foreshore and steep escarpment the most appropriate scale of l_* was found to be a swash-zone length determined below. Due to non-linearity of the modeling system this length oscillates from step to step in the course of numerical procedure.

Sediment transport concept

Sediment transport rates of two kinds are distinguished in the nearshore region (Fig. 3): the rates q_W generated by wave/current mechanisms in wave-shoaling and surf zones, and rates q_R due to run-up in the swash zone (Leont'ev, 1999, 2001). The adopted conventional border between the swash and surf zones, X_W, as seen from Fig. 3, corresponds to a depth equal to the input *rms* of wave height H_{rms0}. Points X_C and X_R denote the positions of the coastline and the upper limit of run-up. Thus the general expressions for sediment transport rates are

$$q_x, q_y = \begin{cases} q_{Wx}, q_{Wy}, & x < X_W \\ q_{Wx} + q_{Rx}, q_{Wy} + q_{Ry}, & X_W \le x \le X_C \\ q_{Rx}, q_{Ry}, & X_C \le x \le X_R \end{cases} \qquad (3)$$

where

$$q_W = \begin{cases} q_W^0 - 2s\sqrt{q_{Wx}^{0\,2} + q_{Wy}^{0\,2}} & x \le X_W \\ q_W(X_W)[(x - X_W)/(X_C - X_W)]^{1.5} & X_W \le x \le X_C \end{cases} \qquad (4)$$

and

$$q_R = \begin{cases} \hat{q}_R[(x - X_W)/(X_C - X_W)]^{0.5} & X_W \le x \le X_C \\ \hat{q}_R[(X_R - x)/(X_R - X_C)] & X_C \le x \le X_R \end{cases} \qquad (5)$$

where $q_W = (q_{Wx}, q_{Wy})$, $q_R = (q_{Rx}, q_{Ry})$ and $s = (s_x, s_y)$ are the local bed slopes ($s_x = -\partial d/\partial x$, $s_y = -\partial d/\partial y$).

Quantities q_{Wx}^0 and q_{Wy}^0 express the cross-shore and longshore sediment discharges over the horizontal bed (with zero slopes)

$$q_{Wx}^0 = GU, \qquad q_{Wy}^0 = GV \qquad (6)$$

where *U* and *V* are the mean flow velocities near the bed (at the edge of wave boundary layer) and *G* is the conventional characteristic of immersed weight of moving grains per unit area depending on the rate of wave energy dissipation (Leont'ev, 1999, 2001).

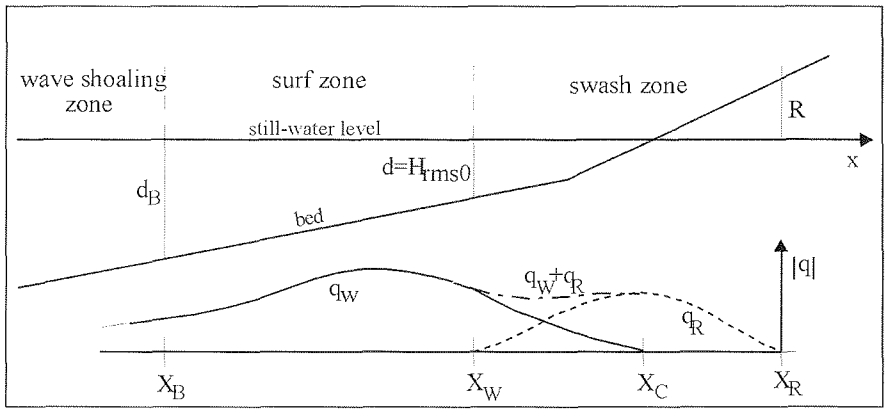

Fig.3. Scheme of the nearshore zone

Velocities *U* and *V* include the contributions of wave-induced mass transport (U_W^B, V_W^B) and horizontal circulation (U_C^B, V_C^B) and also additional currents generated, for instance, by wind (U_{wind}^B, V_{wind}^B):

$$U = U_W^B + U_C^B + U_{wind}^B, \quad V = V_W^B + V_C^B + V_{wind}^B \tag{7}$$

Velocities U_W^B and V_W^B are determined from the semi-empirical equation which is close to the well-known expression of Longuet-Higgins (1953) for the mass transport velocity at the edge of the boundary layer, if there is no wave breaking, and bed ripples are absent (Leont'ev, 1999, 2001).

Quantities U_C^B and V_C^B are derived from the depth-averaged velocities determined, in turn, from the system of momentum and mass balance equations (Leont'ev, 1999, 2001). In a one-dimensional case considered in the present work, U_C^B disappears (as the total cross-shore water flux is zero) and V_C^B is the longshore current velocity generated by obliquely incident waves.

The onshore steady wind creates the shear stress, which is balanced by a pressure gradient due to a mean sea level rise η (wind set-up). As a result the offshore mean flow is generated, of which the near-bed velocity is estimated by (see Appendix):

$$U_{wind}^B = -0.0007 \frac{W^2}{\sqrt{g(h+\eta)}} \cos\Theta_{wind}, \qquad h = d + \zeta \tag{8}$$

where *W* is the wind speed, Θ_{wind} is the angle between the wind direction and the shore normal, and ζ is the wave set-up. In case of relatively steep waves shoaling over a gentle slope, U_{wind}^B may be greater in absolute value than the wave-induced mass-transport velocity U_W^B directed toward the shore outside the breaking region (see Fig. A1). As a result, the offshore transport can dominate over the whole coastal profile. The longshore component V_{wind}^B is usually small compared to the wave-generated longshore current velocities.

The maximum cross-shore sediment discharge in the swash zone ($\hat{q}_{Rx}$ in Eq. 5) is proportional to the height of run-up and depends on the difference between the equilibrium and actual beach slopes $(\beta_{eq} - \beta)$. Sediments move offshore if $\beta > \beta_{eq}$. The expression of β_{eq} is based on the relationship of Kriebel et al. (1991).

The volumetric sediment discharges used in Eq. (1) are obtained by dividing q_x by $g(\rho_s - \rho)(1-\sigma)$, where ρ is the water density, ρ_s and σ are the density and porosity of sediments, respectively.

Coastal evolution in the Varandei region

Varandei and the adjacent coasts of Pesyakov Island and Medynskii Zavorot Peninsula (Fig. 1) are parts of a common morphodynamic system extending about 100 km along the shore. The coast in this region is formed by a 2-6 km wide marine terrace. The seaward edge of the terrace in most places is defined by a 3 to 10 m cliff (Figs. 5, 6). The sediment body is mostly composed of fine sands (mean grain size is about 0.18 mm) with inclusions of organic detrital material. The ice content is not more than 5-10% of the total sediment volume. Thermal abrasion occurs locally and does not play significant role in coastal dynamics (Ogorodov et al., 2001). The amplitude of tide is insignificant (about 0.5 m). In recent times, the coastal cliffs throughout this area have been retreating at the rates of 1-4 m/year. Locations of surveyed reference profiles are denoted in Fig. 1.

The bed slopes over the adjacent inner shelf are much less than 0.01, and bottom topography is rather uniform in alongshore direction (Fig. 4a). These peculiarities result in the restriction of wave parameters (at 10-m depth the once-per-year *rms* heights vary from 1.3 to 1.6 m depending on wave direction) and also provide a relative uniformity of alongshore sediment flux. Fig. 4b shows the computed distributions of the bulk longshore sediment discharge *Q* created by the once-per-year storms of each major direction at various points along the coast. The Q values are obtained by integrating the local transport rates q_y over the cross-shore coastal profile. The *Q* magnitudes are estimated in tens and hundreds of m^3/h, but alongshore gradients $\Delta Q/\Delta y$ are only of the order 10^{-2} $m^3/m/h$. Even with the hypothetical highly exaggerated 100-hours duration of the once-per-year storm event the gradients of sediment discharge would not exceed 1 $m^3/m/year$. In addition, sediment fluxes of the two opposite directions along the coast partly compensate each other.

Thus, within this study area, the term $\Delta Q/\Delta y$ does not contribute significantly to the sediment balance expressed by Eq. (1). Therefore the coast recession can be related to other factors – eolian transport q_{AEOL} carrying sand material landward away from the shore, and q_* representing the net seaward movement of sediment. Erosion due to eolian deflation, as observed by Ogorodov et al. (2001), is highly developed due to numerous interruptions of vegetative cover and actually results in local lowering of the coast. As to the offshore flux q_* across the seaward boundary of the active profile zone, it may be caused by the return flow generated during storm surges.

Since the total sediment discharge $q_{AEOL} - q_*$ is unknown a priori, the preliminary calibration of the predictive model is done using available data on changes in

coastal profile over a sufficiently long period of time (one decade, at least). Data of this kind obtained by Ogorodov et al. (2001) for profile V-5 are presented in Fig. 5a, which shows the coastal recession by approximately 35 m during a 12-year time interval (or about 3 m/year). The task of calibration is to find the optimal value of $q_{AEOL} - q_*$ which provides the best agreement of computed and measured morphological changes. Calculations were performed under typical storm conditions: wind speed = 20 m/s, *rms* wave height = 1.5 m at 10-m depth (corresponding significant height = 2.1 m), mean period = 5.2 s, storm surge level = 1.5 m (all parameters were computed using the data on wind and sea bathymetry). The volume of sediment deficiency was estimated as 10 m^3/m/year. The respective predicted profile 1 is also shown in Fig. 5a.

In case of profile V-5 the swash-zone width determining the active profile length l_* is almost equal to the extension of the beach section located over the mean still water level and submerged during storm surges (with inclusion of the run-up extension). On average the l_* value is approximately 30 m (Fig. 5a) while varying in the range of 15-50 m from step to step (from year to year) during a numerical procedure. Hence the found sediment deficiency corresponds to $\overline{\Delta z_b} / \Delta t = -(q_{AEOL} - q_*)/l_* \approx -0.3$ m/year. In other words, the lack of material results in a sediment layer of about 0.3 m being removed from the beach surface every year.

The computed profile 2 in Fig. 5a refers to the situation if the contribution of wind-driven outflow in the short-term transport rate q_x is ignored ($U^B_{wind} = 0$). Exclusion of this factor, evidently, leads to a significant underestimation of coastal recession. Therefore, the additional offshore mean flow noticeably enhances the erosion capability of waves (especially if the wave period is relatively short, as in this case).

Evolution of coastal profile V-5 over the next 100 years was also simulated with the above estimated value $q_{AEOL} - q_*$=10 m^3/m/year. To assess the influence of relative sea-level rise, the calculations were performed with two different rates (0.01 and 0.005 m/year) and, besides, with a constant sea level. The results obtained are shown in Fig. 5b, c and d. Initial profile shapes remain almost unchanged in the course of the evolution. With a higher rate of water level rise the coast retreats more rapidly, but this difference is not large in general. After 100 years the scarp break is displaced landward by 290 m at w=0.01 m/year, by 260 m at w=0.005 m/year, and by 250 m at w=0. In the first case the averaged rate of the scarp movement is almost kept at a recent level (about 3 m/year), while in the latter case it is reduced by about 17%. That means that under the given environmental conditions the sea level changes play a secondary role as compared with other factors involved.

It can be also seen from Fig. 5b, c and d that in all cases the recession of coast is slightly retarded with time. A possible reason is a gradual decrease in the foreshore slope and accompanied lowering of waves attacking escarpment (since the wave energy is dissipated over a greater extension).

Cross-shore profiles at various points along the Varandei coast (see Fig. 1a) are shown in Fig. 6 (reference morphological data were kindly provided by Dr. S.A. Ogorodov from Moscow State University). Due to variability of reference profile geometry, the long-term losses of sediments in each case may differ significantly.

However having no calibration data we can argue only for two different estimates of sediment deficiency.

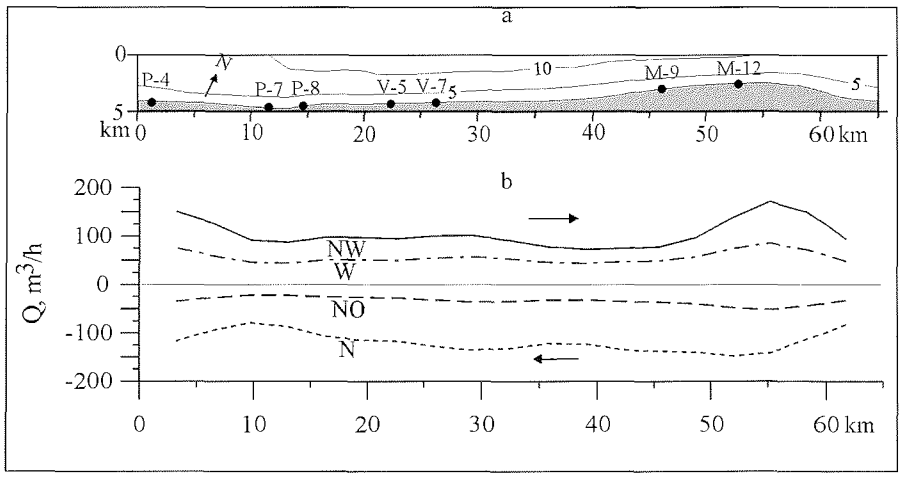

Fig.4. Bottom contours (a) and distributions of total longshore sediment discharges during the once-per-year storms of major directions (b) in Varandei region

Profile V-7, as V-5, is situated within the coast section with the most active erosion. In this case the former quantity of sediment losses of 10 m^3/m/year seems to be appropriate. In adjacent coastal areas, the observed rates of shore recession are reduced on average by half (Ogorodov et al., 2001). It may be expected that the volumes of sediment deficiency diminish there in the same proportion. Based on this assumption, the modeling of long-term behavior of profiles P-4, P-7, P-8, M-9 and M-12 was performed with value $q_{AEOL} - q_* = 5$ m^3/m/year. The results of the calculations are shown in Fig. 6.

Obviously, intensity of coastal recession depends on elevation of escarpment above sea level. In case of a very low and gently sloping beach (profile P-8) the shoreline retreats by about 0.5 km over the next 100 years. Unlike profile V-5 considered above the recession of profile P-8 is strongly influenced by sea-level rise. A passive submergence alone would lead to the coast being displaced by about 180 m.

The behavior of higher coasts (with 4-6 m high cliff) is similar to that of profile V-5. The landward shift of the scarp break is about 260 m in case V-7, while it is 150-160 m in cases P-4 and P-7, for which half the amount of background losses of sediments are supposed. The recession of the highest cliffs M-9 and M-12 elevated by 8-10 m attains only 60-80 m and, as found from computations, only slightly depends on the rate of sea-level rise (in the limits assumed).

When the cliff height does not exceed 6 m, the recession slowly decreases with time as it was previously noted for profile V-5. However the higher scarps (M-9 and M-12) demonstrate almost inverse behavior. Retardation of erosion would be possibly manifested over a greater period of time.

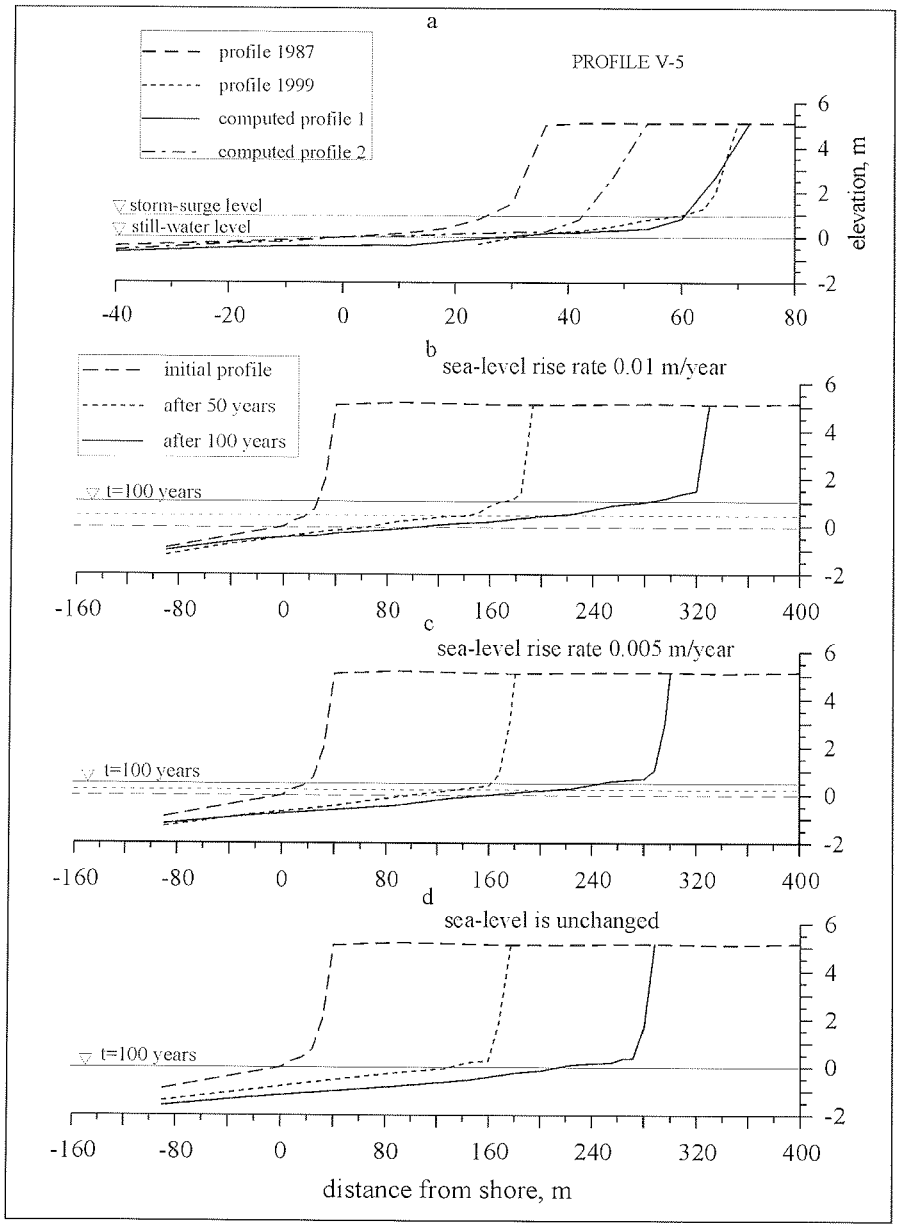

Fig.5. Recent dynamics and predicted evolution of profile V-5 in Varandei region. (a) comparison of observed changes and results of computations with sediment deficiency volume 10 $m^3/m/year$; profiles 1 and 2 are computed with and without contribution of wind-driven outflow, respectively. (b, c, d) profile behavior over the next 100 years for the rates of sea-level rise 0.01 and 0.005 m/year, and constant sea level, respectively.

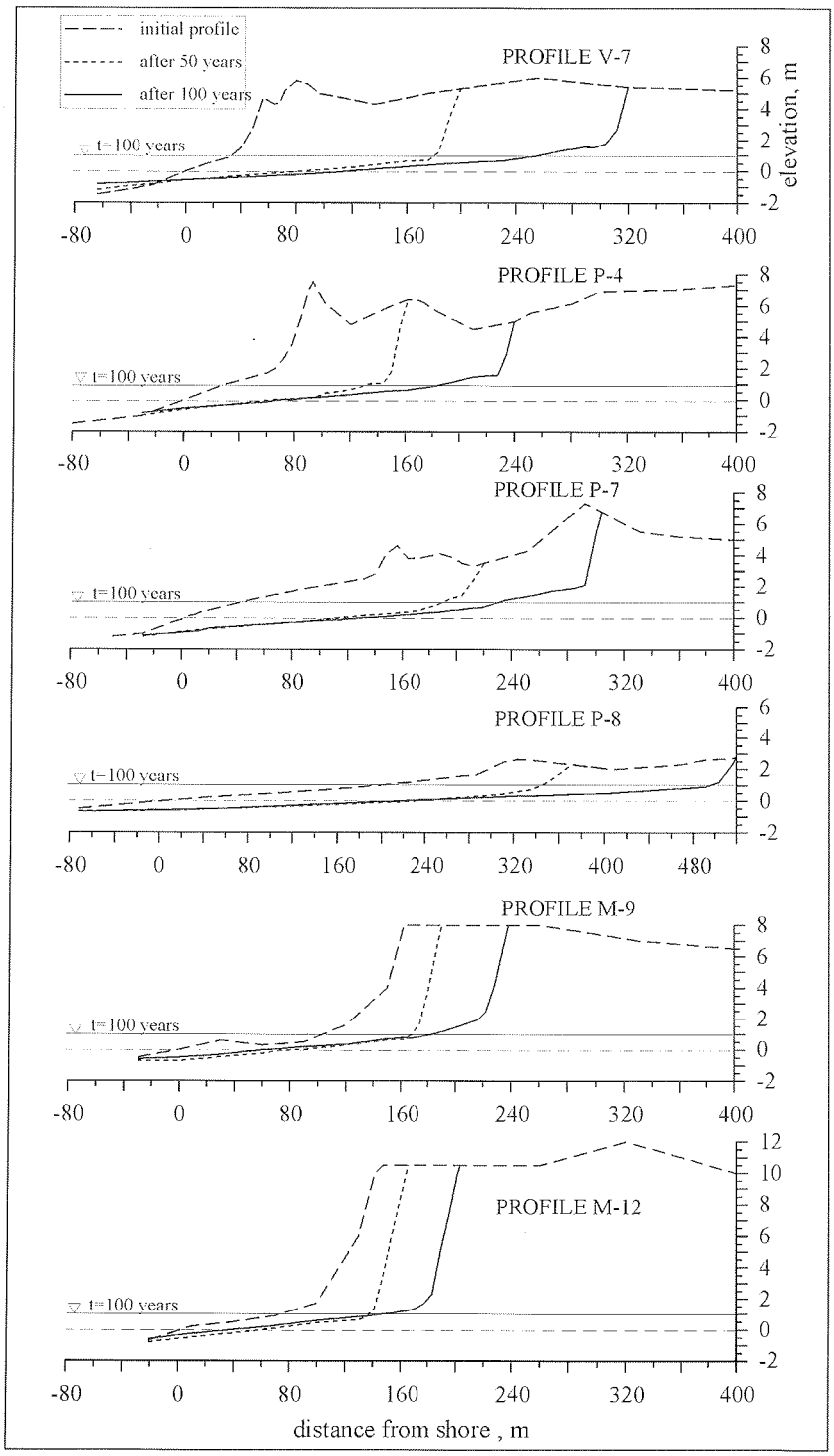

Fig.6. Predicted evolution of coastal profiles in Varandei region

At many sites of the studied area a multiple bar system exists on the coastal slope. This feature, however, causes no limitations in the applicability of the model used, which is capable of generating a break-point bar (Leont'ev, 1999, 2001). An important bar effect is wave lowering due to breaking over the bar crests. As a result the waves at the shoreline are reduced in height as compared with the case of the uniform bed, and in this way a bar system manifests itself as a shore-protecting structure. But with increase in depths during a high storm surge the bar influence weakens and wave lowering should be less pronounced.

Conclusions

Coastal evolution over a given period of time is the aggregated result of morphodynamic processes of various temporal and spatial scales. Accordingly, a mathematical model explaining the observed morphological changes and predicting the future behavior of the coast has to involve the contributions of both short-term storm impacts and relatively slow changes in background environmental conditions. In the present work the modeling evolution at each time step is subdivided into two stages. At first a quasi-equilibrium shoreface profile is determined satisfying the representative storm conditions, and then the profile received is transformed by the influence of parameterized long-term factors.

The results show that the model is capable of reproducing the morphological changes on low-relief sedimentary Arctic coasts. A certain advantage of the present approach is the inclusion of the wind-driven nearshore circulation, in particular, the near-bed outflow ignored in earlier models. In settings characterized by high surge and relatively short-period surface waves, typical of many Arctic coasts including the present study area in the Pechora Sea, the storm-driven outflow is revealed to work as an additional seaward sediment transport mechanism enhancing beach erosion during a storm. This mechanism (along with eolian deflation) can be also responsible for a great part of the long-term loss of sediment material and so may visibly contribute to the observed recession of Arctic coasts.

In the Varandei region a long-term sediment deficiency is evaluated by 5-10 m^3/m/year, while the total erosion volumes (with inclusion of short-term contribution) exceed 15 m^3/m/year in some cases (V-5 in Fig. 5 and V-7 in Fig. 6). The greatest coastline displacements over the next 100 years are estimated to amount to 300-500 m. The typical shoreface profile resulting from the dominant morphodynamic conditions includes a steep scarp and a very gentle foreshore slope (depth gradients < 0.01) to at least 1-2 m depths.

Some recent profiles on coasts of the Varandei region are rather smoothed having only a weakly developed escarpment. That is a sign of low erosion activity due to the present local environmental conditions (for instance, by the peculiarities in bottom topography). This situation can change in the future due to a relative sea-level rise, which can trigger or enhance erosion. The modeling results, however, indicate that the sea-level rise is a minor factor in the future coastal evolution if erosion activity is already high enough and the coast is not very low.

APPENDIX

Wind-driven nearshore circulation

Shear stress τ_x created by steady onshore wind is balanced by a pressure gradient due to a rise of mean sea level η (wind set-up),

$$g\frac{d\eta}{dx}=\frac{\tau_x-\tau_{bx}}{\rho(h+\eta)}, \qquad \tau_x=k\rho W^2\cos\Theta_{wind} \tag{A1}$$

where τ_{bx} is the bed shear stress due to the flow induced, and k is proportionality coefficient of order 10^{-6}. Field studies provide evidence that typically $\tau_x >> \tau_{bx}$ and so the latter value may be neglected (Bretschneider, 1966). The pressure gradient, in turn, must be in balance with the friction forces in the water column. This leads to

$$\nu_Z\frac{d^2U_{wind}}{dz^2}=\frac{\tau_x}{\rho(h+\eta)} \tag{A2}$$

where ν_Z is the vertical eddy viscosity. Integrating Eq. (A2) under conditions of continuity of shear stresses at the free surface and absence of net cross-shore water flux

$$z=h+\eta:\ \nu_Z\frac{dU_{wind}}{dz}=\frac{\tau_x}{\rho}, \qquad \int_0^{h+\eta}U_{wind}dz=0 \tag{A3}$$

we obtain the vertical velocity profile

$$U_{wind}=\frac{\tau_x(h+\eta)}{6\rho\nu_Z}\left(3\tilde{z}^2-1\right), \qquad \tilde{z}=\frac{z}{(h+\eta)} \tag{A4}$$

This profile shown in Fig. A1a along with the laboratory test data of King (1959) indicates the onshore transport in the upper layer and offshore flow in the lower part of the water column ($0\le\tilde{z}\le 1/\sqrt{3}$). With the eddy viscosity in the form (Stive and Wind, 1986)

$$\nu_Z=b(h+\eta)\sqrt{g(h+\eta)} \tag{A5}$$

the near-bed outflow velocity U^B_{wind} (at $\tilde{z}=0$) is determined from Eq. (A4) as

$$U^B_{wind}=-\frac{1}{6}\frac{k}{b}\frac{W^2}{\sqrt{g(h+\eta)}}\cos\Theta_{wind} \tag{A6}$$

The ratio *k/b* as based on the data of King (1959) ranges between 0.0035-0.0051. Taking an average value we have approximately $(1/6)(k/b)\approx 0.0007$ and therefore come to Eq. (8). Computed distributions of U^B_{wind} over a typical coastal profile are shown in Fig. A1b along with the distributions of wave-induced mass transport velocities at the bed U^B_W. In case of relatively short steep waves (*T*=5 s) U^B_{wind}

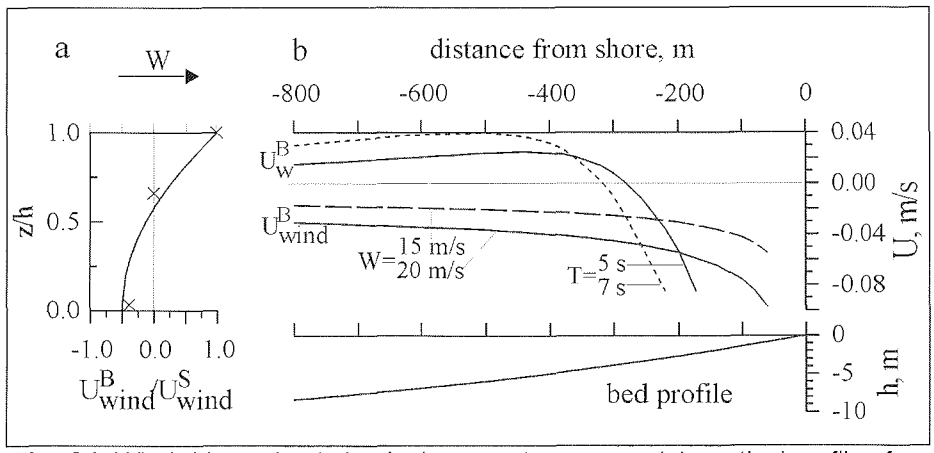

Fig. A1. Wind-driven circulation in the nearshore zone. (a) vertical profile of cross-shore flow velocity. Crosses refer to laboratory test data of King (1959). (b) wind-induced outflow and wave-induced mass transport velocity distributions over a typical coastal profile. Input *rms* wave height is 1.4 m, sand grain size is 0.18 mm

exceeds in magnitude U_W^B outside the breaking region. As a result offshore transport can dominate over a greater part of the nearshore zone.

The depth-averaged longshore velocity of wind-driven circulation $\overline{V}_{wind}$ may be roughly evaluated from the balance between the longshore component of wind stress $\tau_y = k\rho W^2 \sin\Theta_{wind}$ and bed friction stress $\tau_{by} = C_f \rho \overline{V}^2_{wind}$ (implying the longshore pressure gradient is zero),

$$\overline{V}_{wind} = W\sqrt{\frac{k}{C_f}}\sin\Theta_{wind} \qquad \text{(A7)}$$

where C_f is the friction coefficient. With the typical values of k and C_f velocity $\overline{V}_{wind}$ is of the order of $0.01W$ for the shore-parallel wind. This quantity is usually negligible as compared with the wave-generated longshore current velocities.

In the above considerations the Coriolis force $f_c = 2\Omega U \sin\varphi$ is ignored. Its insignificance in the shallow-water nearshore region is proved by comparing with the stress term $\tilde{\tau} = \tau_x / \rho(h+\eta)$ in momentum balance Eq. (A1). With the earth-rotation angular speed Ω=0.73·10^{-4} s^{-1} and U from the Eq. (13) we have in high-latitude (φ=70-80°) regions $f_c \approx 10^{-7} W^2 / \sqrt{g(h+\eta)}$. The value of $\tilde{\tau}$ is about $10^{-6} W^2/(h+\eta)$ and, hence, $f_c/\tilde{\tau} \approx 10^{-1}\sqrt{(h+\eta)/g}$. This means $f_c/\tilde{\tau} \le 10^{-1}$ for the depth (h+η)≤10 m, i.e. the Coriolis force is at least an order of magnitude smaller than other forces influencing the nearshore current system.

References

Anisimov, O., Fitzharris, B., Hagen, J.O., Jeffries, R., Marchant, H., Nelson, F., Prowse, T., Vaughan, D.G., 2001. Polar regions (Arctic and Antarctic). In: VcCarthy, J.J., Canziani, o.f., Leary, N.A., Dokken, D.J., White, K.S. (eds.), Climate change 2001: impacts, adaptation and vulnerability. Contribution of Working Group II to the Third Assessment Report of the Intergovernmental Panel on Climate Change. Cambridge University Press, Cambridge, 801-841.

Are, F.E., 1985. Forecast of thermal-abrasion coasts. Novosibirsk, Nauka, 172 pp. (in Russian).

Bretschneider, C.L., 1966. Engineering aspects of storm surges. In: Estuary and coastline hydrodynamics. Ed. A.T.Ippen. New York, P. 67-91.

Church, J.A., Gregory, J.M., Huybrechts, P., Kuhn, M., Lambeck, K, Nhuan, M.T., Qin, D., Woodworth, P.L., 2001. Change in sea level. In: Houghton, J.T., Ding, Y., Griggs, D.J., Noguer, M., van der Linden, P., Dai, X., Maskell, K., Johnson, C.I. (eds.), Climate change 2001: the scientific basis. Contribution of Working Group I to the Third Assessment Report of the Intergovernmental Panel on Climate Change. Cambridge University Press, Cambridge UK and New York USA, 639-693.

Cowell, P.J., Thom, B.G., 1995. Morphodynamics of coastal evolution. In: Carter, R.W.G., Woodroffe, C.D. (eds.), Coastal evolution: late quarternary shoreline morphodynamics. Cambridge Univ. Press, 33-86.

Cowell, P.J., Roy, P.S., Jones, R.A., 1995. Simulation of large-scale coastal change using a morphological behaviour model. Marine Geol. 126, 45-61.

De Vriend, H.J., 1997. Prediction of aggregated-scale coastal evolution. In: Int. Conf. "Coastal Dynamics'97". Plymouth, 644-653.

Forbes, D.L., Taylor, R.B., 1994. Ice in the shore zone and the geomorphology of cold coasts. Progress in Physical Geography, 18, 59-89.

Hequette, A., Desrosiers, M., Hill, P.R., Forbes, D.L., 2001. The influence of coastal morphology on shoreface sediment transport under storm-combined flows, Canadian Beaufort Sea. Journal of Coastal Research, 17, 507-516.

Kaplin, P.A., Leont'ev, O.K., Lukyanova, S.A., Nikiforov, L.G., 1991. Berega (The coasts). Moscow, Mysl, 480 pp. (in Russian).

King, C.A.M., 1959. Beaches and coasts. London, Edward Arnold, 403 pp.

Kriebel, D.L., Kraus, N.C., Larson, M., 1991. Engineering methods for predicting beach profile response. In: Int Conf. "Coastal Sediments'91". Seattle, 557-571.

Leont'ev, I.O., 1996. Numerical modelling of beach erosion during storm event. Coastal Engineering, 29, 187-200.

Leont'ev, I.O., 1999. Modelling of morphological changes due to coastal structures. Coastal Engineering, 38, 143-166.

Leont'ev, I.O., 2001. Coastal dynamics: waves, currents, sediment transport. Moscow, GEOS, 272 pp. (in Russian).

Longuet-Higgins, M.S., 1953. Mass transport in water waves. Phil. Trans. Royal Soc. London, Ser. A, 245, 903, 535-581.

Nairn, R.B., Southgate, H.N., 1993. Deterministic profile modelling of nearshore processes, 2: sediment transport and beach profile development. Coastal Engineering, 19, 57-95.

Ogorodov, S.A., Kamalov, A.M., Baurchulu, T.S., Ermolov, A.A., 2001. Anthropogenic influence on coastal evolution in region of Varandei. In: The humanity and coastal zone in XX century. Moscow, GEOS, 416-423. (in Russian).

Stive, M.J.F., De Vriend, H.J., 1995. Modelling shoreface profile evolution. Marine Geology, 126, 235-248.

Stive, M.G.F., Wind, H.G., 1986. Cross-shore mean flow in the surf zone. Coastal Engineering, 10, 325-340.